THE ROLE OF INTERFERON GAMMA IN REGULATING ANTIGEN SPECIFIC CD8 T CELL RESPONSES IN A MOUSE MODEL OF INFLUENZA

NAYANA PRABHU PADUBIDHRI

(M.Sc (Biochemistry), Bangalore University, India)

A THESIS SUBMITTED

FOR THE DEGREE OF DOCTOR OF PHILOSOPHY

NUS GRADUATE SCHOOL FOR INTEGRATIVE SCIENCES AND ENGINEERING

NATIONAL UNIVERSITY OF SINGAPORE

2013

Declaration

I hereby declare that the thesis is my original work and it has been written by me in its entirety. I have duly acknowledged all the sources of information, which have been used in the thesis.

This thesis has also not been submitted for any other degree in any university previously.

Nayana Prabhu Padubidhri

05 December 2013

Acknowledgements

I am most grateful to my supervisor, Prof Mike Kemeny for his endless support and guidance. Thank you for giving me not only so many opportunities, but also the freedom to make mistakes. Thank you for teaching me to handle failures and encouraging me through them. Thank you for taking out time always, whether on weekends for meetings or on your vacations to correct different versions of my manuscripts and thesis. Most of all, thank you for teaching me to be a good scientist. I will always value the lessons you've taught me.

I am also thankful to my Thesis Advisory Committee members, Prof. Shazib Pervaiz and Dr. Sivasankar Baalasubramanian for their guidance from time to time. Thank you for directing my project and helping me shape it to what it is today. A special word of thanks to Dr. Shiv for helping me with my paper, I am grateful for your time and encouragement.

I am grateful to Dr. Paul Hutchinson, Guo Hui and Fei Chuin for all their help with the sorting experiments. Special thanks to Paul for teaching me the basics of flow cytometry and for helping me master a few things along these years.

To my lab members, life just would not have been the same without all of you. I cannot imagine getting through these years without all the fun and frolic and all the much-needed morale boosting when experiments were not working so well. Thanks to Adrian for being such a great mentor. Thank you for teaching

me the ropes and for helping me even after you graduated. I will always remember your spirit and unbeatable enthusiasm for science. Thanks to Kenneth for being such a good friend. Thanks for being my sounding board, always willing to listen to my rants and always willing to lend a helping hand. Thanks to Sophie for being a good friend. We've drudged along this path together and now that we're almost there, I'm happy I had you to share these years with me. To Shuzhen and Yafang, it was great travelling to conferences and the trips with you girls. I really enjoyed your company all through. To Pey Yng, thanks for being so "zen" even in times of turmoil. Looking at you always made me feel that things would be all right. Thanks to Suruchi for always lending me a hand ever so often and so willingly and for always having a funny story to tell to lighten up my mood. To Richard, thanks for helping me with my project initially and for mashing those lungs with me, when I had loads of samples to process. To Debbie, thanks for helping me with my experiments and for always volunteering to help to read my paper and thesis. It has been great knowing you. To Laura, I've always looked up to you for guidance and support and you have never let me down. Thanks for everything. A special word of thanks to Benson; for putting up with my umpteen requests for more mice. Thanks for helping out. Thanks to Elsie for helping out with the ordering, even when they were always urgent. To Isaac, Dave, Shin la and Neil, it has been great fun knowing you guys and playing all those fun games in the cave during our breaks. They were such great stress busters.

I am deeply thankful to my family for always believing in me. Ma and Pappa, I could never have done it without you. I also thank my parents-in-law for

their support and blessings during these years and always. To my six sisters, you were my greatest supporters and my biggest fans. All those long skype sessions and telephone calls did a lot to bridge the distance between us. I am so lucky to have you as family. Thanks to Veena, my best friend and my worst critic for the many times you put things into perspective. To my dear husband Ravi, I don't have words to express my gratitude. Thanks for putting up with me through these years, encouraging me every step of the way. Mostly, thanks for just for being there. And finally, thanks to my Mave. You always believed in me and you always encouraged me to be a better person, leading by example. You were always so interested in my research and I regret that I could not tell you everything about it. I feel your absence the most today.

Table of Contents

Summary

Understanding the mechanisms of virus-host interactions and the factors that regulate memory T cell responses are important for generation of efficient vaccines. The factors that regulate the contraction of the $CD8^+$ T cell response and the magnitude of the memory population against localized mucosal infections like influenza are currently undefined. In this study, we use a mouse model of influenza to demonstrate that the absence of IFN-γ or the receptor, IFN-γR1 leads to aberrant contraction of antigen-specific $CD8^+$ T cell responses. The increased accumulation of the effector $CD8^+$ T cell population was independent of viral load and rates of proliferation of the cells. Direct *ex vivo* analysis revealed an increased amount of cell death in influenza-specific-$CD8^+$ T cells from infected WT mice compared to the IFN-$\gamma^{-/-}$ mice. Reduced contraction was associated with an increased fraction of influenza-specific $CD8^+$ T cells expressing the interleukin-7 receptor at the peak of the response, resulting in enhanced numbers of memory precursor cells in IFN-$\gamma^{-/-}$ and IFN-$\gamma R^{-/-}$ compared to WT mice. Blockade of IL-7 within the lungs of IFN-$\gamma^{-/-}$ mice restored the contraction of the influenza-specific $CD8^+$ T cells, indicating that expression and signaling through IL-7R is important for survival and is not simply a consequence of the lack of IFN-γ signaling. Finally, enhanced $CD8^+$ T cell recall responses and accelerated viral clearance were observed in the IFN-$\gamma^{-/-}$ and IFN-$\gamma R^{-/-}$ mice after re-challenge with a heterologous strain of influenza, confirming that higher frequencies of memory precursors are formed in the absence of IFN-γ signaling and these can contribute to heterosubtypic immunity. In summary, we have identified IFN-γ as an

important regulator of localized viral immunity that promotes the contraction of antigen-specific $CD8^+$ T cells and inhibits memory precursor formation, thereby limiting the size of the memory cell population after an influenza infection.

List of tables

List of figures

List of Abbreviations

7AAD	7-amino-actinomycin D
AF488	Alexa Fluor 488
AF549	Alexa Fluor 549
AF647	Alexa Fluor 647
APC	Antigen presenting cell
APC	Allophycocyanin
BAL	Bronchoalveolar Lavage Fluid
BSA	Bovine serum albumin
CD	Cluster of differentiation
CTL	Cytotoxic T Lymphocyte
DC	Dendritic cell
DMEM	Dulbecco's modified eagle's medium
EAE	Experimental Autoimmune Encephalomyelitis
EDTA	Ethylenediaminetetraacetic acid
FACS	Fluorescence activated cell sorting
FCS	Foetal calf serum
FITC	Fluorescein-5-isothiocyanate
IFN	Interferon
HA	Hemagglutinin
HEF	Hemagglutinin Esterase Fusion
HPAI	Highly Pathogenic Avian Influenza
IL	Interleukin
iNOS	inducible Nitric Oxide Synthase
IRF	Interferon Regulatory Factor

JAK	Janus Kinase
mAb	Monoclonal antibody
MDCK	Madine Darby Canine Kidney
MHC	Major Histocompatibility Complex
MFI	Mean Fluorescence Intensity
MMP	Matrix Metalloproteinase
MW	Molecular Weight
NA	Neuraminidase
NK	Natural Killer
NS1	Non-structural protein 1
NP	Nucleoprotein
OT-I	Transgenic $CD8^+$ T-cell with TCR specific for OVA 257-264/Kb
PBS	Phosphate buffered saline
PE	Phycoerythrin
PerCP	Peridinin-chlorophyll protein
PCR	Polymerase Chain Reaction
PFA	Paraformaldehye
PFU	Plaque Forming Units
p.i.	Post Infection
MDCK	Manine Darby Canine Kidney Cell Line
PBS	Phosphate Buffered Saline
RBC	Red Blood Cell
RPMI	Roswell park memorial institute
RSV	Respiratory Synctial Virus

TCR	T-cell receptor
T_{CM}	Central Memory T cell
T_{EM}	Effector Memory T cell
TLR	Toll like receptor
TNF	Tumor Necrosis Factor
TNFR	Tumor Necrosis Factor Receptor
TPCK	L-1-tosylamido-2-phenylethyl chloromethyl ketone
TRAIL	TNF-related apoptosis-inducing ligand
WT	Wild type

Publications

Prabhu N, Ho AW, Wong KHS, Hutchinson PE, Chua YL, Kandasamy M, Lee DC, Baalaubramanian S, Kemeny DM. 2013. Interferon-γ regulates contraction of the influenza-specific CD8 T cell response and limits the size of the memory population. J Virol 87 (23): 12510

Betts RJ, **Prabhu N**, Ho AW, Lew FC, Hutchinson PE, Rotzschke O, Macary PA, Kemeny DM. 2012. Influenza A virus infection results in a robust, antigen-responsive, and widely disseminated Foxp3+ regulatory T cell response. J Virol 86: 2817-25

Ho AW, **Prabhu N**, Betts RJ, Ge MQ, Dai X, Hutchinson PE, Lew FC, Wong KL, Hanson BJ, Macary PA, Kemeny DM. 2011. Lung CD103+ dendritic cells efficiently transport influenza virus to the lymph node and load viral antigen onto MHC class I for presentation to CD8 T cells. J Immunol 187: 6011-21

Chapter 1: Introduction

1.1 Influenza Virus

Influenza virus is a negative single stranded RNA virus from the Orthomyxoviridae family. It is one of the most studied viruses in recent times because of the huge economic burden it causes. The influenza viruses comprise the 3 genera out of the five of the family Orthomyxoviridae: Influenza A, B and C. Influenza viruses A, B and C are very similar in their overall structure and protein composition. They are made of a viral envelope containing glycoproteins, wrapped around a central core containing the viral RNA genome. There are minor differences in their structure: Influenza A viruses have three membrane proteins (Hemagglutinin (HA), Neuraminidase (NA) and Matrix (M2) and a ribonucleoprotein core consisting of eight viral RNA segments and three proteins: PA, PB1 and PB2. Influenza B viruses have four proteins in the envelope: HA, NA, NB and BM2 and eight RNA segments. The Influenza C viruses however have a major envelope protein called HEF (Hemagglutinin-esterase fusion) that performs the functions of both the HA and NA proteins and hence contain only 7 RNA segments.

The influenza A viruses are the most studied because of their ability to cause severe illness in humans, birds, pigs and other animals. They are classified by their surface HA and NA proteins, of which there are 16 HA subtypes and 9 NA subtypes.

1.1.1 Structure and Genetics of the Influenza A virus

The Influenza A virus particle (virion) is 80-120nm in diameter and can exist in both spherical and filamentous forms, although the spherical forms are more common. The virion is made up from the lipid bilayer, derived from the host plasma membrane as the virus buds out of the host. This viral envelope contains two main types of glycoproteins on the surface, hemagglutinin (HA) and Neuraminidase (NA) and encapsulates the ribonucleoprotein core. This central core contains the viral RNA genome made up of 8 strands of negative-sense single-stranded RNA and the other viral proteins that package and protect this RNA (McGeoch et al. 1976). These eight strands of RNA encode for 11 different proteins (listed in table 1.1).

The HA and the NA are the two large spike-like glycoproteins on the surface of the virus. HA is a lectin that mediates the binding of the virus to target cells and facilitates the entry of the virus into the target cell. The proteolytic cleavage of the HA molecule (HA0) into HA1 and HA2 is carried out by trypsin-like enzymes found in the respiratory tract and is necessary for the infectivity of the virus (Klenk et al. 1975). This cleavage exposes the hydrophobic N-terminus of the HA2 subunit, which contains a highly conserved fusion peptide that inserts into the endosomal membrane (Stegmann et al. 1991). Proteolytic cleavage also leads to a conformational change in the HA molecule in response to endosomal acidification and hence leads to the fusion of viral and host membranes, allowing the viral genome to enter the host cell (Bullough et al. 1994). The NA protein is a glycoside hydrolase enzyme that catalyses the hydrolysis of terminal sialic acid residues from the

host cell receptors and is involved in the release of newly formed progeny virus particles from infected cells. The NA is also able to cleave sialic acid residues bound to surface viral proteins, hence preventing the aggregation of the newly formed viral particles, which may hamper infectivity. This function of NA to cleave sialic acid is a pre-requisite for the spread of the virus. These surface proteins are ideal targets for antiviral drugs as interference of their key roles can hamper infectivity of the virus. Influenza neuraminidase inhibitors Zanamivir and Oseltamivir, also known as Relenza and Tamiflu respectively, are effective antivirals known today which act by binding to the active site of the NA and render the virus unable to escape from the host cell, thereby preventing spread of the virus (Hayden 1997; Hayden et al. 1999). Furthermore, the surface HA and NA proteins form antigens against which antibodies can be raised. Neutralizing antibodies against HA and NA also help to prevent virus from spreading.

Another protein that is embedded on the surface of the virus but at a much lower frequency is the M2 matrix protein, a small protein generated by the alternative splicing of the RNA segment encoding the matrix protein. The M2 protein comprises of the ectodomain M2e, a small part exposed to the cell surface, a transmembrane domain with the rest of it localized within the internal portion of the virus (Lamb et al. 1985). The M2 is a proton channel and is also involved in mediating viral entry into the host cell. During the fusion with the host membrane, the M2 proton pump lowers the pH of the virus to permit the dissociation of viral Ribonucleoprotein complexes from the structural M1 protein (Kemler et al. 1994). This allows the viral RNPs tethered to the M1 proteins to be released into the cytoplasm where they can be

imported into the nucleus by nuclear localization signals found on the NP molecule (O'Neill et al. 1995). Antivirals like Rimantidine and Amantidine target the M2 protein prevent the import of the protons into the viral core by blocking the M2 channel (Schnell and Chou 2008), thereby preventing the release of viral RNPs from the M1 protein, and ultimately into the host cell.

The M1 protein is present beneath the lipid-envelope and is the most abundant protein in the virion. It functions as an internal scaffold for the viral RNPs to be anchored together, mediated by interactions between the non-structural NS2 protein bound to the viral RNA and the M1 protein (Yasuda et al. 1993). The M1 protein is also essential for viral assembly and release by resulting in the spontaneous formation of virus-like budding particles at the cell surface (Gomez-Puertas et al. 2000).

Inside the viral core, each viral RNA segment is associated with several viral proteins: the nucleoprotein NP and PA, PB1 and PB2 which are components of the viral RNA dependent RNA polymerase. Each of the 8 viral RNA segments encodes for one or two proteins, the details of which are summarized in table 1.

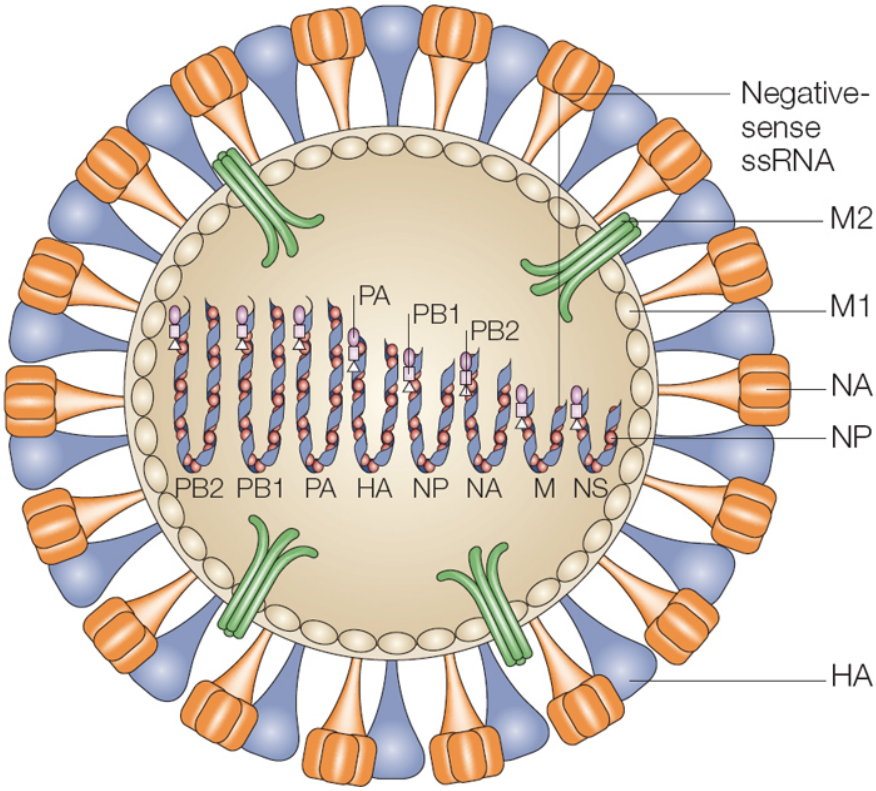

Figure 1.1 Schematic representation of the influenza A virus.

The two major surface glycoproteins of the influenza virus are hemagglutinin (HA) and neuraminidase (NA), which form spike-like projections from the viral envelope. The ribonucleoprotein complex comprises a viral RNA segment associated with the nucleoprotein (NP) and three polymerase proteins (PA, PB1 and PB2). The matrix protein is associated with both the ribonucleoprotein and the viral envelope. Adapted from (Horimoto and Kawaoka 2005)

Viral RNA segment	Size of RNA (bp)	Protein	Approx Mol Wt (kDa)	Function
1	2341	PB2 Basic polymerase	86	Viral polymerase subunit
2	2341	PB1 Basic polymerase	87	Viral polymerase subunit
		PB1-F2 Alternate open reading frame	11	Unknown-inhibits host mitochondrial function and induces apoptosis
3	2233	PA Acid polymerase	83	Viral polymerase subunit
4	1778	HA Hemagglutinin	64	Binding to sialic acid containing cell surface receptors and membrane fusion
5	1565	NP Nucleoprotein	56	Encapsidation of RNA
6	1413	NA Neuraminidase	50	Sialidase- Cleavage of sialic acids to release mature virions from host cell
7	1027	M1 Matrix protein	28	Viral assembly
		M2 Matrix protein	11	Proton channel. Dissociation of viral components during uncoating.
8	890	NS1 Non-structural protein	26	RNA splicing and translation. Antagonism of host immune responses
		NS2 Non-structural protein	14	Nuclear export of RNP

Table 1.1: List of 11 proteins encoded by the influenza RNA segments

1.1.2 The threat of influenza

Influenza A is one of the most successful viruses in terms of the numbers of people it infects each year, not to mention the different pandemics it has caused in the last century. The success of the influenza virus is mainly attributed to the fact that it can undergo antigenic shift and antigenic drift. Antigenic shift is a specialized form of re-assortment, which confers a change in the phenotype of the virus. This occurs normally in a host simultaneously infected with two or more subtypes of the virus, where the surface proteins and viral RNAs recombine to form newer variants of the virus, even different subtypes. This enables the virus to change its surface proteins and hence evade neutralization by host antibodies resulting from an earlier infection. Reassortment of the influenza viruses is known to occur in pigs, which are known to be mixing vessels for the virus and also in waterfowl, as these are natural hosts for multiple subtypes of the virus. Antigenic drift is a mechanism that involves the accumulation of point mutations over time within the genes that can encode for antibody-binding sites. This results in newer strains of viruses, which cannot be inhibited as effectively by the antibodies that were originally targeted against the previous strains. Both antigenic shift and antigenic drift make it easier for the virus to spread in a moderately immune population.

Due to these properties, the influenza A virus is partially able to elude host immunity and hence is able to cause multiple cases of inflection each year through the influenza seasons as well as the pandemics that have been responsible for millions of deaths in the last century. The 1918 influenza pandemic was the most severe pandemic caused by the H1N1 strain, and

resulted in the death of approximately 40 million people worldwide (Reid et al. 2001). There were also pandemics that occurred in 1957 and1968, albeit not as serious as the one in 1918. In fact the most recent scare came only a few years ago in the form of the 2009 H1N1 virus or "swine flu" that claimed many lives (Chowell et al. 2009; Garten et al. 2009). In addition, H5N1 viruses (or bird flu) are also extremely virulent in humans but have not yet acquired the ability for efficient human-to-human transmission. The more recent scare with the new bird flu H7N9, which has already caused 104 confirmed human cases and 21 deaths (Watanabe, T. et al. 2013). The emergence of these new viruses remind us that we are still in danger from influenza and that more research and health preparedness is necessary to combat any further outbreaks.

1.1.3 Clinical symptoms of infection and pathology

Influenza is an acute respiratory infection characterized by the sudden onset of high fever, sore throat, cough, headache, myalgia, malaise and inflammation of the upper respiratory tract and trachea. It is very difficult to diagnose an influenza infection by the clinical symptoms alone as the disease manifestations are very similar to those caused by other respiratory viruses such as Para influenza virus, respiratory syncytial virus and rhinovirus. Acute symptoms and fever can last for 5 to 7 days but weakness and fatigue may linger for weeks. Influenza usually occurs in winter outbreaks or epidemics in the temperate climates. People of all ages are generally afflicted, but the most affected are the children and the aged and those with underlying illnesses. Influenza A and B viruses are the most common causes of Influenza-like-

illnesses (ILI) and at the peak of an influenza epidemic, about one-third of patients with ILI are positive for influenza A (2000).

Influenza A viral replication peaks about 48-72 hours after inoculation and then declines slowly with little virus shedding after about 6 days. The virus can replicate in both the upper and lower respiratory tract. Influenza can be diagnosed by viral culture, demonstration of viral antigens or the viral genetic material or the presence of specific antibody in serum (Taubenberger and Layne 2001).

Although influenza is a self-limiting illness in most individuals, complications and death can occur in groups of people with reduced immune function such as the very young and elderly. People with chronic pulmonary or cardiac disease are also at high risk for developing complications from influenza. Complications include hemorrhagic bronchitis and pneumonia, which can develop within hours followed by dyspnea, cyanosis, pulmonary edema and death may occur in as little as 48 hours after the onset of symptoms (Taubenberger and Morens 2008). Secondary bacterial infections can also contribute to the complications after an influenza infection and was a significant cause for the high mortality during the 1918 pandemic (Morens et al. 2008).

Influenza virus replicates in epithelial cells throughout the respiratory tract and the virus has been recovered from both the upper and lower respiratory tract of people infected naturally or experimentally with influenza. Analysis of lung biopsies by both light and electron microscopy show that influenza results in diffuse inflammation of the larynx, trachea and bronchi, with lymphocyte and

histiocyte cellular infiltration (Walsh et al. 1961). Infection of the ciliated epithelium leads to initial shrinkage and vacuolization of the cells hence leading to necrosis and desquamation of the cells in the luminal space. The lung interstitium may show signs of congestion as the airspaces are filled with fluid, fibrin and the neutrophil infiltration (Taubenberger and Morens 2008).

1.1.4 Natural hosts for Influenza

The influenza virus binds to cell surface glycoproteins containing terminal sialic acid residues, through the HA molecule. The cell tropism of the virus depends on the type of sialic acid glycosylated on the proteins of the glycolipids on the cell surface. Through the HA molecule, the human-specific-viral strains bind to residues with a terminal α2, 6-linked sialic acid. In contrast, the HA of the avian-specific strains binds to α2, 3-linked sialic acid residues. Consequently, α2,6-linked sialic acid linkages are mainly expressed on the apical surfaces of ciliated cells in the tracheal epithelium of humans, whereas the α2,3-linked sialic acid linkages are abundantly present in the upper airways of birds.

α2,3 linked sialic acid residues are also present on the non-ciliated cells of the human trachea, but there are few of these cells and the density of sialic acid residues is also low, which may account for the relatively low transmissibility of avian influenza strains into humans (Matrosovich et al. 2004). In pigs however, the tracheal epithelium expresses both kinds of sialic acid residues and this leads to the infection of pigs with both the avian and human strains of influenza. This facilitates viral reassortment and the generation of novel

human viral strains with the potential of transferring genetic material from the highly pathogenic avian influenza strains.

Wild birds are also known to be natural hosts for all known subtypes of influenza A viruses although they do not become sick when infected. Fowl are also asymptomatic carriers of influenza A viruses and can transmit the virus to birds, pigs, horses, seals, whales and humans.

Ferrets have been identified as excellent models for human influenza after the isolation of human influenza A viruses in 1933. It was reported in a series of papers that the histopathological changes in the respiratory tracts of pigs, ferrets and mice were compatible with those in human influenza virus infection (Shope 1931; Shope 1934; Shope 1935). However, although mice were susceptible to infection with both avian and human strains of influenza, they could not transmit the infection to other mice. In contrast (Shope 1935), both ferrets and pigs were able to transmit the virus to animals they were in contact with (Shope 1934).

1.2 Host innate immune response to influenza

The innate immune system is the first line of defense against the influenza virus. Viral replication peaks in a matter of hours, whereas the adaptive immunity takes days to be initiated and then for the response to peak. In the interim, it is the innate immune response that combats viral replication in the initial phase of the infection, buying precious time until the adaptive immune responses come into play. It consists of components that aim to prevent infection of the respiratory epithelium and control virus replication. Some of these responses are outlined below:

1.2.1 Mucus secretions and the lung epithelium

In the lung, the first line of protection against the influenza virus is provided by the mucus lining of the respiratory tract which contains sialic-acid bearing glycoproteins with anti-hemagglutinating properties. These serve as decoy receptors for the virus and hence prevent binding of the virus to the underlying epitahelial cells. The mucus also contains collectins, such as mannose binding lectin, and surfactant protein D which can bind to glycosylated residues on the HA protein, resulting in either direct blockade of viral binding or opsonization of the virus for clearance by phagocytosis (Reading et al. 1997). The surface of the lung epithelium also has cilia, which push the viral particles trapped in the mucus to the larynx to be swallowed and destroyed by the high acidity in the stomach. Upon infection, the alveolar epithelial cell layer is also able to actively recruit immune cells such as monocytes to the site of infection by up regulating adhesion molecules and secreting chemokines to facilitate leukocyte transepithelial migration (Herold et al. 2006).

1.2.2 Intracellular innate sensing of influenza virus infection

When influenza virus infects respiratory epithelial cells or alveolar macrophages, the single stranded RNA is recognized by PAMP (pathogen Associated Molecular Patterns) via receptors such Toll Like receptor 7 (TLR7), Retinoic acid-inducible gene-I (RIG-I) (Diebold et al. 2004; Pichlmair et al. 2006) and the NOD-like receptor family pryin domain containing 3 (NLRP3) protein (Pang and Iwasaki 2011).

Signaling through these receptors leads to production of pro-inflammatory cytokines and type I interferons, which have strong antiviral activities that inhibit host cell protein synthesis and viral replication (Kumagai et al. 2008). Further, NLRP3 is a part of the inflammasome, a cytoplasmic complex that is associated with immunity against influenza virus. The receptor is activated by influenza virus infection and M2 ion channel activity, leading to the conversion of pro-IL-1β into IL-1β, a cytokine that is involved in the expansion of antigen-specific $CD4^+$ T cells and induction of Th17 responses (Acosta-Rodriguez et al. 2007; Ben-Sasson et al. 2009).

1.2.3 Type I Interferons

Type I interferons (IFNs), IFN-α/β are secreted by epithelial cells and innate immune cells such as macrophages, monocytes and plasmacytoid dendritic cells and are crucial in limiting viral replication in the initial phases of an influenza infection. Type I IFNs also induce IFN stimulated genes (ISGs) via the JAK-STAT signaling pathway. One of the important ISGs is the myxovirus (MX) gene that encodes the MxA protein, a GTPase with strong antiviral activity that can inhibit influenza virus replication (Holzinger et al. 2007). In addition, type I IFNs can induce the production of several inflammatory cytokines and chemokines mediated by NF-kB activation, eg. IL-1β, IL-6, IL-8, TNF-α, CCL2, CCL3, CCL5 and CXCL10, which in turn recruit cells like macrophages and neutrophils to the site of infection (Perrone et al. 2008).

Type I interferons stimulate cells to up regulate their expression of MHC I and hence enhance presentation of viral peptides on the cell surface. They also

stimulate dendritic cells to enhance their antigen presentation to $CD4^+$ and $CD8^+$ T cells thus contributing to initiating the adaptive immune response.

1.2.4 Phagocytes

Macrophages and neutrophils play a critical role in controlling early viral titers during an influenza infection. Depletion of either macrophages or neutrophils prior to a lethal infection with the 1918 HA/NA: Tx91 recombinant virus resulted in uncontrolled virus growth and mortality (Tumpey et al. 2005). But depletion of these cell types 3 or 5 days after infection did not alter disease outcome, indicating that macrophages and neutrophils act primarily to control viral replication during the early stages of infection (Kim, H. M. et al. 2008b). It is likely that the principal contribution of macrophages and neutrophils during early infection is to phagocytose the virus or infected cells, as the introduction of phagocytosis inhibitors into the airways of mice lead to increased lethality after influenza infection (Watanabe, Y. et al. 2005). Although macrophages are highly susceptible to influenza infection, the infection is not productive as synthesis of viral proteins is halted midway and the macrophage undergoes apoptosis before progeny virus can be released (Hofmann et al. 1997). On the other hand, once macrophages become activated, they produce nitric oxide synthase 2 (NOS2) and tumor necrosis factor alpha (TNF-α) and in this way can contribute to the influenza virus induced lung pathology (Jayasekera et al. 2006).

1.2.5 Dendritic cells

Dendritic cells (DCs) are professional antigen-presenting cells in influenza virus infections. DCs act as sentinels of the immune system. They are situated beneath the airway epithelium and monitor the airway lumen via their dendrites that are extended through the tight junctions between the airway epithelial cells. DCs can pick up antigen from infected and dying cells but can themselves, also be infected by the influenza virus. Upon capturing antigen in the lung, the DCs then migrate to the lung draining lymph node, specifically to the posterior mediastinal lymph node and here they present the influenza virus derived antigens to naïve T cells and activate them(GeurtsvanKessel et al. 2008; Ho et al. 2011).

The DC degrades the viral proteins and subsequently presents the peptide bound to MHC I or MHC II molecules on the cell surface. For MHC class I presentation, the virus-derived peptides are liberated into the cytosol by proteasomes and subsequently are transported to the ER where they bind to MHC I molecules. These complexes are then transported to the cell surface for recognition by cytotoxic $CD8^+$ T cells. For MHC II presentation, viral proteins are degraded in endosomes/lysosomes and the resulting peptides bind to MHC II molecules. These complexes are then transported to the cell membrane for recognition by $CD4^+$ T cells.

1.2.6 Natural Killer cells

Natural Killer (NK) cells are important effectors of the innate immune response to influenza infection. They can recognize antibody-bound influenza infected cells and lyse them by a process known as antibody-dependent cell

cytotoxicity (ADCC). These cells can recognize influenza-infected cells by their receptors (NKp44, NKp46) and upon binding of the influenza HA; the receptors trigger the NK cells to lyse the infected cell (Arnon et al. 2001; Mandelboim et al. 2001). It has also been suggested that invariant NKT cells stimulate the induction of cellular immunity and regulate infection-induced pathology (Paget et al. 2011).

1.3 Host adaptive immune responses to influenza

The adaptive immune response is the second line of defense against influenza virus infection and comes into play later in infection to eliminate the influenza virus from the system. It consists of humoral and cellular immune elements mediated by virus-specific B cells/antibodies and T cells respectively. Cellular immunity is mainly mediated directly by cytotoxic $CD8^+$ T cells but $CD4^+$ T cells provide indirect help for optimal generation of antibodies and cytotoxic responses.

1.3.1 Humoral immunity against influenza

Influenza virus infection induces virus-specific antibody responses (Potter and Oxford 1979). These antibodies mediate long-term protection from re-infection by an identical or antigenically similar viral strain. Antibodies specific for the two surface glycoproteins HA and NA are most critical since the presence of these antibodies are known to correlate with protective

immunity (Gerhard 2001). The HA specific antibodies bind to the trimeric globular head of the HA1 subunit and inhibit virus attachment and entry into the host cell. HA-specific antibodies can hence neutralize the virus and facilitate phagocytosis of virus particles by Fc receptor expressing cells. HA-specific antibodies form a solid correlate of protection against influenza provided that they match the virus causing the infection. In contrast to the antibodies targeted to the HA head region, antibodies formed against the highly conserved stem region can recognize and bind to HA molecules from different subtypes and have broad neutralizing ability (Ekiert et al. 2009; Prabhu et al. 2009). Antibodies against the NA protein are protective as well. By binding to NA, antibodies do not directly neutralize the virus but inhibit NA enzymatic activity and thus limit viral spread. Further, NA-specific antibodies facilitate ADCC and also contribute to the clearance of virus-infected cells (Mozdzanowska et al. 1999).

The main antibody subtypes in the influenza-specific humoral immune response are IgA, IgM and IgG. Mucosal or secretory IgA antibodies are produced locally and are transported along the mucus of the respiratory tract by transepithelial transport and afford local protection from infection of airway epithelial cells. These antibodies are also able to neutralize the virus intracellularly (Mazanec et al. 1995). The presence of serum IgA is an indicator of recent infection as these are produced rapidly after influenza A infection (Rothbarth et al. 1999). Serum IgGs chiefly transudate into the respiratory tract and afford long-term protection (Murphy, B. R. et al. 1982). IgM antibodies initiate complement mediated neutralization of influenza virus and are a hallmark of primary infection (Jayasekera et al. 2007).

1.3.2 $CD4^+$ T cell responses to influenza

$CD4^+$ T cells are activated after recognizing virus-derived MHC class II associated peptides on antigen presenting cells that also express co-stimulatory molecules. The role of $CD4^+$ T cells in influenza has not been as extensively studied as their $CD8^+$ counterparts due to the difficulty of detecting antigen-specific $CD4^+$ T cells using MHC II multimers owing to their low binding avidity (La Gruta et al. 2007). Also, unlike the $CD8^+$ T cell response that has several immunodominant epitopes, which account for 75% of total virus-specific $CD8^+$ T cells (Doherty et al. 2006), $CD4^+$ T cell epitopes are widely distributed (Crowe et al. 2006) and hence pose a challenge when trying to obtain a sufficiently large amount for estimating the virus-specific response.

The main role of virus-specific $CD4^+$ T cells during influenza infection is to provide T cell help to augment B cell antibody production and $CD8^+$ T cell cytolysis of infected cells to clear the virus from the respiratory tract. Different subsets of Th cells are distinguished based on their cytokine expression profiles. Th1 cells produce IFN-γ and IL-2 and are involved mainly in cellular immune responses. Th2 cells produce IL-4 and IL-13 and promote B cell responses. Also, regulatory T cells (Tregs) and Th17 cells have been identified that regulate the cellular immune response to influenza virus infection.

Th1 $CD4^+$ T cell responses are important for viral clearance as adoptive transfer of Th1 virus-specific $CD4^+$ T cell clones were able to confer protection against a lethal dose of influenza whereas mice that received Th2 clones fail to survive (Graham et al. 1994). $CD4^+$ T cells are also important for the development of $CD8^+$ T cell memory responses and the absence of $CD4^+$ T

cell help during primary infection resulted in a weaker secondary memory $CD8^+$ response after a heterologous virus challenge (Belz et al. 2002).

1.3.3 $CD8^+$ T cell responses to influenza

The establishment of a robust $CD8^+$ T cell response is a key factor in determining the outcome of a primary influenza infection. Mice deficient in $CD8^+$ T cells exhibit delayed clearance of influenza virus, elevated pulmonary viral titers and increased mortality (Bender et al. 1992). Conversely, adoptive transfer of virus-specific $CD8^+$ T cells confers protection against lethal doses of influenza (Cerwenka et al. 1999; Hamada et al. 2009). This protection was seen even in mice lacking B cells (Graham and Braciale 1997).

Upon influenza infection, $CD8^+$ T cells are activated in the lung draining lymph nodes and are recruited to the site of infection. $CD8^+$ T cells have several effector functions that lead to their antiviral activity and this can be categorized into three groups: First $CD8^+$ T cells promote the lysis of infected cells by the exocytosis of perforin and granzyme containing granules. Perforin permeabilize the membrane of the infected cells and subsequently granzymes enter the cell and induce apoptosis. Second, $CD8^+$ T cells induce tumor necrosis factor receptor (TNFR) family-dependent apoptosis of infected cells by expressing CD95 ligand (FAS-L) or TNF-related apoptosis-inducing ligand (TRAIL). The abrogation of any of these effector molecules results in reduced cytolytic activity and delayed viral clearance (Topham et al. 1997; Brincks et al. 2008). Third, $CD8^+$ T cells also produce pro-inflammatory cytokines such as IFN-γ, TNF-α and GM-CSF in response to virus-infected cells. IL-17 secreting $CD8^+$ T cells have also been identified during influenza infection and

adoptive transfer of these cells conferred protection against lethal challenge (Hamada et al. 2009).

Although effector $CD8^+$ T cells contribute significantly to pro-inflammatory responses, they were also shown to have a crucial immunomodulatory role during acute influenza infection. $CD8^+$ T cells were observed to simultaneously produce large amounts of IL-10 to counterbalance pro-inflammatory responses and the blockade of T-cell derived IL-10 resulted in enhanced pulmonary inflammation and increased viral lethality (Sun, J. et al. 2009).

Antigen specific T lymphocytes recognize antigen in the context of self MHC-class I molecules. During many infections, all T cells undergo cytokine-driven phenotypic changes (called by-stander activation) but only antigen specific T cells undergo multiple rounds of replication to generate robust numbers of effector $CD8^+$ T cells. Although the quality of the $CD8^+$ T cell response is crucial to viral clearance, the quantity of virus-specific cells generated is equally important in determining the outcome of infection. Tetramer staining of $CD8^+$ T cells reveals that there is a strong correlation between the number of virus-specific $CD8^+$ T cells in the lung and viral titer reduction (Flynn et al. 1999; Lawrence et al. 2005). This highlights the importance of generating sufficiently large numbers of effector $CD8^+$ T cell populations during influenza infection.

Naïve $CD8^+$ T cells circulating in the blood and secondary lymphoid organs are quickly recruited to the lung draining lymph node during an influenza infection (Ho et al. 2011). In the lymph node, they encounter viral antigens, presented by MHC class I molecules on the surface of the dendritic cells and

undergo massive proliferation and differentiate into effector cells (GeurtsvanKessel et al. 2008; Kim, T. S. and Braciale 2009). These effector cells then migrate to the site of infection in the lung and undergo further expansion (Lawrence et al. 2005). This leads to a huge increase in the number of antigen specific $CD8^+$ T cells, which mediate effector function as mentioned earlier. Once the pathogen is cleared, the $CD8^+$ T cell pool undergoes extensive contraction and the vast majority of antigen specific $CD8^+$ T cells (~95%) undergo programmed cell death. Only a small proportion of these cells survive the contraction phase to form the memory pool. The magnitude of the $CD8^+$ T cell memory pool depends on the number of cells that survive the contraction phase and further differentiate to form long-lived memory cells(Williams and Bevan 2007). The mechanisms by which this process is regulated are not yet completely understood.

1.4 Memory $CD8^+$ T cells

Immune memory is the essential hallmark of the immune system and indicates a qualitatively and/or quantitatively improved immune response upon successive exposures to the same antigen. This leads to an enhanced secondary immune response, which is greater in magnitude, and speed, is more sensitive to low doses of antigen, and is more effective in the diversity or complexity of secondary effectors produced (Kaech and Wherry 2007; Williams and Bevan 2007; Harty and Badovinac 2008).

A minimal definition of memory $CD8^+$ T cells would be a population of $CD8^+$ T cells that persists long after antigen clearance. The memory cell pool contains two diverse populations: effector memory or T_{EM} ($CD62L^{low}$ $CCR7^{low}$) and central memory or T_{CM} ($CD62L^{hi}$ $CCR7^{low}$) (Sallusto et al.

1999). The two subsets are known to possess distinct functional properties. Studies have shown that human and murine T_{CM} circulate between lymphoid organs, whereas the T_{EM} set is found more in peripheral tissues (Sallusto et al. 1999; Masopust et al. 2001) reflecting the expression of the CD62L lymph-node homing marker. Apart from their anatomical compartmentalization, T_{CM} and T_{EM} memory populations are thought to display a different array of functional properties. T_{EM} cells are generally considered to have a more limited lifespan and weaker proliferative potential compared to their T_{CM} counterparts.

Different cytokines participate in the differentiation of naïve $CD8^+$ T cells to memory $CD8^+$ T cells. Cytokines using the common gamma chain (CD132) receptor family are implicated in the process of memory cell generation. The common gamma chain cytokines act as at-cell growth and survival factors. There are now data to show that Interleukin (IL)-2, IL-4, IL-7, IL-15 and IL-21 are all involved in T cell responses and some of these cytokines are involved in the development and maintenance of memory T cell responses. IL-7 and IL-15 are required during or before the contraction phase to promote memory cell production (Schluns et al. 2000; Schluns et al. 2002).

IL-7 is a potent survival factor for lymphocytes during development and in the periphery (Maraskovsky et al. 1996). The survival effects of IL-7 are due, in part, to the ability of IL-7 to increase expression of Bcl-2, an anti-apoptotic protein (Akashi et al. 1997; Maraskovsky et al. 1997). Analysis of the roles of IL-7 in immune responses has been hampered by the fact that IL-7 is highly essential in normal lymphocyte development and IL-7- and IL-7R- deficient mice are severely immunodeficient. Although naïve $CD8^+$ T cells express high

levels of IL-7Ra, they down regulate it upon activation and slowly regain it throughout the contraction phase. These events are likely to be crucial for the transition from effector to memory T cells. This theory is supported by the finding that virus-specific-TCR-transgenic $CD8^+$ T cells from IL-7Ra deficient mice are rapidly lost after a normal expansion phase, resulting in the poor generation of memory cells (Schluns et al. 2000). Memory T cells have an increased potential to survive *in vivo* compared to naïve T cells (Tanchot et al. 1997). As IL-7 is a survival factor and memory $CD8^+$ T cells express high levels of IL-7Ra (Vella et al. 1998; Schluns et al. 2000; Goldrath et al. 2002), the survival of memory $CD8^+$ T cells rather than their proliferation may be attributed to IL-7.

IL-15 on the other hand is a more potent proliferative agent for memory $CD8^+$ T cells. This is supported by the fact that IL-15- and IL-15Rα deficient mice totally lack memory phenotype $CD8^+$ T cells (Lodolce et al. 1998; Kennedy et al. 2000). Further, antibody mediated blockade of IL-15Rβ inhibited the proliferation of memory $CD8^+$ T cells *in vivo* (Ku et al. 2000). Several studies have shown that IL-15 is involved in the maintenance of antigen-specific memory $CD8^+$ T cells (Becker et al. 2002; Schluns et al. 2002). The antigen specific $CD8^+$ T cell response to infection with VSV or LCMV could be generated in IL-15 and IL-15Rα deficient mice. However, the number of antigen-specific $CD8^+$ T cells in these mice declined over time. Overall, these studies show that IL-15 signaling is required for the maintenance of normal numbers of antigen-specific $CD8^+$ T cells. However, a recent study also shows IL-15 independent generation, maintenance and function of $CD8^+$ T cell memory after influenza infection (Verbist et al. 2011). These studies show that

probably both IL-15-dependent and IL-15-independent memory populations exist.

1.5 Influenza and asthma

Asthma is a chronic airway disease with symptoms such as wheezing, breathlessness, chest tightness and coughing, with variable and reversible airway obstruction accompanied by airway hyper responsiveness (AHR). These symptoms are a result of a range of processes, including contraction of airway smooth muscle, airway inflammation; IgE mediated allergic responses, exposure to pollutants and the stimulation of cholinergic and sensory nerves (Bateman et al. 2008). Allergic airway inflammation and respiratory viral infections are known to have complex interactions. There is evidence to show that respiratory viral infections can initiate, maintain and exacerbate allergic conditions in the respiratory tract of infected individuals. Conversely, immune responses biased towards Th2 can make the immune response ineffective in combating the infection.

T helper cells are classified as Th1 and Th2 sub-populations. Th1 responses are characterized by IFN-γ and promote cell-mediated immunity whereas IL-4, IL-5 and IL-13 are the hallmarks of Th2 responses. Th2 cells promote B cell proliferation, class switching and antibody production. Th1 and Th2 cytokines cause the immune response to polarize toward either Th1 or Th2, depending on the type of the pathogen. Th1 responses are more effective at getting rid of intracellular pathogens such as viruses whereas the Th2 responses are better at combating extracellular pathogens i.e. parasites.

1.5.1 Effect of viral infections on asthma

Two different hypotheses have been proposed to explain the effects of viral infections on allergic sensitizations; the hygiene hypothesis, which regards viral infection as an inhibitor of allergic sensitization and the alternative view that some viral infections can enhance allergic sensitization. There is evidence to support both theories.

The hygiene hypothesis states that repeated exposure to diverse common infections and environmental microbiota during childhood are strongly associated with healthy maturation of the immune system and prevent the development of asthma and allergies later in life. It was hypothesized that infections especially viral infections may induce specific responses that are biased towards a Th1 phenotype. Due to this Th1 bias, allergic reactions requiring Th2 responses occur less effectively (Gern and Busse 2002). This view is reinforced by the fact that populations that lived in environments with diverse microbiological flora were associated with low incidence of asthma whereas populations in environments with low microbiological diversity are associated with a higher incidence of asthma (Ege et al. 2011).

On the other hand, data from various studies show an association between viral infection in the respiratory tract in early life and subsequent childhood asthma. Most studies however, focus on acute bronchiolitis in infants caused by Respiratory Syncytial Virus (RSV). It has been debated whether viral infection increases the risk for asthma by damaging the developing airway and immune system or merely unmasks the genetic predisposition to asthma. Enhanced allergic sensitization after viral infection has been observed in mice. It was shown that IL-13 producing macrophages persisted in the lungs of mice

after they had recovered from viral infection and hence enhanced allergic sensitization (Kim, E. Y. et al. 2008a). Rhinovirus infection triggers exacerbation of asthma by inducing inflammation when the airway is already sensitized (Subrata et al. 2009). Infection causes the recruitment of APCs in high numbers and for long periods following pathogen clearance. Cells expressing CD11c display enhanced antigen presentation long after the resolution of an acute infection by viruses (Beyer et al. 2004). Such cells are long lasting suggesting that an enhanced mature APC compartment assists immunological responses on subsequent exposure to environmental allergens. Viral infection may also affect airway remodeling by up regulating matrix metalloproteinase MMP-9 in airway epithelial cells (Tacon et al. 2010) and induce matrix protein deposition on airway smooth muscle cells (Kuo et al. 2011).

1.5.2 Effect of asthma on influenza virus infections

Data from several *in vitro* and *in vivo* experiments have shown that there is an increased susceptibility to respiratory viral infections after airway allergic sensitization that occurs via two mechanisms: impaired innate and specific immune responses and up regulation of viral receptors on airway epithelium. The allergic immune response is biased toward Th2 polarity. Because effective control and elimination of viral infection requires a Th1 response, pre-existing Th2 bias may interfere with the immune response to viral infection (Hassantoufighi et al. 2007; Message et al. 2008). This bias towards a Th2 response is likely to lead to impairment of interferon production and delayed viral clearance in response to an influenza viral infection.

A recent study has described an up-regulation of both α2,3- and α2,6- linked sialic acid which are receptors for avian and human influenza viruses respectively on the epithelial cells of nasal polyps of allergic individuals (Suptawiwat et al. 2010). Tissue explants for nasal polyps were also more effective for replication of both avian and human influenza viruses than those from normal nasal mucosa. However, it is not clear whether the up regulation of sialic acid resulted from the chronic inflammatory process or was specific to the allergic reaction.

Epidemiological studies have shown that influenza and other respiratory viral infections are a frequent cause of hospitalization in patients with asthma (Mullooly et al. 2007; Miller et al. 2008). Hence it is clear that asthma exacerbation occurs in asthmatic individuals when they are infected with respiratory viruses. Virus-induced asthmatic exacerbations could be due to a combination of a few or all of the above-mentioned factors.

1.6 Cytokine storm in influenza infection

Cytokines (and chemokines) play an important role in the pathology associated with influenza virus infection. Lung epithelial cells are the principal targets for influenza A virus infection. These cells produce large amounts of virus, which can then infect alveolar macrophages (AMs) (Bender and Small 1992). Following infection, epithelial cells and AMs die by necrosis and apoptosis respectively (Fesq et al. 1994). Cell necrosis/apoptosis triggers the production of cytokines TNF-α, IL-1 and chemokines such as monocyte chemoattractant protein (MCP-1), regulated on activation, normal T cell

expressed and secreted (RANTES), MIP-1α/β, interferon induced protein (IP)-10 and IL-8 (Sprenger et al. 1996; Julkunen et al. 2000; Julkunen et al. 2001). Respiratory epithelial cells can up regulate these pro-inflammatory mediators following *in vitro* infection (Adachi et al. 1997; Chan et al. 2005). *In vivo*, it is likely that the initial release of inflammatory mediators by infected lung epithelium and AMs result in the extravasation of macrophages and neutrophils and then T cells, from the peripheral blood across the endo-epithelial barrier into the infected lung tissue within the first three days after influenza A virus infection (Ada and Jones 1986). This early inflammatory pathology can contribute to severe disease, especially with the highly pathogenic H5N1 viruses.

Although there is little direct evidence from the immunopathology caused by the 1918 pandemic virus, both this and the avian H5N1 viruses are believed to induce cytokine storms, characterized by dysregulated and exaggerated production of inflammatory cytokines which are in turn associated with massive pulmonary edema, primary and secondary pneumonias and alveolar hemorrhage with acute bronchopneumonia (Taubenberger et al. 1997). Chemokines are the main factors, which enable monocytes and T lymphocytes to migrate from the peripheral blood via the vascular endothelium into the site of inflammation. Reverse mutant viruses expressing the HA and NA of the 1918 influenza virus induced significantly higher levels of IFN-γ, TNF-α, MIP-2, MIP-1α, MCP-1, MIP-1β, MIP-3α, IL-1, IL-6, IL-12, IL-18 and G-CSF in the lungs of infected mice clearly indicating that elevated cytokine and chemokine levels were a hallmark of the human disease during the 1918 pandemic (Kobasa et al. 2004; Tumpey et al. 2005).

The roles of TNF-α in lung pathology have been well studied (Bruder et al. 2006) and high quantities of TNF-α can induce numerous clinical and pathological abnormalities, associated with acute inflammatory response in leukocytes and respiratory tract epithelium. Elevated levels of TNF-α have found to be correlated with severity of gross and histologic lung lesions in influenza infected mice (Peper and Van Campen 1995). Furthermore studies in which influenza infected mice were treated with blocking antibody to TNF-α showed reduced pulmonary cell infiltration and less severe pathology, associated with prolonged survival of the mice (Peper and Van Campen 1995; Hussell et al. 2001). These studies also show that neutralization of TNF-α has no deleterious effect on either lung viral loads or clearance of virus.

The roles of IFN-γ however, have not been so well studied. Although, IFN-γ is known to have a protective role in many viral infections including vaccinia, herpes simplex, cytomegalovirus and lymphocytic choriomeningitis virus (LCMV), multiple studies of influenza virus infection in mice lacking functional IFN-γ, demonstrate little requirement for this cytokine in efficient viral clearance (Baumgarth and Kelso 1996; Bot et al. 1998; Nguyen et al. 2000). While little attention has been paid to the possible effects of IFN-γ on influenza immunopathology, a study of influenza-infected mice receiving WT or IFN-$\gamma^{-/-}$ HA specific $CD8^{+}$ T cells showed that the presence of IFN-γ actually ameliorated the severity of inflammation and lung damage (Wiley et al. 2001).

The immunopathological effects of TNF-α and IFN-γ in influenza virus infections may also be indirectly mediated in individuals undergoing a secondary bacterial infection. This is particularly relevant, as several patients

infected with the highly pathogenic strains of influenza are known to develop and succumb to secondary bacterial pneumonia (Zhang et al. 1996).

1.7 Interferons

Interferons (IFNs) are cytokines that play key roles in the immune system, in the resistance of mammalian hosts to pathogens. They are glycoproteins made by the host cells in response to the presence of pathogens, to allow communication with the immune system to trigger the defenses to get rid of the pathogens. Interferons have been named after their ability to "interfere" with viral replication in host cells. They have been divided into three IFN classes, based on the type of receptors they signal through:

Type I IFNs:

These interferons bind to cell surface receptor complexes known as the IFN-α receptor (consisting of IFN-αR1 and IFN-αR2 chains). The type I interferons are IFN-α, IFN-β and IFN-ω. Type 1 interferon is secreted by all virus-infected cells.

Type II IFNs

These bind to the IFN-γR that consists of IFN-γR1 and IFN-γR2 chains. It consists of only one interferon i.e. IFN-γ. Also known as gamma interferon, this is secreted mainly by T cells and NK cells.

Type III IFNs

These signal through a receptor complex consisting of IL-10R2 (CRF2-4) and IFNLR1. Acceptance of this classification is less universal than that of type I and type II. This class consists of three IFN-l molecules called IFN-λ1, IFN-λ2 and IFN-λ3.

1.8 Interferon gamma

Interferon gamma (IFN-γ) is one of the master cytokines of the immune system with pleiotropic roles. Although interferon gamma was originally defined as an agent with direct antiviral activity (Wheelock 1965), the properties of IFN-γ include regulation of several aspects of the immune response, stimulation of bactericidal activity of phagocytes, stimulation of antigen presentation, effects on cell proliferation and apoptosis and the control of several genes whose functional significance is still unknown.

The principal cell types that produce IFN-γ are activated NK cells (Perussia 1991), activated T helper cells of the Th1 subset (Mosmann and Coffman 1989), and activated $CD8^+$ T cells of the Tc1 phenotype (Sad et al. 1995). In NK cells, IFN-γ production is stimulated by cytokines produced by macrophages like TNF-α and IL-12 and is auto stimulated by IFN-γ itself. In T cells however, the main inducer of IFN-γ is the cross-linking of the T cell receptor (TCR) complex.

Both human and mouse IFN-γ is encoded by a single gene copy, generating a single 1.2 kb mRNA species (Derynck et al. 1982) and a polypeptide of 166 residues including a cleaved hydrophobic signal of 23 residues (Rinderknecht et al. 1984). Biologically active IFN-γ is in the form of a non-covalent 34 kDa

homodimer (Fountoulakis et al. 1992) and its structure has been confirmed by X-ray analysis (Ealick et al. 1991). IFN-γ binds to its receptor on different cells and signals a downstream flurry of events, which include turning on of several genes, which may also be transcription factors.

IFN-γ binds to a specific cell surface receptor, which is ubiquitously but not uniformly present on all nucleated cells, although its expression is highest outside the lymphoid system (Valente et al. 1992; Farrar and Schreiber 1993). The IFN-γ–receptor consists of two subunits, the high affinity α chain (IFN-γR1) with ligand binding properties and the β chain (IFN-γR2), which is required for signaling. Each subunit is associated with a specific Janus Kinase (JAK); the IFNγ-R1 chain with JAK1 and the IFNγ-R2 chain with JAK2 (Igarashi et al. 1994). Signal transduction starts with an interaction of the IFN-γ homodimer with two IFN-γR1 chains, thereby inducing their dimerization. The association of IFN-γR2 with the IFN-γR1 complex leads to the transphosphorylation and reciprocal activation of the JAKs. Tyrosine phosphorylation of the IFN-γR1 on residue 440 provides a docking site for the SH2 domain of the latent STAT1 transcription factor. Docked STAT1 is phosphorylated in the C-terminus on tyrosine Y701, enabling a homodimer of tyrosine-phosphorylated STAT1 to form and dissociate from the receptor. This phosphorylated STAT1 homodimer translocates to the nucleus and initiates transcription of genes containing a Gamma activated sequence (GAS) (Decker and Kovarik 2000) in their promoter region. To a lesser extent, IFN-γ stimulation can activate an ISRE binding complex (Schroder et al. 2004). The importance of the JAK-STAT pathway in IFN-γ signaling is clearly evident because defects in anti-viral immunity observed in STAT-1 deficient mice,

grossly resembles the phenotypes of IFN-γ/IFNγR knockout mice (Durbin et al. 1996; Meraz et al. 1996). Moreover, enhanced susceptibility to viral and mycobacterial infections in humans is associated with STAT1 mutations as well as IFN-γR mutations (Dupuis et al. 2001; Picard and Casanova 2004).

The generation of mice lacking functional IFN-γ (Dalton et al. 1993) (IFN-$\gamma^{-/-}$) or IFN-γ receptor (Huang et al. 1993)(IFN-$\gamma R^{-/-}$) has permitted the assessment of the role of this cytokine during different bacterial and viral infections. Both IFN-$\gamma^{-/-}$ and IFN-$\gamma R1^{-/-}$ mice showed many subtle failures in immune function that became explicit when the mice were challenged with infectious organisms. Increased susceptibility to many intracellular pathogens such as Leishmania major (Wang, Z. E. et al. 1994), Listeria monocytogenes (Huang et al. 1993), mycobacteria (Cooper et al. 1993) and different viruses e.g. vaccinia virus (Muller et al. 1994) but not to the influenza virus (Graham et al. 1993) have been reported. Furthermore, over-expression of IFN-γ in transgenic mice under the control of various tissue-specific promoters generates sites of inflammation with subsequent severe tissue destruction (Young and Hardy 1995).

In humans, complete IFN-γR1 deficiency is associated with frequent infection and ultimately death from the poorly virulent mycobacterium- Bacille Calmette-Guerin (Jouanguy et al. 1996). Patients with partial IFN-γR deficiency have a similar but milder clinical presentation (Jouanguy et al. 1997). The inability to secrete IFN-γ or the development of autoantibodies to IFN-γ, led to the death of a patient by overwhelming mycobacterial infection (Doffinger et al. 2004). More subtle immune defects have also been observed

in patients unable to secrete IFN-γ, these patients have poor neutrophil trafficking and weak NK cell activation (Davies et al. 1982).

1.8.1 Immunomodulatory roles of IFN-γ on $CD4^+$ T cell responses

IFN-γ is known to play an important role in immune regulation by modulating T cell responses. Such a role has been studied in several models and several functions of IFN-γ have thus been identified. Addition of IFN-γ to $CD4^+$ T cells *in vitro* increases the number of $Foxp3^+$ regulatory T (T_{reg}) cells (Wang, Z. et al. 2006). In addition, the numbers and function of T_{reg} cells is reduced in IFN-$\gamma^{-/-}$ mice in a mouse model of experimental autoimmune encephalomyelitis (EAE) leading to increased severity of disease (Wang, Z. et al. 2006). Also, lowered T_{reg} function in IFN-$\gamma R^{-/-}$ mice contributes to greater disease severity in the collagen-induced arthritis model (Kelchtermans et al. 2005). In addition, IFN-γ suppresses the development of the IL-17 producing effector T cells from naïve CD4+ precursor cells in both EAE (Langrish et al. 2005) and type II collagen induced arthritis (Murphy, C. A. et al. 2003) models. Infection of IFN-$\gamma^{-/-}$ mice with Bacillus Calmette-Guerin results in an exacerbated inflammatory response, which has been attributed to increased numbers of Th17 cells produced due to the absence of IFN-γ (Cruz et al. 2006).

Several recent studies speculate on the role of IFN-γ in the homeostatic control of T cells. A progressive expansion of $CD4^+$ T cells was seen in IFN-$\gamma^{-/-}$ mice infected with mycobacteria and this expansion was not due to persistence of bacteria but due to a role for inducible NO synthase (iNOS) in apoptosis of activated $CD4^+$ T cells during BCG infection (Dalton et al. 2000). Aberrant

contraction of antigen specific CD4+ T cells has been observed in the absence of IFN-γ in Listeria infection (Haring and Harty 2006) and also during immune responses in EAE (Chu et al. 2000). The mechanism by which IFN-γ regulates T cell expansion, survival and contraction are unclear and several studies have attempted to shed light on this. One such study by Refaeli et al shows that IFN-γ is required in Activation Induced Cell Death of CD4+ T cells downstream of the ligation of Fas by the activation of the caspase-8-dependent apoptosis (Refaeli et al. 2002). Another study in a mycobacterial infection shows that IFN-γ promotes apoptosis in CD4+ T cells by inducing components of both the intracellular and extracellular apoptotic machinery (Li, X. et al. 2007). Th2 cells more than Th1 cells are also known to undergo autophagy mediated cell death upon growth factor withdrawal (Li, C. et al. 2006). There is some evidence that IFN-γ may induce autophagy-mediated cell death in CD4+ T cells (Feng et al. 2008).

1.8.2 Immunomodulatory roles of IFN-γ on $CD8^+$ T cell responses

Studies have focused on the immunomodulatory roles of IFN-γ in the $CD8^+$ T cell response to systemic infections such as LCMV, CMV, VSV and *L.monocytogenes* (Badovinac et al. 2004), ((Badovinac et al. 2000; Christensen et al. 2004; Tewari et al. 2007; Andrews et al. 2008). Mice lacking IFN-γ or the IFN-γ-receptor exhibit impaired apoptosis or delayed contraction of activated antigen-specific CD8+ T cells in the spleen during immune responses to Listeria or LCMV infections (Badovinac et al. 2002). The contraction of $CD8^+$ T cells in a Listeria infection is also known to be

controlled by early inflammation and IFN-γ production (Badovinac et al. 2004). The responsiveness of antigen specific $CD8^+$ T cells to IFN-γ correlated with the expression of IFN-γR2 but not with that of IFN-γR1 (Haring et al. 2005). Activation induced cell death was induced by super antigens in human $CD8^+$ T cells in a fratricide dependent manner (Gorak-Stolinska et al. 2001; Gorak-Stolinska et al. 2002) and is dependent on Fas and granzyme B (Gorak-Stolinska et al. 2001).

Thus far, however, no role for IFN-γ in regulating the responses after an acute localized infection has been reported. Although, IFN-γ was found to play a critical role in the contraction of $CD8^+$ T cells following LCMV and *L. monocytogenes* infection (Badovinac et al. 2000; Tewari et al. 2007), this process was reported to be independent of IFN-γ in VSV and CMV infections (Christensen et al. 2004; Andrews et al. 2008). However it remains to be determined whether IFN-γ is involved in mediating $CD8^+$ T cell contraction during a localized infection like influenza.

1.9 Interferon gamma signaling in influenza

The earliest reports show that mice lacking IFN-γ did not display a reduced ability to recover from primary infection with influenza and mounted cytotoxic T lymphocyte (CTL) activity comparable to that of their wild type counterparts in a killing assay (Graham et al. 1993). However, the absence of IFN-γ led to increased production of influenza-specific IgG1, IL-4 and IL-5 as compared to WT mice. Administration of anti-IFN-γ antibodies to beta-2-microglobulin mice showed delayed viral clearance but did not switch the

response to a Th2 phenotype (Sarawar et al. 1994). Furthermore, CTL clones from IFN-$\gamma^{-/-}$ mice, adoptively transferred into wild-type recipients previously challenged with influenza virus mediated effective recovery from primary infection (Wiley et al. 2001).

There are conflicting reports about the roles of $CD8^+$ T cell derived IFN-γ in mediating influenza-virus-associated immunopathology. While $CD8^+$ T cell production of IFN-γ enhanced lung pathology in one study (Moskophidis and Kioussis 1998), it ameliorated damage in another system (Wiley et al. 2001). Reduced survival rates in the IFN-$\gamma^{-/-}$ mice were observed during recall responses to heterologous strains of the influenza virus (Bot et al. 1998), although the reason for this was unclear. In another study it is reported that a lack of IFN-γ did not impair cross-reactive virus-specific $CD8^+$ immune responses to lethal infection with influenza virus (Nguyen et al. 2000). Hence there is no clear consensus on the role of IFN-γ in protective role after a heterologous re-challenge.

It was demonstrated that IFN-γ signaling differentially regulates both antigen-specific CTL homeostasis in secondary lymphoid organs and trafficking to a site of virus infection (Turner et al. 2007). Although, IFN-γ facilitates adaptive immunity against influenza, it also inhibits the initial bacterial clearance from the lung by alveolar macrophages during a secondary bacterial infection (Belz et al. 1998; Sun, K. and Metzger 2008). Although there is some evidence that antigen-specific $CD8^+$ T cells are destroyed in the liver during the control and resolution phases of an influenza infection (Belz et al. 1998), the mechanism by which this happens is not known. Though it has been reported that CD27 signaling directs the IL-2 production that is essential to sustain the survival of

virus-specific CTLs in non-lymphoid tissue (Peperzak et al. 2010), the mechanism by which these virus-specific $CD8^+$ T cells die after the infection is resolved is far from clear.

IFN-γ orchestrates a remarkable range of distinct cellular programs. Although some of these roles have been studied in influenza infection, the role played by IFN-γ in programs of immune regulation is evidently of great interest but still remain obscure. In this study, we attempt to study the role of IFN-γ in a mouse model of influenza and also to identify the mechanisms by which IFN-γ modulates the T cell responses in a respiratory viral infection. We present evidence that IFN-γ has direct effects on $CD8^+$ T cell homeostasis and plays a key role in mediating T cell death.

1.10 Specific aims of this study

While some studies have examined briefly, the role of IFN-γ in an influenza infection, there is no data so far examining the roles of IFN-γ in regulating the immune responses to influenza. The essential immunomodulatory role of such an important cytokine in a respiratory infection where it is made in large quantities remains poorly understood. Further there is no consensus about the role played by IFN-γ in the heterosubtypic immunity against a re-challenge with influenza virus. In the present study we sought to examine such roles of IFN-γ in influenza infection and studied whether this could influence rational vaccine design that is able to provide optimal $CD8^+$ T cell mediated immunity.

Specific Aims

1. Establish a mouse model of influenza and broadly characterize the immune response.
2. Characterize and compare the antigen-specific $CD8^+$ T cell response in the presence and absence of IFN-γ signaling.
3. Characterize the mechanisms by which IFN-γ regulates antigen-specific $CD8^+$ T cell responses to influenza.
4. Establish a model for heterologous influenza re-challenge
5. Characterize the roles played by IFN-γ signaling during a recall response to influenza

Chapter 2: Materials and Methods

2.1 Buffers and Media

2.1.1 PBS Buffer

PBS buffer, ultrapure grade was commercially obtained from 1st Base (Singapore) as a 10X stock. The 10X stock consists of 137mM NaCl, 2.7mM KCl and 10mM Phosphate buffer. The buffer was diluted to 1X with 9 parts of distilled water. The pH of the buffer was then adjusted to 7.4 with 1M HCl.

2.1.2 MACS Buffer

MACS Buffer consists of 1X sterile PBS supplemented with 2% FCS and 5mM EDTA. The pH of the buffer was adjusted to 7.4 with 1M HCl.

2.1.3 FACS Buffer

FACS buffer consists of 1X PBS supplemented with 1% FCS (Biowest, France; Sciencewerke, Singapore) and 5mM EDTA. Sodium Azide (0.05%) is added as a preservative to permit use and storage under non-sterile conditions. The pH of the buffer is adjusted to 7.2-7.4 with 1M HCl.

Note: Although the components of the FACS and MACS buffer are similar, FACS buffer cannot be used in place of MACS buffer to isolate cells for culture because it contains sodium azide, which may inhibit certain metabolic functions of the cells.

2.1.4 Permeabilization Buffer for Intracellular staining

Cell permeabilization buffer consists of 0.1% BSA, 0.1% Saponin and 0.1% sodium azide. The pH of the buffer was adjusted to 7.4 with 1M HCl. Alternatively, commercially available fixation/permeablization buffer and permeabilization buffers were purchased from eBioscience, (eBioscience, USA; ImmunoCell, Singapore).

2.1.5 Red Blood Cell lysis buffer

RBC lysis buffer was made as a 10X stock consisting of Ammonium Chloride (8.3g), Sodium Bicarbonate (0.84g) and EDTA (0.03g) in water. The pH of the buffer was adjusted to 7.4 with 1M HCl. The stock was diluted with water to a 1X working solution.

2.1.6 Liberase Enzyme Blend for lung digestion

Liberase TL Research Grade (low thermolysin concentration) was obtained from Roche (Roche Applied Science, Switzerland; Roche diagnostics Asia-pacific, Singapore) and dissolved in plain RMI-1640 to obtain a concentration of 2mg/ml, which corresponds to a collagenase activity of 0.52 Wunsch units/ml. This forms a 10X Liberase stock solution, which was stored in aliquots at -30^0C. For digestion of tissues, the 10X Liberase stock solution was diluted 10-fold with plain RPMI-1640 and supplemented with 1% v/v FCS, which is added to preserve the viability of the cells during digestion.

2.1.7 Buffers for ELISA

Wash buffer for ELISA

Wash buffer for ELISA consisted of 1X PBS with 0.5% v/v Tween-20. The pH of the buffer was adjusted to 7.4 with 1M HCl.

Blocking Buffer for ELISA

Blocking buffer for ELISA consisted of 1X PBS with 1% w/v BSA.

2.1.8 Alsever's solution for storage of Guinea Pig RBCs

Alsever's solution was made with the following components:

a) Citric Acid 55mg

b) Sodium Citrate 800mg

c) Sodium Chloride 420mg

d) D-Glucose 205mg

The components were dissolved in distilled water, and the pH was adjusted to 6.1 with 1M HCl and made up to 100ml.

2.1.9 Complete RPMI Medium for cell culture

Complete RPMI was prepared using RPMI-1640 with L-Glutamine (Gibco, Invitrogen, Singapore) supplemented with the following:

a) FCS (Biowest, France; Sciencewerke, Singapore),
10% v/v
(heat inactivated for 30 mins at 55^0C)

b) Non-essential amino acids (Sigma-Aldrich, Singapore) 1X
(from a 100X stock)

c) Sodium Pyruvate (Sigma-Aldrich, Singapore) 1mM

d) Beta-mercaptoethanol (Sigma-Aldrich, Singapore) 50uM

e) Penicillin (100IU/ml) and Streptomycin (0.1mg/ml) 1X (from a 10X stock) (Sigma-Aldrich, Singapore)

2.1.10 Complete DMEM for cell culture

Complete DMEM was prepared using Dulbecco's Modified Eagle Medium with L-Glutamine and 4.5g/L D-glucose (Gibco, Invitrogen, Singapore) and supplemented with the same components as complete RPMI.

2.1.11 Plain DMEM at 2X concentration

DMEM with L-Glutamine and 4.5g/L D-Glucose in powdered form was purchased from Gibco and dissolved in half the recommended volume of sterile water. 3.7g/L of Sodium bicarbonate was added. The pH of the solution was adjusted to 7.4 with 1M HCl and supplemented with 2% v/v Non-essential amino acids (Sigma-Aldrich, Singapore), as well as 200IL/ml Penicillin and 0.2mg/ml Streptomycin (Sigma-Aldrich, Singapore) before sterile filtration through a 0.22micron filter (Nalgene, USA; Fisher Scientific, Singapore)

2.2 Mice

C57BL/6 mice (8-10 weeks old) were obtained from National University of Singapore (NUS) CARE. IFN-$\gamma^{-/-}$ and IFN-$\gamma R^{-/-}$ mice were purchased from Jackson Laboratory (Bar Harbor, ME, USA). OT-1 mice were obtained from Charles River Laboratories (France). All mice were maintained under specific pathogen-free conditions within the National University of Singapore's animal holding unit. C57BL/6 mice used were 8-10 weeks old. OT-1 and OT1 X IFN-$\gamma^{-/-}$ mice were 7-10 weeks old. Mice were age and sex-matched for each experiment. All experiments were performed in accordance with guidelines of the National Advisory Committee for Laboratory Animal Research

(NACLAR), Singapore. The Institutional Animal Care and Use Committee (IACUC) of the National University of Singapore approved the protocols (Protocol numbers 137/08 and 087/10). All mice were maintained under pathogen-free conditions in the satellite animal housing unit and were transferred to the ABSL2 facility for experiments involving influenza infections.

2.2.1 Infection of mice

Mice were anesthetized by intraperitoneal injection of Ketamine, 100mg/kg (Parnell Laboratories, Australia) and Medetomidine, 15mg/kg (Pfizer, NewZealand). Intranasal challenge of mice with influenza was carried out with the required dose of the virus in 20µl of PBS. Atipamezole (Pfizer, Australia), 5mg/kg was administered by intraperitoneal injection to reverse the effects of the anesthetic. All the experiments in this study were performed using C57BL/6 mice.

2.3 Influenza virus

2.3.1 Culture of influenza virus in embryonated chicken eggs

1. 9-10 day old embryonated chicken eggs were obtained from Bestar, Singapore or Chew's Poultry Farm, Singapore.
2. The eggs were candled to mark the location of the air cell and the large blood vessels.
3. A 21-gauge needle was used to puncture the eggshell just below the air cell, taking care to avoid any large blood vessels.

4. A fine needle was used to inject the influenza virus stock, diluted 100 times in sterile PBS (dilution of lower than 2HAU), into the allantoic cavity through the hole.
5. The hole was then sealed with melted max in order to maintain sterility.
6. The eggs were then incubated in a 37^0C incubator for 2.5 days and observed regularly to check the viability of the embryo.
7. After 2.5 days, the eggs were then incubated at 4^0C for 4 hours to sacrifice the embryos.
8. The shell was then cut open along the air cell and the allantoic fluid collected.
9. The allantoic fluid was clarified by centrifugation at 3000g for 20 min and then sterile filtered using 2micron filters.
10. The virus was then stored at -80^0C as small aliquots.

2.3.2 Culture of influenza virus in MDCK cells

1. Madine Darby Canine Kidney (MDCK) cells (ATCC CCL-34, ATCC, USA) were grown to confluence in T75 tissue culture flasks (NUNC, USA) using complete DMEM.
2. On the day of infection, the cells were washed with sterile PBS to remove any traces of serum, which may inhibit viral growth.
3. 10ml of plain DMEM supplemented with 4mg/ml of TPCK treated trypsin (Pierce, USA) was added to the flask followed by the virus stock.

4. The cells were incubated at 37^0C with 5% CO_2 and visualized under the microscope daily to check for signs of cytopathological effects.
5. When more than 90% of the MDCK cells exhibited cytopathological effects, the media was harvested and centrifuged at 3000g at 4^0C for 5 min to pellet the floating cells and other large debris.
6. The clear supernatant was decanted and frozen at -80^0C.

2.3.3 Titration of virus by Plaque assay

1. MDCK cells were seeded at 3-3.5 × 10^5 cells/well in a 24-well plate and cultured in complete DMEM until fully confluent and the spaces between cells barely distinguishable. This typically takes 24h. The cells were not grown for longer as this would lead to multiple layers of MDCK cells.
2. Immediately before infection, the medium was aspirated and the cells washed once with PBS to remove any traces of serum, which affects the ability of the virus to bind to the cells.
3. The influenza virus (viral stock or lung homogenate) was serially diluted 10-fold in plain DMEM and introduced to the MDCK cells and incubated for 1 hour at 37^0C to allow the virus to adsorb onto the cells. The volume of the inoculum was kept small, typically 250µl per well so as to ensure maximal adsorption of the virus onto the cells.
4. During the incubation period, a 2% agarose solution in sterile water was prepared by microwaving the agarose solution until it was completely molten. The agarose solution was cooled and kept in the molten state by incubating in a water bath at 47^0C.

5. At the same time, 2X DMEM was warmed to 37^0C and TPCK Trypsin was added to a final concentration of 4µg/ml.
6. After 1-hour incubation the molten 2% agarose was mixed with an equal volume of 2X DMEM to obtain a 1X DMEM agarose solution. This solution was kept in the molten state inside the BSC by placing it in a beaker of water taken from the 47^0C water bath.
7. The virus inoculum was quickly removed starting from the highest dilution to minimize any carry-over effect and gently overlaid with the DMEM-agarose solution. The agarose overlay was left to cool inside the BSC until it hardened before incubating for 3 days at 37^0C to allow plaques to form.
8. To visualize plaques on the third day, 0.5 to 1ml of PBS was added on top of the agarose layer to facilitate removal of the agarose overlay and a bent needle was used to gently dig out the agarose layer above the cells. Care was taken to avoid scratching the bottom of the plate.
9. The plaques were visualized by adding 0.2ml of 0.5% aqueous crystal violet and incubating for at least 5 minutes. Excess stain was removed by washing the plate under running tap water.
10. The plaques were then counted to calculate the total titer/ plaque forming units of the viral stock or the lung isolates.

2.3.4 RBC Hemagglutination assay

1. Fresh guinea pig Red Blood Cells (RBCs) were obtained from NUS CARE.
2. The RBCs were washed twice in Alsever's solution and stored for up to 2 weeks at 4^0C.

3. For the hemagglutination assay, the RBCs in Alsever's solution were washed twice in PBS and pelleted.
4. A 1% RBC solution was obtained by adding the required volume of the pellet to a 1X PBS solution.
5. The influenza virus was serially diluted two-fold in 25µl volume across a 96-well V bottomed plate.
6. 25µl of the 1% RBC solution was then added to each well using a multichannel pipette and left for 2h.
7. Viral titer was determined by taking the reciprocal of the last virus dilution that exhibited hemagglutination activity (e.g. for a dilution of 512-fold, the titer would be 512HA/25µl, which is equivalent to 20.48HA/µl).

2.3.5 Hemagglutination Inhibition assay

1. Mouse serum was treated with receptor destroying enzyme (RDE) II (Denka Seiken, Japan; AllEights, Singapore) to remove non-specific hemagglutination inhibiting activity by adding 4 parts of RDE to 1 part of serum and incubating at 37^0C overnight.
2. After digestion, the RDE was destroyed by addition of an equal volume (5 parts) of 1.6% sodium citrate and incubating at 56^oC for half hour. This results in a final 10-fold dilution of serum.
3. One part of neat guinea pig RBC pellet was added to 10 parts of RDE treated serum and incubated for a further half hour at room temperature to remove any non-specific binding of RBCs to the serum. The RBCs

were spun down and the supernatant containing the serum was removed. This does not cause further dilution, as the RBCs do not add significantly to the volume of the serum.

4. Serial 2-fold dilutions of the serum were made in 96-well U-bottom plates at 25µl per well following which 25µl of influenza virus containing 4 HA units were added. The plate was incubated for half an hour to allow the antibodies to bind to the virus.
5. Finally, 50µl of 1% guinea pig RBC were added and the HAI titer was determined 2 hours later, defined as the reciprocal of the maximum dilution of serum that resulted in inhibition of virus hemagglutination activity.

2.4 Cell Isolation

2.4.1 Isolation of $CD8^+$ T cells from spleens and lymph nodes of naïve mice

1. Spleens and lymph nodes were harvested from euthanized mice and mechanically disrupted by pushing through a 61µm cell strainer (Fisher Scientific, Singapore) to obtain a single cell suspension.
2. Single cell suspensions were then washed once with MACS buffer and then layered on Ficoll-Paque (GE Healthcare, Scimed, Singapore) and centrifuged at 600g for 20 min at room temperature.
3. Cells accumulating at the interface were collected, washed twice with MACS buffer and counted.
4. The cells were pelleted and the supernatant decanted to remove as much liquid as possible.

5. The cell pellet so obtained was resuspended and then incubated with anti-CD8α conjugated MACS beads (Miltenyi Biotec, Singapore) at a concentration of 4μl per million cells.
6. The cells were incubated at 4^0C in the dark for 30 min with occasional flicking of the tube to prevent the cells from settling down.
7. The cell pellet was washed with MACS buffer and then re-suspended in 1ml of MACS buffer.
8. The re-suspended cells were then loaded on a pre-equilibrated LS MACS column (Miltenyi Biotec, Singapore).
9. The MACS column was then washed 3-4 times with 3ml of MACS buffer each to remove any unbound or loosely bound non-$CD8^+$ T cells.
10. The bound $CD8^+$ T cells were then eluted with 5ml of complete RPMI medium.

2.4.2 CFSE Labeling of $CD8^+$ T cells and adoptive transfer

1. The harvested cells were washed in sterile PBS twice and re-suspended in warm (~37^0C) PBS at a concentration of 20 million cells/ml for CFSE labeling.
2. The CFSE (Invitrogen, Singapore) stock was diluted 5 times to a final concentration of 10mM.
3. The cells were mixed with the CFSE solution at a 1:1 ratio, making the final concentration of cells at 10 million cells/ml and concentration of CFSE 5mM.
4. The cells were incubated at 37^0C in the dark for 15 minutes.

5. The reaction was stopped by quenching the cells with complete RPMI and incubating on ice for 5 min.
6. The cells were then centrifuged at 600g for 5min, washed twice with PBS and re-suspended in PBS at the required concentration.
7. Recipient mice were restrained using a mouse restrainer after application of lidocaine on the tails and sufficient heating using a heat lamp for 2-4 min, until the tail veins become visible.
8. The required cells were then injecetd into the mouse through the tail vein.

2.4.3 Isolation of T cells from the Broncho Alveolar Lavage fluid of infected mice

1. Mice were sacrificed using carbon dioxide asphyxiation.
2. BAL samples were collected by 3 x 0.7ml instillations of PBS into the trachea of cannulated mice.
3. RBCs were lysed using RBC lysis buffer and incubated for 2-3 min and then quenched with MACS buffer.
4. The cells were then centrifuged at 600g for 5 min and the cell pellet stained with appropriate antibodies for Flow Cytometry.

2.4.4 Isolation of T cells from the lungs of infected mice

1. Lungs were harvested from euthanized mice and excised into small pieces in 0.5mg/ml Liberase enzyme blend (Roche Diagnostics, Singapore) and digested for 45 min at 37^0C. The suspension was homogenized using a Pasteur pipette after 20 min digestion.

2. The digested lungs were physically disrupted into a single cell suspension by passing through a 61mm-cell strainer (Fisher Scientific, Singapore).
3. Single cell suspensions were washed with FACS/MACS buffer twice.
4. The washed cell suspensions were then layered on Ficoll-Paque (GE Healthcare, Scimed, Singapore) and centrifuged at 600g for 20 min at room temperature.
5. Cells accumulating at the interface were collected, washed twice with MACS buffer, suspended in 5ml of MACS buffer and counted.
6. The cells were then used for further staining with antibodies for flow cytometry or for *in vitro* cell culture.

2.4.5 Isolation of Lung Dendritic cells (DCs)

1. Lungs were finely excised using scissors in 1 × Liberase enzyme blend supplemented with 1% v/v FCS to preserve the viability of DCs and incubated at 37^0C for 20 min. The partially digested lung tissue was then re-suspended with a Pasteur pipette to break it up further and incubated for another 20 min.
2. The resulting digested cells were then pushed through a 61μm cell strainer (Fisher Scientific, Singapore) to obtain a single cell suspension. The cells were washed twice in MACS buffer to remove any traces of Liberase.
3. After the second wash, the cell pellet was raked vigorously and re-suspended in 3ml of OPTIPREP (g=1.064g/ml) (Sigma-Aldrich, Singapore) following which 2ml of FCS was gently overlaid on top of

the OPTIPREP cell solution. The cells were spun at 1700g for 10 min at 4^0C with brakes and acceleration set to zero.

4. The low-density cells that accumulated at the interface between OPTIPREP and FCS were harvested and transferred into a fresh tube and washed twice with MACS buffer to remove any OPTIPREP present in the solution. The cell pellet was raked to re-suspend cells.
5. Fc block (2.4G2) was added at 0.2µg/million cells and incubated for 10 min at 4^0C. This is to increase the purity of the cells isolated and remove contaminating B-cells, which can otherwise non-specifically bind to the MACS beads via the Fc receptor.
6. Anti-CD11c MACS beads were added to the cells at a volume of 10µl per 10 million cells with a minimum of 10µl of beads being used if cell numbers were below 10 million. The mixture was incubated at 4^0C for 10 min and the cells washed by addition of 3ml of MACS buffer and centrifuged at 350g to pellet the cells. As much of the supernatant was decanted as possible and the cell pellet resuspended in 1ml of MACS buffer before being placed in a LS MACS column that has been pre-equilibrated with MACS buffer.
7. Once all the cells have entered, the column was washed with 3ml of MACS buffer for 4 times before eluting with 4ml of complete RPMI.

Note: CD11c is also expressed by lung macrophages, thus for isolating $CD11c^+$ cells by positive selection, approximately 50% of the cells will be macrophages. Nonetheless, this technique is useful for the enrichment of lung DCs for *in vitro* experiments and facilitates analysis by removing a large number of irrelevant cells from the preparation.

2.5 Flow cytometry and cell sorting

2.5.1 Staining of cell surface markers for flow cytometry

1. Single cell suspensions were transferred to flow cytometry tubes. About 1ml of FACS buffer was added to each of the tubes
2. The cells were then centrifuged at 600g for 5 min to pellet down the cells.
3. After centrifugation, the supernatant was discarded and the tubes were blotted on tissue paper to reduce the amount of liquid left with the cell pellet. The tubes were then vigorously raked on the tube racks to re-suspend the cell pellet.
4. Fc block (2.4G2) was added at 0.2µg per million cells and incubated for 5 min at 4^0C to prevent non-specific binding of antibodies via Fc receptors.
5. Antibodies directly conjugated to fluorophores were added to the cells at 0.02µg per million cells and incubated in the dark at 4^0C for 30 min.
6. After incubation, the cells were washed twice with 1ml of FACS buffer to remove unbound antibodies.
7. After the second wash, the cell pellet was re-suspended and fixed with 350ml of 1% Paraformaldehyde (PFA). To prevent formation of cell clumps during fixing, the cell pellet was well disrupted by raking several times on the tube racks and then vortexed at 3000 rpm while simultaneously adding 1% PFA.

2.5.2 Intracellular staining for flow cytometry

1. Intracellular staining of antigens was performed after staining of cell surface markers. Cells were stained following the protocol above and washed with FACS buffer.
2. The cell pellet was re-suspended and 1ml of Fix-Perm solution (eBioscience, USA; ImmunoCell, Singapore) added while constantly vortexing the samples. The samples were then kept in the dark for 30 min.
3. After 30 min, 1 ml of permeabilization buffer (eBioscience, USA; ImmunoCell, Singapore) was added and the tubes centrifuged at 600g for 5 min. The cells were then washed with permeabilization buffer and centrifuged 600g for 5 min to obtain a cell pellet and the supernatant discarded before raking the tube to re-suspend the cell pellet.
4. Antibodies directly conjugated to fluorophores were added to the cells at 0.02µg per million cells and incubated in the dark at 4^{o}C for 30mins, while for intra nuclear transcription factors, the incubation was done for 1h at 4^{o}C.
5. After incubation, cells were washed twice with at least 1ml of permeablization buffer to remove unbound antibodies. Cells were finally re-suspended in 350µl of FACS buffer for analysis.

Intracellular Cytokine Staining

For intracellular staining of cytokines in cells, synthesis of cytokines was stimulated by addition of the appropriate stimulus. Cytokine secretion from the cell was blocked by the addition of Brefeldin A (BD Biosciences,

Singapore) and Golgi stop (BD Biosciences, Singapore) containing monensin to the culture medium. Both Brefeldin A and Golgi stop was added at 1µl per 1ml of culture medium. After 4-6 hours, cells were harvested, transferred into FACS tubes before proceeding for surface staining of markers, followed by intracellular staining for cytokines.

2.5.3 Sorting of naïve $CD8^+$ T cells by flow cytometry

1. Spleen and lymph node cells were enriched for T cells using Ficoll-Paque as described earlier. The cells accumulating at the Ficoll-Paque and MACS buffer interface were collected, counted and then spun down in sterile FACs tubes. Where single stains were required for multi-colored cell sorting, small amount of cells were taken for single stains at this point.
2. The concentration of the cells was adjusted to approximately 50 million cells/ml using MACS buffer.
3. Fc Block (2.4G2) was added at 0.2µg per million cells and incubated for 5 mins at 4^oC to prevent non-specific binding of antibodies to Fc receptors. Antibodies directly conjugated to fluorophores (B220, CD8, CD62L and CD44) were added to the cells at 0.02µg per million cells and incubated in the dark at 4^oC for 30 min.
4. After incubation, cells were washed once with 2 to 3ml of MACS buffer. Cells were then re-suspended in 2 ml of MACS buffer and passed through a 61µm strainer to filter out cell clumps or any tissue pieces, which may clog the cell sorter.
5. The filtered cells were then spun down once more to obtain a cell pellet. Cells were finally resuspended to a concentration of between

20-50 million cells/ml and NP_{366}^{+} $CD8^{+}$ T cells were sorted using the MOFLO (Beckman Coulter, USA).

6. Naive $CD8^{+}$ T cells were collected in sterile FACS tubes containing complete RPMI or neat FCS.

2.5.4 Sorting of flu-specific lung NP_{366}^{+} $CD8^{+}$ T cells by flow cytometry

1. Lung cells were enriched for T cells using Ficoll-Paque as described earlier. The cells accumulating at the Ficoll-Paque and MACS buffer interface were collected, counted and then pelleted in sterile FACs tubes.
2. The concentration of the cells was adjusted to approximately 50 million cells/ml using MACS buffer. Where single stains were required for multi-colored cell sorting, small amount of cells were taken for single stains at this point.
3. Fc Block (2.4G2) was added at 0.2µg per million cells and incubated for 5 min at 4°C to prevent non-specific binding of antibodies to Fc receptors. Antibodies directly conjugated to fluorophores (CD11c, Gr1, CD8) were added to the cells at 0.02µg per million cells. NP_{366} pentamer was added to the cells at 10µl/5 million cells and incubated in the dark at 4°C for 30min to 1 hour.
4. After incubation, cells were washed once with 2 to 3ml of MACS buffer. Cells were then re-suspended in 2 ml of MACS buffer and passed through a 61µm strainer to filter out cell clumps or any tissue pieces, which may clog the cell sorter.
5. The filtered cells were then spun down once more to obtain a cell pellet. Cells were finally re-suspended to a concentration of between

20-50 million cells/ml and NP_{366}^{+} $CD8^{+}$ T cells were sorted using the MOFLO (Beckman Coulter, USA).

6. NP_{366}^{+} $CD8^{+}$ T cells were collected in sterile FACS tubes containing complete RPMI or neat FCS.

2.5.4 List of Antibodies used

Primary Antibodies

Target	Host	Clone	Conjugation	Source
B220	Rat	RA3-6B2	FITC	BD Biosciences, Singapore
CCR7	Rat	3B12	Biotin	eBioscience, USA, ImmunoCell, Singapore
CD3e	Hamster	500A2	eFluor450	eBioscience, USA, ImmunoCell, Singapore
	Rat	17A2	APC	eBioscience, USA, ImmunoCell, Singapore
CD4	Rat	RM4-5	PB	BD Biosciences, Singapore
	Rat	RM4-5	PE	BD Biosciences, Singapore
	Rat	RM4-5	APC	eBioscience, USA, ImmunoCell, Singapore
CD8	Rat	53-6.7	PB	BD Biosciences, Singapore
	Rat	53-6.7	PE	BD Biosciences, Singapore
	Rat	53-6.7	PE-Cy7	BD Biosciences, Singapore
CD11b	Rat	M1/70	PE	BD Biosciences, Singapore
	Rat	M1/70	PE-Cy7	eBioscience, USA, ImmunoCell, Singapore

	Rat	M1/70	APC	BD Biosciences, Singapore
CD11c	Hamster	N418	FITC	BD Biosciences, Singapore
	Hamster	HL3	PE	BD Biosciences, Singapore
	Hamster	N418	PerCP Cy5.5	eBioscience, USA, ImmunoCell, Singapore
	Hamster	N418	AF647	Biolegend, USA; Genomax Technologies, Singapore
CD16/32	Rat	2.4G2	None	Biolegend, USA; Genomax Technologies, Singapore
CD19	Rat	1D3	PE	BD Biosciences, Singapore
CD25	Rat	PC61	PCP/Cy5.5	BD Biosciences, Singapore
CD40	Rat	3/23	FITC	BD Biosciences, Singapore
CD44	Rat	IM7	APC	BD Biosciences, Singapore
CD62L	Rat	MEL-14	FITC	BD Biosciences, Singapore
CD69	Rat	H1.2F3	FITC	eBioscience, USA, ImmunoCell, Singapore
CD70	Rat	FR70	PE	eBioscience, USA, ImmunoCell, Singapore
CD80	Rat	16-10A1	FITC	BD Biosciences, Singapore
CD86	Rat	GL1	FITC	BD Biosciences, Singapore
CD103	Rat	2E7	PE	eBioscience, USA, ImmunoCell, Singapore
	Rat	2E7	APC	eBioscience, USA, ImmunoCell, Singapore
CD107α	Rat	eBio1D4B	AF488	eBioscience, USA, ImmunoCell, Singapore

CD122	Rat	TM-b1	FITC	Biolegend, USA; Genomax Technologies, Singapore
CD127	Rat	A7R34	BV421	Biolegend, USA; Genomax Technologies, Singapore
CD132	Rat	TUGm2	APC	Biolegend, USA; Genomax Technologies, Singapore
CD215	Rat	DNT15Ra	APC	eBioscience, USA, ImmunoCell, Singapore
Bcl-2	Mouse	BCL/10C4	AF647	Biolegend, USA; Genomax Technologies, Singapore
Eomesodermin	Rat	DAN11MAG	APC	eBioscience, USA, ImmunoCell, Singapore
H-2Kb	Mouse	28-8-6	FITC	eBioscience, USA, ImmunoCell, Singapore
IL-2	Rat	JES6-5H4	AF488	BD Biosciences, Singapore
IFN-γ	Rat	XMG1.2	PE-Cy7	BD Biosciences, Singapore
Ki-67	Rat	SolA15	PE-Cy7	eBioscience, USA, ImmunoCell, Singapore
Ly6G	Rat	1A8	APC	Biolegend, USA; Genomax Technologies, Singapore
	Rat	1A8	PE	BD Biosciences, Singapore
IA/IE	Rat	M5/ 114.15.2	eFluor450	eBioscience, USA, ImmunoCell, Singapore
	Rat	M5/ 114.15.2	PE	BD Biosciences, Singapore
	Rat	M5/ 114.15.2	PerCP Cy5.5	eBioscience, USA, ImmunoCell, Singapore
PD-1	Mouse	25-D1.16	FITC	eBioscience, USA,

				ImmunoCell, Singapore
SiglecF	Rat	E50-2440	PE	BD Biosciences, Singapore
T-bet	Mouse	4B10	PCP/Cy5.5	eBioscience, USA, ImmunoCell, Singapore
TNF-α	Rat	MP6-XT22	APC	Biolegend, USA; Genomax Technologies, Singapore

2.6 Culture and activation of $CD8^+$ T cells

Freshly isolated $CD8^+$ T-cells were cultured at a concentration of 1×10^5 per 96-well U-bottom well plate. PMA (10mg/ml) (Sigma Aldrich, USA) and ionomycin (400mg/ml) (Sigma Aldrich, USA) was added to the $CD8^+$ T cells. For experiments requiring addition of IFN-γ, recombinant IFN-γ (Peprotech, USA; Gene-Ethics, Singapore) was added at the required concentrations. Cells were incubated in a 37^0C incubator for 48 or 72h and then harvested.

2.7 Measurement of Cytokines

Levels of cytokines (IL-5, IL-10, IL-13, IL-17, Eotaxin and IFN-γ) were detected using the commercially available DuoSet ELISA kits (R&D systems, USA; ImmunoCell, Singapore)

Coating of the ELISA plate and blocking

1. Capture antibodies were diluted to the working concentration in PBS without the carrier protein and a 96-well microplate coated with 100μl per well of the diluted capture antibody. The plate was then sealed and incubated at room temperature overnight.

2. The next day, each well was aspirated and washed with the wash buffer three times. After the last wash, the plate was inverted and blotted it on clean paper towels to remove any remaining wash buffer.
3. The plate was then blocked by addition of 200µl of blocking buffer and incubating for 1h at room temperature. The plate was then washed as in step 3.

Assay procedure

4. 100µl of sample or standard in the blocking buffer was added to the wells, the plate sealed and incubated for 2h at room temperature.
5. The plate was then washed as in step 3.
6. A working dilution of Streptavidin-HRP (100µl) was then added to each well, the plate covered and incubated for 20 min at room temperature in the dark.
7. The plate was washed as in step 3.
8. 100µl of substrate solution was added to each well and incubated for 20 min at room temperature in the dark.
9. 50µl of the stop solution was added to each well and the plate was gently tapped to ensure thorough mixing.
10. The Optical Density of each well was then determined using a microplate reader set to 450nm.

Note: The readings made directly at 450nm may be less accurate. Hence it is recommended that if wavelength correction is available, set it to 540nm or 570 nm. If wavelength correction is not available, the readings at 540nm or 570nm

may be subtracted from the readings at 450nm. This subtraction will correct for optical imperfections in the plate.

2.8 CTL killing assays

2.8.1 ^{51}Cr release assay

The chromium release assay was performed under sterile conditions with complete RPMI medium.

1. Target EL-4 cells were cultured and then centrifuged in a 15ml falcon tube at 450g for 5 min at room temperature.
2. The supernatant was discarded and 50mCi of ^{51}Cr was added to the cells in a BSL2 cabinet.
3. The plates were then labeled with hazard tape and then placed in a 37^0C incubator with 5% CO_2 for 1h.
4. The labeled cells were washed with pre-warmed (~ 37^0 C) complete RPMI and then spun down at 450g for 5min at room temperature.
5. The cells were re-suspended in pre-warmed (~ 37^0 C) complete RPMI at $1x10^6$ cells/ml concentration. The cells were then split into two 15ml falcon tubes. ASNENMETM peptide at 5mM was added to one of the tubes while control peptide GP_{33-41} was added to the other. Both tubes were incubated for 30min at 37^0C incubator with 5%CO_2.
6. Effector cells were plated in to a 96-well U-bottomed plate at the desired ratios (100:1, 30:1, 10:1, 3:1, 1:1, 1:3etc.) 100mL of pre-warmed (~ 37^0 C) complete RPMI was added to the cells without effector cells. For total lysis, 80mL of pre-warmed medium was added with 20mL of 10% Triton-X.

7. The peptide pulsed target cells were washed with 5ml of pre-warmed medium at 300g for 5min at room temperature.
8. The target cells were counted and then re-suspended at a concentration of 4 x 10^4 cells/ml.
9. 100mL of the target cells were added to each of the wells (4 x10^3/ well).
10. The plates were incubated at 37^0C with 5% CO_2 for 4-6h, harvested from the assay plate using the cell harvester and then transferred to appropriate 96-well Luma plate.
12. The Luma plate was then dried in an oven at 50^0C for 2h or O/N at room temperature.
13. The Beckman Top Count was used for the radioactive count.

Cytotoxic activity was the calculated as follows:

% Cytotoxic activity = (Sample lysis-spontaneous lysis) / (Total lysis-spontaneous lysis) x100.

% Specific lysis is determined by subtracting the cytotoxic killing of peptide pulsed targets versus non-peptide pulsed controls.

2.8.2 CD107α de-granulation assay

This assay was performed under sterile conditions with complete RPMI as the medium.

1. 100µl of effector cells (1x10^6 cells/ml) were plated into a 96-well U-bottomed plate.
2. 100µl of medium containing PMA (10mg/ml) (Sigma Aldrich, Singapore), ionomycin (400mg/ml) (Sigma Aldrich, USA) Ionomycin, Brefeldin (5mg/ml) (BD biosciences, Singapore), Monensin (5mg/ml)

(BD biosciences, Singapore) and anti-CD107a- APC (10mg/ml) (eBioscience, USA;) was added to each well.

3. The plates were incubated at 37^0C/5% CO_2 for 4-6h, cells harvested and surface staining performed for CD3, CD8 and with the NP_{366} pentamer.

2.9 Reverse Transcription

2.9.1 Isolation of RNA from the isolated cells

1. Total RNA was obtained from sorted or harvested cells using the RNeasy kit (Qiagen, Singapore).
2. Cells were pelleted and then lysed with 350µl of RLT buffer and then passed through a QIAshredder column (Qiagen, Singapore) to homogenize the lysate. One volume of 70% isopropanol was added to precipitate the RNA and then the solution was added to the column. The column was then centrifuged at maximum speed for 2 min.
3. The column-bound RNA was washed once with 700µl of RW buffer, followed by two washes with 500ml of RPE buffer. The column was centrifuged again to ensure complete removal of residual ethanol from the RPE buffer.
4. RNA was eluted by addition of 15µl of RNase-free water and the eluate so collected was again put back through the column to enhance the yield.
5. cDNA was obtained using Quantitect Reverse Transcription kit (Qiagen, Singapore) according to manufacturer's instructions. The cDNA was then stored at -80^0C.

2.9.2 Isolation of RNA from the lungs

1. Pieces of lungs were stored in RNAlater® at 4^0C for up to a week.
2. The lung pieces were taken from the RNAlater® (Qiagen, Singapore) and mashed with the bottom of a syringe in RLTplus® buffer from the kit (with beta mercapto-ethanol).
3. The tissue was then made into a single cell suspension by passing it through a needle with a syringe.
4. The cell suspension was then put through a QIAshredder column (Qiagen, Singapore) and the eluate collected.
5. Total RNA was obtained from whole lungs using the RNeasy Plus Mini kit (Qiagen, Singapore).

2.9.3 Primers

All primers were obtained from AIT Biotech, Singapore. The primer sequences are as follows:

Target	Primer sequences
GAPDH	F: AGGCCGGTGCTGAGTATGTCG R: GCAGAAGGGGCGGAGATGAT
M-protein	F: GGACTGCAGCGTTAGACGCTT R: CATCCTGTTGTATATGAGGCCCAT
Beta-actin	F: AGAGGGAAATCGTGCGTGAC R: CAATAGTGATGACCTGGCCGT

2.9.4 Real Time PCR

Real time PCR was performed using an ABI7500 Real-time PCR system with SYBR Green detection reagent (Applied Biosystems, Singapore). In all experiments, the primers were used at 300nM and the reaction volume maintained at 25μl. The relative quantities of target gene expression were quantified by comparative C_T method and normalized to GAPDH or beta-actin levels in the cells.

2.10 Lung Histology

2.10.1 Preparation of lung tissue

1. The mice were sacrificed using CO_2 asphyxiation and mounted on its back on a paraffin block with all the limbs spread apart.
2. After exposing the abdomen of the mouse, a cut was made at the renal artery to drain circulating blood.
3. The diaphragm was then cut laterally on both sides to expose the heart. A cut was made at the left atrium to allow blood and perfusion fluid to be released.
4. Using a pair of forceps, ventral tip of the heart was grasped with the left hand while making a small cut at the right ventricle, just enough for the cannula tip.
5. The cannula was then inserted and directed up through the right ventricle until the tip of the cannula was visible within the aorta.

6. The lung was perfused with PBS using a 50ml syringe until the lung turned pale white.
7. After perfusion, the trachea was cannulated with a needle and plastic tubing and 0.7ml of 4%Paraformaldehyde or 1% Formalin to fix the lung.
8. The perfused and fixed lung tissues were then placed in 4% Paraformaldehyde or 1% Formalin for 2-5 days before processing.

2.10.2 Processing of lung tissue

The fixed lung tissues were treated in a Leica tissue processor as follows:

1. 1h in 75% ethanol
2. 1h in 80% ethanol
3. 1h in 90% ethanol
4. 1.5h in 100% ethanol
5. 1.5h in 100% ethanol
6. 1.5h in 100% ethanol (Merck, Sigma Aldrich, Singapore)
7. 2h in Histoclear (Sigma Aldrich, Singapore)
8. 2h in Histoclear
9. 2h in Histoclear
10. 2.5h in wax
11. 2.5h in wax

2.10.3 Mounting the tissue and sectioning

1. The processed tissue was transferred from wax to the embedding mould
2. The cassette was placed on top of the mould to hold the tissue in place.
3. The cassette was then topped up with enough hot wax to hold the tissue.

4. The mould with the cassette in hot wax was transferred to a cold surface and left there until the wax solidified.
5. The embedded tissue was then removed from the mould using a pair of forceps.
6. The cassette was then mounted in a microtome for sectioning the tissue.
7. The tissue was cut into 3.5 to 5mM thick sections for staining.

2.10.4 Deparafinizing the tissues

The sections were then deparaffinized and rehydrated by treating them in the following solutions:

1. 10 min in Histoclear
2. 10 min in Histoclear
3. 2 min in 100% ethanol
4. 2 min in 100% ethanol
5. 10 dips in 95% ethanol
6. 10 dips in 70% ethanol
7. Rinsed in distilled water.

2.10.5 Hematoxylin and Eosin staining

1. After deparaffinizing and rinsing, the tissue sections were stained in Hematoxylin (Sigma-Aldrich, Singapore) for 5 min and then rinsed in distilled water.
2. The sections were differentiated in 0.3% acidic ethanol (0.3% HCl in 70% ethanol) for 30sec to 1 min and then rinsed in distilled water.
3. The sections were blued in Scott's tap water (3.5g Sodium carbonate (Na_2CO_3) and 20g magnesium sulfate ($MgSO_4 * 7H_2O$) in 1L distilled

water) for 1 min and again rinsed in distilled water.

4. The slides were checked under the microscope for blue nuclear chromatin and blued again in Scott's tap water if bluing is insufficient.
5. The slides were stained in alcoholic eosin (Sigma-Aldrich, Singapore) for 30 sec and then rinsed in 70% ethanol.
6. The sections were finally dehydrated and cleared by dipping 10 times in 95% ethanol and then 10 times in 100% ethanol and finally in Histoclear for 10 min.
7. The slides were then mounted with mounting medium, Histomount (Invitrogen, Singapore)
8. In the resultant slides, nuclear chromatin was visible as blue, the nucleoli were visible and the cytoplasm of the cells was stained pinkish to pinkish-purple.

2.10.6 Periodic Schiff staining

1. After de-paraffinizing and rinsing, tissue sections were oxidized in Periodic acid solution for 5 min and rinsed in distilled water.
2. The sections were then placed in Schiff's reagent for 15 min and the rinsed under running water for 5 min.
3. The sections were counterstained in Hematoxylin for 1.5 min and then washed in tap water.
4. The sections were finally dehydrated and cleared by dipping 10 times in 75

   % ethanol, 10 times in 95% ethanol and then 10 times in 100% ethanol and finally in Histoclear for 10 min.

5. The slides were then mounted with mounting medium, Histomount (Invitrogen, Singapore)
6. In the resultant slides, the nuclear chromatin in the cells was visible as blue, the nucleoli were visible and the mucus was visible as pink to pinkish-purple.

2.11 Statistical Analyses

Unpaired Students t test was used for comparison between two groups with a normal distribution and Mann-Whitney test was used for comparison between two groups with a skewed distribution. One-way ANOVA was used for comparison between multiple groups. Data is expressed as Mean +/- SEM. Statistical significance was indicated as $p<0.05$, $p<0.01$ and $p<0.001$. For Flow cytometric profiles and histology, plots and pictures are representations of repeated experiments.

Chapter 3: Mouse model of influenza and characterization of the general immune responses.

3.1 Introduction

Animal models make an important contribution to the study of infectious diseases, both for the characteristics of the infection as well as in the development of vaccines and therapeutics. Animal models that can accurately reflect the human disease characteristics and the protective immune responses they induce are indispensable tools for research. Animal models have been crucial in the study of immunology to characterize the immune responses in general and the behavior of specific immune cells in particular. Several animal models have been used for the study of influenza viruses and therapeutics targeting the virus. Animals such as mice, ferrets, cotton rats, guinea pigs, macaques and hamsters have been used to study influenza infections. Each animal model presents several unique advantages and disadvantages. Due to their similarity with human disease (ferrets) or the ease with which they can be used and the availability of inbred and genetically modified strains (mice) some animals are most commonly used.

Ferrets are naturally susceptible to influenza viruses and hence influenza viruses can replicate efficiently in the respiratory tract of these animals without prior adaptation. The clinical symptoms of illness are very similar to human infection, including fever, sneezing, rhinorrhea and weight loss. Neurologic and gastrointestinal symptoms are seen following infection with some Highly Pathogenic Avian Influenza (HPAI) viruses. Furthermore the receptor distribution is very similar to humans: α 2,6 in the upper respiratory

tract and α 2,3 in the alveoli. In spite of these advantages, it is difficult to obtain animals that are seronegative for human influenza viruses. In addition, the high expense involved, limited immunological reagents available and the requirement of special housing requirements for these animals form major deterrents against using ferrets to study influenza.

Although influenza virus is not a natural pathogen of mice, mice have been good models of this infection. Human influenza viruses replicate in the respiratory tract without prior adaptation but require adaptation for some strains to cause disease. The receptor distribution in the respiratory tract of mice: α 2,3 in the ciliated airway and type II alveolar epithelial cells are unlike those found in humans. In spite of these drawbacks, mice are the most commonly used animal models for influenza research. In terms of size of the animal, cost involved and husbandry requirements, the murine model is very convenient. A wide range of immunological reagents is available for studying humoral and cellular immune responses. The availability of species-specific reagents and the ability to manipulate mice genetically offers a system in which the host response to infection can be studied in depth. Using the mouse model is also the most economical way to produce statistically robust data. For our study, we use a mouse model of influenza and because all the transgenic mice needed for the study were available on the C57BL/6 background, we chose to do all our experiments with the C57BL/6 mice.

Several strains of influenza have been used for experimental studies. The influenza viruses A/PR/8/1934 (H1N1) and A/Aichi/2/1968-x31 (a reassortant H3N2 virus) are commonly used strains in immunology research. The A/PR/8/1934 (H1N1) strain, (abbreviated as PR/8) is an influenza vaccine

reference strain that has been extensively passaged in the laboratory and is known to grow to very high titers in embryonated chicken eggs (Robertson et al. 1992). The PR/8 strain is pathogenic at low doses of the virus as in a physiological course of an influenza infection. It is known to have a LD_{50} (50% lethal dose) of 200 PFU (Plaque Forming Units) (Quan et al. 2008). The A/Aichi/2/1968-x31, (abbreviated as X31) strain of virus is a genetically engineered virus such that it has the same internal proteins as that of the PR/8 strain but surface proteins from the A/Aichi (H3N2) strain (Kilbourne 1969). This strain is much less pathogenic compared to the PR/8 strain and has a LD_{50} of $7x10^5$ PFU (Quan et al. 2008). Hence high challenge doses have generally been used in previous studies. We had access to both strains of the virus and hence we used both strains of the virus.

In this chapter, we sought to establish a mouse model of influenza. We compared the two strains of viruses to choose the appropriate viral strain and dose for all the following studies. We also characterized the immune responses to this strain at different infectious doses of influenza. We studied weight loss, production of pro-inflammatory cytokines in the bronchoalveolar space, the kinetics of cellular infiltration into the bronchoalveolar space and the T cell responses (both CD4 and CD8) as well as the humoral responses induced in response to an influenza infection.

3.2 Choosing the viral strain and dose of virus

We compared viral infections with both strains of viruses: the A/PR/8/H1N1 and A/HK-X31/H3N2. The PR/8 strain is known to have a LD_{50} of 200 PFU

(Quan et al. 2008). The HK-x31 on the other hand is a much less virulent with an LD_{50} of $7x10^5$ PFU (Quan et al. 2008). We chose to start with a very low dose of virus i.e. 5 PFU of PR/8 keeping in view that it is more physiological in terms of the levels of virus one is exposed to during an infection but a much higher dose of the HK-x31 strain of virus i.e. 10^5 PFU.

Both viruses were grown in 9-day old embryonated chicken eggs and the viral titers were determined by the plaque assay using MDCK cells. The virus was diluted accordingly and C57BL/6 mice infected with 5 plaque-forming units of PR/8 or a 10^5 PFU of HK-x31.

Signs of clinical sickness include ruffled fur, labored breathing, hunching, hypothermia, weight loss and mortality (we avoided the latter by sacrificing animals when their weight loss exceeded 25% of body weight). Loss of body weight is an excellent indicator of the level of sickness in mice due to an influenza infection. The extent of weight loss coincides with other markers of sickness. It also provides a non-invasive way to determine the extent of influenza infection in the mice so that mice can be sacrificed if they are too sick. Mice were weighed at roughly the same time everyday for a better representation of their weight loss.

The C57BL/6 mice were infected intra-nasally with a 5 PFU dose of virus and their weights were recorded every day for 14 days until they completely returned to their original body weight (Figure 3.1). The PR/8 strain of influenza caused significant morbidity in the infected mice at the low dose of virus used (5 PFU) but did not lead to the death of the mice. Hence, it is a sub-lethal dose. The 5 PFU infected C57BL/6 mice infected with PR/8 influenza started to show weight loss typically from day 5 after infection. There was a

slight decrease in body weight at day 3-post infection (p.i), which may have been due to the effects of the anesthetic but this dip was quickly recovered by the next day. The influenza related weight loss started around day 5 p.i. and the mice continuously lost weight from then on until about day 8 or 9. Apart from the weight loss, the mice also showed signs of morbidity in that they were lethargic and were poorly groomed. The weight loss was greatest at day 8 or day 9. At this point, along with a thin appearance the mice were visibly lethargic and their fur was unkempt. After day 9, the mice began to regain body weight and completely recovered from the infection by day 14 p.i.

The C57BL/6 mice infected with HK-x31 influenza started to show weight loss immediately and lost a maximum of 12% body weight by day 4 p.i. but quickly recovered from there on. This was in contrast with the PR/8 infection, but this early loss of weight was probably due to the high dose of virus used for this strain. However, these mice quickly recovered from the infection and did not show signs of significant morbidity in spite of using such a high dose of virus for infection. This finding was in line with earlier studies that this viral strain was much less pathogenic than the PR/8 strain of virus. Hence, we chose to use the PR/8 strain of influenza with a dose of 5 PFU for all our studies with responses to primary infection with influenza.

For the re-challenge experiments however, using the same virus for both infections would mean inducing neutralizing antibodies, which would confound the studies of the protective $CD8^+$ T cell responses due to the primary infection. Hence, we used both the above-mentioned strains in combination. The PR/8 and the HK-x31 strains of virus have the same internal proteins but they have different surface glycoproteins (Hemagglutinin and

Neuraminidase). The $CD8^+$ T cell responses to influenza are targeted towards the internal proteins but the antibody responses are aimed at the surface proteins. It is known that the neutralizing antibody response to the surface proteins of these two viruses is not cross-reactive (Flynn et al. 1998). Hence the protective response of the mice to the secondary challenge is solely attributable to the $CD8^+$ T cells and not to the neutralizing antibodies. For studying the responses to secondary infections, the HK-x31 strain was used for the primary infection and 5 PFU or higher doses of the PR/8 strain were used for the re-challenge experiments.

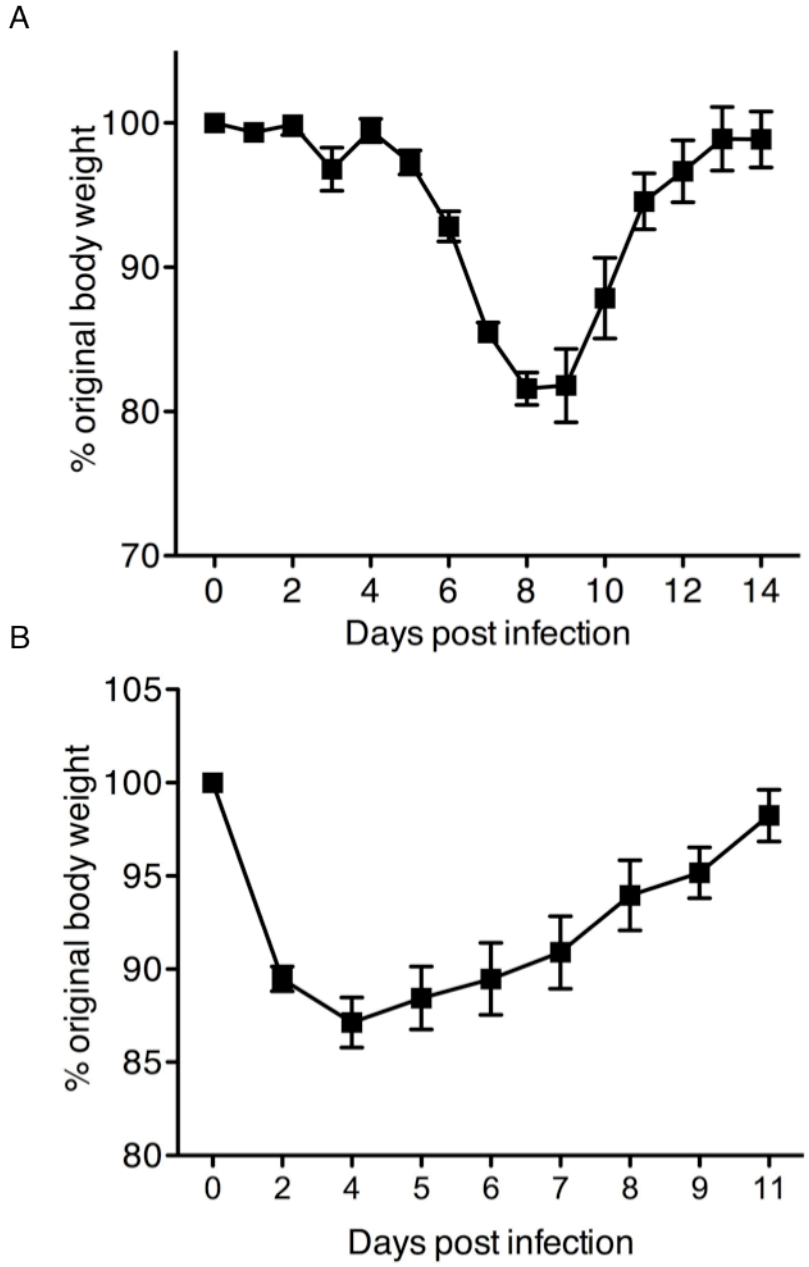

Figure 3.1 Percentage weight loss in C57BL/6 mice infected with different strains of influenza

(A) Infection with 5 PFU of PR/8 (n=15)
(B) 150,000 PFU of X31 (n=5)
Graphs show mean ± S.E. Data representative of 2-3 experiments

3.3 Kinetics of cellular infiltration into the BAL after a 5 PFU influenza infection

We studied the progression of 5 PFU influenza infection in WT mice by looking at the extent of cellular infiltration into the airways of the lungs at different points in time after infection. For this purpose, WT C57BL/6 mice were infected with 5 PFU PR/8 and the kinetics of different cell types entering the airways were determined by analyzing the BAL fluid of the lungs of the infected mice, every day for 10 days after infection.

The mice were sacrificed on the indicated days post infection and the trachea was cannulated and the lung flushed with MACS buffer to harvest the BAL fluid. The cells from this extracted BAL fluid were analyzed by flow cytometry. The cells were stained with CD11c, CD3, SiglecF and Ly6G to identify different cell types (figures 3.2A and 3.3A) by their staining profiles as follows:

Eosinophils: $CD11c^{-}$ $SiglecF^{+}$

Neutrophils: $CD11c^{-}$ $Ly6G^{+}$

Macrophages: $CD11c^{+}$ $SiglecF^{+}$

T cells: $CD11c^{-}$ $CD3^{+}$

We observed that before infection, the number of cells in the BAL fluid of the mice was very low. Most of the cells were macrophages. There were no neutrophils, eosinophils or T cells in the BAL fluid of uninfected mice. The number of macrophages fell by day 2 p.i. and was reduced considerably after that and remained lower for the rest of the infection (figure 3.2B). Few eosinophils were detected although a small number was seen on day 9 (figure 3.2C).

The number of neutrophils peaked at day 4 p.i. and then was reduced significantly after that (figure 3.3B).Most importantly, the T cells came into play only at about day 7 p.i and from then on increased in numbers even as long as day 9 p.i. (Figure 3.3 C).

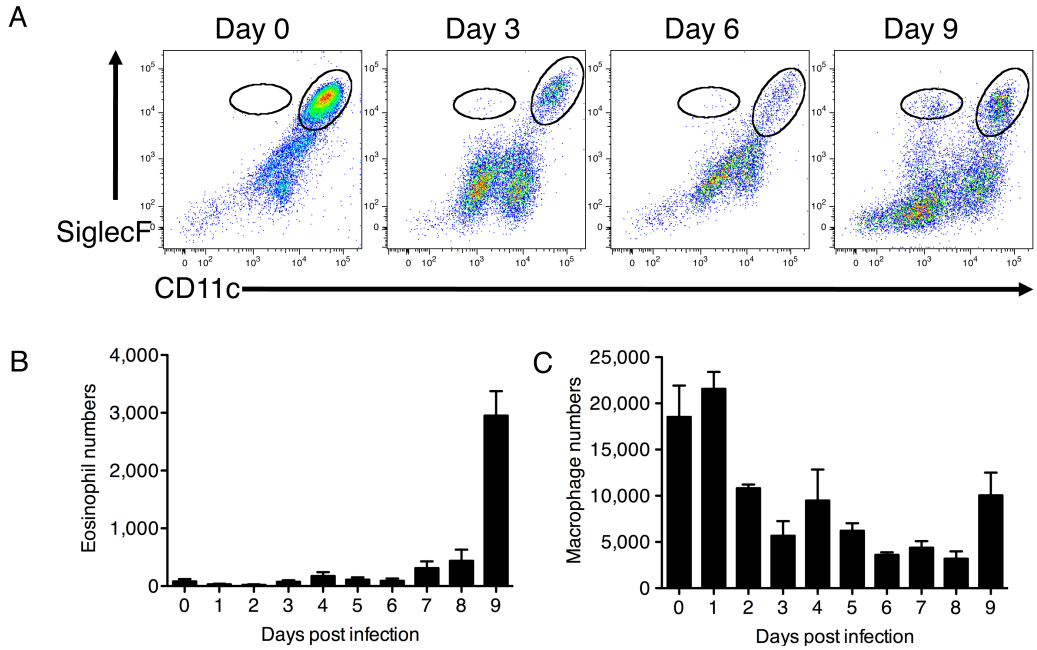

Figure 3.2 Cellular infiltration in the BAL fluid after influenza infection: Kinetics of Eosinophils and Macrophages

The BAL fluid was harvested from infected mice at different time points after infection. The cells from the BAL fluid were counted and stained for flow cytometry. (A) Representative plot of Eosinophils ($CD11c^-$ $SiglecF^+$) and macrophages ($CD11c^+$ $SiglecF^+$) at different time points after infection.
(B) Kinetics of eosinophil infiltration into the BAL fluid of WT mice after a 5 PFU influenza infection.
(C) Kinetics of macrophage infiltration into the BAL fluid of WT mice after a 5 PFU influenza infection.
Data are representative of 2 independent experiments with n=3-5 per experiment.

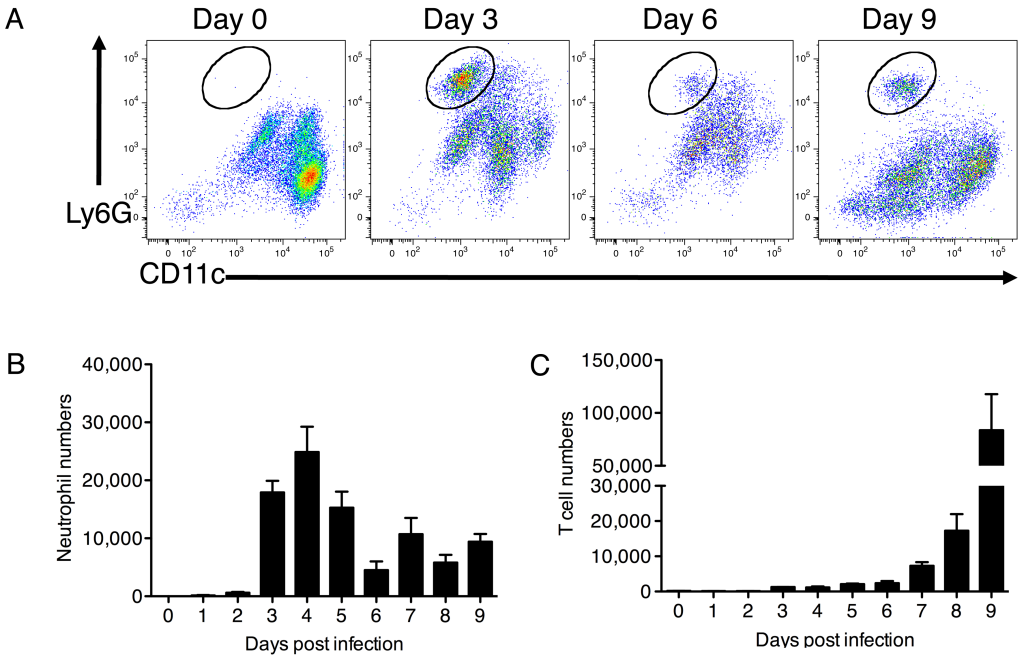

Figure 3.3 Cellular infiltration in the BAL fluid after influenza infection: Kinetics of Neutrophils and T cells

BAL fluid was harvested from infected mice at different time points after infection. The cells from the BAL fluid were counted and stained for flow cytometry.
(A) Representative plot of Neutrophils ($CD11c^-$ $Ly6G^+$) and T-cells ($CD11c^-$ $CD3^+$) at different time points after infection.
(B) Kinetics of neutrophil infiltration into the BAL fluid of WT mice after 5 PFU influenza infection.
(C) Kinetics of T cell infiltration into the BAL fluid of WT mice after 5 PFU influenza infection.
Data are representative of 2 independent experiments with n=3-5 per experiment. This data was from the same set of experiments as figure 3.2.

3.4 Kinetics of pro-inflammatory cytokines Interferon gamma (IFN-γ) and Tumor Necrosis Factor alpha (TNF-α) after a 5 PFU influenza infection

To determine the extent of airway inflammation, we looked at the kinetics of the cytokine IFN-γ in the infected mice (figure 3.4A). Bronchoalveolar lavage fluid was harvested from infected mice every day after infection and the levels of IFN-γ and TNF-α were determined by an ELISA based protocol.

IFN-γ was not detected in the BAL fluids of the infected mice during the early days of infection. Although low levels of IFN-γ were recorded on day 4 and 5, the levels of IFN-γ peaked at about days 6 and 7 p.i. and remained high for the following 2-3 days. The levels again dropped by day 10 p.i. and were not detected after day 11 p.i.

Similar kinetics was also observed for TNF-α. The levels of TNF-α were low in the broncho alveolar lavage fluid for the first few days after infection (figure 3.4B). The levels started to increase by day 6 p.i. and peaked at day 7 p.i. In common with IFN-γ, the levels of TNF-α also fell by day 10 p.i. and were undetected after day 11 p.i.

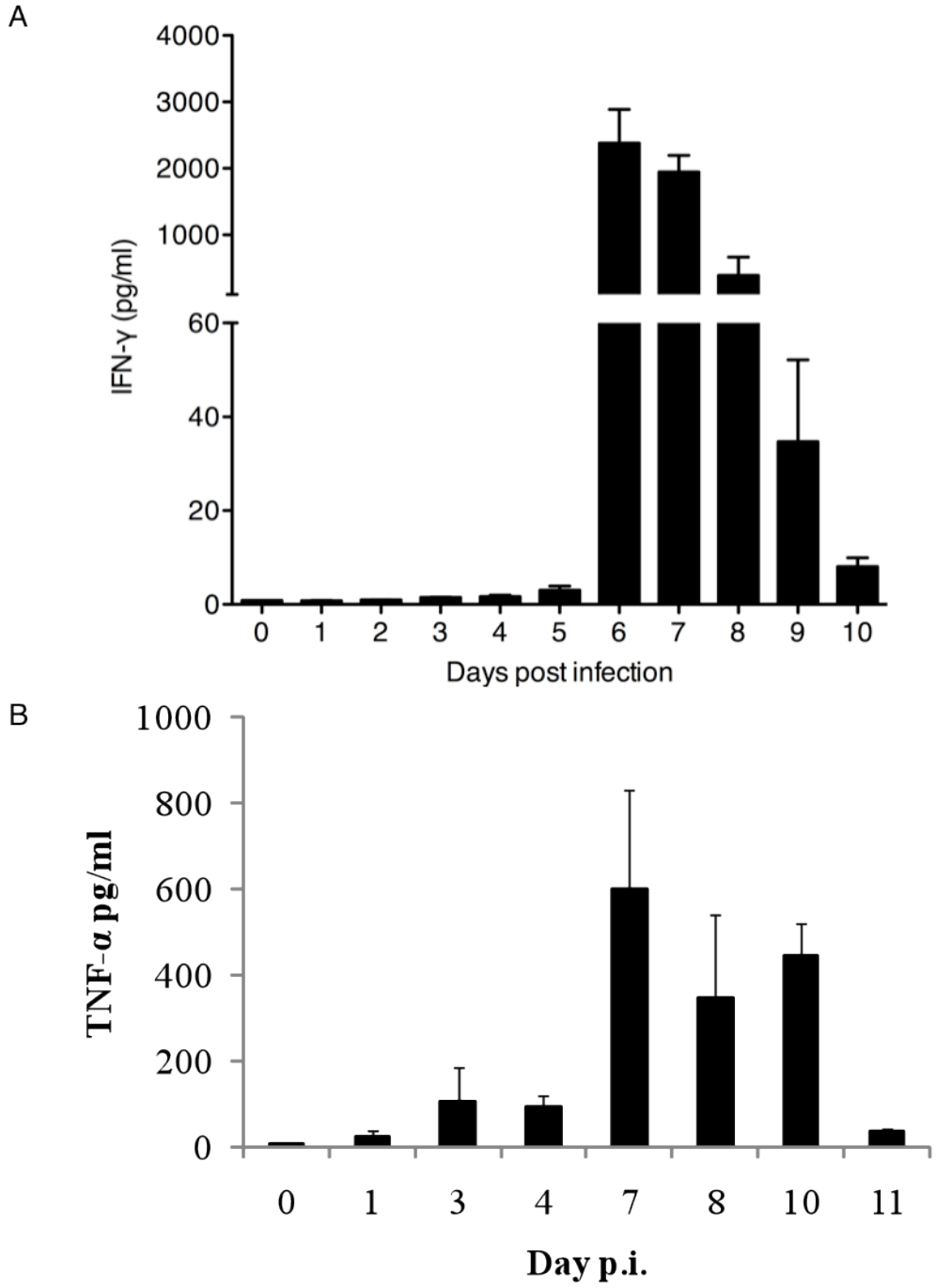

Figure 3.4 Kinetics of pro-inflammatory cytokines in the BAL fluid of C57BL/6 mice infected with 5 PFU of PR/8 influenza

The BAL fluid was harvested from infected mice at different time points after infection. The supernatant from the BAL fluid was used for ELISA to detect the respective cytokines. Kinetics of (A) IFN-γ and (B) TNF-α in the BAL fluid after infection
Graphs show mean ± S.E. Data is representative of 2 independent experiments.
n = 3-5 for the set of data shown

3.5 Adaptive immune responses to a 5 PFU influenza infection

The adaptive immune response to influenza is established much later in the infection, at a time point when the viral titers have already fallen and comprises the $CD8^+$ T cells, $CD4^+$ T cells and the antibody responses.

3.5.1 $CD8^+$ T cell responses and antigen specific $CD8^+$ T cells

The $CD8^+$ T cells form a very important component of the immune protection against viral infections, mediating viral clearance (Yap et al. 1978; McMichael et al. 1983; Topham et al. 1997) and thereby host recovery.

Total $CD8^+$ T cell numbers were enumerated in the lung tissue of the mice at different time points after infection. The lungs were harvested from the mice and digested to harvest the cells from the lungs, which were then stained with antibodies anti-CD11c and Gr-1 to gate out the auto fluorescent cells (macrophages, neutrophils and some dendritic cells). The cells were also stained with antibodies against CD3, CD4 and CD8 to enumerate $CD4^+$ and $CD8^+$ T cells. The total number of cells was counted and the numbers of cells staining positive for the appropriate markers were then used to calculate the absolute numbers of T cells. The cells were gated on live lymphocytes and singlets before looking at $CD3^+$ and $CD8^+$ populations (Figure 3.5A). $CD8^+$ T cells were readily detectable at day 8 and peaked at day 11 p.i. (Figure 3.5B). After the peak, the numbers of $CD8^+$ T cells decreased, marking the contraction phase of the response.

To study the antigen specific $CD8^+$ T cell responses to 5 PFU PR/8 influenza infection, we used the MHC I pentamer for $NP_{366\text{-}374}$ 'ASNENMETM-H-$2K^b$',

an immunodominant epitope, to detect for influenza-specific $CD8^+$ T-cells (Figure 3.5A). $NP_{366-374}$ specific $CD8^+$ T-cells followed similar kinetics to the total $CD8^+$ T cells, although their numbers were smaller. Flu-specific $CD8^+$ T cells were readily detectable in the lung tissue from day 8 p.i. with the peak response seen at day 11 p.i. (Figure 3.5C). Day 14 had lower numbers, again marking the contraction of the response.

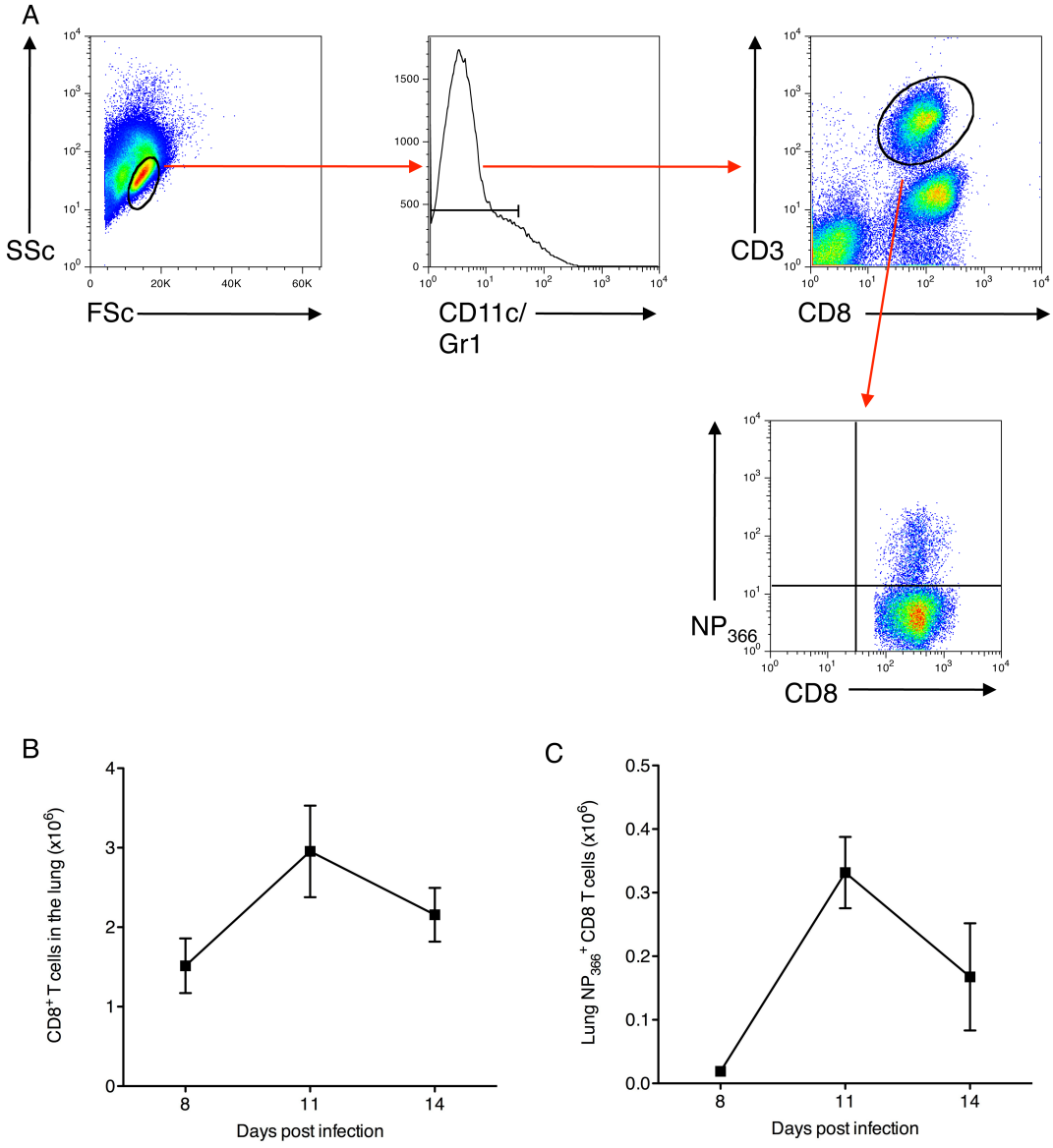

Figure 3.5 Kinetics of total and antigen-specific $CD8^+$ T cells in the lungs of infected mice after 5 PFU PR/8 influenza infection.

(A) Representative flow cytometry plots to show the gating strategy for the total and NP_{366}^+ $CD8^+$ T cells,
(B) kinetics of total $CD8^+$ T cell numbers post influenza infection,
(C) kinetics of antigen specific NP_{366}^+ $CD8^+$ T cells after 5 PFU PR/. Graphs show mean +/- SE. Data is representative of 3 independent experiments n=10 per group per time-point.

3.6 $CD4^+$ T cell responses

Although $CD4^+$ T cell responses are not very important in a primary influenza infection, they are known to play a crucial role in the memory responses. We characterized the $CD4^+$ T cell responses after a 5 PFU influenza infection. Due to the lack of $CD4^+$specific tetramers, we only looked at the total $CD4^+$ T cell numbers to give us a general idea of the $CD4^+$ T cell response.

The lungs were harvested from the mice and digested to harvest the cells from the lungs, which were then stained with antibodies to CD11c and Gr-1 to gate out the auto fluorescent cells (macrophages, neutrophils and some dendritic cells). The cells were also stained with antibodies against CD3 and CD4 to characterize the $CD4^+$ T cell responses. The gating for the $CD4^+$ T cells was done similar to the $CD8^+$ T cells initially and then gated on $CD3^+$ and $CD4^+$ T cells (Figure 3.6A). The total number of cells was counted and the numbers of cells staining positive for the appropriate markers were then used to calculate the numbers of $CD4^+$ T cells.

The kinetics of the total $CD4^+$ T cell response was similar to what was observed with the $CD8^+$ T cells, although the numbers of $CD4^+$ T cells was far lower than for $CD8^+$ T cells. The numbers of $CD4^+$ T cells were detectable at day 8 p.i. and peaked at day 11 p.i, (Figure 3.6B).

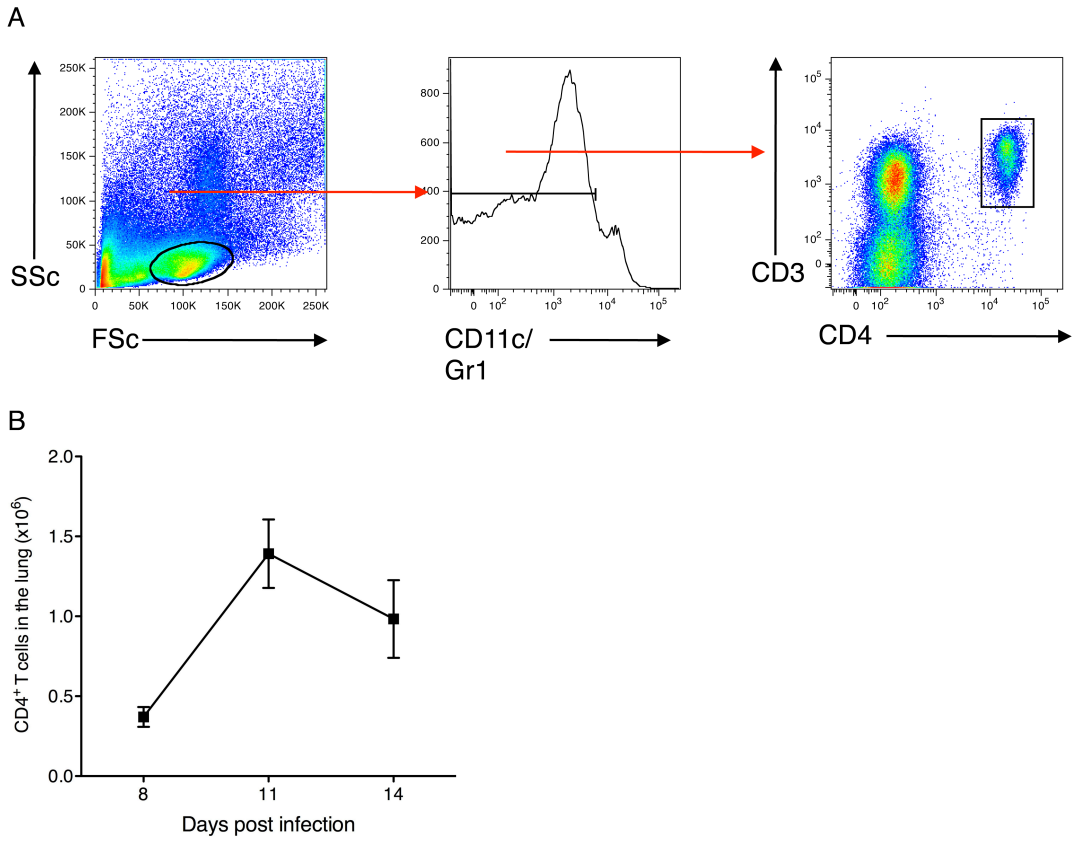

Figure 3.6 Kinetics of total CD4$^+$ T cells in the lungs of infected mice after 5 PFU PR/8 influenza infection.

(A) Representative flow cytometry plots to show the gating strategy for the total CD4$^+$ T cells, (B) kinetics of total CD4$^+$ T cells post influenza infection. Graphs show mean +/- SE. Data is representative of 3 independent experiments n=10 per group per time-point.

3.7 Neutralizing antibody responses

The humoral response is important for an influenza infection for mediating viral clearance. Mice deficient in antibodies were found to be incapable of clearing the virus after a primary influenza viral challenge (Kris et al. 1985). Neutralizing antibodies against influenza virus are generally directed against the surface glycoproteins, Hemagglutinin and Neuraminidase of the virus. We determined the titers of virus neutralizing antibodies in the serum of mice infected with 5 PFU PR/8 influenza by using a hemagglutination inhibition (HAI) assay. Serum HAI titers of 40 in human serum are regarded as the minimum titers for seroprotection. It was observed that hemagglutination-inhibiting titers of virus were detected in the sera of infected mice at day 8 p.i. and increased by day 11 p.i (Figure 3.7). This indicates that the neutralizing titers against influenza were rapidly engendered after influenza infection.

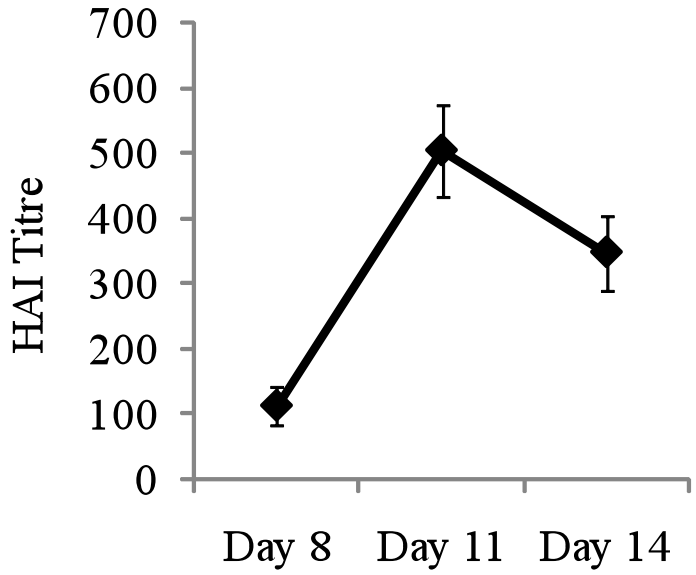

Figure 3.7 Serum Neutralizing antibody titers after 5 PFU PR/8 influenza infection

Serum was harvested at different time points after infection from the infected mice. The serum was treated with RDE before subjecting the samples to a Hemagglutination Inhibition assay with 4HAU of virus. Graph shows mean +/- SE. Data is pooled of 3 independent experiments n=10 per group per timepoint.

3.8 Discussion

In this chapter, we have established a mouse model of influenza with the C57BL/6 mice using a 5 PFU dose of PR/8 influenza. We have also broadly characterized the immune responses to the infection, mainly the T cell responses and neutralizing antibody responses. We decided to base our model on the 5 PFU dose of influenza, considering that it is presumably similar to the dose a person would encounter/ inhale when the virus is transmitted. This dose of virus also caused enough morbidity for us to track the infection and monitor the engendered immune responses.

The innate immune responses to influenza infection kick in quite early and the neutrophils are found to infiltrate into the airways as early as day 3 p.i. but start to go down at later points. The eosinophils do not seem to play such an important role here as they are found in very small numbers and although there is a peak at day 9 p.i., it was not significant. As innate immune responses were not the focus of our study, we did not investigate them in greater detail.

The adaptive immune response, i.e. the T cells as well as the antibody titers come into play much later in the infection, as late as day 8 p.i. We detected $CD4^+$ and $CD8^+$ T cells in the lung tissue of the infected mice only at around day 7-8. Although this is not the peak of the $CD4^+$ or $CD8^+$ T cell response, peak levels of pro-inflammatory cytokines were secreted into the BAL fluid at this time-point. These findings also correlated with the fact that the mice were sickest at this point, indicated by the maximum loss in body weight. The peak in the pro-inflammatory cytokines in the BAL correlated very well with the weight loss, indicating that the severe loss in body weight/sickness may be due to the cytokine storm, so often linked to an influenza infection. But there is a

discrepancy in that, although the levels of cytokines seemed to peak at day 7 p.i., the levels of $CD4^+$ and $CD8^+$ T cells only seem to peak much later i.e. at day 11 p.i. This is not surprising as $CD8^+$ T cells are known to produce prominent levels of cytokines during their proliferation and $CD8^+$ T cells are known to continue their proliferation even after reaching the lung (Lawrence et al. 2005).

The magnitude of the memory $CD8^+$ T cell response is directly determined by the clonal burst of the virus-specific $CD8^+$ T cell response to the infection (Hou et al. 1994). The continued proliferation of the virus-specific $CD8^+$ T cells in the lung is required to establish a robust memory response. However, the levels of cytokines seem to be very low or non-existent during the peak of the T cell responses. Recent studies have shown that $CD8^+$ T cells in the lung have to interact with lung dendritic cells in order for them to secrete pro-inflammatory cytokines (Hufford et al. 2011). It is possible the decline in numbers of lung dendritic cells at such late points after influenza infection is responsible for the reduced pro-inflammatory cytokines. This may indicate an efficient way of controlling the inflammatory cytokine environment and reducing lung pathology due to cytokine storm even when maintaining high numbers of $CD8^+$ T cells to establish a robust memory response.

Although the influenza-specific $CD8^+$ T cell numbers peak at day 11, there is a decline in their numbers by day 14p.i. This marks the contraction phase of the $CD8^+$ T cell response during which many of the cells undergo apoptosis. The cells that survive the contraction phase of the response go on to form the memory population. The factors that determine the contraction phase of the influenza-specific $CD8^+$ T cell response are still unknown. Several cytokines

such as IL-2, IL-7 and IL-15 play a homeostatic role in maintaining primary and memory $CD8^+$ T cells. IL-2 is known to support the generation of terminal effector $CD8^+$ T cells as opposed to memory cells (Kalia et al. 2010; Pipkin et al. 2010). IL-7 and IL-15 on the other hand support the formation of long-lived memory T cells(Schluns et al. 2000; Becker et al. 2002).

Chapter 4: The role of Interferon gamma in the adaptive immune responses to influenza

4.1 Introduction

Interferon gamma is a well-studied master cytokine, which has effects on multiple cell types and hence plays multiple roles in the immune system. Some of the pleiotropic roles of IFN-γ have been highlighted in the introduction. Our main aim was to study its' function in the adaptive immune response to influenza. Most cells express the IFN-γR and hence can respond to IFN-γ. It is because of this fact that it plays important roles in a variety of infections, both systemic and local.

In the previous chapter, we established a mouse model of influenza using the PR/8 strain of influenza and demonstrated that infection of mice intra-nasally with 5 PFU of PR/8 could induce a robust immune response to influenza in the C57BL/6 strain of mice. We used this model for further experiments to study the role of IFN-γ signaling in the immune response to a primary influenza infection. The availability of mice deficient in IFN-γ and mice deficient for IFN-γR make it truly possible to study the immune response in the absence of IFN-γ signaling.

IFN-γ is an important cytokine in influenza as it is one of the pro-inflammatory cytokines produced in very high quantities in an influenza infection and adds to the cytokine storm linked to an influenza infection. Earlier studies in IFN-γ deficient mice have had varying results based on viral strain and the doses of viruses used for the experiments. The first study of influenza infection in the IFN-γ deficient mice used A/Japan/305/57 (H2N2)

strain of virus (Graham et al. 1993). In this study, IFN-$\gamma^{-/-}$ mice showed similar susceptibility to C57BL/6 wild type mice to intranasal infection with the influenza virus. Another study used the BALB/c model and blocked IFN-γ *in vivo* (Baumgarth and Kelso 1996). These mice showed a significant reduction in the titers of virus-specific IgG2a and IgG3 in the serum. Although the authors did not observe any change in the viral titers in the lung tissue, they observed reduced cellular infiltration in the lungs of the mice with *in vivo* neutralization.

The roles of IFN-γ have been studied in a wide variety of viral and bacterial infections. But most of these studies focus on systemic infections like LCMV and Listeria. There are few studies that explore the role of IFN-γ in localized infections like influenza. However, most of these studies use re-assortant viruses (like HK-x31) and hence use very high doses of virus to elicit a response to study the infection. In our study we chose to use a laboratory-adapted strain PR/8 and a dose of 5 PFU, a physiological dose i.e. the amount of virus one would encounter from the environment, from a sneeze etc. Our study is comprehensively looking at all the roles IFN-γ might have on the adaptive immune response in a localized respiratory infection like influenza.

One of our main aims for this project was to understand the role of IFN-γ in regulating the adaptive immune response and especially the T cell response in a mouse model of influenza. For this we made use of mice deficient in IFN-γ or in IFN-γ receptor. These tools gave us a better understanding of how IFN-γ contributed to the protection and/or pathology after an influenza infection and what cell types contributed to this particular phenotype. Our study mainly

focused on the $CD8^+$ T cells and the role, played by IFN-γ in the modulation of the virus-specific $CD8^+$ T cell responses.

4.1.1 Tools for deciphering the role of IFN-γ in an influenza infection

The main aim of this project was to understand the role of IFN-γ signaling in an influenza infection. Hence, we made use of gene knock out mice: transgenic mice that were deficient in IFN-γ (IFN-$\gamma^{-/-}$) and transgenic mice which were deficient in IFN-γR1 (IFN-$\gamma R^{-/-}$). These mice were obtained from Jackson Laboratories with the following stock numbers: IFN-$\gamma^{-/-}$ mice: 002287 and IFN-$\gamma R^{-/-}$ mice: 003288.

The IFN-$\gamma^{-/-}$ mice were made by the insertion of a neomycin gene into exon 2 of the IFN-γ gene, which induced a termination codon after the first 30 amino acids of the mature protein (Dalton et al. 1993). Mice with this targeted mutation were reported to be viable, fertile and normal in a "clean" environment but had reduced macrophage function in response to pathogens. Their macrophages were shown to have impaired production of antimicrobial products and reduced expression of MHC II antigens. They were also observed to have reduced resting natural killer cell activity.

IFN-$\gamma R^{-/-}$ mice were made by insertion of a neomycin cassette into the exon V of the IFN-γ receptor 1 gene, which encodes an extracellular membrane-proximal portion of the receptor (Huang et al. 1993). Mice with this targeted mutation were viable and fertile with no overt abnormalities. They were also

shown to have normal T cell responses but had increased susceptibility to infection by *Listeria monocytogenes* and *vaccinia* virus.

4.2 Response to influenza infection in the absence of IFN-γ signaling

4.2.1 Comparison of weight loss after a 5 PFU influenza infection

To understand the role of IFN-γ signaling in our model of influenza infection, WT C57BL/6 mice, IFN-$\gamma^{-/-}$ mice and IFN-$\gamma R^{-/-}$ mice were infected with 5 PFU of PR/8 influenza and their responses to infection were characterized. All the mice survived the ensuing infection, irrespective of their ability to make or respond to IFN-γ. We measured weight loss in all the infected mice for a period of 14 days after the infection. IFN-$\gamma^{-/-}$ and IFN-$\gamma R^{-/-}$ mice showed similar weight loss characteristics to WT mice after infection. They also displayed similar symptoms as WT mice, including labored breathing, poor grooming, ruffled fur, reduced responses to external stimuli a week p.i. The highest weight loss was recorded around day 8-9 p.i at about 20 % of their original body weight. They also recovered from the infection regaining their original body weight by day 14 p.i. The kinetics as well as the extent of weight loss was similar to what was observed in WT mice. This indicated that the loss of IFN-γ or its receptor did not increase the susceptibility of the mice to a 5 PFU dose of PR/8 influenza. Our results are in agreement with previous findings with other strains of influenza virus, which show that the IFN-$\gamma^{-/-}$ mice are not more susceptible to an influenza infection (Graham et al. 1993).

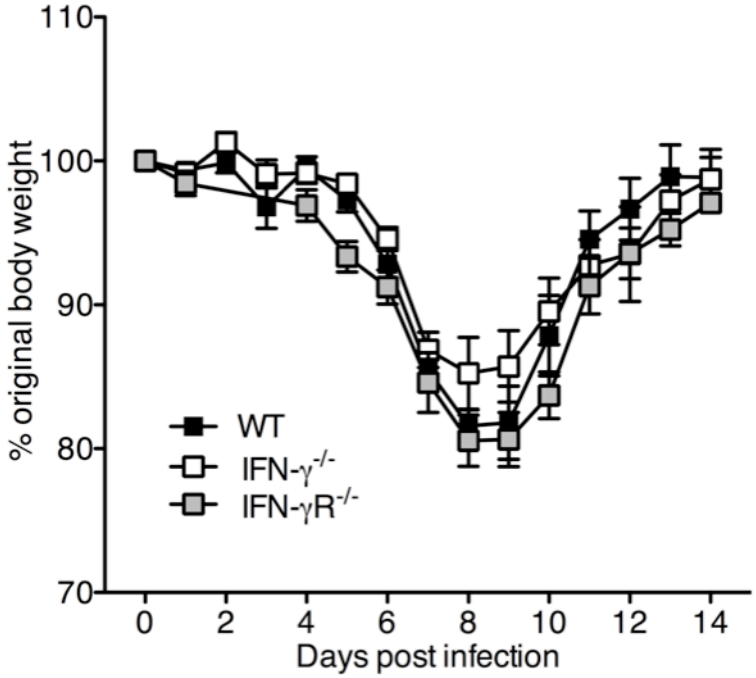

Figure 4.1 Comparison of loss of body weight in response to a 5 PFU PR/8 influenza infection in WT, IFN-$\gamma^{-/-}$ and IFN-$\gamma R^{-/-}$ mice.

C57BL/6 WT, IFN-$\gamma^{-/-}$ and IFN-$\gamma R^{-/-}$ mice were infected with 5 PFU of influenza A/PR/8/34. Weight loss of mice over a course of 14 days following infection. Data represents mean+/- SEM. n=15/ group

4.2.2 Comparison of viral load in the lungs of mice after 5 PFU influenza infection

We measured viral titers in the lungs of infected mice at different time points after infection to determine the kinetics of viral clearance. The lungs of the mice were harvested on days 2, 4, 6 and 8 after infection and the lungs homogenized. Viral titers in the supernatant were measured by the plaque assay. In the C57BL/6 mice, viral titers peaked at day 4 p.i. and no virus could be detected in the lungs of WT mice at day 8 p.i. using the plaque assay (Figure 4.2). Viral titers in the lungs of IFN-$\gamma^{-/-}$ and IFN-$\gamma R^{-/-}$ mice were similar to WT mice at all times measured. The kinetics of viral clearance from the lungs of IFN-$\gamma^{-/-}$ and IFN-$\gamma R^{-/-}$ mice was similar to what was observed in the WT mice (Figure 4.2). This gave us an indication that IFN-γ signaling did not play a role in the clearance of the viral antigen and other mechanisms are probably able to compensate for its absence.

We could only detect significant viral titers until day 6 p.i. using the plaque assay. As the sensitivity of this assay is limited, we decided to measure the viral RNA in the lungs of the infected mice. We compared the levels of viral RNA for the M-protein in the lungs of the infected mice by using a qRT-PCR assay (Figure 4.3). Although, we could detect viral RNA till about day 10 we did not observe any differences in the number of copies of viral RNA between the WT, IFN-$\gamma^{-/-}$ and IFN-$\gamma R^{-/-}$ mice lungs. With this, we confirmed that IFN-γ does not have an irreplaceable role in clearance of the influenza virus.

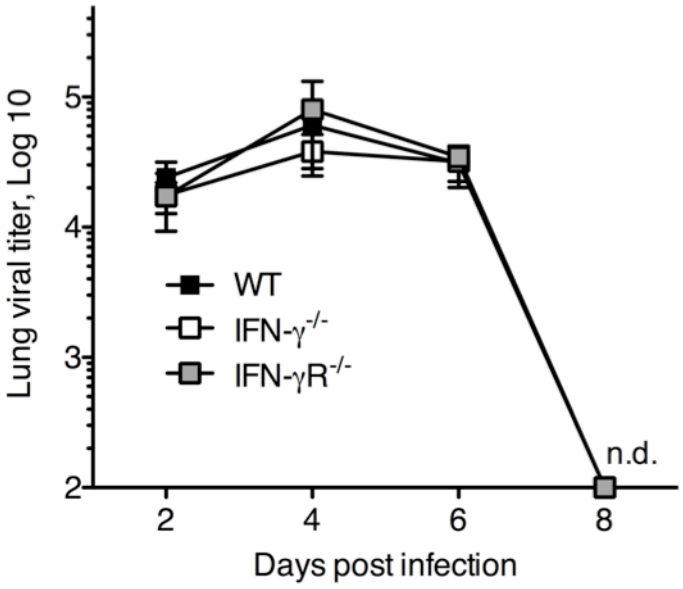

Figure 4.2 Kinetics of viral clearance after 5 PFU PR/8 influenza infection

C57BL/6 WT, IFN-$\gamma^{-/-}$ and IFN-$\gamma R^{-/-}$ mice were infected with 5 PFU of influenza A/PR/8/34. The viral loads in the lung tissue of the infected mice were measured with a plaque assay over a period of 8 days after infection. Data represent mean +/- SEM. n=6-10/group

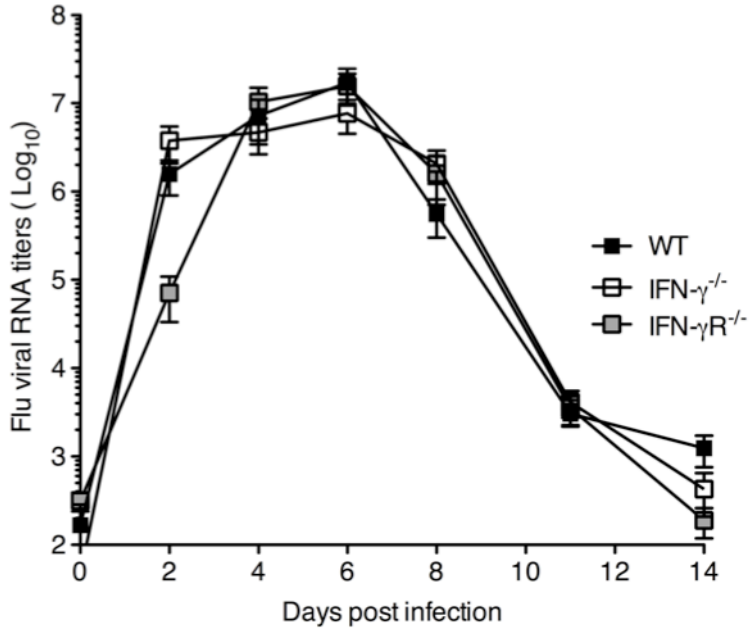

Figure 4.3 Kinetics of viral RNA after 5 PFU PR/8 influenza infection

C57BL/6 WT, IFN-$\gamma^{-/-}$ and IFN-$\gamma R^{-/-}$ mice were infected with 5 PFU of influenza A/PR/8/34. The viral RNA in the lung tissue of the infected mice was measured over a period of 14 days after infection by qRT-PCR. Graph showing relative RNA levels of viral M-protein in the lungs of infected mice. Data represent mean +/- SEM n= 5 mice/group.

4.3 Th2 responses to influenza in the absence of IFN-γ signaling

IFN-γ is the hallmark of a Th-1 response. In the absence of IFN-γ, CD4 T cells are known to polarize to a Th2 phenotype (Maggi et al. 1992). Influenza elicits a strong Th1 response. We wanted to check if there was a tendency to skew the response to Th2 in the absence of IFN-γ signaling. Since influenza is a respiratory infection, the appearance of a Th2 phenotype can be measured by the presence of Th2 cytokines in the BAL fluid as well as the presence of eosinophils in the airways.

4.3.1 Cellular infiltration in the airways of the IFN-$\gamma^{-/-}$ and IFN-$\gamma R^{-/-}$ mice after 5 PFU PR/8 infection

We studied cellular infiltration into the airways of infected mice in the absence of IFN-γ signaling. The BAL fluid was harvested from the airways of the infected mice with the same protocol as described in Chapter 3.3 and the cells in the pellet analyzed by flow cytometry. The supernatant was saved and the levels of cytokines measured.

In the infected WT mice, a very low count of eosinophils was seen in the BAL after influenza infection (Figure 3.2). We found that airways of both IFN-$\gamma^{-/-}$ and IFN-$\gamma R^{-/-}$ mice had significantly higher infiltration of eosinophils when compared to the WT mice at days 8, 11 and 14 after influenza infection. The numbers of eosinophils peaked at day 11 p.i. but reduced only slightly at day 14 p.i. (Figure 4.4). The presence of significant numbers of eosinophils in the IFN-$\gamma^{-/-}$ and IFN-$\gamma R^{-/-}$ mice indicates that there may be a slight bias towards a Th2 phenotype in the absence of IFN-γ signaling. IFN-$\gamma^{-/-}$ mice also had an increased level of macrophages at day 11 and 14 p.i. (Figure 4.4B). The

numbers of neutrophils however, were similar to what was observed in the WT mice (Figure 4.4C).

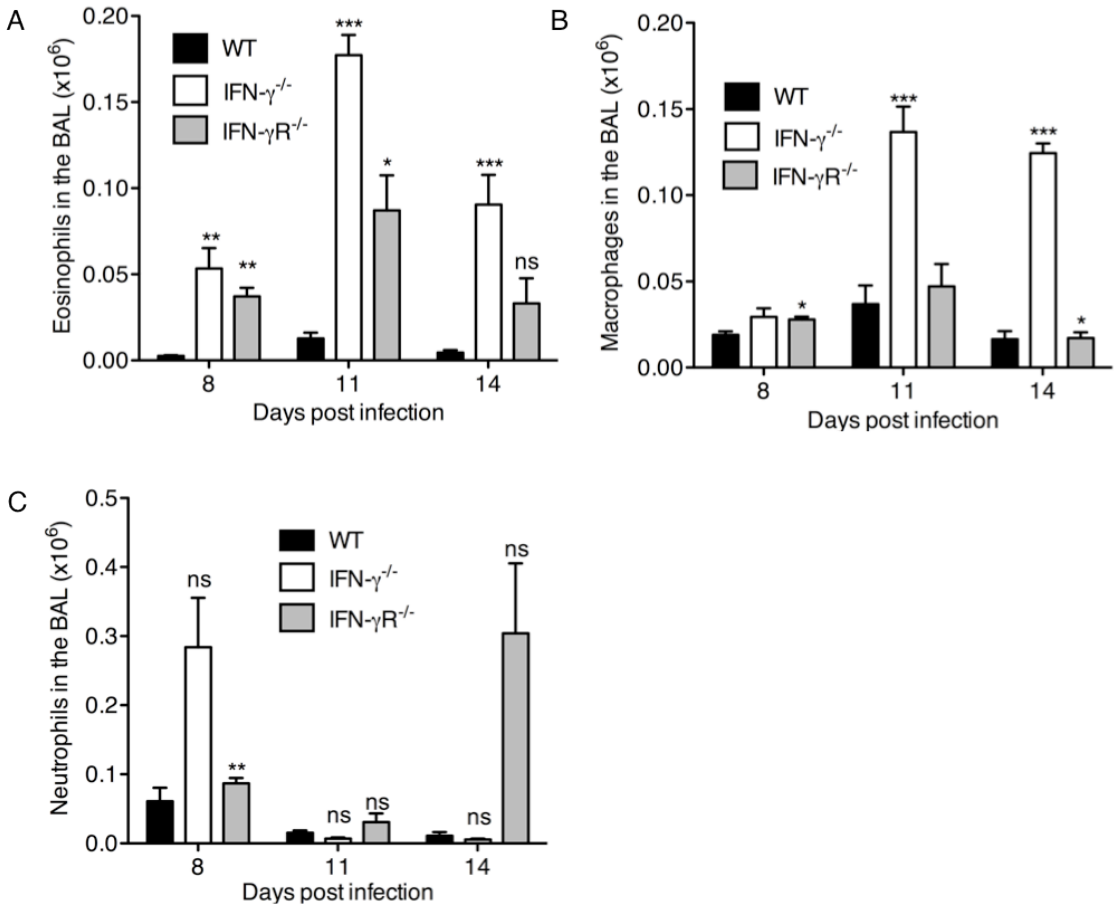

Figure 4.4 Cellular infiltration in the lung airways of WT, IFN-$\gamma^{-/-}$ and IFN-$\gamma R^{-/-}$ mice after 5 PFU influenza infection

C57BL/6 WT, IFN-$\gamma^{-/-}$ and IFN-$\gamma R^{-/-}$ mice were infected with 5 PFU of influenza A/PR/8/34. BAL fluid was harvested from infected mice at different time points after infection. Cells from the BAL fluid were counted and stained with anti-CD3, anti-CD11c, anti-Ly6G and anti-SiglecF and then analyzed by flow cytometry. Kinetics of (A) Eosinophils ($CD11c^{-}$ $SiglecF^{+}$)
(B) Macrophages ($CD11c^{+}$ $SiglecF^{+}$) and
(C) Neutrophils ($CD11c^{-}$ $Ly6G^{+}$) at days 8, 11 and 14 following 5 PFU PR/8 infection Data represent mean+/- SEM of 10 mice.

4.3.2 Comparison of Th2 cytokine levels in the lung airways of infected mice

We compared the various cytokines present in the airways of the infected mice by measuring the cytokine levels in the BAL fluid of WT and IFN-$\gamma^{-/-}$ mice at different time-points after 5PFU PR/8 infection. The supernatants from the BAL fluid samples were used to measure the cytokines by ELISA.

Significantly higher levels of IL-5 were found in the IFN-$\gamma^{-/-}$ mice at day 8 p.i. (Figure 4.5A). The levels of IL-13 however did not seem to be different on day 8 but were significantly higher in the WT mice at day 11 and day 14 p.i. It should be noted that the levels of IL-13 were below 100pg/ml (Figure 4.5B). Increased levels of IL-10 were found in the BAL fluid of the IFN-$\gamma^{-/-}$ mice at all times, although the levels of IL-10 were highest at day 8 p.i (Figure 4.5C). This indicated that there was a moderate skewing towards a Th2 phenotype in the IFN-$\gamma^{-/-}$ mice.

We also found that there was a significantly higher level of Eotaxin in the IFN-$\gamma^{-/-}$ mice on day 8 p.i (Figure 4.5D). Eotaxin is a chemotactic factor for the migration of eosinophils (Garcia-Zepeda et al. 1996). This could be the reason that there is increased infiltration of eosinophils in the airways of IFN-$\gamma^{-/-}$ mice.

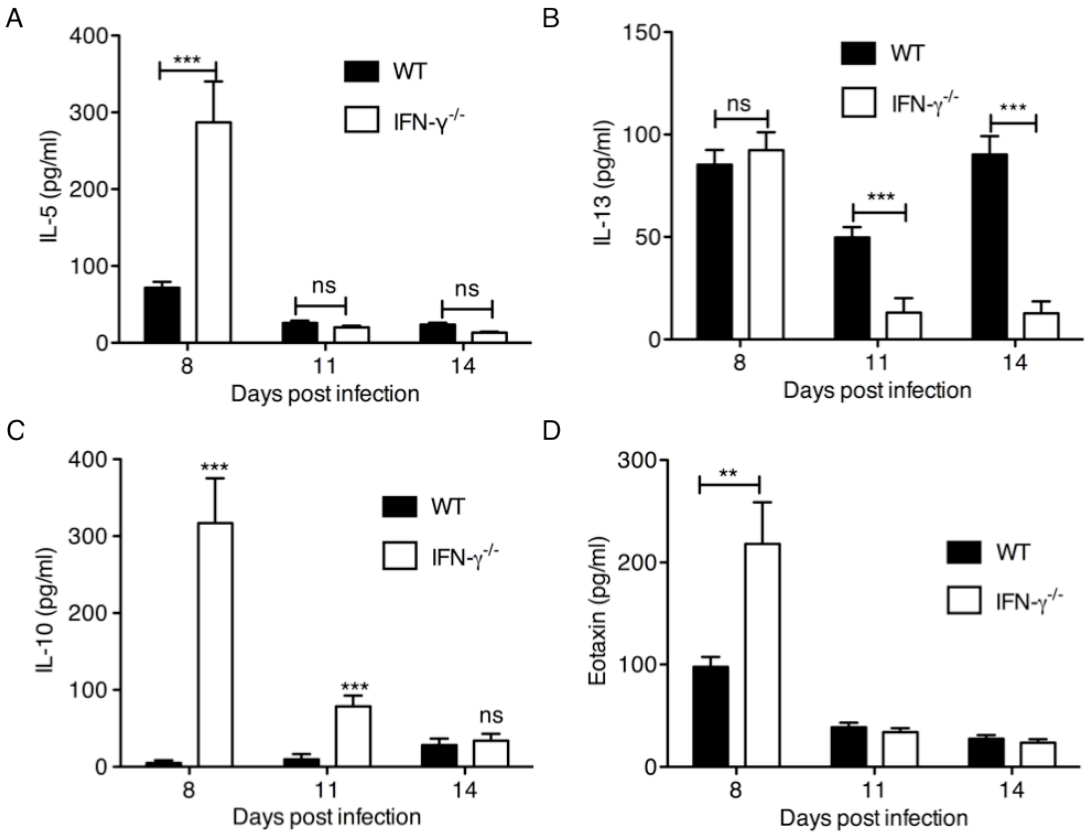

Figure 4.5 Cytokine profiles in the airways of the influenza infected mice detected by ELISA

C57BL/6 WT and IFN-$\gamma^{-/-}$ mice were infected with 5 PFU of influenza A/PR/8/34. The BAL fluid was harvested from infected mice at days 8,11 and 14 after infection. The levels of different cytokines (A) IL-5, (B) IL-13, (C) IL-10 and (D) Eotaxin were measured in the supernatant using ELISA.
Data represent mean +/- SEM of 10 mice.

4.4 Adaptive immune responses to influenza

In order to study the roles of IFN-γ signaling on the adaptive immune response to influenza and specifically on the T cell response, we compared the T cell responses between the WT, IFN-$\gamma^{-/-}$ and IFN-$\gamma R^{-/-}$ mice after 5PFU PR/8 influenza infection.

4.4.1 $CD8^+$ T cell responses to influenza in the absence of IFN-γ signaling

$CD8^+$ T cells respond to an influenza infection by killing virus infected cells and hence are important for viral clearance (Bender et al. 1992). $CD8^+$ T cells form the majority of the cellular infiltrate in the lung at later time points after infection (Lawrence et al. 2005). The $CD8^+$ T cell response affects not only viral clearance but also the extent of inflammation in the lungs of the infected host as well. Earlier studies in our laboratory have shown that the influenza-specific $CD8^+$ T cell response is initiated in the posterior mediastinal lymph node that drains the lung (Ho et al. 2011). Although $CD8^+$ T cells start to proliferate and get activated in the lymph nodes as early as day 5 p.i, they reach the lung only slightly later. From the kinetics of cell infiltration in the BAL fluid (Figure 3.3), it was evident that the $CD3^+$ T cells start to accumulate in the lung tissue only 7-8 days after infection. Hence, we looked at days 8, 11 and 14 as suitable time-points to examine the various phases of the influenza-specific $CD8^+$ T cell response. We identified influenza-specific $CD8^+$ T cells as $CD3^+CD8^+$ T cells that bound to the MHC I pentamer NP_{366} 'ASNENMETM-H-$2K^b$', an immunodominant epitope, (ProImmune, UK). In

addition to the lung tissue, we also compared $CD8^+$ T cells in the BAL fluid to those in the lung parenchyma.

Kinetics of the antigen specific $CD8^+$ T cell response to influenza

A small percentage (2-3%) of NP_{366}^+ $CD8^+$ T cells started to accumulate in the lung tissues of the infected mice on day 8 p.i. (Figure 4.6A). This frequency increased greatly by day 11 p.i. This was a result of higher numbers of flu-specific $CD8^+$ T cells migrating to the lung as well as the proliferation of the $CD8^+$ T cells in the lung itself (McGill et al. 2008; McGill and Legge 2009). But at day 14 p.i., the frequencies of the flu-specific $CD8^+$ T cells in the lungs of the WT mice had started to decline. This decline in frequencies of flu-specific $CD8^+$ T cells was not seen in the lungs of the IFN-$\gamma^{-/-}$ and IFN-$\gamma R^{-/-}$ mice.

A similar trend was observed when the total numbers of the antigen-specific $CD8^+$ T cells in the BAL fluid (figure 4.6 B) and lung tissue was calculated (figure 4.6 C) Although a similar number of NP_{366}^+ $CD8^+$ T cells were present in the lungs of all the infected mice on day 8 p.i., it was only at day 11 p.i., that the cell numbers peaked. There were no differences in the numbers of flu-specific $CD8^+$ T cells in the lungs of the WT and the IFN-γ signaling-deficient animals on days 8 or 11. This showed that the expansion and the peak phases of the response were unaffected by the absence of IFN-γ or IFN-γR. On day 14 p.i., however, the numbers of NP_{366}^+ $CD8^+$ T cells in the lungs of the WT mice showed a decline, marking the contraction phase of the response. However, this phenomenon was not observed in the lungs of the IFN-$\gamma^{-/-}$ and IFN-$\gamma R^{-/-}$ mice and the numbers of NP_{366}^+ $CD8^+$ T cells were higher than what was

observed in the WT mice, indicating that the absence of IFN-γ signaling might have an affect on the contraction phase of the antigen-specific $CD8^+$ T cell response to influenza. Although the numbers of NP_{366}^+ $CD8^+$ T cells were smaller than what was observed in the lung tissue, their kinetics in the BAL fluid showed a similar pattern, emulating what was observed in the lung tissue (Figure 4.6 B).

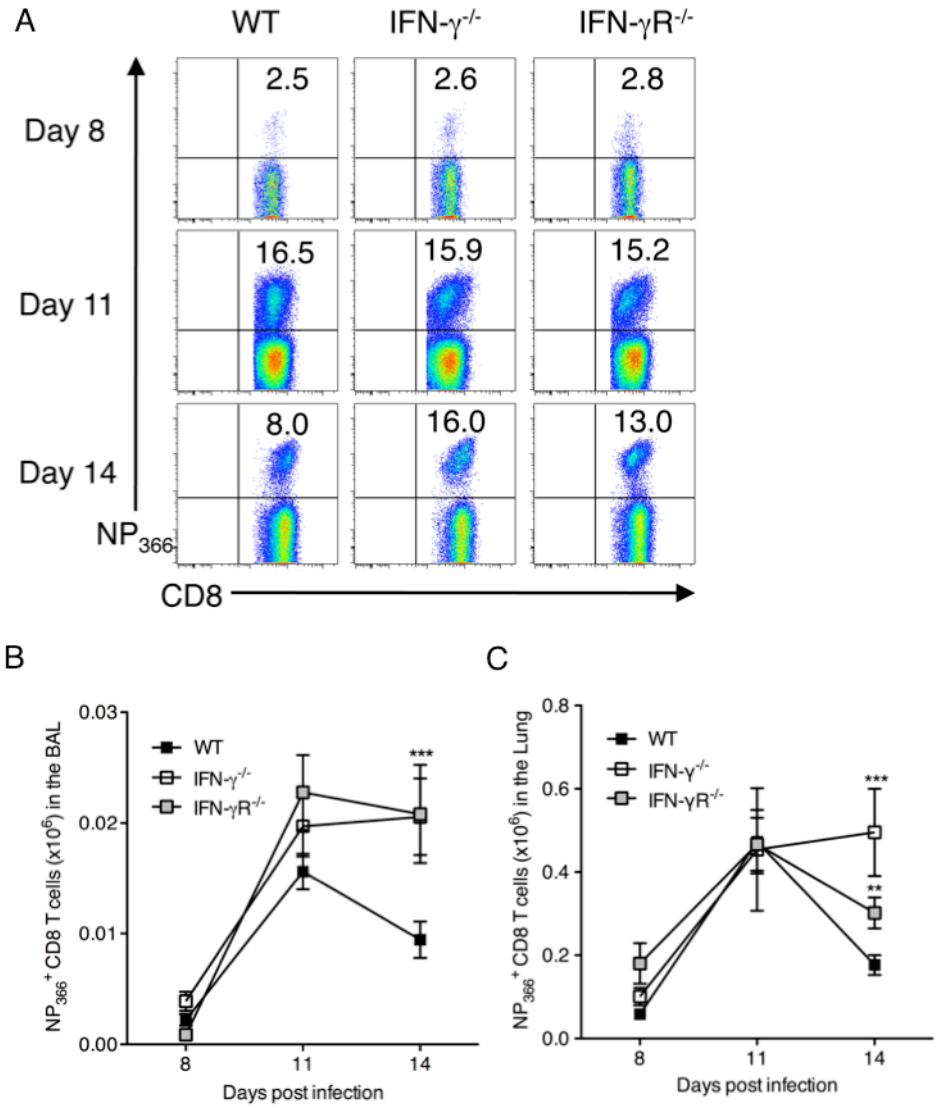

Figure 4.6 Kinetics of antigen specific $CD8^+$ T cells in BAL and lungs of IFN-$\gamma^{-/-}$ and IFN-$\gamma R^{-/-}$ mice after influenza infection

C57BL/6 WT, IFN-$\gamma^{-/-}$ and IFN-$\gamma R^{-/-}$ mice were infected with 5 PFU of influenza A/PR/8/34. BAL and lungs were harvested on the indicated days and cells stained with anti-CD3, anti-CD8 and H2-D^b NP_{366} pentamer on the indicated days. (A) Representative flow cytometry plots of the proportion of $CD8^+$ T cells specific for NP_{366} (ASNENMETM) in the lung tissue of WT, IFN-$\gamma^{-/-}$ mice and IFN-$\gamma R^{-/-}$ mice. Cells are gated on $CD3^+CD8^+$ T cells. Numbers represent percentages of $CD8^+$ T cells in the lungs, which are NP_{366}^+. Total NP_{366}^+ $CD8^+$ T cell numbers in the BAL fluids (B) and lung tissues (C) across a time-course following influenza infection in the WT, IFN-$\gamma^{-/-}$ and IFN-$\gamma R^{-/-}$ mice. Data are pooled from three independent experiments with 4-5 mice/group/experiment (*$p<0.05$ and **$p<0.001$ determined using Mann-Whitney test).

4.5 Effects of IFN-γ deficiency on the function of influenza-specific $CD8^+$ T cells

The most important effector functions of $CD8^+$ T cells in the context of an influenza infection are killing of virus-infected cells and the production of cytokines. We wanted to assess the role of IFN-γ in regulating these two functions. Hence, we decided to compare the cytotoxic killing ability and the cytokine secretion capabilities of the $CD8^+$ T cells in the WT and the IFN-γ-signaling deficient mice.

4.5.1 Cytotoxic killing ability of influenza-specific $CD8^+$ T cells

We compared the cytotoxic potential of the NP_{366}^+ $CD8^+$ T cells isolated from the lungs of infected WT, IFN-$\gamma^{-/-}$ and IFN-$\gamma R^{-/-}$ mice by the expression of the degranulation marker CD107α in these $CD8^+$ T cells at days 7 and 11 after influenza infection. A higher percentage of NP_{366}^+ $CD8^+$ T cells expressed CD107α on day 7 compared to day 11 p.i. This is probably due to the fact that higher viral loads are present at day 7 and the cytotoxic ability is more relevant at this timepoint. On day 7, all the NP_{366}^+ $CD8^+$ T cells had similar levels of degranulation, measured by the accumulation of CD107α on the cell surface (Figure 4.7A). On day 11 however, we observed that the IFN-$\gamma^{-/-}$ $CD8^+$ T cells had a slightly reduced expression of CD107α (Figure 4.7B). Since this was quite variable, this set of experiments was repeated many times. It was observed that the levels of CD107a expression was slightly reduced compared to the WT, in the IFN-$\gamma^{-/-}$ mice but not in the IFN-$\gamma R^{-/-}$ mice. Since CD107α is only a marker of the potential to kill, we decided to compare the actual killing ability by using the chromium (^{51}Cr) release assay. This assay would be more relevant and accurate in determining the differences in the cytotoxicities of the

cells and hence the role of IFN-γ in influencing the killing ability of the influenza -specific $CD8^+$ T cells.

The ^{51}Cr release was measured in the ^{51}Cr labeled peptide pulsed target cells after incubation with $CD8^+$ T cells harvested from infected lungs at different target to effector ratios. The killing assay revealed that there were no differences in the killing ability of the NP_{366} $CD8^+$ T cells from the WT, IFN-$\gamma^{-/-}$ and the IFN-$\gamma R^{-/-}$ mice on day 7 (Figure 4.7 C) or day 11 (Figure 4.7 D). These results suggested that although IFN-γ may influence the expression of CD107α, IFN-γ signaling does not affect the killing ability of the influenza-specific $CD8^+$ T cells. This also indicates that although there were higher frequencies of antigen-specific $CD8^+$ T cells in the lungs of the infected IFN-$\gamma^{-/-}$ and IFN-$\gamma R^{-/-}$ mice, these cells were not deficient in their killing ability.

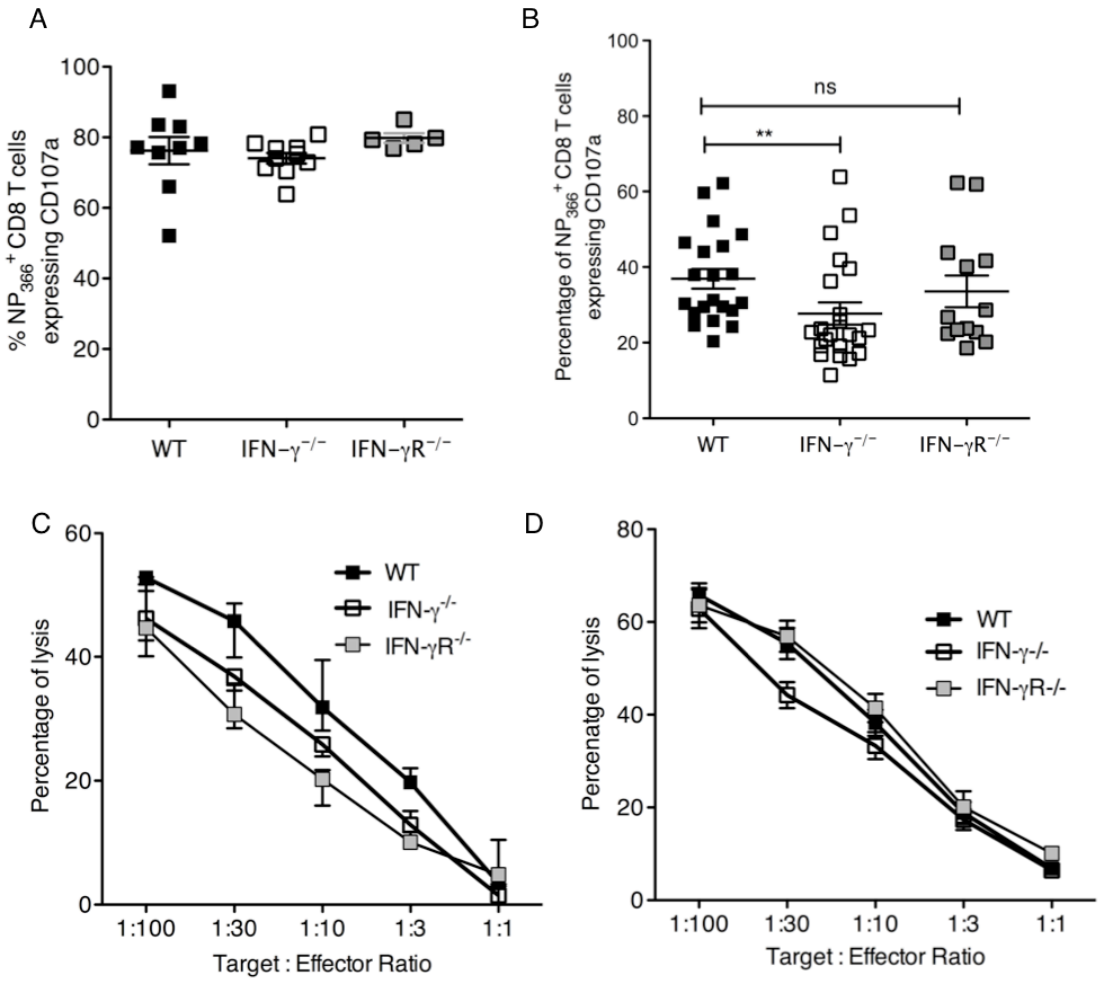

Figure 4.7 IFN-γ deficiency does not affect the killing ability of antigen-specific CD8$^+$ T cells after influenza infection

C57BL/6 WT, IFN-$\gamma^{-/-}$ and IFN-$\gamma R^{-/-}$ mice were infected with 5 PFU of influenza A/ PR/8/34 and CD107α expression was measured on the $NP_{366}{}^+$ $CD8^+$ T cells on days 7 (**A**) and 11 p.i. (**B**) . Graphs representing the percentage of $NP_{366}{}^+$ CD8 T cells expressing CD107α in the lungs of the infected mice are shown (**A & B**). Cytotoxic profiles of $CD8^+$ T cells from the lung on day 7 (**C**) and day 11 p.i (**D**) determined by ^{51}Cr assay, expressed as percentage of specific lysis of target cells. (*$p<0.05$ and **$p<0.001$ determined using Student's t test).

4.5.2 Cytokine secretion by influenza-specific $CD8^+$ T cells

From the cytokines detected by ELISA in the BAL fluid of infected WT mice (Figure 3.4), we found that the level of cytokines is at the maximum around day 7-8 p.i., when some of the virus is still present. Although there were fewer $CD8^+$ T cells in the lung tissue around this time as compared to the peak of the response, the levels of cytokines secreted seemed to be quite high indicating that the T cells secrete much of their cytokines around this point. In order to assess if IFN-γ influenced the secretion of other cytokines by the $CD8^+$ T cells, we compared the levels of cytokines IL-2, TNF-α and IFN-γ made by the NP_{366}^+ $CD8^+$ T cells in the lungs of the WT, IFN-$\gamma^{-/-}$ and the IFN-$\gamma R^{-/-}$ mice, upon *ex vivo* stimulation with NP_{366} peptide.

Both the WT and IFN-$\gamma R^{-/-}$ $CD8^+$ T cells produced IFN-γ at day 8, although the levels produced by the IFN-$\gamma R^{-/-}$ $CD8^+$ T cells were slightly higher (Figure 4.8A). No differences were observed in the production of IL-2 and TNF-α (Figure 4.8 B, C). When we looked at the ability of these cells to produce cytokines on day 11 p.i., we could not detect any cytokine production by the flu-specific $CD8^+$ T cells. This is in agreement with our earlier data where the levels of IFN-γ and TNF-α are very low in the BAL fluids at the later phases of the $CD8^+$ T cell response in the lung.

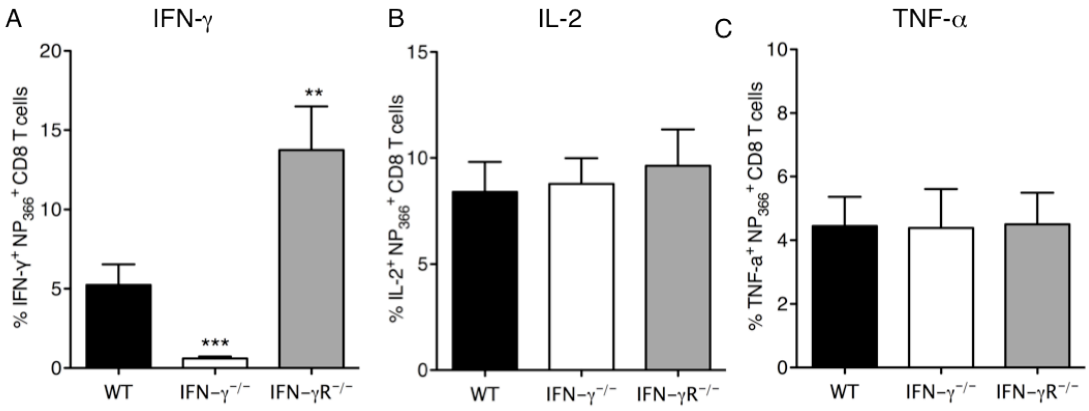

Figure 4.8 IFN-γ deficiency does not affect the ability of antigen-specific CD8$^+$ T cells to produce cytokines after influenza infection.

C57BL/6 WT, IFN-$\gamma^{-/-}$ and IFN-$\gamma R^{-/-}$ mice were infected with 5PFU of influenza A/ PR/8/34 and cytokine secretion by the $NP_{366}{}^+ CD8^+$ T cells were measured on day 8 p.i. Graphs representing the percentages of $NP_{366}{}^+ CD8^+$ T cells from the lungs expressing IFN-γ (A), IL-2 (B) and TNF-α (C) after ex vivo stimulation with NP_{366} peptide for 6h are shown (*$p<0.05$ and **$p<0.001$ determined using Student's t test).

4.5.3 Transcription factors in the influenza-specific $CD8^+$ T cells

Transcription factors like T-bet and Eomesodermin (eomes) play an important role in regulating the properties of $CD4^+$ and $CD8^+$ T cells. While T-bet is associated with Th1 responses, GATA-3 is associated with Th2 responses in $CD4^+$ T cells. Since earlier studies show that IFN-γ is known to have a direct effect on levels of T-bet in $CD4^+$ T cells, we decided to look at the levels of T-bet and its paralogue eomes in the NP_{366}^+ $CD8^+$ T cells in the lungs of the WT and the IFN-$\gamma^{-/-}$ mice. Since the levels of cytotoxicity as well as cytokine secretion were highest at day 7 p.i., we decided to look at the levels of these transcription factors at the day 7 p.i. (Figure 4.9)

At day 7 p.i, almost all the NP_{366}^+ $CD8^+$ T cells expressed T-bet and neither the number of cells expressing T-bet or the level of expression were affected by the absence of IFN-γ signaling (Figure 4.9A, B, D). No significant differences were observed in the levels of T-bet between the NP_{366}^+ $CD8^+$ T cells in the lungs of the WT and IFN-$\gamma^{-/-}$, whether in the percentage of cells expressing T-bet or in their MFI. However, there was a slight decrease in the number of eomes-producing flu-specific $CD8^+$ T cells in the absence of IFN-γ (Figure 4.9 A, C). The levels of expression of Eomes were lower as well, as measured by the MFI of the cells (Figure 4.9 E).

This difference may be attributed to the fact that eomes plays a more important role in $CD8^+$ T cells than T-bet. Although IFN-γ influences the levels of eomes, this difference does not seem to reflect in the functional

capabilities of the $CD8^+$ T cells after an influenza infection, since the levels of cytotoxicity and cytokines expressed were not significantly different.

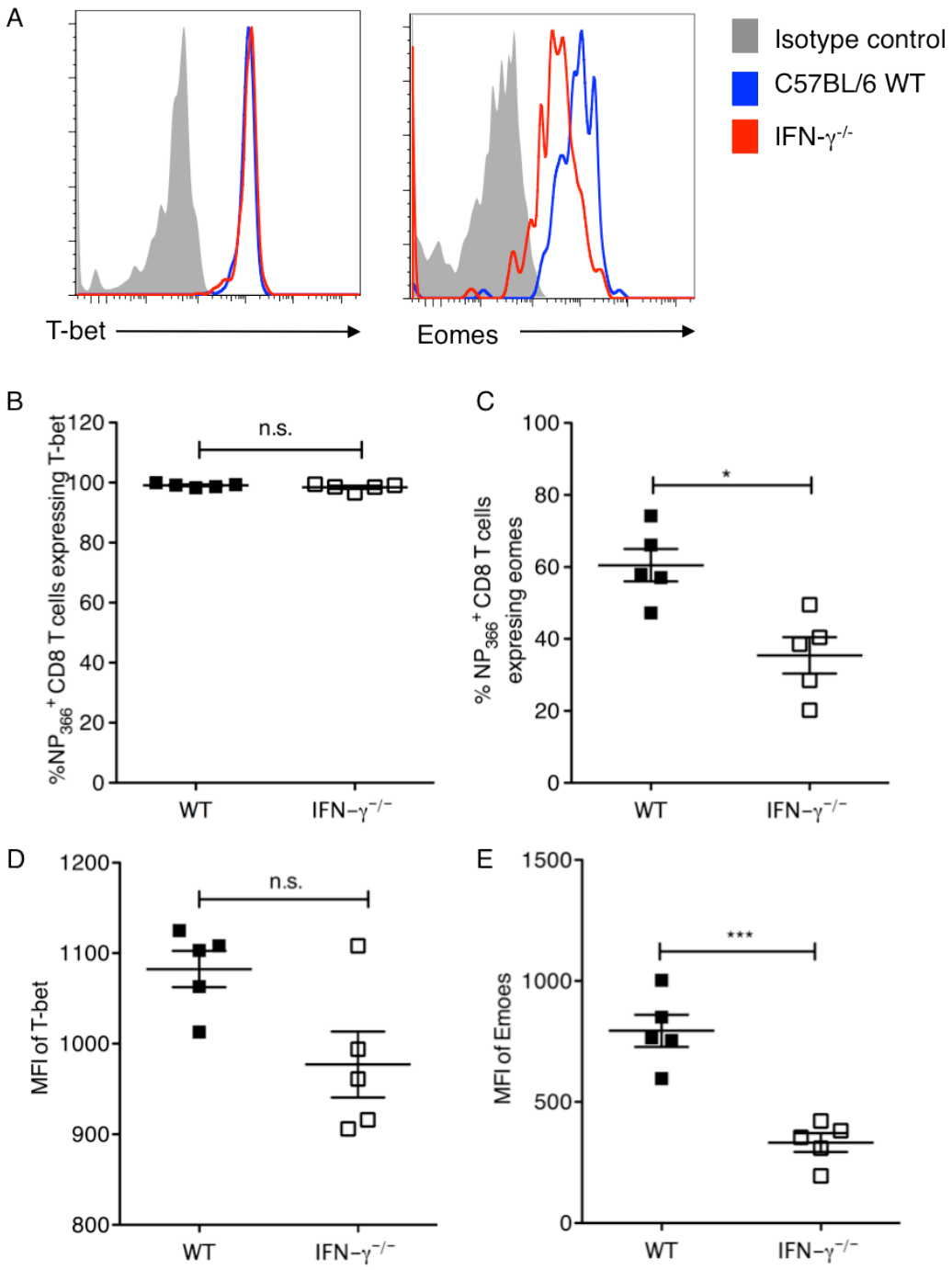

Figure 4.9 IFN-γ deficiency affects the transcription factors produced by the antigen-specific CD8$^+$ T cells after influenza infection

C57BL/6 WT and IFN-γ$^{-/-}$mice were infected with 5 PFU of influenza A/ PR/8/34 and levels of transcription factors in the NP_{366} $^+$ $CD8^+$ T cells were measured by Intracellular staining on day 7 p.i. (A) Representative histograms showing the expression of transcription factors, T-bet and Eomesodermin on the NP_{366}^+ $CD8^+$ T cells in the lung. Graphs comparing the percentages of flu-specific $CD8^+$ T cells expressing T-bet (B) and eomes (C) on day 7 p.i. Graphs comparing the expression in terms of MFI of T-bet (D) and Eomes (E) on the flu specific $CD8^+$ T cells on day 7 p.i. Data is representative of three independent experiments. (*$p<0.05$ and ***$p<0.001$ using Student's t test).

4.6 $CD4^+$ T cell responses to influenza in the absence of IFN-γ signaling

Subsequently we analyzed $CD4^+$ T cell responses in the lungs of the mice after infection. Because of the lack of MHC class II tetramers for the identification of antigen specific $CD4^+$ T cells, we could only study the total $CD4^+$ T cells in the lungs of the mice after different time points after a 5PFU PR8 infection.

To check whether the lack of IFN-γ has an effect on the $CD4^+$ T cells, we compared $CD4^+$ T cell responses to influenza in the WT, IFN-$\gamma^{-/-}$ and the IFN-$\gamma R^{-/-}$ mice. We chose similar time-points to measure the total numbers of $CD4^+$ T cells as we used for the $CD8^+$ T cells i.e. days 8, 11 and 14 after infection (Figure 4.10). We examined $CD4^+$ T cell numbers at the site of infection i.e. in the lung tissue. $CD4^+$ T cells also followed similar kinetics to the $CD8^+$ T cells, peaking at day 11 p.i. Although the kinetics seems to be similar to the $CD8^+$ T cells, the numbers of $CD4^+$ T cells are much lower than total $CD8^+$ T cell numbers in the lung tissue after infection.

$CD4^+$ T cell numbers were similar between the lungs of the WT, IFN-$\gamma^{-/-}$ and the IFN-$\gamma R^{-/-}$ mice at all the time points measured (Figure 4.10). The $CD4^+$ response was seen to be contracting on day 14 in both the WT and IFN-$\gamma^{-/-}$or IFN-$\gamma R^{-/-}$ mice. Although IFN-γ signaling plays a role in the contraction of the influenza specific $CD8^+$ T cell response, such an effect seems to be absent where the $CD4^+$ T cells are concerned.

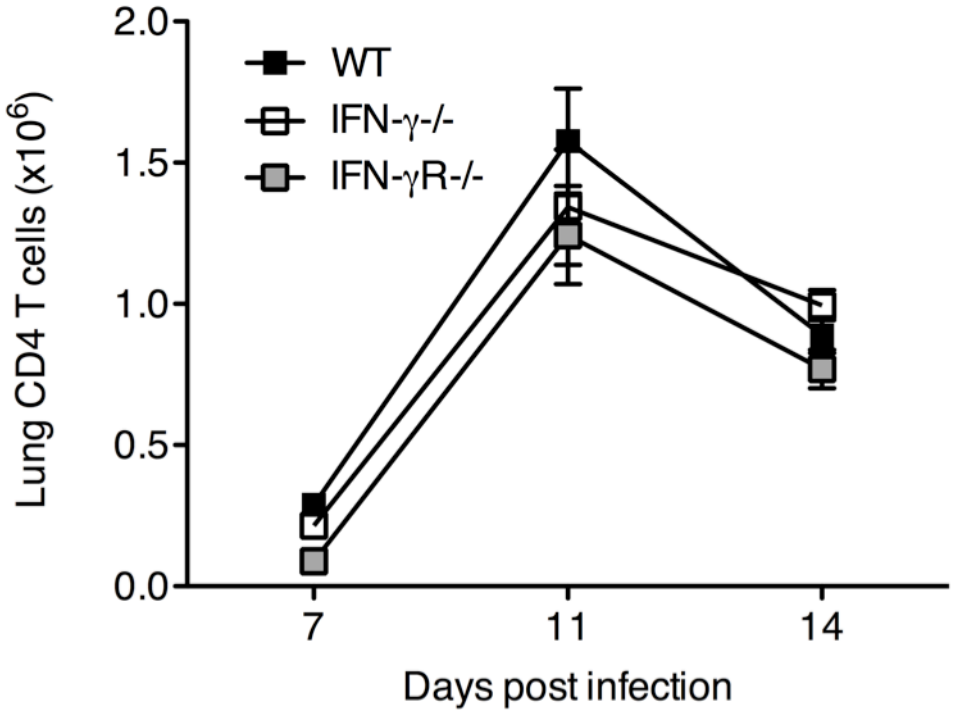

Figure 4.10 IFN-γ does not affect the total $CD4^+$ T cell responses after a 5PFU influenza infection.

C57BL/6 WT, IFN-$\gamma^{-/-}$ and IFN-$\gamma R^{-/-}$ mice were infected with 5PFU of influenza A/PR/8/34. Lungs were harvested on the indicated days and cells were stained with the anti-CD3 and anti-CD4 antibodies on the indicated days. Total $CD4^+$ T cell numbers in the lung tissue across a time-course following influenza infection in the WT, IFN-$\gamma^{-/-}$ and IFN-$\gamma R^{-/-}$ mice. Data are pooled from three independent experiments with 4-5 mice/group/experiment (*$p<0.05$ and **$p<0.001$ determined using Mann-Whitney test).

4.7 Role of IFN-γ in controlling lung damage after an influenza infection

Although there were no differences in the number of $CD8^+$ T cells in the lungs of the WT, IFN-$\gamma^{-/-}$ and IFN-$\gamma R^{-/-}$ mice infected with influenza at the expansion and peak phases of the response, there was a significant difference in the numbers of $CD8^+$ T cells persisting in the lungs of the infected mice at day 14 p.i. $CD8^+$ T cells can cause severe lung damage during a virus infection due to their ability to kill virus-infected cells and to secrete cytokines. Hence, we looked at the damage inflicted on the lungs of the infected mice at different points in time after influenza infection.

We studied the lung damage using pulmonary histopathology in lung sections of the WT, IFN-$\gamma^{-/-}$ and IFN-$\gamma R^{-/-}$ mice at different time points after influenza infection (Figure 4.11A). Using a four point system we scored lung damage blindly and compared the level of inflammatory cell infiltrate in the 3 strains (Figure 4.11B). Before the infection, the lung sections of all the mice looked normal in all three strains of mice showing that there were no gross abnormalities in the lungs in the absence of IFN-γ or IFN-γR1. By day 3 p.i, all mice exhibited a similar extent of inflammatory cell infiltration into the airways, which increased significantly by day 7 p.i. and partial resolution of inflammation was seen by day 14 p.i. The histological findings suggested that the absence of IFN-γ signaling does not affect lung damage post influenza infection.

We also examined the leakage of albumin into the BAL fluid as an indicator of lung damage (Figure 4.11C). Although we did not observe any changes after 8 days we observed slightly increased levels of albumin leakage in the BAL

fluid of WT mice when compared to the IFN-$\gamma^{-/-}$ mice on days 11 and 14, indicating that there may be decreased inflammation in the absence of IFN-γ signaling later in the infection. We concluded that the lack of IFN-γ does not grossly affect lung pathology and although there was abnormal contraction of $CD8^{+}$ T cells in the IFN-$\gamma^{-/-}$ mice, this did not exacerbate the immunopathology due to influenza infection.

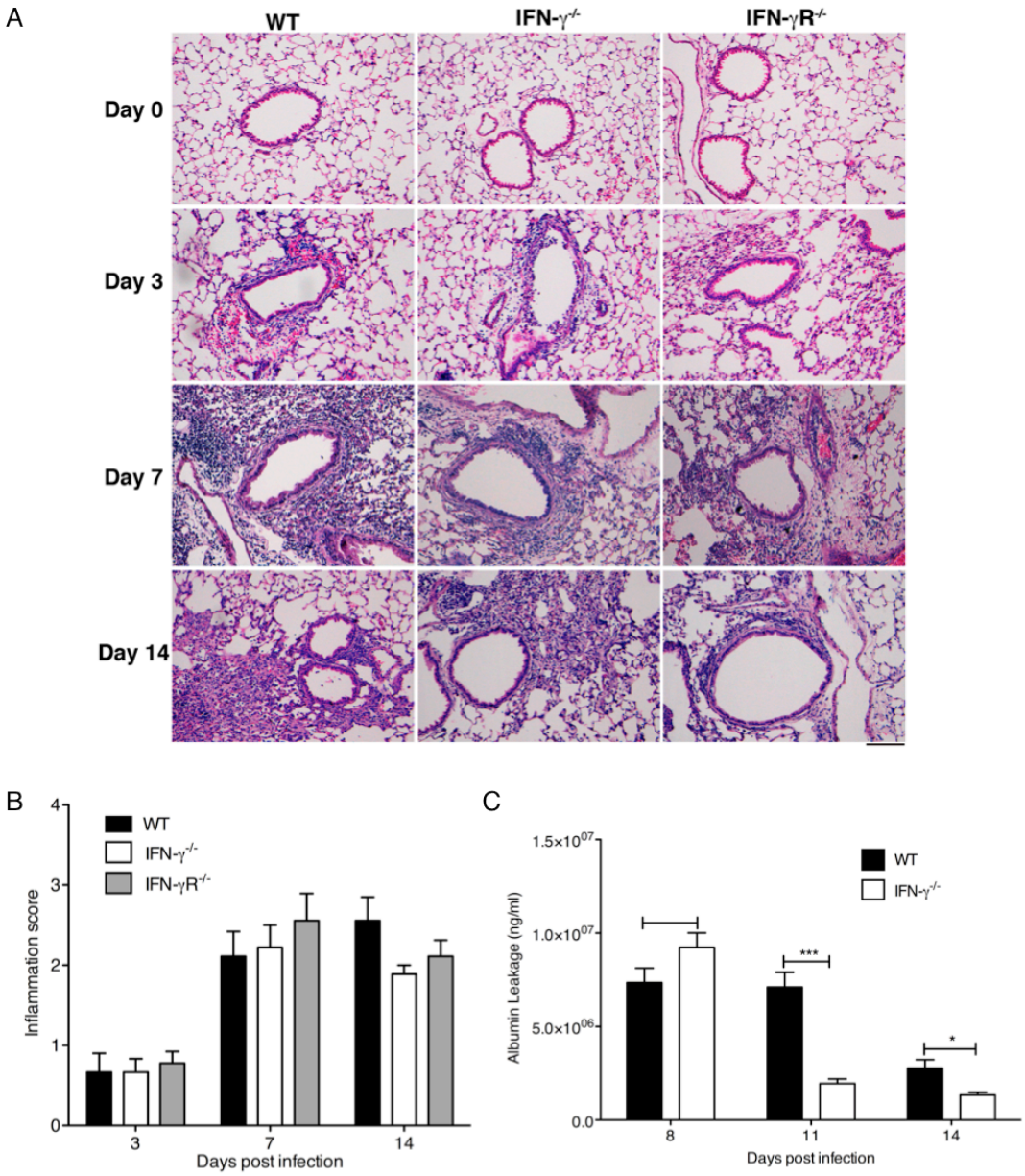

Figure 4.11 IFN-γ or IFN-γR deficiency does not lead to changes in the lung damage due to a 5PFU influenza infection.

C57BL/6 WT, IFN-$\gamma^{-/-}$ and IFN-$\gamma R^{-/-}$mice were infected with 5PFU of influenza A/ PR/8/34 and the lungs perfused and harvested before infection (day 0) or on days 3,7 and 14 p.i. for Hematoxylin and Eosin (H&E) staining. Representative images for the H&E sections are shown (**A**). The lung sections scored blind, using a 5-point scoring system as follows **0**- no infiltrating cells, **1**-only1-2 airways or vessels have cell infiltration (<3 cell deep), **2**- 25-50% of the whole section has inflammation (>3 cell deep), **3**-50-75% of the whole section has inflammation (>3 cell deep), **4**- >75% of the whole section has inflammation (>3 cell deep). Multiple lung sections were scored per lung and 3 lungs were scored per group per time point and the means +/- SEM were plotted (**B**). (**C**) Albumin leakage into the BAL fluid of the infected mice was measured using ELISA at days 8, 11 and 14 p.i..

4.8 IFN-γ influences the contraction phase of the $CD8^+$ T cell response

We observed from our previous experiments (Figure 4.6) that the levels of influenza-specific $CD8^+$ T cells were higher in IFN-$\gamma^{-/-}$ and IFN-$\gamma R^{-/-}$ mice at day 14 p.i., after resolution of the infection. Due to this, we hypothesized that IFN-γ played a role in regulating the contraction phase of the flu-specific $CD8^+$ T cell response. In order to confirm this, we examined influenza-specific $CD8^+$ T cell responses on day 28 p.i. This is a time-point at which all the mice have essentially recovered from the infection and the $CD8^+$ T cell response should have contracted considerably. In the lungs of the WT mice, we observed a much-reduced number of NP_{366}^+ $CD8^+$ T cells, than was seen on day 14 p.i. But the numbers of NP_{366}^+ $CD8^+$ T cells in the BAL of the IFN-$\gamma^{-/-}$ and IFN-$\gamma R^{-/-}$ mice were much higher than what was observed in the WT mice (Figure 4.12A). A similar trend was observed in the NP_{366}^+ $CD8^+$ T cells in the lung tissue (Figure 4.12B) and in the spleens of these mice (Figure 4.12C). This confirmed our hypothesis that IFN-γ signaling plays an important role in the contraction of the antigen-specific $CD8^+$ T cell response after influenza infection and that the absence of IFN-γ signaling leads to a defective contraction phase in these mice.

To further determine the extent of the reduced contraction, we also looked at a much later time point i.e. day 120 p.i. At this time point, the numbers of antigen-specific $CD8^+$ T cells in the lungs (Figure 4.13A) and spleens (Figure 4.13B) of the infected mice were higher in the IFN-γ and IFN-γR deficient mice, indicating not only a reduced contraction phase in the absence of IFN-γ signaling, but also an increased memory $CD8^+$ T cell population in the lungs and spleens of the deficient mice.

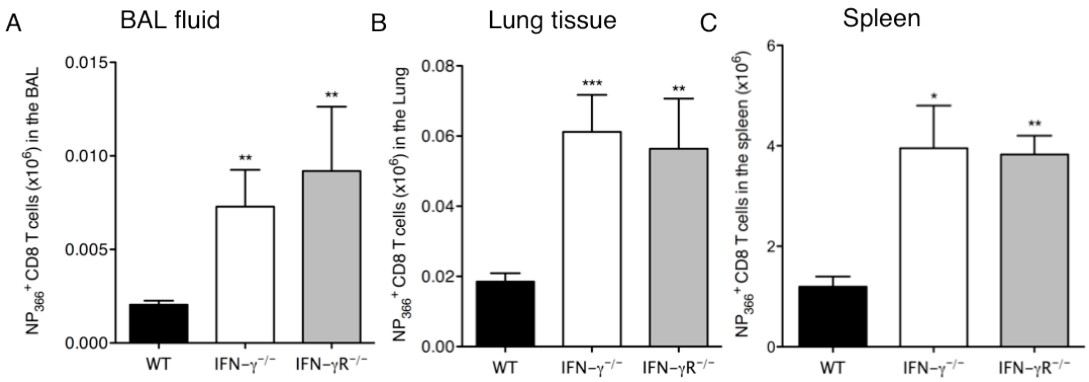

Figure 4.12 Reduced contraction of antigen-specific $CD8^+$ T cell responses in IFN-$\gamma^{-/-}$ and IFN-$\gamma R^{-/-}$ mice after influenza infection.

C57BL/6 WT, IFN-$\gamma^{-/-}$ and IFN-$\gamma R^{-/-}$ mice were infected with a 5PFU dose of influenza A/PR/8/34. NP_{366}^+ $CD8^+$ T cell numbers were examined in the BAL fluid (A) and lung tissue (B) and spleens (C) of the mice on day 28 p.i. The numbers of $CD8^+$ NP_{366}^+ cells (mean+/-SEM) shown are calculated from the total counts and the percentages of cells staining positive. (*$p<0.05$ and **$p<0.001$ determined using Student's t test). Data are representative of at least 3 independent experiments with n=4-5 per group.

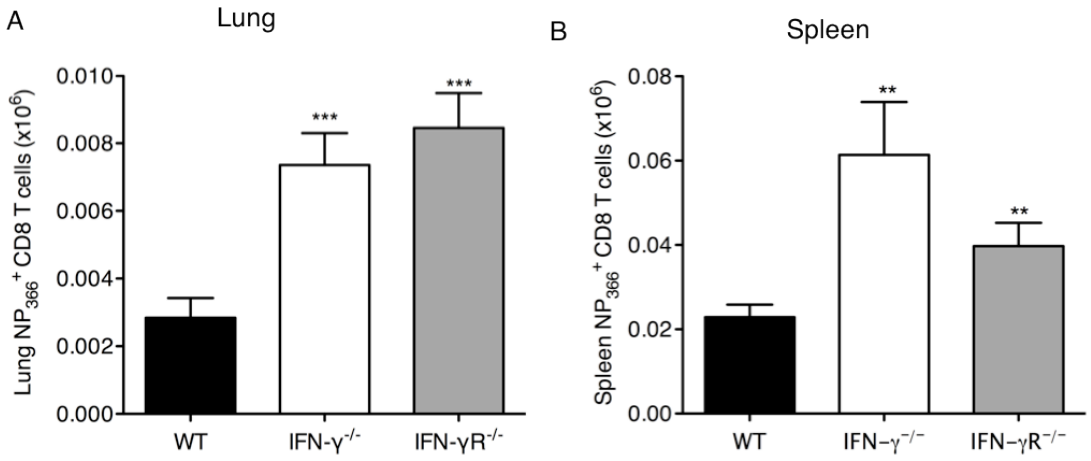

Figure 4.13 Reduced contraction of antigen-specific $CD8^+$ T cell responses and increased memory cells in IFN-$\gamma^{-/-}$ and IFN-$\gamma R^{-/-}$ mice after influenza infection.

C57BL/6 WT, IFN-$\gamma^{-/-}$ and IFN-$\gamma R^{-/-}$ mice were infected with a 5PFU dose of influenza A/PR/8/34. NP_{366}^+ $CD8^+$ T cell numbers were examined in the lung tissue (**A**) and spleens (**B**) of the mice on day 120 p.i. The numbers of $CD8^+$ NP_{366}^+ cells (mean+/-SEM) shown are calculated from the total counts and the percentages of cells staining positive. (*$p<0.05$ and **$p<0.001$ determined using Student's t test). Data are representative of 2 independent experiments with n=4-5 per group.

4.9 Memory T cell distribution in the absence of IFN-γ signaling

After the resolution of the infection, the $CD8^+$ T cell response contracts and only some of the cells survive to form the memory population. The magnitude of the memory cell pool is a function of both the expansion and subsequent contraction of the $CD8^+$ T cell response. Memory cells are differentiated into central and effector memory cell types based on their expression of CD62L (or CCR7). Since the number of influenza specific $CD8^+$ T cells was significantly increased in the absence of IFN-γ signaling, we next examined the memory distribution of the NP_{366}^+ memory $CD8^+$ T cells in the lungs and spleens of the WT, IFN-$\gamma^{-/-}$ and IFN-$\gamma R^{-/-}$ mice.

At day 28 p.i, higher frequencies of effector memory ($CD62L^{low}$) than central memory ($CD62L^{high}$) NP_{366}^+ $CD8^+$ T cells were observed in the lung tissue of the WT, IFN-$\gamma^{-/-}$ and IFN-$\gamma R^{-/-}$ mice. However, the increased numbers of NP_{366}^+ $CD8^+$ T cells in the lungs of IFN-$\gamma^{-/-}$ and IFN-$\gamma R^{-/-}$ mice were equally distributed in both the effector and central memory compartments in the lung tissue (Figure 4.14A, B). This trend was observed even at day 120 p.i. (Figure 4.14D), although a higher frequency of cells showed the central memory phenotype ($CD62L^{high}$) (Figure 4.14C). This clearly indicated that IFN-γ did not affect the distribution of NP_{366}^+ $CD8^+$ T cells in the different memory cell compartments at the site of infection.

When we looked at the spleens (Figure 4.15), however, we observed that there was a higher frequency of effector memory $CD8^+$ T cells in the IFN-$\gamma^{-/-}$ and IFN-$\gamma R^{-/-}$ mice as compared to the WT mice. This was clearly reflected even in the total number of effector memory $CD8^+$ T cells in the spleen. This indicated

that IFN-γ influenced the expression of CD62L on the antigen specific $CD8^+$ T cells, hence causing an accumulation of $CD62L^{low}$ cells.

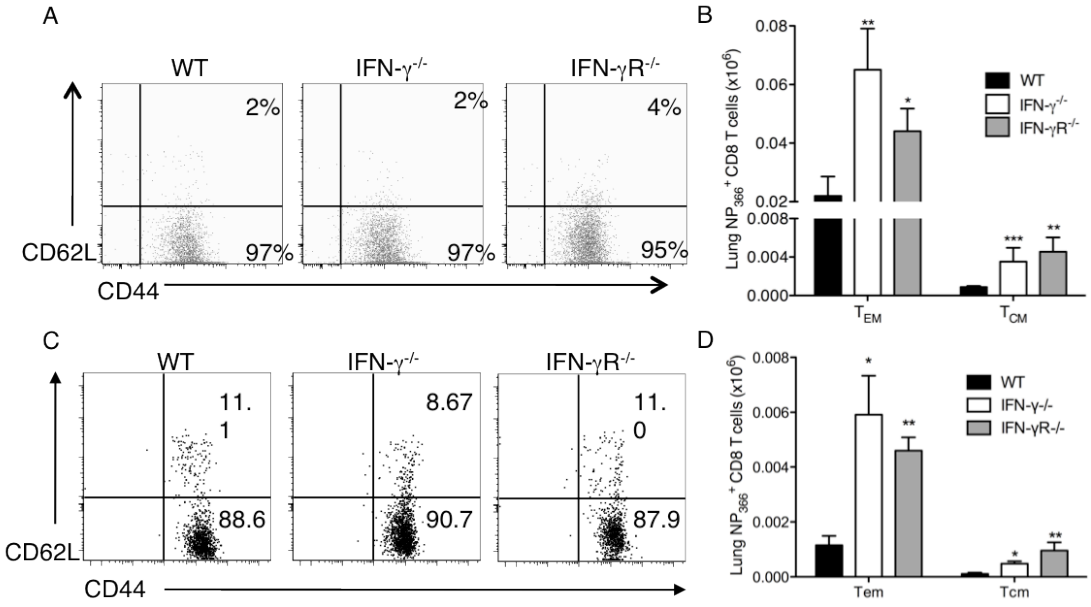

Figure 4.14 Unaltered distribution NP_{366}^{+} cells in the different memory compartments in the IFN-$\gamma^{-/-}$ and IFN-$\gamma R^{-/-}$ mice

NP_{366}^{+} $CD8^{+}$ T cells were examined in the lung tissue of mice on day 28(A & B) and day 120 p.i. (C & D) for their expression of CD44 and CD62L. Representative flow cytometry plots are shown (A and C). The numbers of effector memory ($CD44^{hi}CD62L^{lo}$) and central memory ($CD44^{hi}CD62L^{hi}$) $CD8^{+}$ NP_{366}^{+} cells (mean+/-SEM) shown were calculated from the total counts and the percentage of cells staining positive in the lungs of the infected mice on day 28 (B) and 120 (D) p.i. The numbers of NP_{366}^{+} $CD8^{+}$ cells (mean +/-SEM) shown is calculated from the total counts and the percentages of cell staining. Data are pooled for two or three independent experiments (n=15). (*$p<0.05$ and **$p<0.01$ were determined using Mann-Whitney test).

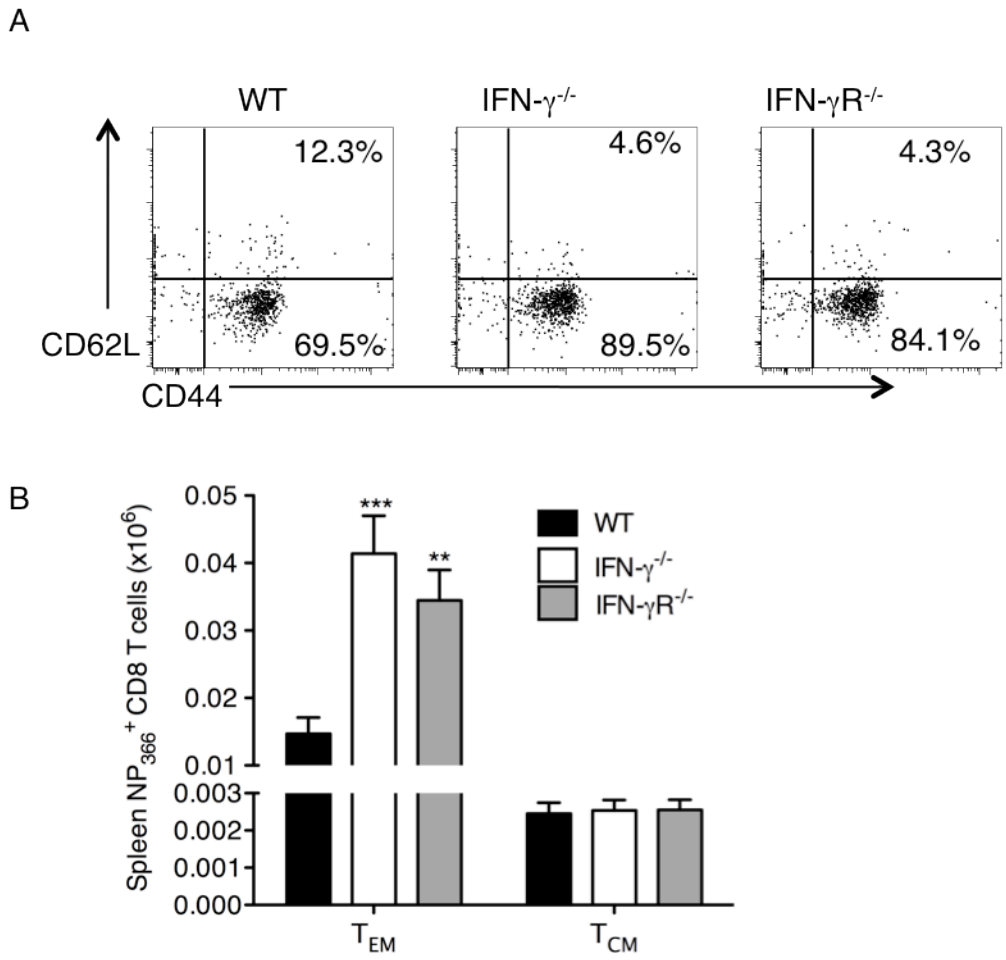

Figure 4.15 Distribution of NP_{366}^{+} cells in the different memory compartments in the spleens of the IFN-$\gamma^{-/-}$ and IFN-$\gamma R^{-/-}$ mice

NP_{366}^{+} $CD8^{+}$ T cells were examined in the spleens of mice on day 28 for their expression of CD44 and CD62L. Representative flow cytometry plots are shown (A). The numbers of effector memory ($CD44^{hi}CD62L^{low}$) and central memory ($CD44^{hi}CD62L^{hi}$) $CD8^{+}$ NP_{366}^{+} cells (mean +/- SEM) shown were calculated from the total counts and the percentages of cells staining positive in the lungs of the infected mice on day 28 (B) Data are pooled for two independent experiments (n=10). (*$p<0.05$ and **$p<0.01$ were determined using Mann-Whitney test).

4.10 Discussion

Understanding the immune response to influenza infection and the specific interactions between the influenza virus and the host is fundamental to our management of this infection and to the development of better vaccines. This is especially true for influenza vaccines in which current vaccine strategies lack the ability to elicit lasting $CD8^+$ T cell memory responses. In the present study we show that IFN-γ-IFN-γR signaling plays a key role in the modulation of antigen-specific $CD8^+$ T cell contraction and memory development in response to influenza infection. We have shown that in the absence of IFN-γ signaling, the contraction phase of the $CD8^+$ T cell responses is aberrant, resulting in the accumulation of antigen-specific $CD8^+$ T cells as far as day 120 p.i. when the responses in the WT mice declined significantly.

Although several recent studies show that IFN-γ may influence the trafficking and contraction of the $CD8^+$ T cell response against LCMV and Listeria infections (Badovinac et al. 2000; Tewari et al. 2007), other studies have reported that IFN-γ does not play a role in the contraction of $CD8^+$ T cell responses after CMV and VSV infection (Christensen et al. 2004; Andrews et al. 2008). This suggests that the effects of IFN-γ on the magnitude of $CD8^+$ T cell contraction may be specific to the particular pathogen. A likely explanation is that the inflammatory cytokine milieu induced by the pathogen may counter the effect of IFN-γ signaling on the $CD8^+$ T cells to influence their survival and contraction. In our influenza model we observed that large amounts of IFN-γ are produced during the acute phase of influenza infection (Figure 3.4). Hence, we thought that IFN-γ might play a role in programming of the $CD8^+$ T cell response during an influenza infection. Although we

studied the various aspects of the flu-specific immune response in the IFN-$\gamma^{-/-}$ mice and IFN-$\gamma R^{-/-}$ mice, we observed defects only in the contraction phase of the $CD8^+$ T cell response. The other aspects such as the $CD4^+$ T cell response, viral clearance, effector function of the $CD8^+$ T cells and lung damage seem unchanged in the IFN-$\gamma^{-/-}$ and IFN-$\gamma R^{-/-}$ mice. Although we observed increased levels of Th2 cytokines and eosinophilia in the lungs of the IFN-$\gamma^{-/-}$ mice, this did not lead to more lung damage or exacerbated illness in these mice.

In our model of influenza infection, the viral titers peaked at day 4-6 p.i. The $CD8^+$ T cells appeared in the lung at day 8 p.i. and were secreting cytokines and displayed cytotoxic potential even in the absence of IFN-γ signaling. Although the viral titers peaked so early, the peak of the $CD8^+$ T cell response was only seen on day 11 p.i. Although an enhanced cytotoxic ability was still present on day 11 p.i., we did not observe any cytokine production by the $CD8^+$ T cells at this time-point. The IFN-$\gamma^{-/-}$ and IFN-$\gamma R^{-/-}$ mice in all aspects of the $CD8^+$ T cell response studied appeared similar except for the contraction phase of the response. The transcription factors T-bet and Eomesodermin (eomes) were studied at day 7 p.i. Although, no differences were observed in the levels of T-bet, we observed decreased levels of its paralogue, eomes. Further study is required to highlight the significance of this finding, which was beyond the scope of this thesis.

The response of the IFN-$\gamma^{-/-}$ mice to influenza infection was first studied in 1993 (Graham et al. 1993). In this study the authors noted that the absence of IFN-γ led to an increased production of flu-specific IgG1 and that IL-4 and IL-5 were elevated compared with the WT animals. Furthermore, these authors

did not note any differences in the development of an effective CTL response in the WT and the IFN-γ-deficient mice. Our findings are in agreement with that study and we found no differences in the CTL response in the knock out mice. However, we observed differences in the levels of CD107α between the WT and IFN-$\gamma^{-/-}$ $CD8^+$ T cells on day 11 p.i. CD107a (LAMP-1) is a marker for degranulation and is an indirect readout of $CD8^+$ T cells cytotoxic function. However, since $CD8^+$ T cells kill target cells by Fas-FasL (Topham et al. 1997) and TRAIL (Brincks et al. 2008) in addition to the release of granzyme and perforin during degranulation, we realized that CD107α staining may not be give a complete picture of actual $CD8^+$ T cell cytotoxic function. As we have already assessed the true ability of the flu-specific $CD8^+$ T cells to kill in a chromium release-killing assay, we concluded that IFN-γ does not affect the cytotoxic function of the $CD8^+$ T cells.

Several studies have also shown that IFN-γ influences the $CD4^+$ T cell responses to a variety of infections and especially the contraction phase of the response (Haring and Harty 2006). Hence we looked at total $CD4^+$ T cell numbers in our model throughout the infection. Although, we did not track the antigen-specific $CD4^+$ T cell response, we did not observe any differences in the total $CD4^+$ T cell numbers throughout the 5 PFU PR/8 influenza infection. However, as we focused more on the $CD8^+$ T cell response, we did not examine in detail, the properties or the functions of the $CD4^+$ T cells during the infection.

The reduced contraction of the flu-specific $CD8^+$ T cell response found in the IFN-$\gamma^{-/-}$ and IFN-$\gamma R^{-/-}$ mice consequently lead to an increase in the memory population in these mice. When we looked at their CD62L expression in the

lungs, we observed equal levels of CD62L expression on the NP_{366}^{+} $CD8^{+}$ T cells in the IFN-$\gamma^{-/-}$ and IFN-$\gamma R^{-/-}$ mice as compared to the WT mice. However, in the spleens, a higher number of $CD62L^{low}$ cells were present in the IFN-$\gamma^{-/-}$ and IFN-$\gamma R^{-/-}$ mice as compared to the WT mice. This anomaly can be explained by the fact that CD62L is a lymph node homing receptor and its expression decides the location of the $CD8^{+}$ T cells. Cells expressing high CD62L migrate into the spleens and lymph nodes (Kaech et al. 2002). Hence, although there is no difference in the CD62L expression on the NP_{366}^{+} cells in the lung tissue, this difference is manifested in the spleens. Since there are a higher number of memory cells in the IFN-$\gamma^{-/-}$ and IFN-$\gamma R^{-/-}$ mice as compared to the WT mice, this differences in CD62L could be a division-linked differentiation (Schlub et al. 2010), where it was described that there was a link between CD62L expression and cell division. It is evident that IFN-γ regulates CD62L expression but it is still unclear whether this leads to faulty T cell trafficking after influenza infection. Since the differences between T_{CM} and T_{EM} is present only in the spleens, it could be possible that the trafficking back to the spleen after contact with antigen in the lung is dependent on the up-regulation of CD62L, which is in turn regulated by IFN-γ. The role of CD62L in lymph node homing has been well studied but it has also been shown that equal numbers of effector and central memory $CD8^{+}$ T cells can develop in the absence of CD62L mediated lymph node trafficking (Wirth et al. 2009).

In summary, we found that the contraction of the influenza specific $CD8^{+}$ T cell response is influenced by IFN-γ and hence increased numbers of antigen specific $CD8^{+}$ T cells were present in the IFN-$\gamma^{-/-}$ and IFN-$\gamma R^{-/-}$ mice even at

day 120 p.i., leading to increased memory cells in these mice. However, the effector function of the $CD8^+$ T cells and the viral clearance were not affected by the absence of IFN-γ signaling.

In the next chapters, we investigate the possible causes and mechanisms of the reduced contraction of the $CD8^+$ T cell response to an influenza infection. Further, we also study the effects the reduced contraction phase has during a recall response to a re-challenge with a heterologous strain of influenza.

Chapter 5: Identifying the mechanisms by which IFN-γ regulates the contraction of influenza-specific $CD8^+$ T cell response

5.1 Introduction

IFN-γ has long known to be important in the regulation of immune responses. Our aim was to study specifically, the roles it plays in the regulation of $CD8^+$ T cell responses to an influenza infection. In Chapter 4, we have shown that IFN-γ regulates the contraction phase of the $CD8^+$ T cell response to influenza. In this chapter, we set out to identify the underlying mechanism/s by which IFN-γ modulates the influenza-specific $CD8^+$ T cell response.

Several studies have looked at the roles of IFN-γ in regulating Th1 responses by suppressing Th2 responses (Gajewski and Fitch 1988). It has also been contemplated that IFN-γ can slow/arrest the proliferation of T cells (Novelli et al. 1996). There have been studies that show that IFN-γ causes apoptosis of T cells *in vitro* (Refaeli et al. 2002). The role of IFN-γ in the activation induced cell death of T cells has been well studied (Liu and Janeway 1990; Gorak-Stolinska et al. 2002). Our initial efforts concentrated on identifying whether increased proliferation or reduced survival was the reason for the reduced $CD8^+$ T cell contraction phase in the absence of IFN-γ signaling. We also studied the role of IFN-γ regulated PD-1, a marker for cell exhaustion on the contraction phase of the response.

Furthermore, we looked at the downstream effectors of IFN-γ signaling by which this regulation of contraction could be brought about. Since we identified increased survival as the reason for increased cell numbers in the

IFN-$\gamma^{-/-}$ and IFN-$\gamma R^{-/-}$ mice, we studied the receptors on the NP_{366}^+ $CD8^+$ T cells, for the cytokines involved in providing survival signals.

In this chapter, we show with *in vitro* and *in vivo* experiments that IFN-γ does not control the rates of proliferation of $CD8^+$ T cells during an influenza infection. We also show that IFN-γ is responsible for inducing the cell death of antigen specific $CD8^+$ T cells in the lungs of influenza-infected mice. We also identify some of the downstream effectors by using a PCR array of molecules involved in pathways of cell death. Further, we found that the expression of IL-7R on the NP_{366}^+ $CD8^+$ T cells and hence the survival signals received by these cells during an influenza infection are controlled by IFN-γ. Finally, we show that the reduced contraction in the IFN-$\gamma^{-/-}$ mice comes back to WT levels when IL-7 is blocked in the lung during the peak of the $CD8^+$ T cell response to the influenza infection.

5.2 Determination of precursor frequencies of NP_{366}^+ $CD8^+$ T cells in the IFN-$\gamma^{-/-}$ and IFN-$\gamma R^{-/-}$ mice

The extent of $CD8^+$ T cell clonal expansion is a function of the initial endogenous precursor frequency of the $CD8^+$ T cells in the immune system. We compared the precursor frequencies of NP_{366}^+ $CD8^+$ T cells in naïve uninfected WT, IFN-$\gamma^{-/-}$ and IFN-$\gamma R^{-/-}$ mice (Figure 5.1). The spleen, inguinal, cervical, axial and brachial lymph nodes were pooled from individual uninfected healthy mice in an attempt to collect all the naïve T cell population. $CD8^+$ T cells were purified by MACS separation and stained with NP_{366} Pentamer and the entire sample was analyzed by flow cytometry.

We found that there were about 300-600 NP_{366}^+ $CD8^+$ T cell precursors in a naive uninfected WT mouse. Similar numbers of NP_{366}^+ $CD8^+$ T cells were also found in IFN-$\gamma^{-/-}$ and IFN-$\gamma R^{-/-}$ mice. This showed that IFN-γ does not influence the naïve $CD8^+$ T cell frequencies and the reduced contraction was not due to an increase in the naïve influenza-specific $CD8^+$ T cell frequency in the IFN-$\gamma^{-/-}$ and IFN-$\gamma R^{-/-}$ mice.

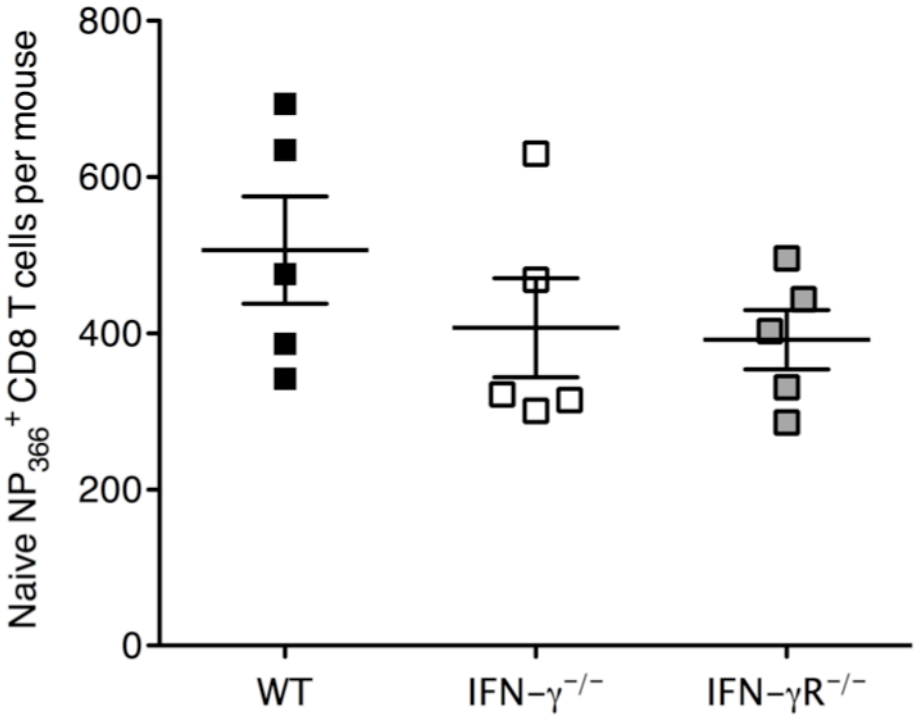

Figure 5.1 Precursor frequency of NP_{366}^+ $CD8^+$ T cells is not different in uninfected WT, IFN-$\gamma^{-/-}$ and IFN-$\gamma R^{-/-}$ mice

NP_{366}^+ $CD8^+$ T cells were examined in the spleens and pooled lymph nodes of naïve-uninfected mice by flow cytometry. The numbers of $CD44^{low}CD62L^{Hi}$ $CD8^+$ NP_{366}^+ cells (mean +/- SEM) shown were counted per animal. Data are pooled for two independent experiments (n=5).

5.3 Rates of proliferation of $CD8^+$ T cells in the absence of IFN-γ signaling

Earlier studies have shown that IFN-γ can regulate the rate of proliferation of $CD8^+$ T cells. We wanted to examine if this was true in our model. First of all, we compared the rates of proliferation of naïve WT and IFN-$\gamma^{-/-}$ $CD8^+$ T cells after activation *in vitro*. Naïve $CD8^+$ T cells were isolated from the spleens and lymph nodes of naïve WT and IFN-$\gamma^{-/-}$ mice and purified. The cells were then labeled with CFSE and stimulated with PMA and Ionomycin for 48 hours. The IFN-$\gamma^{-/-}$ $CD8^+$ T cells were also cultured in the presence of rIFN-γ to observe its effects on the deficient cells. After 48h, the cells were stained with CD3 and CD8 and a live/dead stain. The extent of proliferation in these cells after 48h of culture was compared between the two cell-types (Figure 5.2). Similar results were also seen when antibodies to CD3 and CD28 were used for *in vitro* stimulation of the $CD8^+$ T cells.

Both the WT and IFN-$\gamma^{-/-}$ cell cultures had undergone equal numbers of cell divisions. We examined the proliferation statistics using FlowJo software. We compared the proliferation index of the cells. Proliferation Index is the total number of divisions undergone by the number of cells that went into division. We observed that both cell types had similar proliferation indices indicating that the rates of proliferation were not different in the absence of IFN-γ. We also did not observe any difference in the culture with IFN-$\gamma^{-/-}$ $CD8^+$ T cells cultured in the presence of IFN-γ. This indicated that IFN-γ did not influence the rates of proliferation of $CD8^+$ T cells when stimulated *in vitro*.

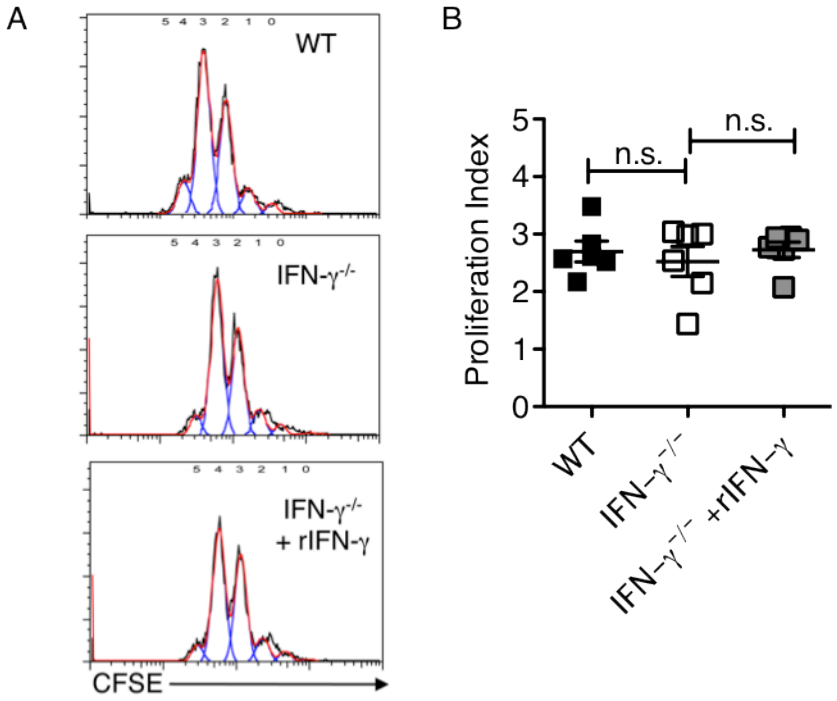

Figure 5.2 Comparison of proliferation rates of naïve WT and IFN-γ$^{-/-}$ CD8$^+$ T cells after *in vitro* stimulation.

CD8$^+$ T cells were purified from WT and IFN-γ$^{-/-}$ mouse spleens and lymph nodes, labeled with CFSE and stimulated *in vitro* with PMA and ionomycin and stained with antibodies after 48 hours. IFN-γ$^{-/-}$ CD8$^+$ T cells were also cultured in the presence of rIFN-γ. (A) Representative flow plots of the proliferation of CD8$^+$ T cells in culture after stimulation for 48h (B) Proliferation indices of *in vitro* activated CD8$^+$ T cells from A.

We also examined the rates of proliferation of antigen specific $CD8^+$ T cells *in vivo* during an influenza infection. For this set of experiments, we used $CD8^+$ T cells isolated from OT-1 and OT-1 x IFN-$\gamma^{-/-}$ mice. Naïve $CD8^+$ T cells were isolated from the spleens and lymph nodes of these mice, purified, CFSE-labeled and transferred into WT and IFN-$\gamma^{-/-}$- mice respectively. Recipient mice were infected with PR8-OT1 (PR/8 virus with SIINFEKL expressed on the surface NA stalk) after 24h. The mice were sacrificed at day 4 after infection and the lymph nodes harvested and the labeled cells were examined for their extent of proliferation.

Both sets of mice showed similar numbers of transferred $CD8^+$ T cells. When we looked at the dilution of the CFSE labeling, we observed that both groups of cells had undergone similar numbers of divisions (Figure 5.3A). Both cell types had undergone 8 divisions with similar kinetics. When we compared the proliferation statistics using proliferation indices, we did not observe a difference in their rates of proliferation (Figure 5.3B). We concluded that the IFN-γ does not influence the rates of proliferation of naive $CD8^+$ T cells while responding to an influenza infection.

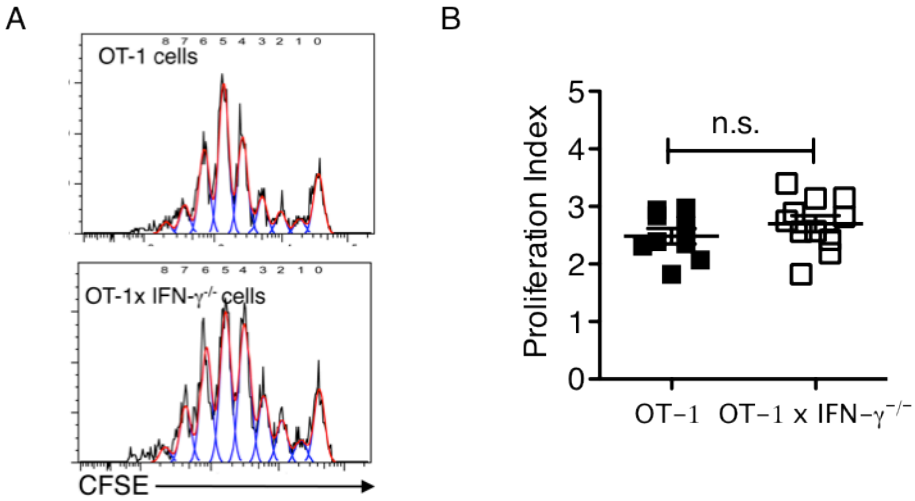

Figure 5.3 Comparison of proliferation rates of antigen specific OT-1 and OT-1 x IFN-γ$^{-/-}$ CD8$^+$ T cells *in vi*vo after infection with PR8-OT1

Naïve CD8$^+$ T cells were purified from the spleens and lymph nodes of OT-1 and OT-1 x IFN-γ$^{-/-}$ mice, labeled with CFSE, transferred into WT or IFN-γ$^{-/-}$ mice respectively, and infected with 50 PFU of PR8-OT1 strain of influenza. Lung draining lymph nodes were harvested on day 4 p.i. and stained for CD3 and CD8.
(A) Representative flow plots of proliferation of labeled CD8$^+$ T cells determined using FlowJo software. (B) Proliferation indices of the transferred CD8$^+$ T cells in A. Data are pooled from 3 independent experiments with n=3-5 mice/group/ experiment.

The differences between the numbers of NP_{366}^+ $CD8^+$ T cells in the WT, IFN-$\gamma^{-/-}$ and IFN-$\gamma R^{-/-}$ during an influenza infection is non-existent on day 11 but is evident only on day 14 p.i.. To determine the contribution of cell proliferation to this phenomenon, we compared proliferation of WT, IFN-$\gamma^{-/-}$ and IFN-$\gamma R^{-/-}$ NP_{366}^+ $CD8^+$ T cells at these time-points by their expression of Ki-67. The antigen Ki-67 is a nuclear protein that is associated with cellular proliferation and is generally used as a marker of proliferation. It is associated with ribosomal RNA transcription and inactivation of Ki-67 leads to inhibition of ribosomal RNA synthesis and hence blocks cell proliferation.

Cells were harvested from the lungs of the WT, IFN-$\gamma^{-/-}$ and IFN-$\gamma R^{-/-}$ mice on days 11 and 14 p.i. and the intracellular levels of Ki-67 were measured on the NP_{366}^+ $CD8^+$ T cells (Figure 5.4). We observed that most NP_{366}^+ $CD8^+$ cells in the lungs of the WT mice expressed Ki-67. This was also true for NP_{366}^+ $CD8^+$ cells from the lungs of IFN-$\gamma^{-/-}$ and IFN-$\gamma R^{-/-}$ mice. No differences were observed in the proportion of NP_{366}^+ cells expressing Ki-67 or in the levels of Ki-67 they expressed. More cells were found to express Ki-67 on day 11 than on day 14 p.i.

We considered that all cells were undergoing some degree of basal proliferation and hence expressed high levels of intra-nuclear Ki-67. However, with this experiment we could absolutely conclude that cellular proliferation is not a contributing factor to the reduced contraction that is seen in the absence of IFN-γ signaling.

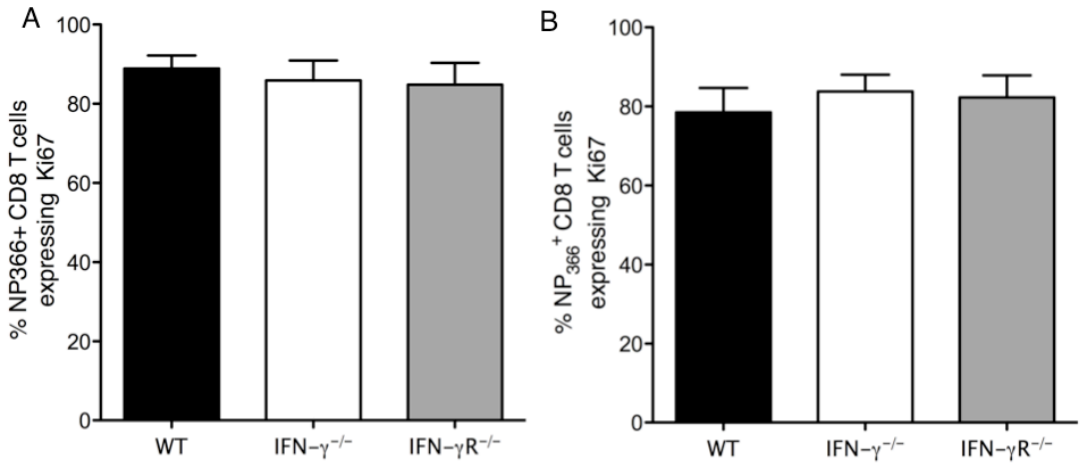

Figure 5.4 Comparison of nuclear antigen Ki67 to determine extent of cellular proliferation in the NP_{366}^+ $CD8^+$ T cells after influenza infection

WT, IFN-$\gamma^{-/-}$ and IFN-$\gamma R^{-/-}$ mice were infected with 5PFU of influenza A/ PR/8/34 and the lungs were harvested on day 11 and day 14 p.i.. The $CD8^+$ T cells from the lungs were isolated and surface stained with anti-CD3, anti-CD8 and NP_{366} pentamer and after fixation and permeabilization with anti-intracellular Ki67 nuclear antigen. The percentage of NP_{366}^+ $CD8^+$ T cells positive for Ki67 on day 11 (B) and day 14 p.i (C) were plotted. Data are pooled from two independent experiments with n=5 per group.

5.4 Interferon gamma and cell death

5.4.1 Rate of survival of CD8$^+$ T cells in the absence of IFN-γ signaling

From our earlier experiments, we could establish that the rates of proliferation are not regulated by IFN-γ and hence do not contribute to the reduced contraction phase of the CD8$^+$ T cells in its absence. Next we assessed whether IFN-γ controls the rates of death or survival of the CD8$^+$ T cells. The first set of experiments look at the rates of survival of naïve CD8$^+$ T cells after stimulation *in vitro*. We purified CD8$^+$ T cells from the spleens and lymph nodes of WT and IFN-γ$^{-/-}$ mice and cultured them in the presence of PMA and ionomycin for 72h. After 3 days, we determined the percentages of live cells in the WT and IFN-γ$^{-/-}$ CD8$^+$ T cell cultures. We observed that there were fewer living cells in the WT than in the IFN-γ$^{-/-}$ CD8$^+$ T cell cultures (Figure 5.5A).

We hypothesized that IFN-γ induced cell death in the WT CD8$^+$ T cell cultures and hence the higher percentage of cells in the IFN-γ$^{-/-}$ cultures was due to the absence of IFN-γ induced cell death. We examined if we could induce death in the IFN-γ$^{-/-}$ CD8$^+$ T cells by adding in recombinant rIFN-γ into the cell culture and observed a dose dependent decrease in the percentage and number of living cells upon addition of increasing amounts of IFN-γ (Figure 5.5B & C). We tried the same experiment using a different approach by blocking IFN-γ signaling on WT CD8$^+$ T cell cultures by using blocking antibodies to IFN-γ and IFN-γR1 (Figure 5.5D) and found that a higher percentage of CD8$^+$ T cells survived after IFN-γ signaling was blocked as compared to the cultures

without the blocking antibodies. We inferred that IFN-γ induces cell death in $CD8^+$ T cell cultures upon *in vitro* stimulation.

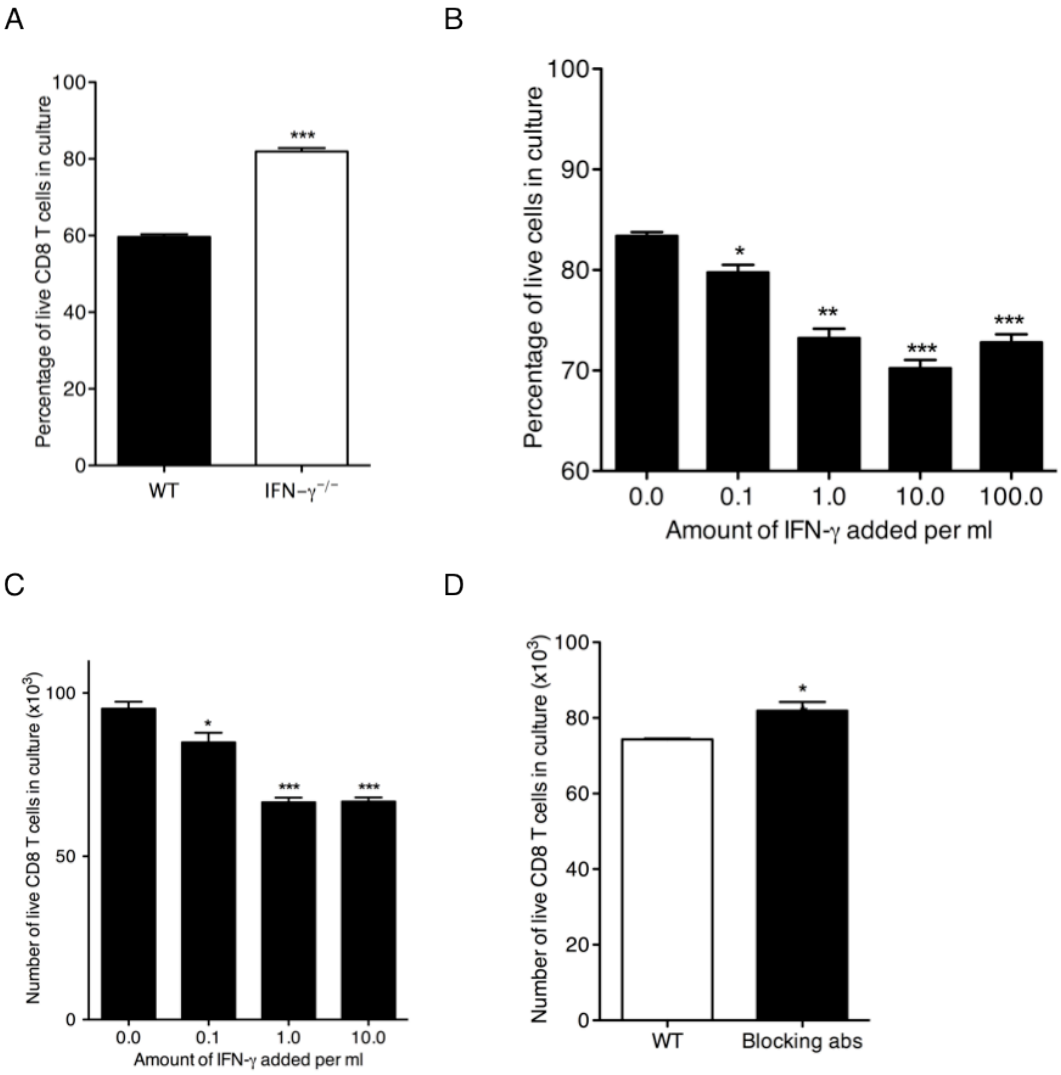

Figure 5.5 Interferon gamma induces death of activated CD8$^+$ T cells *in vitro*

CD8+ T cells were purified from the spleens and lymph nodes of WT and IFN-γ$^{-/-}$ mice. (A) WT and IFN-γ$^{-/-}$ CD8$^+$ T cells were stimulated *in vitro* with PMA and ionomycin and cultured cells were stained with anti-CD3 and anti-CD8 antibodies and 7-AAD. Live cells (7-AAD negative) were counted in all cultures and plotted. (B and C) IFN-γ$^{-/-}$ CD8$^+$ T cells were stimulated *in vitro* with PMA and ionomycin and cultured in the presence of increasing amounts of rIFN-γ and percentages (B) and numbers (C) of live cells after 48h were plotted. (D) WT CD8$^+$ T cells were stimulated in the presence or absence of blocking antibodies to IFN-γ and IFN-γR1 for 48h. Live cells were counted and plotted after 48h. Data are representative of at least 3 independent experiments.

5.4.2 Increased survival of influenza-specific $CD8^+$ T cells in the lungs of IFN-$\gamma^{-/-}$ mice

We concluded from the previous experiments that IFN-γ induces cell death in activated $CD8^+$ T cells. Next we wanted to examine if IFN-γ regulated the contraction of $CD8^+$ T cells by inducing cell death in the antigen specific $CD8^+$ T cells in the lungs of influenza infected mice. We hypothesized that if this was the case, then antigen specific $CD8^+$ T cells in the lungs of IFN-$\gamma^{-/-}$ mice would undergo lower levels of death than those in the WT mice. To verify this hypothesis, we harvested the lungs of influenza infected WT and IFN-$\gamma^{-/-}$ mice, at day 12 p.i. and compared levels of apoptosis in the $CD8^+$ T cells. This time-point was chosen because it was after the peak of the response and the time point at which contraction of the $CD8^+$ T cell response should have begun. To determine whether the $CD8^+$ T cells from the influenza infected IFN-$\gamma^{-/-}$ mice had decreased apoptosis, we stained freshly isolated $CD8^+$ T cells from the lungs of WT and IFN-$\gamma^{-/-}$ mice for CD8, NP_{366} pentamer, Annexin-V and 7-AAD and gated on the antigen specific $NP_{366}{}^+$ $CD8^+$ T cells. We observed that an increased percentage of $NP_{366}{}^+$ cells stained positive for Annexin-V and 7-AAD in the WT mice as compared to the IFN-$\gamma^{-/-}$ mice (figure 5.4.2). This was true of late apoptotic (Annexin-V^+ 7-AAD^+) (Figure 5.6B) and all Annexin-V^+ $NP_{366}{}^+$cells (Figure 5.6C). We concluded that the antigen specific $CD8^+$ T cells from IFN-$\gamma^{-/-}$ mice are refractory to apoptosis after an influenza infection, which supports our theory that IFN-γ induces apoptosis in the antigen specific $CD8^+$ T cells in the lungs after an influenza infection.

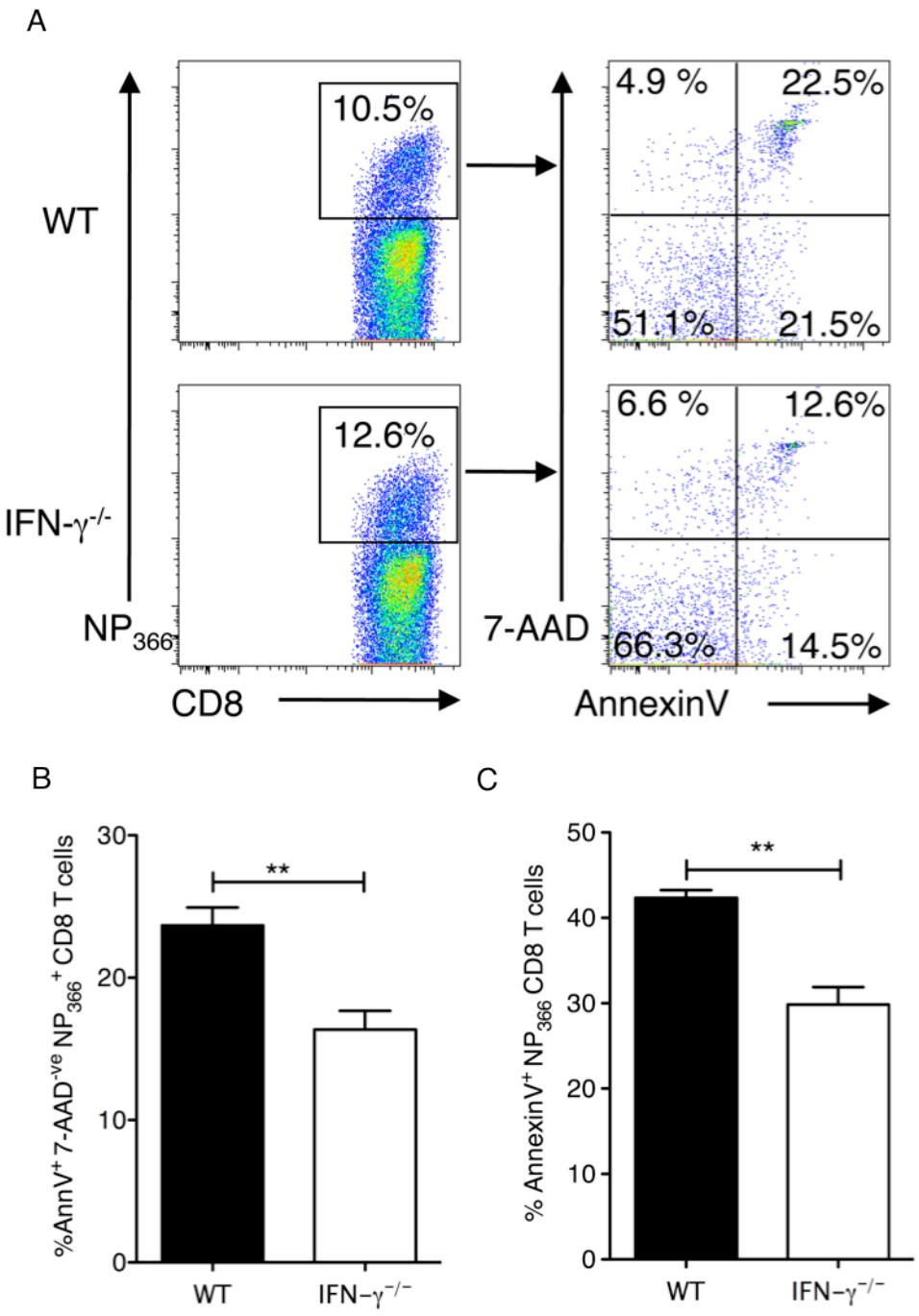

Figure 5.6 Decreased apoptosis in flu-specific CD8$^+$ T cells in the IFN-γ$^{-/-}$ mice

WT or IFN-γ$^{-/-}$ mice were infected with 5PFU of influenza A/ PR/8/34 and the lungs were harvested on day 12 p.i.- The CD8$^+$ T cells from the lungs were isolated and stained with Annexin-V and 7-AAD. (A) Representative flow cytometry plots of Annexin-V and 7-AAD staining of WT and IFN-γ$^{-/-}$ mice. (B and C) The percentage of cells positive for Annexin-V and 7-AAD (B) and all Annexin-V$^+$ (C) were plotted.

5.5 Addition of rIFN-γ increases cell death in *ex vivo* cultures of lungs from influenza-infected IFN-$\gamma^{-/-}$ mice as well as *in vivo*

From the previous experiments, we concluded that antigen specific $CD8^+$ T cells from IFN-$\gamma^{-/-}$ mice are refractory to apoptosis. We next investigated whether we could induce or enhance cell death in the flu-specific $CD8^+$ T cells from the IFN-$\gamma^{-/-}$ mice by the addition of exogenous IFN-γ *ex vivo*. IFN-$\gamma^{-/-}$ mice were infected with 5PFU of PR/8 influenza and the lungs harvested on day 14 p.i. (Figure 5.7). Single cell suspensions of these lungs were enriched for lymphocytes and cultured for 24h in the presence or absence of recombinant IFN-γ. After 24h the cells were stained with antibodies against CD3, CD8 and NP_{366} pentamer and the numbers of live $CD3^+CD8^+NP_{366}^+$ cells that were 7-AAD^{-ve} (live) enumerated (Figure 5.7A). Addition of IFN-γ to the cell cultures resulted in a decrease in the percentage of live NP_{366}^+ $CD8^+$ T cells from the IFN-$\gamma^{-/-}$ cultures compared to the cultures without rIFN-γ (Figure 5.7B). This confirmed that IFN-γ regulates cell survival and induces cell death in the antigen specific $CD8^+$ T cells.

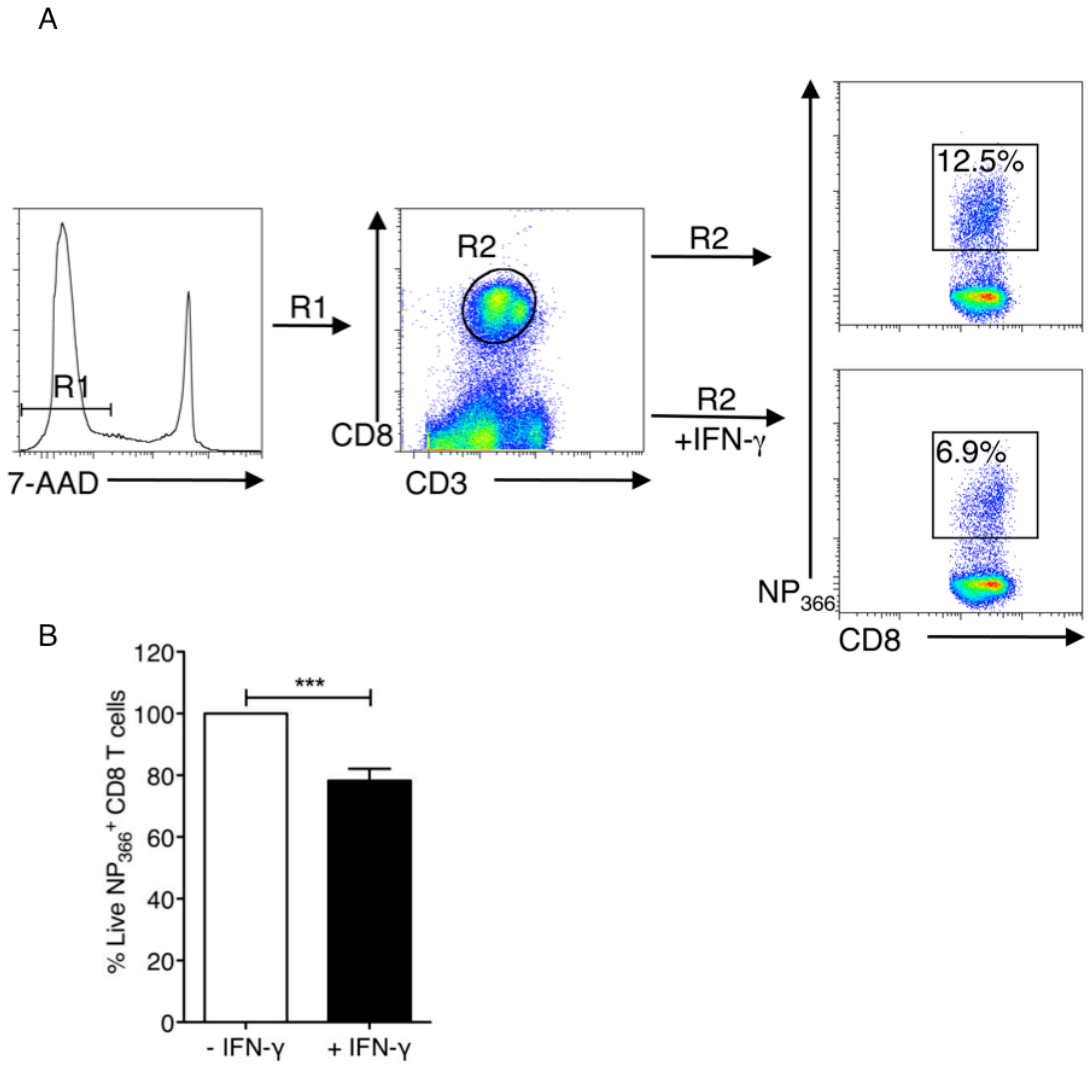

Figure 5.7 Addition of rIFN-γ increases cell death in *ex vivo* cultures of lungs from influenza-infected IFN-γ$^{-/-}$ mice

IFN-γ$^{-/-}$ mice were infected with 5 PFU of influenza A/ PR/8/34 and CD8$^+$ T cells were harvested on day 14 p.i. The Ficoll-enriched cells were cultured in the presence or absence of rIFN-γ for 24h. Live NP$_{366}^+$ CD8$^+$ T cell proportions were examined in the culture according to the gating strategy (A). The NP$_{366}^+$ CD8$^+$ T cells in the cultures without IFN-γ were considered as 100% and the percentage of live NP$_{366}^+$ CD8$^+$ T cells in the cultures with IFN-γ were calculated accordingly (B). Mean+/-SEM shown is calculated from the percentage of cells staining positive. Data are representative of two independent experiments (*p<0.05 and ***p<0.001)

We have shown so far that IFN-γ induces cell death of the antigen specific $CD8^+$ T cells *in vitro* and *ex vivo*. The next logical step was to see if administration of exogenous IFN-γ into IFN-$\gamma^{-/-}$ mice during an ongoing influenza infection would reverse the abnormal contraction phase of the flu-specific $CD8^+$ T cell response in these mice. We decided to administer rIFN-γ into the lungs of the flu-infected IFN-$\gamma^{-/-}$ mice at various time points after infection. We chose time points where the local concentration of IFN-γ would be high in the lungs of WT mice. As per our previous observation, we had seen that the levels of IFN-γ in the BAL fluid of flu-infected mice were highest at days 5, 6 and 7 after infection. Hence, we chose to administer rIFN-γ or PBS (as control) into the lungs of IFN-$\gamma^{-/-}$ mice at day 5 and 7 p.i. via the intra tracheal route. We chose not to do this multiple time points as this would lead to added stress in the lungs of the flu-infected animals. The mice were allowed to rest for the next week and the animals were sacrificed at day 14 p.i, their lungs were harvested and the NP_{366}^+ $CD8^+$ T cells were enumerated.

The influenza infected mice which received rIFN-γ had lower numbers of NP_{366}^+ $CD8^+$ T cells in the lungs when compared to the mice that got PBS (Figure 5.8). This indicated that the presence of IFN-γ in the lung environment programs antigen specific $CD8^+$ T cells to undergo cell death in influenza infected mice and hence regulates the contraction phase of the influenza specific $CD8^+$ T cell response.

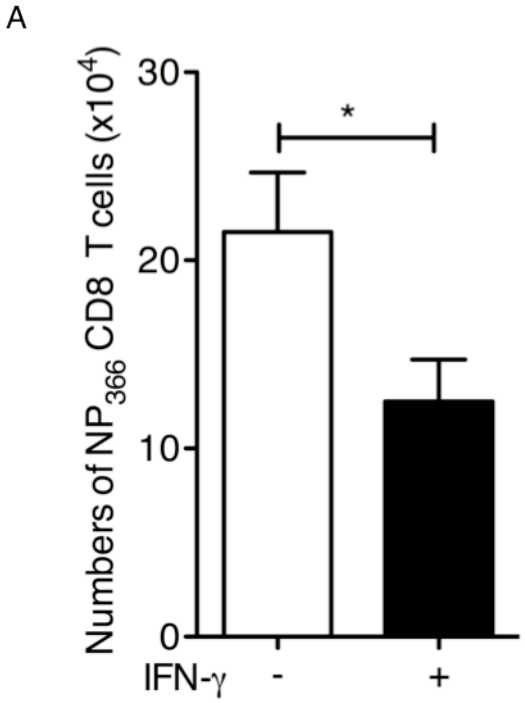

Figure 5.8 ***In vivo*** **administration of rIFN-γ into the IFN-$γ^{-/-}$ mice reduces the $CD8^+$ T cell accumulation in the lungs after influenza infection**

IFN-$γ^{-/-}$ mice were infected with 5 PFU influenza infection and PBS or rIFN-γ was administered i.t. to the lungs of these mice at days 5 and 7 p.i. The mice were sacrificed on day 14 p.i, the lungs were harvested and the antigen specific NP_{366}^+ $CD8^+$ T cells were enumerated. Mean+/-SEM shown is calculated from the number of cells staining positive. Data are representative of two independent experiments (*$p<0.05$ and ***$p<0.001$)

5.6 PCR array to look at the molecules associated with cell death (apoptosis, autophagy and necrosis)

Various pathways can induce cell death. Apoptosis (programmed cell death) and necrosis are the two major types of cell death. Autophagy has been proposed as a third kind of cell death in which cells digest their own organelles. All these three forms of cell death can be induced by programmed control mechanisms involving several players. Some of these key players may have a role to play in more than one pathway. In order to identify the pathways activated by IFN-γ, we used the mouse cell death pathway finder from SA Biosciences. This array profiles the expression of 84 key genes important for all the three mechanisms of cell death. The mechanisms behind the cell death pathways overlap and more than one form of cell death can occur simultaneously. The array uses real-time PCR to analyze the expression of a focused panel of genes involved in cellular death pathways. The genes profiled as part of this array are included in table 5.1.

Apoptosis: Pro-Apoptotic: Abl1, Apaf1, Atp6v1g2, Bax, Bcl2l11, Birc2 (c-IAP2), Casp1 (ICE), Casp3, Casp6, Casp7, Casp9, Cd40 (Tnfrsf5), Cd40lg (Tnfsf5), Cflar (Casper), Cyld, Dffa, Fas (Tnfrsf6), Fasl (Tnfsf6), Gadd45a, Nol3, Spata2, Sycp2, Tnf, Tnfrsf1a, Tnfrsf10b, Trp53. Anti-Apoptotic: Akt1, Bcl2, Bcl2a1a (Bfl-1/A1), Bcl2l1 (Bcl-x), Birc3 (c-IAP1), Casp2, Igf1r, Mcl1, Tnfrsf11b, Traf2, Xiap. **Autophagy:** Akt1, App, Atg12, Atg16l1, Atg3, Atg5, Atg7, Bax, Bcl2, Bcl2l1 (Bcl-x), Becn1, Casp3, Ctsb, Ctss, Esr1 (ERa), Fas (Tnfrsf6), Gaa, Htt, Ifng, Igf1, Ins2, Irgm1, Map1lc3a, Mapk8 (Jnk1), Nfkb1, Pik3c3 (Vps34), Rps6kb1, Snca, Sqstm1, Tnf, Trp53, Ulk1. **Necrosis:** 9430015G10Rik, Atp6v1g2, Bmf, Ccdc103, Commd4, Cyld, Defb1, Dennd4a, Dpysl4, Eif5b, Foxi1, Galnt5, Grb2, Hspbap1, Jph3, Kcnip1, Mag, Olfr1404, Parp1 (Adprt1), Parp2, Pvr, Rab25, S100a7a, Spata2, Sycp2, Tmem57, Tnfrsf1a, Txnl4b. **Housekeeping genes**: beta-2-microglobulin, beta-actin, GAPDH, Ribosomal protein L3a, HPRT1

Table 5.1: Genes profiled in the cell death pathway finder PCR array

IFN-γ induced death in the NP_{366}^+ $CD8^+$ T cells in the lungs of infected mice.

We have already stained for Annexin V (Figure 5.9) and have hence confirmed that IFN-γ induces the apoptotic program to induce cell death in the NP_{366}^+ $CD8^+$ T cells. We wanted to confirm if apoptosis was the only pathway induced by IFN-γ or if other death pathways were also activated by IFN-γ.

We purified NP_{366}^+ $CD8^+$ T cells from the lungs of WT and IFN-$\gamma^{-/-}$ mice by Fluorescence-Activated Cell Sorting (FACS) after staining with antibodies to CD8 and NP_{366} pentamer. The RNA was isolated from these cells and then subjected to the above-mentioned PCR-array.

The IFN-$\gamma^{-/-}$ NP_{366}^+ $CD8^+$ T cells had up-regulated anti-apoptotic molecules like Birc3 and Bcl-2 but had down regulated several genes involved in apoptosis (Akt1 and Casp3), necrosis (Mcl-1, Pvr and Tnfrsf1a) and autophagy (Atg16l1, App, Esr1, Gaa and Irgm1). Since the array also included the IFN-γ gene, this was down regulated several fold in the IFN-$\gamma^{-/-}$ cells, which worked as an excellent internal control. Surprisingly, certain apoptotic genes like Casp6, ApaF1 and Fasl were also up regulated in these cells. This showed that the pathways induced by IFN-γ were not dependent on a single pathway or a single set of molecules. IFN-γ influenced more than one type of cell death pathway.

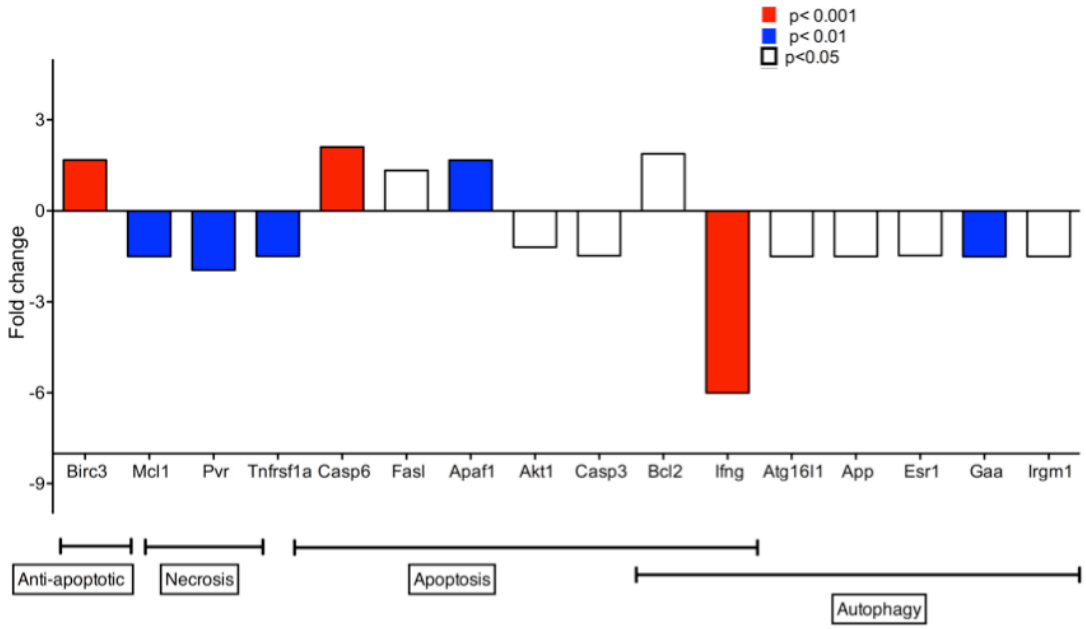

Figure 5.9 PCR array of molecules involved in different cell death pathways

NP_{366}^+ $CD8^+$ T cells were sorted from the lungs of influenza infected WT and IFN-$\gamma^{-/-}$ mice on day 14 p.i. and the RNA was subjected to the Cell death pathway finder PCR array, the details of which are described above and the list of genes profiled are found in table 5.1. Data is pooled from three independent experiments.

5.7 The absence of IFN-γ does not alter levels of exhaustion marker PD-1 on NP_{366}^+ $CD8^+$ T cells

The inhibitory receptor PD-1 contains a classic immunoreceptor tyrosine-based inhibitory motif (ITIM) and its engagement has been shown to induce T cell apoptosis and inhibit proliferative responses in response to TCR engagement (Freeman et al. 2000). It is an inhibitory receptor expressed on activated $CD8^+$ T cells for immune regulation and to reduce immunopathology during infection. The primary function of PD-1 is to attenuate the immune response. Hence, the expression of PD-1 is associated with cell exhaustion and immune suppression.

IFN-γ is known to influence the levels of PD-1 expression on $CD8^+$ T cells (Bos et al. 2012). Hence, we determined the levels of expression of PD-1 on the NP_{366}^+ $CD8^+$ T cells at the peak of the $CD8^+$ T cell response i.e. at day 11 p.i. (Figure 5.10). A high percentage of NP_{366}^+ $CD8^+$ cells was found to express PD-1 at this time-point in the WT mouse lungs. A similar proportion of NP_{366}^+ $CD8^+$ cells in the IFN-$\gamma^{-/-}$ and IFN-$\gamma R^{-/-}$ mice also expressed such high levels of PD-1, indicating that the levels of $CD8^+$ T cell exhaustion and immune suppression were similar in the absence of IFN-γ signaling, indicating that levels of PD-1 did not play a role in the reduced contraction observed in the IFN-$\gamma^{-/-}$ and IFN-$\gamma R^{-/-}$ mice.

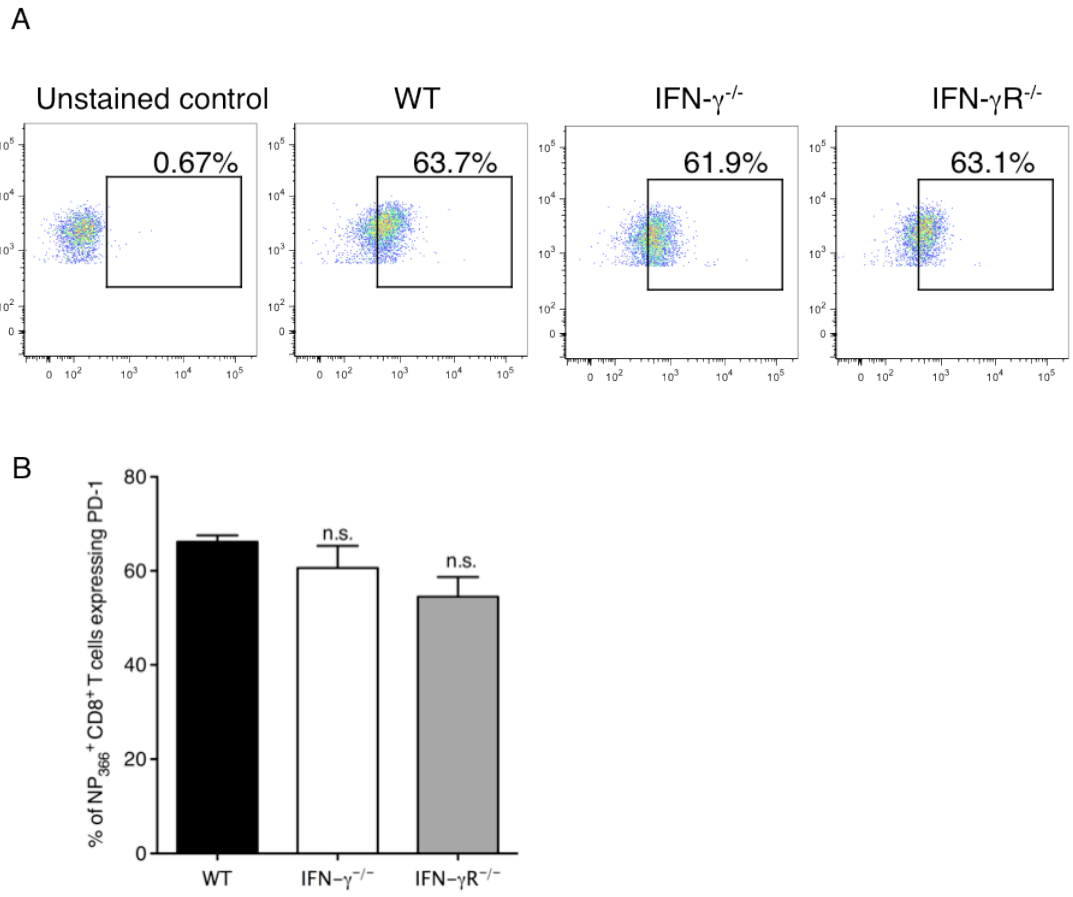

Figure 5.10 The absence of IFN-γ does not alter levels of exhaustion marker PD-1 on the NP_{366}^+ $CD8^+$ T cells.

C57BL/6 WT, IFN-$\gamma^{-/-}$ and IFN-$\gamma R^{-/-}$ mice were infected with 5PFU of influenza A/ PR/8/34 and PD-1 expression was measured on the NP_{366} $^+$ $CD8^+$ T cells on day 11 p.i. Representative flow plots showing the percentage of NP_{366} $^+$ $CD8^+$ T cells expressing PD-1 in the lungs of the infected mice (A). Graph representing the percentages of NP_{366} $^+$ $CD8^+$ T cells from the lungs expressing PD-1 (B). Data are pooled from 3 independent experiments with n=4-5 per group.

5.8 Contribution of DCs to the abnormal contraction in the absence of IFN-γ signaling after influenza infection

DCs are the sentinels of the lung airway and play a very important role in the initiation of the immune response to an influenza infection. They are the first group of cells that interact with the virus, acquire viral antigen and migrate to the draining lymph node to present this to naive $CD8^+$ T cells (Belz et al. 2004). Studies in our lab have shown that lung DCs migrate to the lung draining lymph node (Ho et al. 2011). These cells play an important role in programming the $CD8^+$ immune response to the influenza infection. In order to see how IFN-γ signaling regulates the characteristics of the DCs, we first characterized the dendritic cell population in the draining lymph node i.e. the posterior pMLN at day 5 p.i. (Figure 5.11).

There were no differences in the proportions of total $CD11c^+$ DCs in the lungs of the infected WT, IFN-$\gamma^{-/-}$ and IFN-$\gamma R^{-/-}$ mice. When the levels of Class I and Class II MHC molecules were measured on the surface of the $CD11c^+$ DCs, we did not see any down regulation in the absence of IFN-γ signaling. We observed a slight decrease in the MFI of expression of Class II on IFN-$\gamma^{-/-}$ DCs but not in their class I expression (figure 5.11B). No differences were observed in the expression of the co-stimulatory molecules measured CD40, CD70, CD80 and CD86 (figure 5.11C). This showed that the DCs do not depend on IFN-γ for their expression of co-stimulatory molecules or their expression of MHC class I or class II molecules during the initiation of the response to influenza in the lung draining lymph nodes**.**

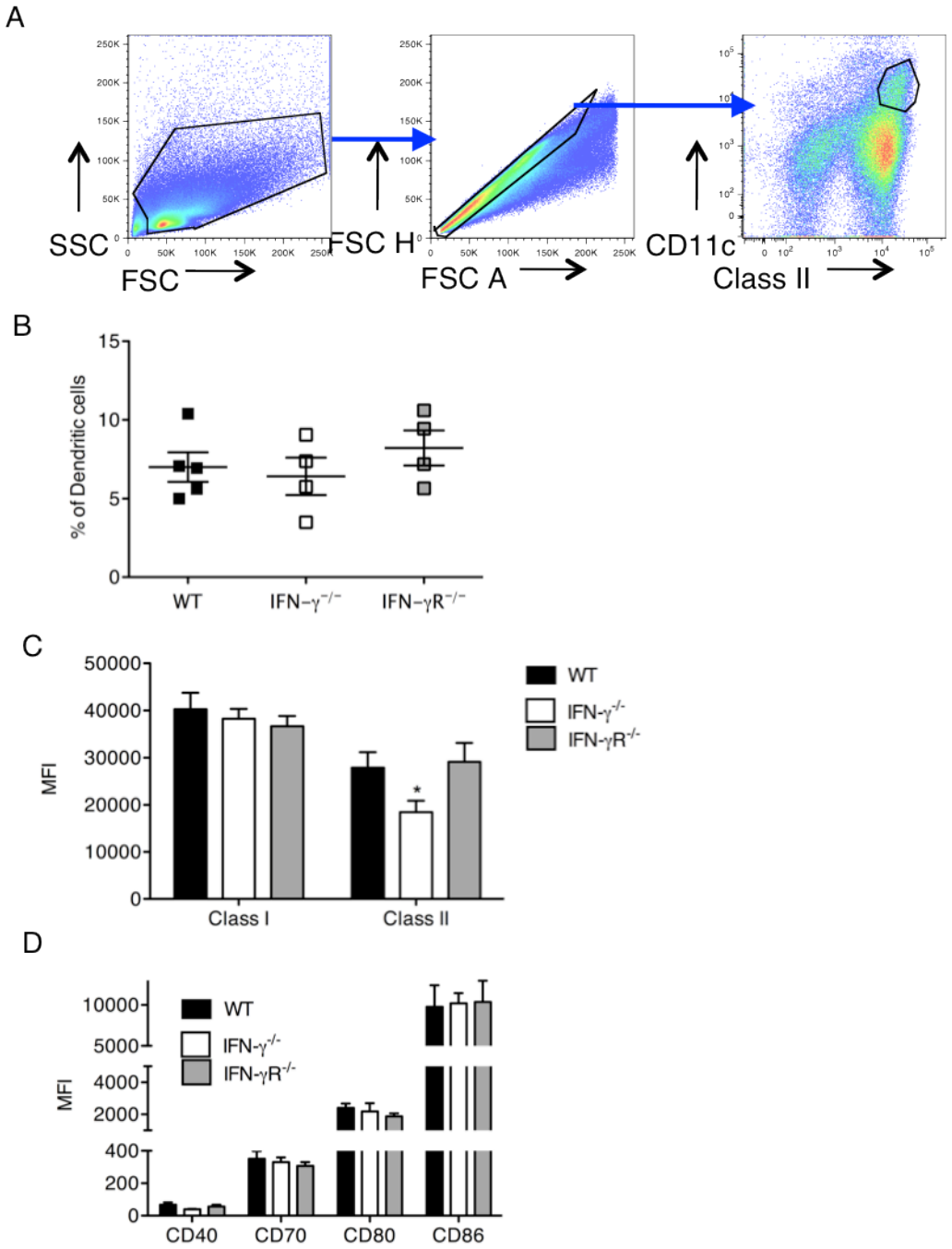

Figure 5.11 No differences in the dendritic cell characteristics at the initiation of the immune response to influenza in the lung draining lymph node.

C57BL/6 WT, IFN-γ$^{-/-}$ and IFN-γR$^{-/-}$ mice were infected with 5 PFU of influenza A/ PR/8/34 and DCs were harvested from the lung draining lymph nodes on day 5 p.i . (A) Gating strategy for lymph node dendritic cells. Graph representing the percentages of DCs from the lymph nodes (B), their expression of Class I and Class II MHC molecules (C) and co-stimulatory molecules (D). Data are representative from 2 independent experiments with n=4-5 per group.

DCs are also important mediators of $CD8^+$ T cell survival in the lung tissue after influenza infection (Dolfi et al. 2008; Peperzak et al. 2010). Since there were higher numbers of antigen specific $CD8^+$ T cells in the lungs of the mice deficient in IFN-γ signaling, we thought that the survival signals from the DCs might be different in these mice. Hence, we also characterized the DC population in the lungs of the infected mice on day 14 p.i. (Figure 5.12)

We harvested the lungs from infected mice on day 14 p.i, isolated the $CD11c^+$ DCs and compared their characteristics between the WT, IFN-$\gamma^{-/-}$ and IFN-$\gamma R^{-/-}$ mice. We observed that the proportion of DCs was significantly lesser in WT lungs as compared to those from IFN-$\gamma^{-/-}$ and IFN-$\gamma R^{-/-}$ mice. But we figured that the reason for this could be the high numbers of influenza-specific $CD8^+$ T cells in the lungs of the IFN-$\gamma^{-/-}$ and IFN-$\gamma R^{-/-}$ mice. Since we did not compare the total cell counts of the DCs, we could not conclusively decide whether this was affecting the lung $CD8^+$ response.

Furthermore, we looked at the levels of expression of MHC class I and MHC class II on the DCs and we observed significantly lower expression of MHC I on the DCs from the IFN-$\gamma^{-/-}$ and IFN-$\gamma R^{-/-}$ mice. When the levels of co-stimulatory molecules were compared however, we did not see any significant differences in the levels of CD40 and CD86 but slightly lower levels of CD80 was observed on the DCs in the lungs of the IFN-$\gamma^{-/-}$ mice but not in the IFN-$\gamma R^{-/-}$ mice.

We also studied the DCs at steady state in the lungs of naïve mice. We found that in the steady state, the percentage of DCs was comparable in the lung in the presence or absence of IFN-γ signaling (Figure 5.13).

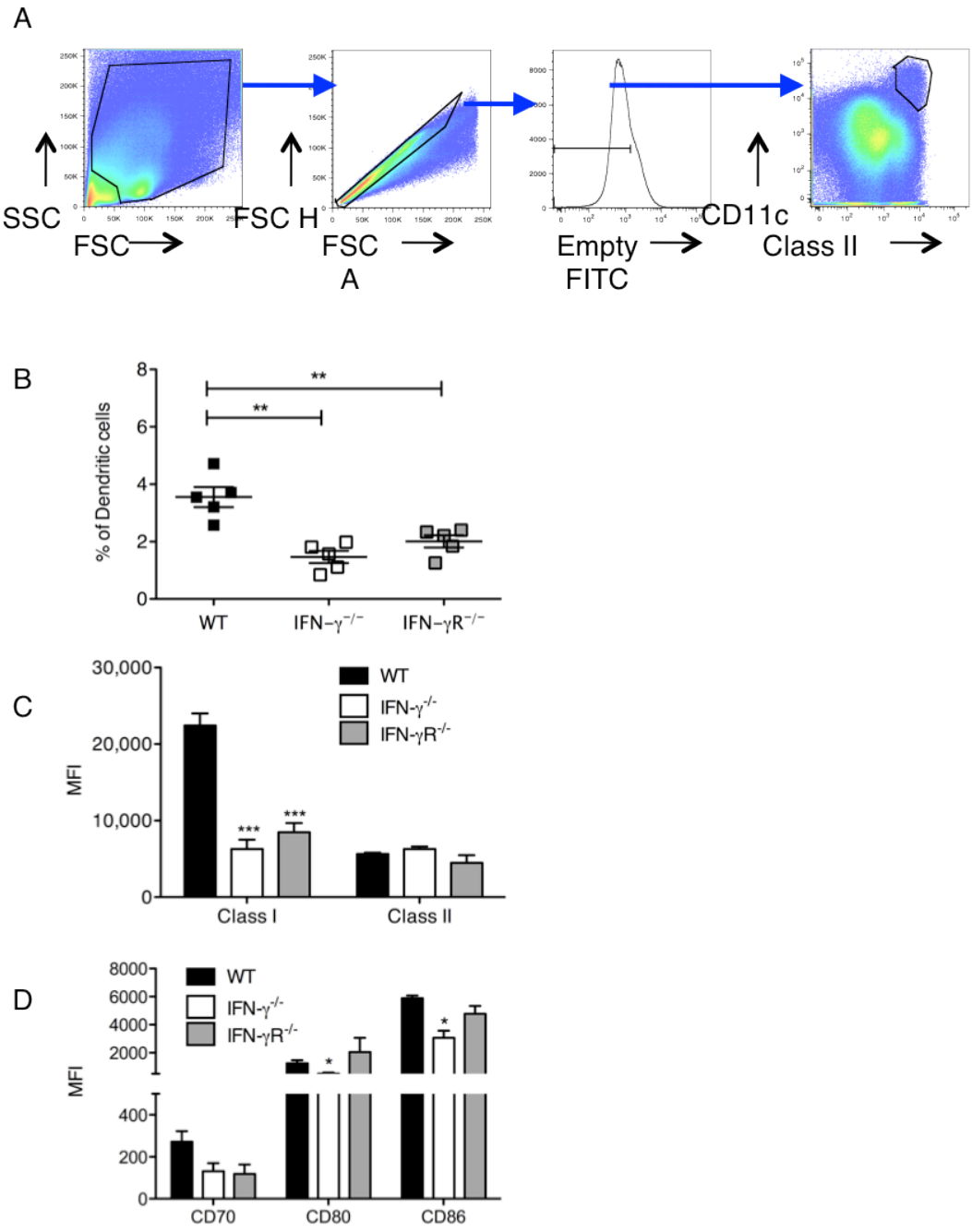

Figure 5.12 Comparison of the dendritic cell characteristics in the lungs of infected mice on day 14 p.i.

C57BL/6 WT, IFN-γ$^{-/-}$ and IFN-γR$^{-/-}$ mice were infected with 5 PFU of influenza A/ PR/8/34 and DCs were harvested from the lungs on day 14 p.i. (A) Gating strategy for lung DCs. Graph representing the percentages of DCs from the lung tissues (B), their expression of Class I and Class II MHC molecules (C) and co-stimulatory molecules (D). Data are representative from 2 independent experiments with n=4-5 per group.

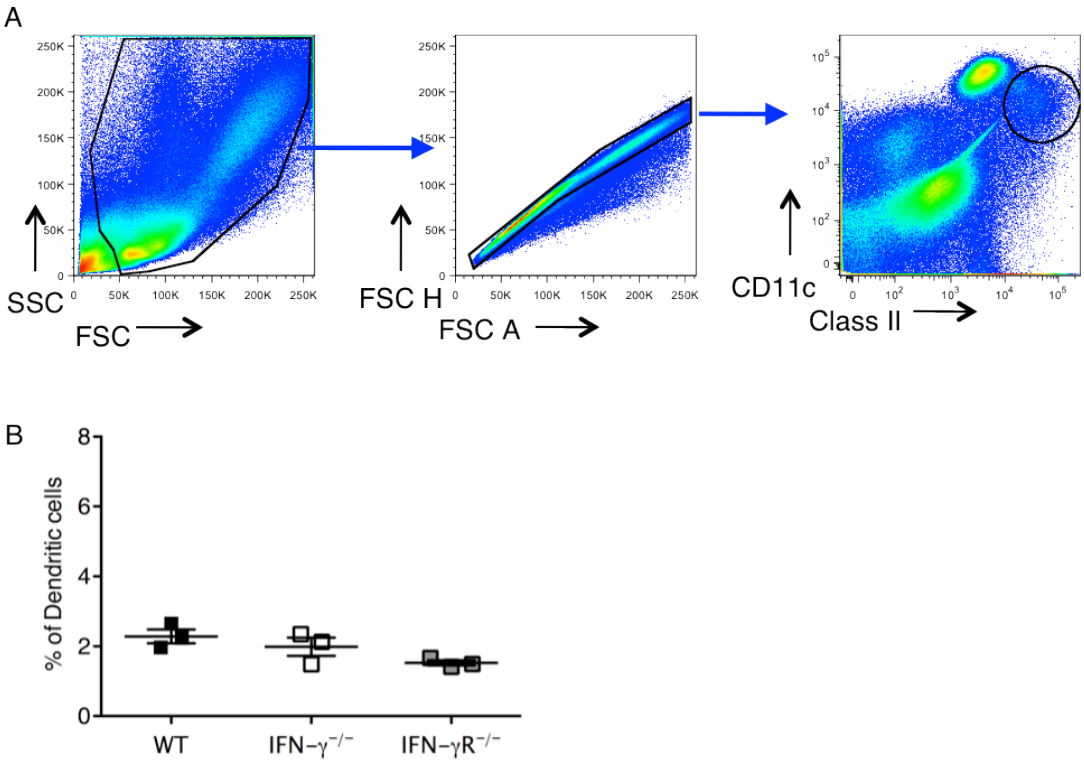

Figure 5.13 Comparison of the dendritic cell characteristics in the lungs of mice at steady state.

Naïve C57BL/6 WT, IFN-γ$^{-/-}$ and IFN-γR$^{-/-}$ mice were sacrificed and DCs were harvested from the lungs. (A) Gating strategy for lung DCs. (B) Graph representing the percentages of DCs from the lung tissues. Data are representative from 2 independent experiments with n=3 per group.

Furthermore we wanted to confirm that there was no extended duration of antigen presentation in the IFN-$\gamma^{-/-}$ and IFN-$\gamma R^{-/-}$ mice. Although, we have confirmed that the viral titers and the kinetics of viral clearance were similar in the lungs of the WT, IFN-$\gamma^{-/-}$ and IFN-$\gamma R^{-/-}$ mice, we wanted to know if clearance of virus coincides with antigen disappearance. To assess this, we infected WT, IFN-$\gamma^{-/-}$ and IFN-$\gamma R^{-/-}$ mice with the PR8-OT1 virus and then harvested the APCs (antigen presenting cells) from the lung draining lymph node on day 5 p.i (as controls) and from the lungs on day 11 p.i. to measure their antigen presentation. These APCs were then cultured with naïve CFSE-labeled OT-1 cells for 72h. We chose the day 11 time-point as this is when the virus was totally cleared and viral RNA was very low. The extent of CFSE dilution measured the cell proliferation and indirectly the extent of antigen presentation by the isolated APCs (Figure 5.14).

We observed that there was a very high dilution of CFSE in the OT-1 cells cultured with all the day 5 APCs, indicating high cell proliferation and hence high levels of antigen presentation. However, we did not observe any cell proliferation in any of the cultures with APCs isolated from the day 14 p.i. lungs. This trend was maintained in the WT, IFN-$\gamma^{-/-}$ and IFN-$\gamma R^{-/-}$ mice, indicating that there is no extended antigen presentation in the absence of IFN-γ signaling.

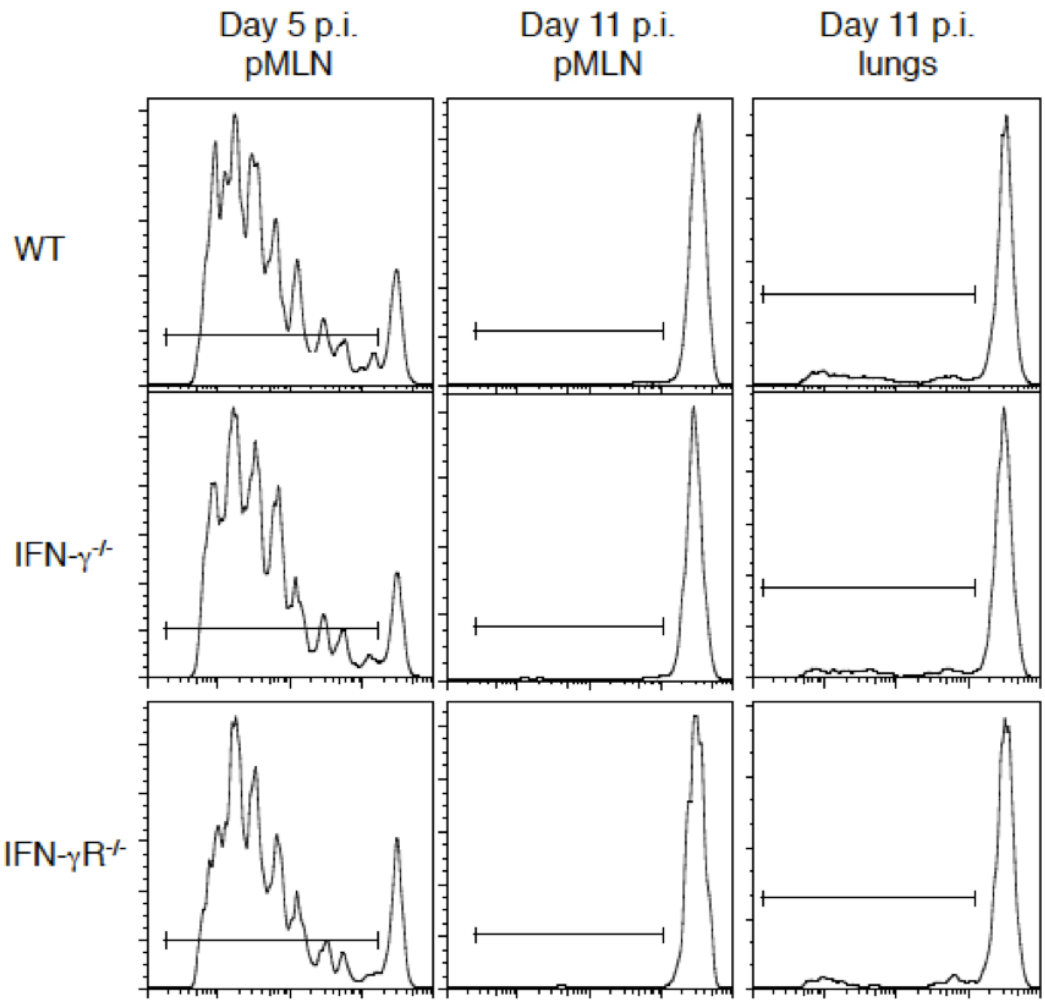

Figure 5.14 No persistence of viral antigen presentation in the absence of IFN-γ signaling.

DCs were harvested from the lung draining lymph nodes (pMLNs) and lungs of mice infected with SIINFEKL-PR/8 influenza and cultured with CFSE-labelled naïve OT-1 cells for 3 days. After 3 days the CFSE dilution was analyzed. Representative flow plots of proliferation of labeled $CD8^+$ T cells determined using FlowJo software.

5.9 IFN-γ regulates number of memory precursors as determined by the expression of IL-7Rα (CD127) on the antigen specific $CD8^+$ T cells in the lungs of influenza infected mice

Memory T cells display enhanced survival when exposed to certain cytokines that are known to boost rates of survival and proliferation in responding cells. The gamma chain cytokines are particularly known for this function. T cells can only respond to these cytokines provided they express the relevant receptors for these cytokines. As antigen specific $CD8^+$ T cells in the lungs of IFN-$\gamma^{-/-}$ and IFN-$\gamma R^{-/-}$ mice displayed enhanced survival during the contraction phase, we hypothesized that these cells may be memory precursors. In order to confirm this and to assess whether these cells could respond better to the cytokine milieu, we measured the levels of expression of receptors for key cytokines that can regulate survival and differentiation into memory cells (viz. IL-2, IL-7, IL-15). We examined levels of all subunits for IL-2R (α CD25, β CD122 and γ CD132), IL-7R (α CD127 and γ CD132) and IL-15R (α CD215, β CD122 and γ CD132) on the surface of the NP_{366}^+ $CD8^+$ T cells at the peak of the infection i.e. at day 11 p.i. (Figure 5.15). Although we noted a slight increase in the level of CD122 on the flu-specific cells of the IFN-$\gamma R^{-/-}$ mice, this was not seen in the IFN-$\gamma^{-/-}$ mice. We did not observe any differences in the levels of expression of CD25, CD132 and CD215. However, we observed significant differences in the levels of CD127 (IL-7Rα) expression in both the IFN-$\gamma^{-/-}$ and IFN-$\gamma R^{-/-}$ mice.

A

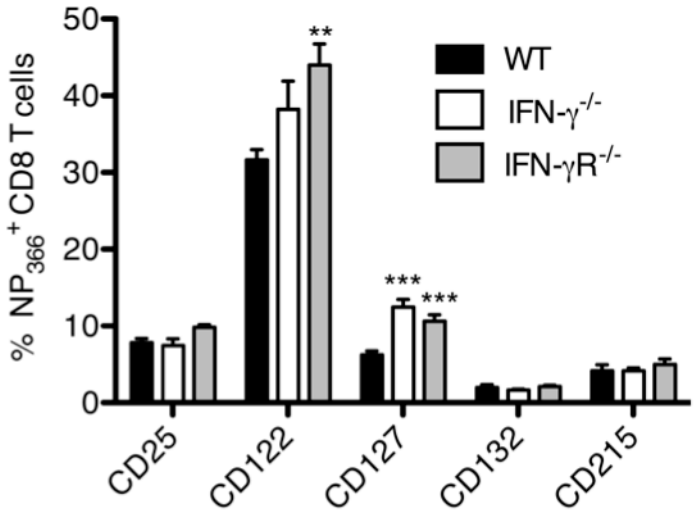

Figure 5.15 Expression of cytokine receptors on antigen specific $CD8^+$ T cells in the lungs of WT, IFN-$\gamma^{-/-}$ and IFN-$\gamma R^{-/-}$ mice.

WT, IFN-$\gamma^{-/-}$ and IFN-$\gamma R^{-/-}$ mice were infected with 5PFU PR/8 influenza. NP_{366}^+ $CD8^+$ T cell proportions were examined in the lung tissue for expression of different receptors on day 11 p.i. (A) Graphs showing the percentages of NP_{366}^+ $CD8^+$ T cells in the lung expressing the receptor sub-units for IL-2 (CD25, CD122 and CD132), IL-7 (CD127, CD132) and IL-15 (CD215 and CD132) on day 11 p.i.

The increased expression of IL-7Rα on $CD8^+$ T cells at the peak of the response is thought to identify those effector $CD8^+$ T cells that will eventually differentiate into memory cells (Kaech et al. 2003). When we examined the levels of IL-7Rα expression on the antigen specific $CD8^+$ T cells at the peak of the influenza infection, we found that only about 3-7 % of the NP_{366}^+ $CD8^+$ T cells from WT mice expressed IL-7Rα. This is consistent with the percentage of cells that survive to become long-lived memory cells in WT mice. However, in the IFN-$\gamma^{-/-}$ and IFN-$\gamma R^{-/-}$ mice, we observed that a significantly higher percentage (~10-15%) of antigen specific $CD8^+$ T cells expressed IL-7Rα at this point (Figure 5.16A and B). This observation is consistent with our previous results that more antigen specific $CD8^+$ T cells survive in these mice. We concluded that in the absence of IFN-γ signaling, a higher number of memory precursor cells are formed. We further examined the kinetics of the IL-7Rα expression on these cells on day 14 after infection (Figure 5.16 A and C). Although the percentage of cells expressing IL-7Rα at this time point showed an increase compared to day 11 p.i, the expression of IL-7Rα was still higher in both IFN-$\gamma^{-/-}$ and IFN-$\gamma R^{-/-}$ mice. These data suggest that one mechanism that IFN-γ may use to control the survival of antigen-specific $CD8^+$ T-cells is to regulate the expression of IL-7Rα during the contraction phase to promote death of effector $CD8^+$ T cells.

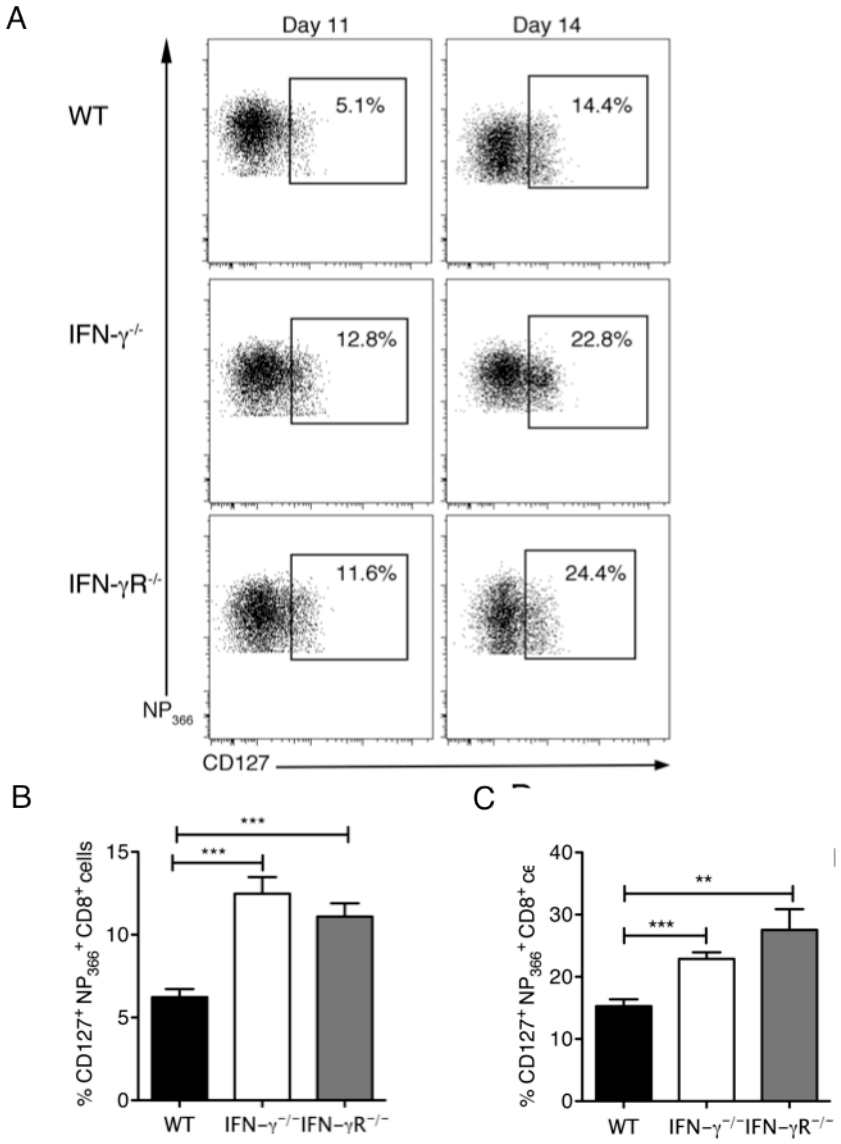

Figure 5.16 Expression of IL-7Rα on antigen specific $CD8^+$ T cells in the lungs of WT, IFN-$\gamma^{-/-}$ and IFN-$\gamma R^{-/-}$ mice

WT, IFN-$\gamma^{-/-}$ and IFN-$\gamma R^{-/-}$ mice were infected with 5PFU PR/8 influenza. NP_{366}^+ $CD8^+$ T cell proportions were examined in the lung tissue for expression of IL-7Rα (CD127) on day 11 p.i. (A) Representative flow cytometry plots and (B and C) graphs showing the percentage of cells expressing IL-7Rα in the WT, IFN-$\gamma^{-/-}$ and IFN-$\gamma R^{-/-}$ mice on day 11 p.i. (A & B) and day 14 p.i. (A & C). Data were pooled from two or three independent experiments with 4-5mice/group/experiment. (*$p<0.05$ and **$p<0.001$ determined using Student's t test).

Next we co-stained for the T cell degranulation marker CD107α as well as CD127 (IL-7Rα) at day 11 p.i. We observed that at the peak of the response, the NP_{366}^+ $CD8^+$ T cells that were IL-7Rα^{low} expressed CD107α whereas the IL-7Rα^{high} cells did not Figure 5.17). This could be an indication that the IL-7Rα^{lo} cells may be the short-lived effector cells whereas the IL-7Rα^{high} cells do not have effector function and may be memory precursors.

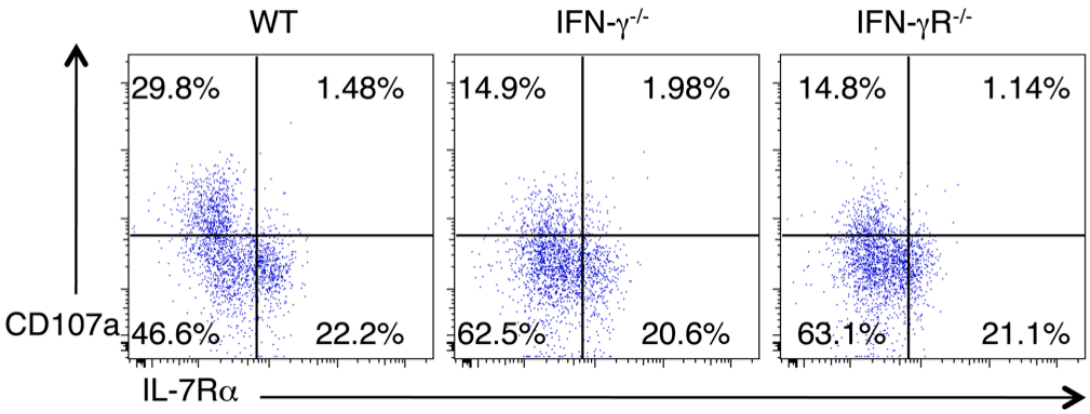

Figure 5.17 Differential expression of degranulation marker CD107α on the IL-7Rα^{hi} and IL-7Rα^{low} antigen specific CD8$^+$ T cells.

C57BL/6 WT, IFN-γ$^{-/-}$ and IFN-γR$^{-/-}$ mice were infected with 5PFU of influenza A/ PR/8/34 and the percentage CD107α expression measured on the NP_{366} $^+$ CD8$^+$ T cells on day 11 p.i. (A) Representative flow cytometry plots showing the relative expression of CD107α and IL-7Rα(CD127) on the NP_{366}^+ CD8+ T cells in the lungs of mice on Day 11 p.i. Data are representative of at least 3 independent experiments with n=4-5 per group.

5.10 Increased IL-7R expression in the $CD8^+$ T cells increases their survival by increasing the levels of anti-apoptotic molecule Bcl-2 inside the cell

We also examined the levels of intracellular Bcl-2 expressed by the antigen specific IL-$7R^{hi}$ and IL-$7R^{lo}$ cells (Figure 5.18A). We observed that the IL-7Rhi cells express higher levels of the anti-apoptotic molecule Bcl-2, indicating that these are refractive to apoptosis and hence may be long-lived memory precursors (Figure 5.18 B).

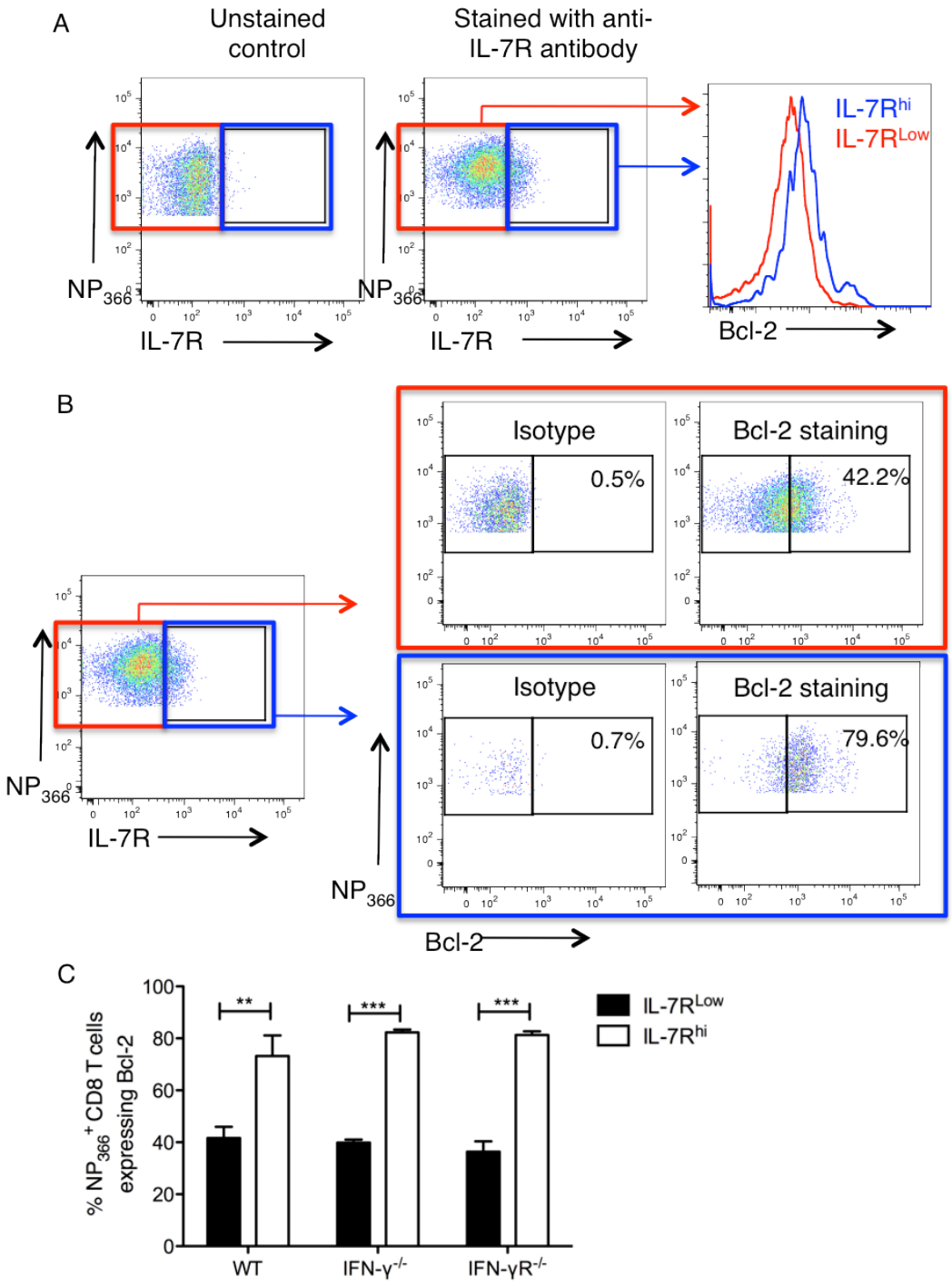

Figure 5.18 Levels of expression of intracellular Bcl-2 on the IL-7Rα^{hi} and IL-7Rα^{low} antigen specific CD8$^+$ T cells.

(A and B) Representative flow cytometry plots showing the level of Bcl-2 in the IL-7R^{hi} and IL-7R^{lo} population of antigen specific CD8$^+$ T cells. (C) Graph showing percentages of IL-7R^{low} and IL-7R^{hi} NP$_{366}$ CD8$^+$ T cells expressing Bcl-2. Representative plots are shown from three independent experiments. (*p<0.05 and **p<0.001 determined using Student's t test).

5.11 Blocking IL-7 in the lungs of infected IFN-$\gamma^{-/-}$ mice returns the contraction phase to normal WT levels

To confirm whether IL-7R expression was indeed key to the survival of the influenza-specific $CD8^+$ T cells *in vivo*, we blocked IL-7 in the lungs of infected mice. We delivered IL-7 neutralizing antibody or control isotype IgG to the lungs of infected WT and IFN-$\gamma^{-/-}$ mice on day 11 p.i. by the intranasal route and quantified NP_{366}^+ $CD8^+$ T cells in the lung tissues of the treated mice on day 14 p.i. Blocking IL-7 enhanced the death of the NP_{366}^+ $CD8^+$ T cells and significantly fewer cells survived in the lungs of the IFN-$\gamma^{-/-}$ mice, compared to the control treated IFN-$\gamma^{-/-}$ mice (Figure 5.19).

When IL-7 was blocked in the lungs of WT mice, a similar induction of cell death was observed. Even fewer NP_{366}^+ $CD8^+$ T cells survived in the lungs of WT mice treated with anti-IL-7. This finding demonstrates that IL-7R expression on the NP_{366}^+ $CD8^+$ T cells is functionally important in their survival during the contraction phase of the response.

This experiment confirmed that the expression of IL-7R is functionally important for receiving survival signals. Hence, the increased frequency of IL-7Rα (CD127) on the NP_{366}^+ $CD8^+$ T cells in the absence of IFN-γ signaling enhances their survival and consequently their ability to develop into memory cells.

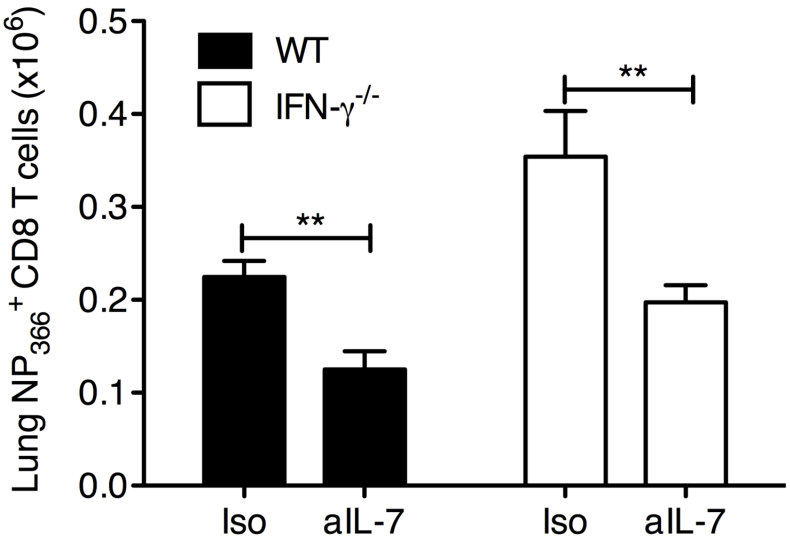

Figure 5.19 Administering IL-7 neutralizing antibodies to the lungs of infected mice leads to reduced survival of NP_{366}^+ $CD8^+$ T cells

Infected WT and IFN-$\gamma^{-/-}$ mice were treated with intranasal 0.05mg of anti-IL-7 pAb (aIL-7) or control isotype Goat IgG (Iso) on D11 p.i. and NP_{366}^+ $CD8^+$ T cells were enumerated in the lungs of these mice on D14 p.i. Representative plots are shown from three independent experiments. (*$p<0.05$ and **$p<0.001$ determined using Student's t test).

5.12 Discussion

There is increasing evidence that IFN-γ regulates the contraction of $CD8^+$ T cell responses in systemic infections although our study is the first to examine its role in localized infections. Although these studies show that IFN-γ regulates the contraction of the $CD8^+$ T cell response, they fail to identify the mechanism/s for this. In the present study we demonstrate that IFN-γ-IFN-γR signaling regulates the reduction of $CD8^+$ T cells even in localized mucosal infections like influenza. We have shown in chapter 4 that in the absence of IFN-γ signaling the contraction phase of the $CD8^+$ T cell response is aberrant, resulting in the accumulation of antigen specific $CD8^+$ T cells as far as day 120 p.i. Our data also suggests that IFN-γ can act directly on antigen specific $CD8^+$ T cells to induce cell death during an influenza infection as we observed when we cultured IFN-$\gamma^{-/-}$ effector cells in the presence of IFN-γ. We postulate that IFN-γ can act on the influenza-specific $CD8^+$ T cells by multiple mechanisms activating several downstream effectors including the receptor for Interleukin 7. We showed that the IL-7R expression was functionally important for the survival of effector cells during the contraction phase. We have also identified some of the other molecules that IFN-γ can activate which may be involved in inducing $CD8^+$ T cell death in an influenza-infected lung.

IFN-γ is known to influence the rates of proliferation and apoptosis in activated T cells (Gajewski and Fitch 1988; Liu and Janeway 1990; Refaeli et al. 2002). Therefore, we thought that the increased accumulation of antigen specific $CD8^+$ T cells in the lungs of influenza infected IFN-$\gamma^{-/-}$ and IFN-$\gamma R^{-/-}$

mice could be a result of either the rates of cell proliferation and/or death. However, analysis of *in vitro* and *in vivo* proliferation indirectly, indicated that IFN-γ deficiency did not alter the rates of proliferation of $CD8^+$ T cells. Expression of Ki67, a nuclear marker for cellular proliferation (Scholzen and Gerdes 2000), on flu-specific $CD8^+$ T cells in the lung was not affected by IFN-γ. Indeed, we observed decreased rates of cell death in antigen specific $CD8^+$ T cells in the IFN-$\gamma^{-/-}$ mice. We could also induce cell death in antigen specific $CD8^+$ T cells by the addition of recombinant IFN-γ to *ex-vivo* cultures. This mechanism is consistent with findings from other studies which show that IFN-γ contributes to activation-induced-cell death of *in vitro* activated T cells (Vukmanovic-Stejic et al. 2000; Refaeli et al. 2002). We further identified several molecules acting downstream of IFN-γ that induce cell death, in a cell death pathway finder PCR array.

The levels of homeostatic cytokine receptors may be differentially expressed in the absence of IFN-γ signaling and hence responsible for increased rates of survival of $CD8^+$ T cells in the IFN-γ and IFN-γR deficient mice. Studies in LCMV showed that IFN-γ had an effect on expression of IL-7R (Tewari et al. 2007). Also, expression of IL-7Rα (CD127) on antigen specific $CD8^+$ T cells at the peak of the response is known to identify cells that will survive to become memory precursor populations (Kaech et al. 2003). We observed that IFN-γ could influence levels of IL-7Rα expression on the effector $CD8^+$ T cells in an influenza infection. IL-7 is one of the homeostatic cytokines, which delivers survival signals to the $CD8^+$ T cells by increasing expression of anti-apoptotic molecules such as Bcl-2 (Kaech et al. 2003). We found that this was also true for influenza and observed increased frequencies of cells expressing

IL-7Rα at the peak of the response in the absence of IFN-γ signaling and showed that these cells also expressed higher levels of Bcl-2. This agreed with our initial finding that increased numbers of cells survived the contraction phase in the absence of IFN-γ signaling. We could confirm that expression of IL-7Rα was functionally significant by IL-7 blocking *in vivo*. Neutralizing IL-7 in the IFN-γ-deficient mice reduced the numbers of flu-specific $CD8^+$ T cells to WT levels. Hence, the higher expression of IL-7Rα is one reason that more cells in these mice are resistant to cell death and hence survive the contraction phase to form a higher percentage of memory cells. In addition to IL-7Ra, other molecules may also regulate the survival of these cells and further studies will be needed to identify the factors responsible.

Antigen specific $CD8^+$ T cells in IFN-$\gamma^{-/-}$ and IFN-$\gamma R^{-/-}$ mice exhibited higher IL-7Rα expression at the peak of expansion and their numbers did not contract compared with antigen specific $CD8^+$ T cells in WT mice. However, it remains to be determined if early IFN-γ signals in T cells directly regulate which effector cells will or will not up regulate IL-7Rα. Thus, determining how antigen-specific $CD8^+$ T cells directly respond to IFN-γ signals during infection may provide important clues to how the immune system regulates the survival of only a small proportion of effector $CD8^+$ T cells for memory cell generation. T-bet is a transcription factor that regulates the levels of IL-7Rα and T-bet deficiency leading to increased levels of IL-7Rα expressing $CD8^+$ T cells at the peak of the response (Intlekofer et al. 2007). Inhibition of T-bet expression due to IFN-γ deficiency could lead to the increased levels of IL-7Rα on the virus-specific $CD8^+$ T cells.

There is evidence to suggest that memory $CD8^+$ T cells may derive from effector cells (Joshi et al. 2007; Sarkar et al. 2008; Bannard et al. 2009). However, it is also possible that memory $CD8^+$ T cells represent a separate lineage that is resistant to contraction. We show here that the memory $CD8^+$ T cells are formed from a population of effector cells which are IL-7Rα^+ but do not express cytotoxic molecules like CD107α and that only the IL-7R$\alpha^{lo/neg}$ cells express CD107α but not the IL-7R$\alpha^{hi/pos}$ cells. This indicates that the IL-7R$\alpha^{hi/pos}$ cells may be memory precursors and is in agreement with the finding that $CD127^+$(IL-7R$\alpha^{hi/pos}$) $CD8^+$ T cells display low levels of cytotoxicity and effector function and progressively differentiate into memory cells (Bachmann et al. 2005).

Chapter 6: Role of IFN-γ in CD8$^+$ T cell response to a heterologous re-challenge

6.1 Introduction

The essential hallmark of the adaptive immune system is its ability to engender antigen-specific memory, which can protect against repeated infections with the same or a similar pathogen (Pulendran and Ahmed 2006; Sallusto et al. 2010; Pulendran and Ahmed 2011). This ability is termed immunological memory and is based on the induction of long-lived T and B cells after infection or vaccination (Ahmed and Gray 1996; Gourley et al. 2004). Memory cells are highly responsive to antigenic stimulation and proliferate swiftly to differentiate into effector cells to confer protection against the invading pathogen (Veiga-Fernandes et al. 2000; Whitmire et al. 2008). The extent to which the host is protected from a re-challenge is dependent on the quality and quantity of memory T cells formed (Swain et al. 2004; Hand and Kaech 2009). Understanding the mechanisms that regulate the formation of efficient T cell memory is important for the development of effective vaccines.

CD8$^+$ T cells are important contributors to immunity against viral infections, such as influenza, by promoting viral clearance (Yap et al. 1978; McMichael et al. 1983; Topham et al. 1997). During a CD8$^+$ T cell response, naïve CD8$^+$ T cells proliferate and differentiate into effectors. In the case of an influenza infection, the peak of the CD8$^+$ T cell expansion is reached at around day 11 p.i after which most of the cells are fated to die, leaving only a small pool of long-lived antigen-specific memory CD8$^+$ T cells. The number of memory

cells depends on the magnitude of expansion and contraction of the CD8$^+$ T cell response. The molecules that control the differentiation of effector cells into memory cells during the contraction of the response and the mechanisms behind this conversion are not yet fully understood.

In earlier chapters, we have shown that IFN-γ regulates the contraction of the antigen-specific CD8$^+$ T cell response to an influenza infection and hence contributes to increased numbers of antigen specific CD8$^+$ T cells persisting in the lungs and other tissues (eg. spleen) of infected mice in the absence of IFN-γ signaling long after the infection has been resolved. We have also shown that the expression of IL-7R by the influenza-specific CD8$^+$ T cells is important for their survival through the contraction phase and that this expression of IL-7R is also regulated by IFN-γ signaling. Furthermore, we wanted to assess if the large numbers of memory CD8$^+$ T cells generated in the absence of IFN-γ, can respond to a re-infection and if they are efficient in eliminating the second viral infection.

It has been shown that memory CD8$^+$ T cells isolated from the lungs can participate in recall responses (Ely et al. 2003). In this chapter, we set out to establish a re-infection model for influenza by using two different viruses differing only in their surface proteins. Using this model, our main aim was to determine whether the increased numbers of antigen-specific CD8$^+$ T cell generated in the IFN-γ$^{-/-}$ and IFN-γR$^{-/-}$ mice could respond to a re-challenge and if whether they offered any advantage over CD8$^+$ T cells from WT mice. We hypothesized that if the increased memory generated in the absence of IFN-γ signaling confers an advantage over WT animals, then it would be a

potential avenue to pursue for establishing better immune $CD8^+$ T cell memory with vaccinations.

6.2 Model for secondary challenge

It is generally believed that memory $CD8^+$ T cells recognize epitopes in the conserved internal proteins of influenza and hence contribute to heterosubtypic immunity to a secondary challenge. To evaluate the role of IFN-γ to a recall $CD8^+$ T cell response, we decided to use a well-established mouse model that has been previously used for the detection of heterosubytpic immunity. We used a pair of influenza strains, A/HK-X31 (X31) and A/PR/8/34 (PR8), that express different HA and NA subtypes. Since X31 expresses the H3N2 subtypes of HA and NA coat proteins and PR8 expresses the H1N1 subtypes of HA and NA, antibodies generated to X31 do not neutralize PR8 and vice versa. However, the internal proteins of both viruses are the same and hence contain epitopes that stimulate $CD8^+$ T cell responses to both viruses. These cross-reactive $CD8^+$ T cells are thought to mediate the effects of heterosubtypic immunity. These two viruses provided us with a model to study the recall $CD8^+$ T cell responses without any interference from their B-cell counterparts.

Our study compared the recall $CD8^+$ T cell responses in the presence and absence of IFN-γ signaling. Protective immunity following challenge was assessed by determining weight loss in infected mice, their rates of survival, and lung viral titers. Given the reduced $CD8^+$ T cell contraction phase in the absence of IFN-γ signaling, we were mainly interested to see how this would

influence the recall response. Furthermore, we wanted to ascertain whether the increased numbers of memory $CD8^+$ T cells in the absence of IFN-γ signaling, could actually respond to a re-challenge and if they could afford better protection in a secondary infection.

6.3 Primary infection with PR8 followed by a re-challenge with X31

Considering that we had used the PR8 virus for all the primary infection experiments, we first chose to use the same strain for primary infection for the re-challenge experiments. Mice that were infected with a 5PFU of PR8 virus were then re-infected with 1000 PFU of X31 virus. The mice were monitored for morbidity and mortality for 8 days p.i (Figure 6.1). We found that the mice did not lose any weight in response to a re-challenge with 1000 PFU of X31. The only slight weight loss that was observed early in the infection was probably a result of the innate immunity or could be an effect of the anesthetic drugs. But this slight weight loss was quickly followed by a steady weight gain until day 8 p.i. None of the mice showed any signs of sickness.

Further, to look at the $CD8^+$ T cell responses to this re-challenge, we measured the antigen specific $CD8^+$ T cells in the lung using the NP_{366} pentamer (Figure 6.2). We found that there were higher numbers of NP_{366}^+ $CD8^+$ T cells responding to the re-challenge at day 8 p.i than was observed at day 8 p.i after a primary infection. Our data is in agreement with earlier studies that established T cell memory confers at best a 2-3 day advantage in the rate of effector T cell development and localization to the influenza virus infected respiratory tract (Bennink et al. 1978).

We also found that there were a significantly larger number of NP_{366}^+ $CD8^+$ T cells in the lungs of IFN-$\gamma^{-/-}$ and IFN-$\gamma R^{-/-}$ mice. This meant that the cells that were present in the IFN-$\gamma^{-/-}$ and IFN-$\gamma R^{-/-}$ mice after the primary infection could respond to a re-challenge and higher numbers of influenza-specific $CD8^+$ T cells that survive the contraction phase translated to enhanced $CD8^+$ T cell responses to a re-infection.

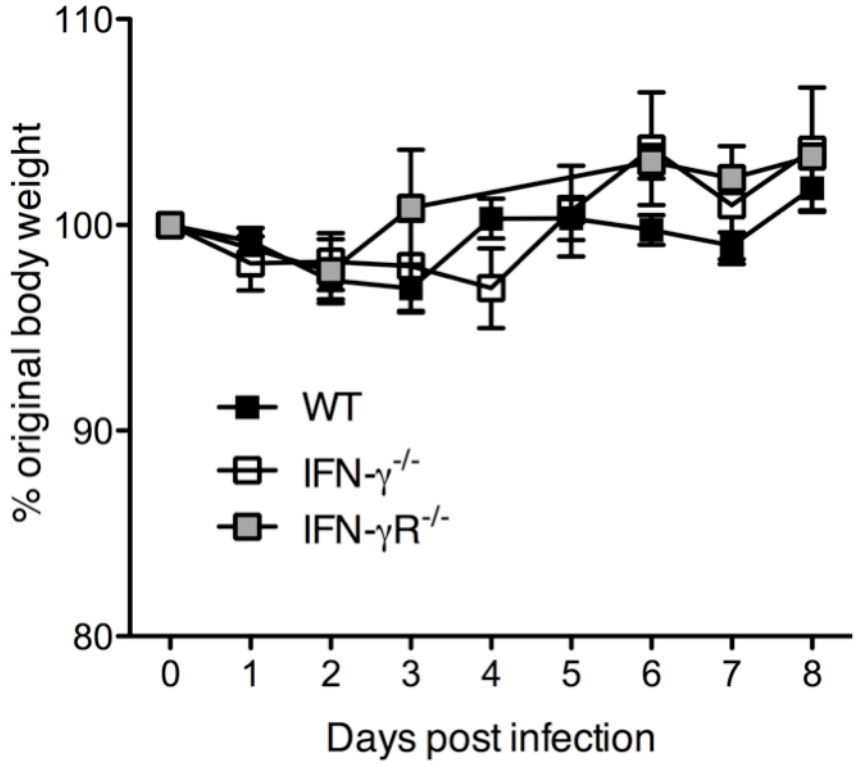

Figure 6.1 Weight loss in response to a 1000 PFU X31 influenza re-infection after a primary infection with 5 PFU PR8.

C57BL/6 WT, IFN-γ$^{-/-}$ and IFN-γR$^{-/-}$ mice were infected with 5 PFU PR/8 and 30 days later with a 1000 PFU of influenza A/HKx31/(H3N2). Weight loss of mice over a course of 12 days following infection. Data represents mean+/- SEM. n=5/ group

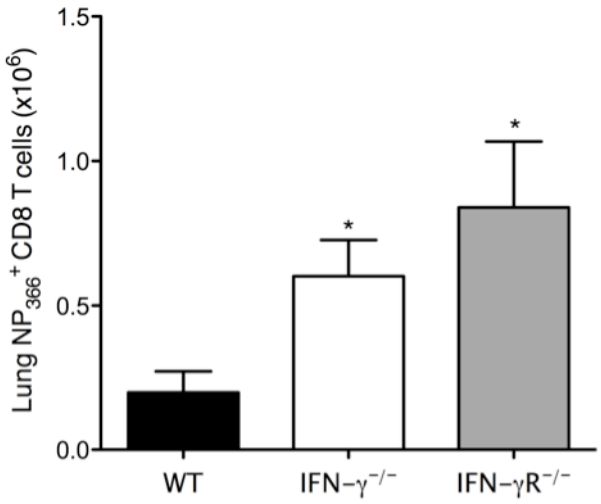

Figure 6.2 Antigen specific CD8$^+$ T cell response to an X31 rechallenge after a PR8 primary infection

C57BL/6 WT, IFN-γ$^{-/-}$ and IFN-γR$^{-/-}$ mice were infected with a sub-lethal dose of influenza A/ PR/8/34 (H1N1) and after 30 days, mice were infected with a second virus HK/X31 (H3N2) and monitored for 8 days after infection. Total NP_{366}^+ CD8$^+$ T cell numbers in the lung tissue at day 8 after re-infection. The numbers of NP_{366}^+ CD8$^+$ cells (mean+/-SEM) shown is calculated from the total counts and the percentage of cell staining. (n=5).

However, with this model of re-infection, we could not see any weight loss after re-infection even with 1000 PFU of X31. And although we could see enhanced numbers of antigen-specific $CD8^+$ T cells in the IFN-$\gamma^{-/-}$ and IFN-$\gamma R^{-/-}$ mice, we could not determine if they could afforded better protection against a re-challenge. Hence, we decided to alter the model for re-challenge: primary infection with X31 followed by re-challenge with PR8, as we could increase the doses of PR8 much higher (5PFU to 500PFU) than we could with X31. But to use the new model, we first had to confirm if we saw the same phenotype of reduced contraction in the IFN-$\gamma^{-/-}$ and IFN-$\gamma R^{-/-}$ mice after primary infection with X31.

6.4 Comparing the primary $CD8^+$ T cell response to an X31 infection

The A/HK/X31 (X31) virus is a recombinant strain that expresses the surface Hemagglutinin (HA) and Neuraminidase (NA) proteins of A/Aichi (H3N2) and the internal components of PR/8 (Kilbourne 1969). Neutralizing antibody responses to the surface HA and NA glycoproteins of these two viruses are not cross-reactive, so protection and recall responses seen are restricted to $CD8^+$ T cells.

The X31 strain of virus is much less pathogenic when compared to PR/8. The extent of weight loss in the infected mice is also very low and about 15-20% which can be only achieved after using very high doses of the X31 virus (i.e. 1000 PFU). This weight loss is comparable to what can be seen with only 5 PFU of the PR/8 strain of virus. The kinetics of weight loss with X31 virus was somewhat different to PR8. Animals started losing weight earlier, which may reflect the higher dose of virus given. Maximum weight loss and recovery

were comparable. To compare the responses to X31 virus, WT C57BL/6 mice, IFN-$\gamma^{-/-}$ mice and IFN-$\gamma R^{-/-}$ mice were infected with 1000 PFU of X31 influenza and their responses to the infection determined. All infected mice survived the ensuing infection, irrespective of their ability to make or respond to IFN-γ. We measured weight loss in all the infected mice for a period of 14 days after the infection (Figure 6.3). IFN-$\gamma^{-/-}$ and IFN-$\gamma R^{-/-}$ mice showed similar weight loss to WT mice after infection. All X31 infected mice exhibited reduced symptoms compared with mice infected with PR/8 including: poor grooming, ruffled fur, reduced responses to external stimuli after a week p.i. The highest weight loss was recorded around day 8-9 p.i, i.e. about 20 % of their original body weight. They also recovered from the infection regaining their original body weight by day 12 p.i. This indicated that the loss of IFN-γ or its receptor does not increase the susceptibility of the mice to a 1000 PFU dose of X31 influenza. Our results are in agreement with previous findings with our earlier studies with the PR8 strain of influenza virus.

Further, we compared the antigen-specific $CD8^+$ T cell responses to the X31 infection (Figure 6.4) by enumerating $CD3^+CD8^+$ T cells that bound to the MHC I pentamer NP_{366} 'ASNENMETM-H-$2K^b$', an immunodominant epitope, similar to the approach used earlier with the PR8 strain. Since we were only interested in checking if the reduced contraction phase that is seen with the PR8 strain is also evident with the X31, we looked examined later time points in the infection i.e. day 28 p.i. We found an increase in the numbers of NP_{366}^+ $CD8^+$ T cells in the BAL fluid and lung tissue of IFN-$\gamma^{-/-}$ and IFN-$\gamma R^{-/-}$ mice even after X31 infection. This was even true in the spleens

of these mice, indicating a reduced contraction phase and hence an increased memory population in the absence of IFN-γ signaling. To confirm the findings, we even looked at a later time point i.e. day 120 p.i, at which all mice have returned to a state of normalcy (Figure 6.5). The WT mice had very low numbers of flu-specific $CD8^+$ T cells but there were higher numbers present in the IFN-$\gamma^{-/-}$ and IFN-$\gamma R^{-/-}$ mice. This provided the confirmation we needed to use X31 as the strain for primary infection and then re-challenge with PR8 for our re-challenge model.

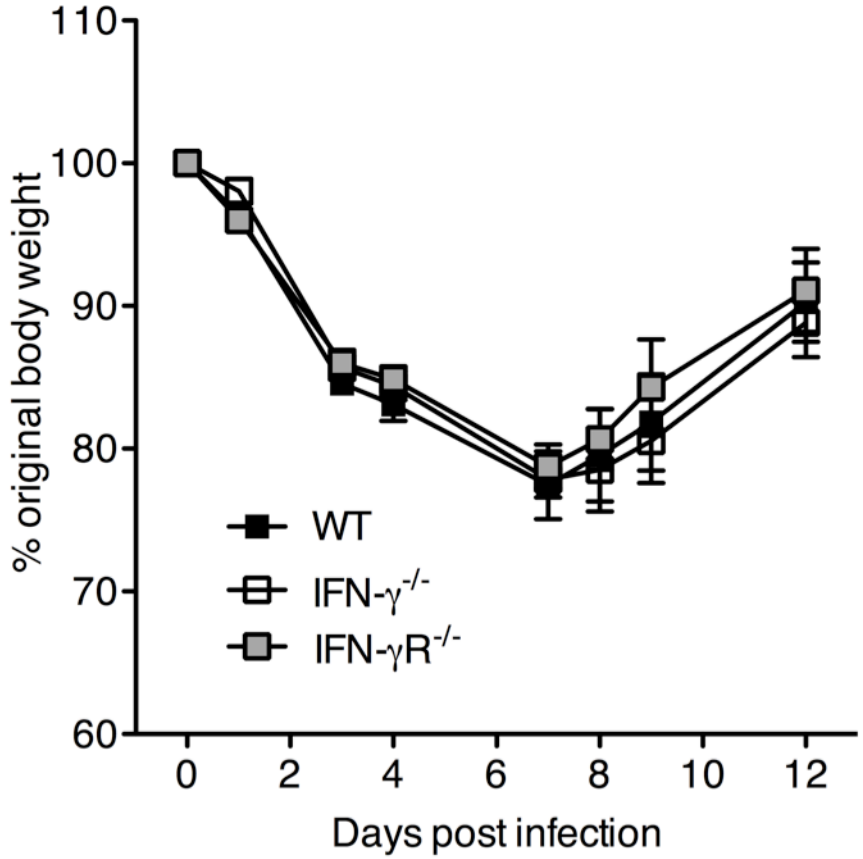

Figure 6.3 Comparison of loss of body weight in response to a 1000 PFU X31 influenza infection in WT, IFN-γ$^{-/-}$ and IFN-γR$^{-/-}$ mice

C57BL/6 WT, IFN-γ$^{-/-}$ and IFN-γR$^{-/-}$ mice were infected with 1000 PFU of influenza A/HKx31/ (H3N2). Weight loss of mice over a course of 12 days following infection. Data represents mean+/- SEM. n=5/ group

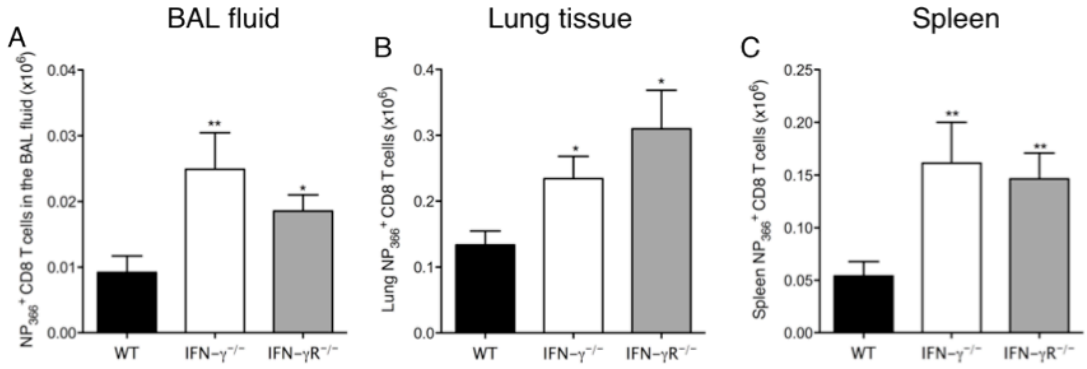

Figure 6.4 Increased numbers of antigen-specific CD8$^+$ T cells in the IFN-γ$^{-/-}$ and IFN-γR$^{-/-}$ mice after X31 infection on day 28 p.i.

C57BL/6 WT, IFN-γ$^{-/-}$ and IFN-γR$^{-/-}$ mice were infected with a 1000 PFU dose of influenza A/HK/X-31. NP$_{366}^+$ CD8$^+$ T cell numbers were examined in the BAL fluid (A), lung tissue (B) and spleens (C) of the mice on day 28 p.i. The numbers of CD8$^+$ NP$_{366}^+$ cells (mean+/-SEM) shown are calculated from the total counts and the percentages of cells staining positive. (***p<0.001 determined using Student's t test). Data are representative of at least 2 independent experiments with n=4-5 per group

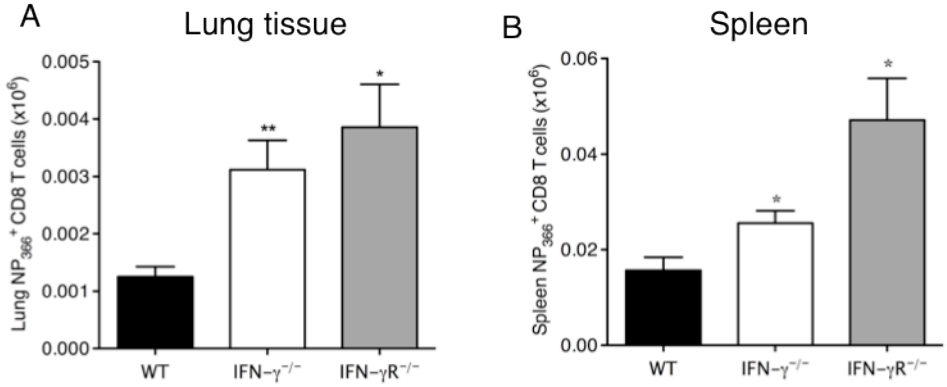

Figure 6.5 Increased numbers of antigen-specific CD8$^+$ T cells in the IFN-γ$^{-/-}$ and IFN-γR$^{-/-}$ mice after X31 infection on day 120 p.i.

C57BL/6 WT, IFN-γ$^{-/-}$ and IFN-γR$^{-/-}$ mice were infected with a 1000 PFU dose of influenza A/HK/X-31. NP_{366}^+ CD8$^+$ T cell numbers were examined in the lung tissue (A and spleens (B) of the mice on day 120 p.i. The numbers of CD8$^+$ NP_{366}^+ cells (mean+/-SEM) shown are calculated from the total counts and the percentages of cells staining positive. (***$p<0.001$ determined using Student's t test). Data are representative of at least 2 independent experiments with n=4-5 per group

6.5 Model for re-challenge: Primary infection with X31 followed by re-challenge with PR8

We decided to use X31 as the strain for the primary infection but we still needed to decide on the dose of PR8 to be used for the re-challenge experiments. Hence, we infected mice with a series of doses of PR8 virus (Figure 6.6). C57BL/6 WT, IFN-$\gamma^{-/-}$ and IFN-$\gamma R^{-/-}$ mice were infected with 5 PFU PR8 as a primary infection (Figure 6.6A) or as a re-infection 35 days after X31 infection and monitored for a period of 8 days. Naïve mice that were infected with 5PFU PR8 behaved similarly to primary PR8 infections shown in chapter 4. They lost about 15-20% of their body weight but regained it by day 14 p.i. Mice that received 5 PFU PR8 as a re-challenge, however did not lose any weight. All the re-infected mice showed no signs of sickness and although did not gain weight in the initial days as uninfected mice would, but started to gain weight after day 5 p.i.

When a higher dose of 50 PFU was used (Figure 6.6B), naïve mice with the primary infection showed signs of sickness and severe weight loss and lost about 20-25% of their body weight and hence had to be euthanized by day 8. These mice would have succumbed to the infection if they had not been sacrificed. Mice that received 50 PFU as a re-infection after an initial infection of X31 showed some weight loss in the initial days of infection but recovered quickly by day 8 p.i. There were no severe signs of sickness observed in these mice and none died. But all three groups of mice infected behaved in a similar manner and hence showed that increasing the virus dose did not have an effect on the mice in the absence of IFN-γ signaling.

When a lethal dose of 500 PFU was used (Figure 6.6C), naïve mice that received this dose as a primary infection lost weight quickly and showed severe signs of infection: lethargy, poor grooming with ruffled fur, hunched backs and lack of response to external stimuli. These mice lost 20-30% of their original body weight and were euthanized. Mice that received this high dose as a reinfection lost about 7-12% of their body weight by day 4 but quickly regained their original weight by day 8 p.i. The mice did not show any signs of sickness. Although the WT mice seemed to lose slightly less weight than the IFN-$\gamma^{-/-}$ and IFN-$\gamma R^{-/-}$ mice, these differences were not statistically significant. Since 500 PFU of PR8 seemed to be the dose of virus with which mice showed weight loss even during a re-infection, we decided to use this dose of virus for our re-infection model. For all experiments carried out after this, we used 1000 PFU of X31 as the primary infection and 500 PFU of PR8 for the second infection. Mice were allowed to recover and generate memory responses for a period of 35 days in between the two infections.

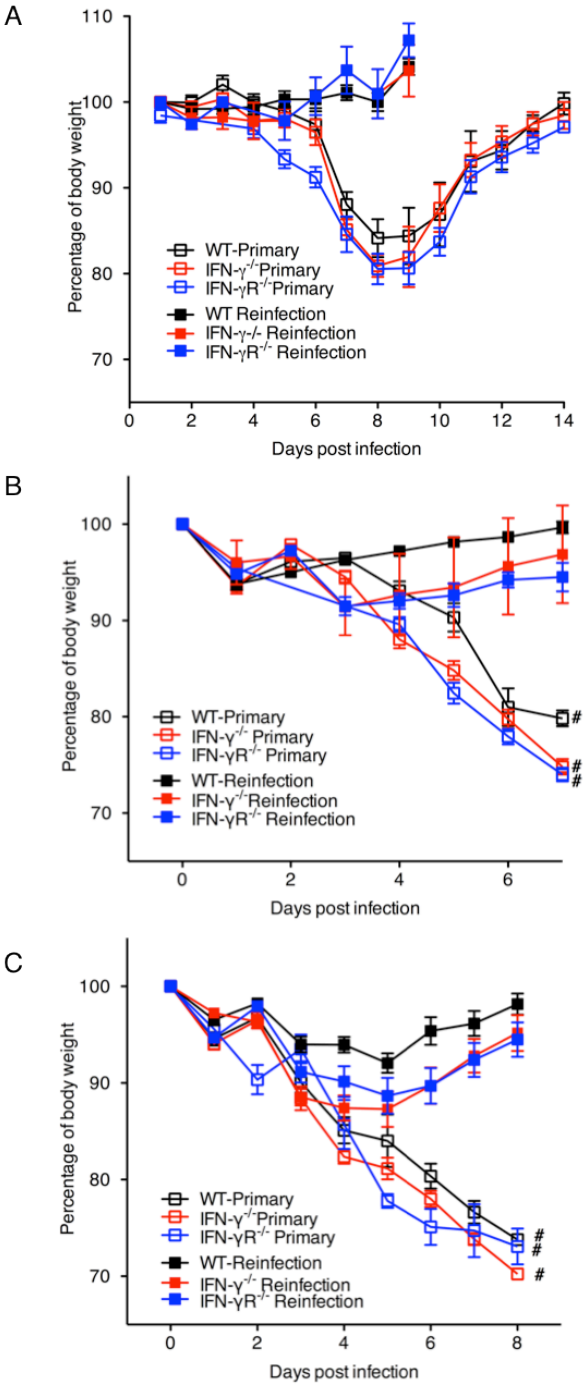

Figure 6.6 Weight loss curves with Primary infection with X31 followed by re challenge with PR8.

C57BL/6 WT, IFN-γ$^{-/-}$ and IFN-γR$^{-/-}$ mice were either infected with a primary infection of 5 PFU (A), 50 PFU (B) or 500 PFU(C) of PR/8 virus or first infected with X31 and then re-infected with the same doses of PR8 after 35 days. Mice infected with a primary infection are shown in open squares and mice with the re-infection are shown as closed squares. (#) indicates mice which were euthanized for loss of excessive weight. Data are pooled from at least 3 independent experiments with n=20 per group.

6.6 Influenza specific CD8$^+$ T cell responses after re-challenge

In order to confirm that the increased frequencies of IL-7Rα expressing cells resulting from the reduced contraction in the absence of IFN-γ signaling were indeed memory precursor cells, we compared recall CD8$^+$ T cell responses in these mice after a secondary challenge with a heterologous strain of influenza. For this set of experiments, mice were infected with X31 (H3N2), and then re-infected after 35 days with 500 PFU of PR/8. As expected for a recall response, we observed an earlier CD8$^+$ T cell response and higher frequencies of antigen specific CD8$^+$ T cells in the lungs of the infected mice, when compared to a primary infection. However, the differences between the CD8$^+$ responses of WT, IFN-γ$^{-/-}$ and IFN-γR$^{-/-}$ mice were greatly enhanced after the secondary challenge, as the NP_{366}^+ CD8$^+$ T cells accounted for ~30% of the CD8$^+$ T cells in the WT mice but in the IFN-γ and IFN-γR deficient mice, these cells accounted for >50% of the CD8$^+$ T cells (Figure 6.7A).

There was a sharp increase in the numbers of antigen specific CD8$^+$ T cells in the lungs and BAL fluid of infected mice when compared to that seen after a primary infection. There was also a dramatic difference in the total numbers of NP_{366}^+ CD8$^+$ T cells in the BAL of IFN-γ$^{-/-}$ and IFN-γR$^{-/-}$ compared to WT mice (Figure 6.7B) and in the lungs as well (Figure 6.7C). The re-infection was done after a period of 120 days after the primary infection with similar results (results not shown).

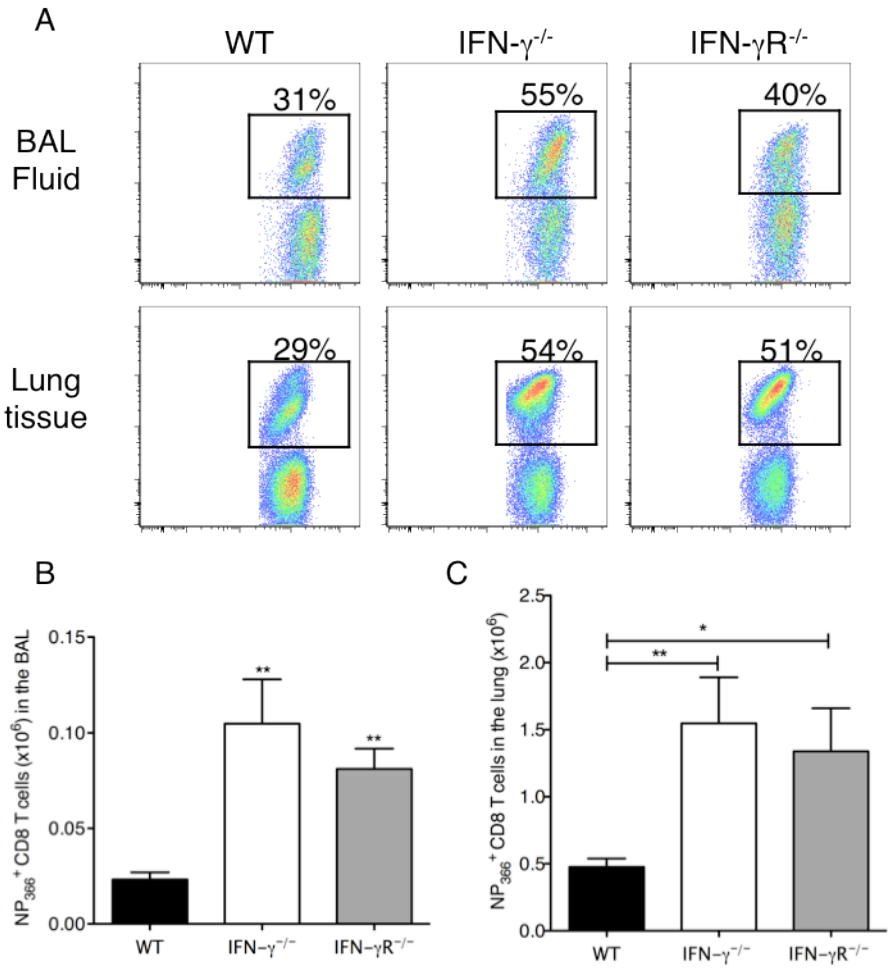

Figure 6.7 Enhanced Antigen-specific CD8$^+$ T cell responses to a re-infection with 500 PFU PR8.

C57BL/6 WT, IFN-γ$^{-/-}$ and IFN-γR$^{-/-}$ mice were infected with a sub-lethal dose of influenza HK/X31 (H3N2) and after 30 days, mice were infected with a second virus A/ PR/8/34 (H1N1) and monitored for 8 days after infection. (A) Representative flow cytometry plots of the proportion of NP$_{366}^+$ CD8$^+$ T cells in the BAL fluid and lung tissue of mice re-infected with 500 PFU of PR/8. Cells are gated on the CD3$^+$CD8$^+$ T cells. Numbers represent percentage of CD8$^+$ T cells, which are NP$_{366}^+$. Total NP$_{366}^+$ CD8$^+$ T cell numbers in the BAL fluid (B) lung tissue (C) at day 8 after re-infection. The numbers of NP$_{366}^+$ CD8$^+$ cells (mean+/-SEM) shown are calculated from the total counts and the percentages of cell staining. Data are pooled for three independent experiments.

6.7 Cytotoxic potential of $CD8^+$ T cells responding to re-infection with 500 PFU PR8

To determine whether the enhanced numbers of $CD8^+$ T cells generated in response to PR8 re-infection were functional, we wanted to assess their ability to kill influenza-infected cells. We decided to study their expression of CD107α as a surrogate marker of their cytotoxic potential. Lung tissues were enriched for T cells and the resulting cells were cultured in the presence of PMA-Ionomycin and anti-CD107α antibodies for 6h in the presence of Brefeldin A and Monensin. The cells were then stained for other cell surface markers and with the NP_{366} tetramer and then analyzed by flow cytometry. The levels of CD107α indicate the potential of the cells to degranulate and hence act as an indirect marker for measuring cytotoxic potential. All the NP_{366}^+ $CD8^+$ T cells expressed high levels of CD107α at day 4 p.i. (Figure 6.8A) but the percentage of cells expressing CD107α decreased by day 8 p.i (Figure 6.8B). This is probably because the virus is cleared by day 8, since this is a re-infection and higher $CD8^+$ T cell numbers are already present in the lung tissue to NP_{366}^+ $CD8^+$ T cell expressing CD107α in the WT, IFN-$\gamma^{-/-}$ and IFN-$\gamma R^{-/-}$ mice. This indicated that the $CD8^+$ T cells generated in the recall response were comparable in their ability to kill infected cells and maintained their functional abilities in the absence of IFN-γ signaling.

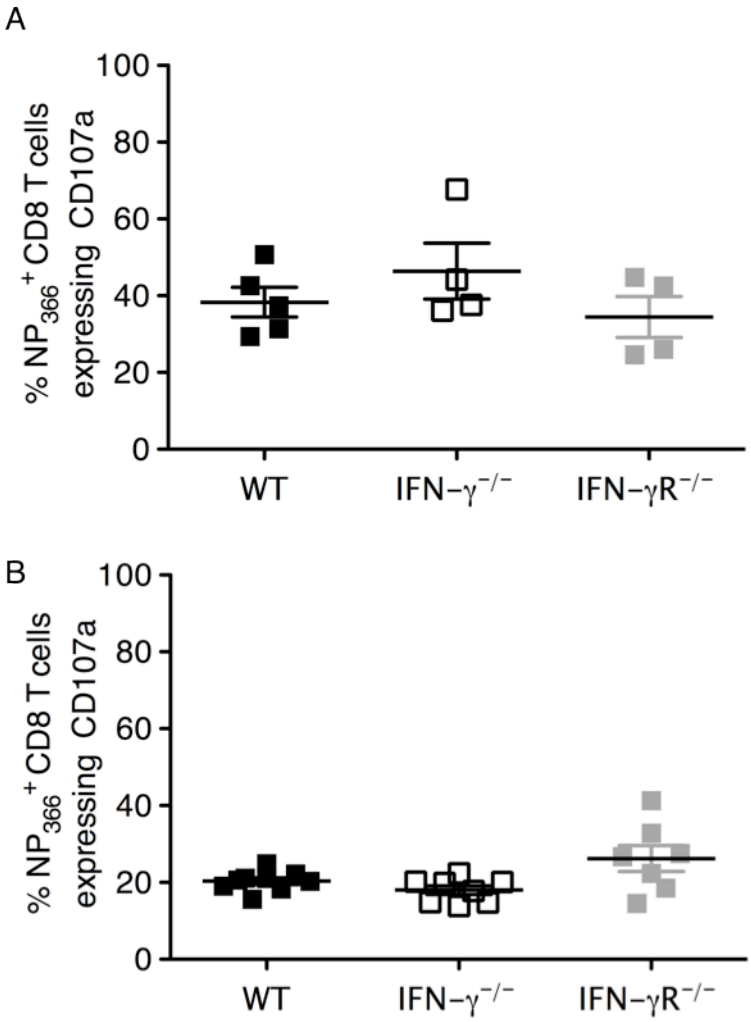

Figure 6.8 Cytotoxic potential of flu-specific CD8$^+$ T cells after 500 PFU re-infection.

C57BL/6 WT, IFN-γ$^{-/-}$ and IFN-γR$^{-/-}$ mice were infected with a sub-lethal dose of influenza HK/X31 (H3N2) and after 35 days, mice were infected with a second virus A/ PR/8/34 (H1N1) and monitored for 8 days after infection. The CD8$^+$ T cells were enriched from the lung tissues and their CD107a levels were measured on day 4 p.i (A) and day 8 p.i (B). Data are pooled for two-three independent experiments with 4-5 mice/group.

6.8 Lung damage after re-infection with 500 PFU PR8

Next we wanted to measure the extent of lung damage due to the re-infection with 500 PFU of PR8. In our earlier experiments with the primary infection, we did not see any differences in the extent of lung damage in the WT and IFN-$\gamma^{-/-}$ mice. We measured the albumin leakage in to the airways as an indirect measure of the lung damage as higher albumin leakage into the airways translates to increased lung damage. We collected the BAL fluid from the infected mice at day 4 and 8 p.i. and the supernatant was used to measure the albumin using an ELISA protocol (Figure 6.9).

We found that there were similar levels of albumin leakage in to the BAL fluid on both days 4 (Figure 6.8A) and day 8 p.i. (Figure 6.9B) The extent of albumin leakage was similar in the WT, IFN-$\gamma^{-/-}$ and IFN-$\gamma R^{-/-}$ mice, both on days 4 and 8 p.i. This indicated that in spite of having higher numbers of flu-specific $CD8^+$ T cells in the lungs of the IFN-$\gamma^{-/-}$ and IFN-$\gamma R^{-/-}$ mice, this did not translate into additional lung damage.

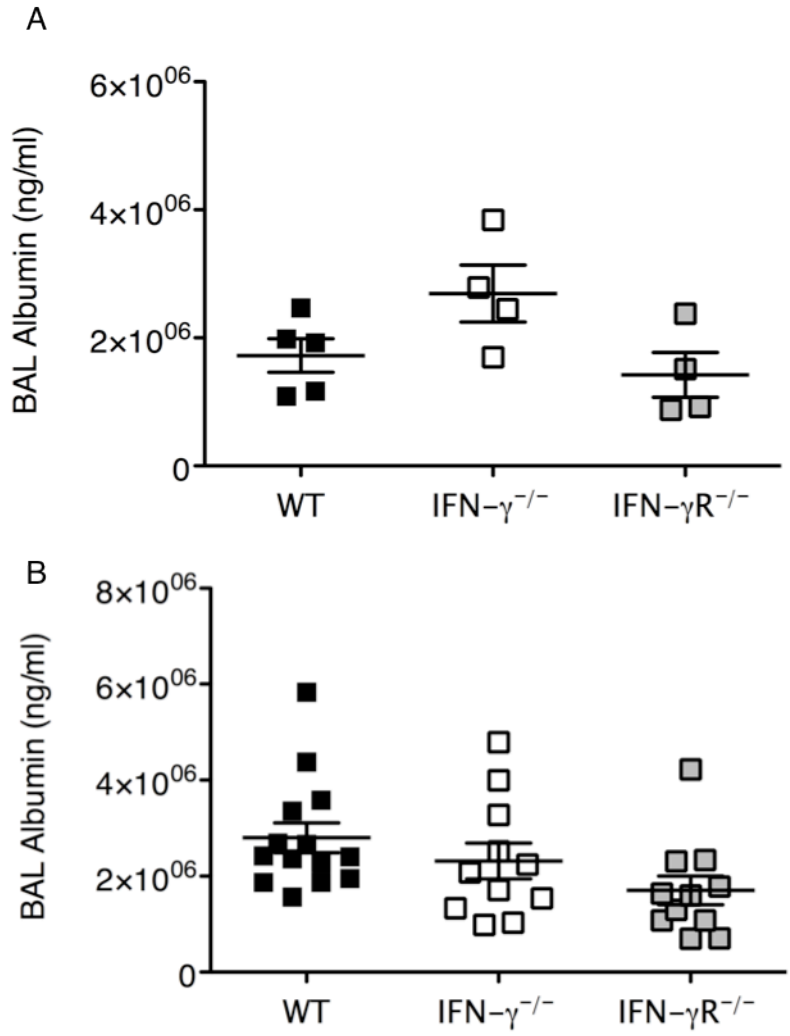

Figure 6.9 Albumin leakage in the lungs as a measure of lung damage after re-infection with 500 PFU of PR8.

C57BL/6 WT, IFN-γ$^{-/-}$ and IFN-γR$^{-/-}$ mice were infected with a sub-lethal dose of influenza HK/X31 (H3N2) and after 35 days, mice were infected with a second virus A/ PR/8/34 (H1N1) and monitored for 8 days after infection. The BAL fluid was collected from the mice and albumin was measured by an ELISA based assay. Albumin leakage into the airway (BAL fluid) on day 4 p.i (A) and day 8 p.i (B). Data are pooled for two- three independent experiments with 4-5 mice/group.

6.9 $CD4^+$ T cell response after re-infection with 500 PFU PR8

Influenza-specific $CD8^+$ T cell responses were enhanced in the absence of IFN-γ signaling. Hence, we could ascertain that the increased NP_{366}^+ $CD8^+$ T cells generated in the IFN-$\gamma^{-/-}$ and IFN-$\gamma R^{-/-}$ mice could respond to a recall response and hence confirmed that increased memory precursors were generated in the absence of IFN-γ signaling. $CD4^+$ T cells are known to play a role in the memory responses to influenza infection (Belz et al. 2002). Since the primary $CD4^+$ T cell responses were not different in the absence of IFN-γ signaling, we studied the $CD4^+$ T cell responses after a re-challenge with 500 PFU PR8 infection.

We studied the $CD4^+$ T cell response to get a general idea if IFN-γ is involved in regulating the $CD4^+$ T cell responses. Since, tetramers are not yet available to study the antigen specific $CD4^+$ T cells; we chose to look at total $CD4^+$ T cell numbers during influenza infection instead. The total $CD4^+$ T cell numbers in the lung tissue were measured at days 4 (Figure 6.10A) and 8 p.i. (Figure 6.10B). The numbers of $CD4^+$ T cells increased from day 4 to day 8 in all the mice. However, no differences were observed between the WT, IFN-$\gamma^{-/-}$ and IFN-$\gamma R^{-/-}$ mice. Although we did not study the properties of the $CD4^+$ T cells in greater detail, we could confirm that IFN-γ did not play a role in regulating the $CD4^+$ T cell responses to influenza and this did not influence the regulation of the influenza-specific $CD8^+$ T cell responses.

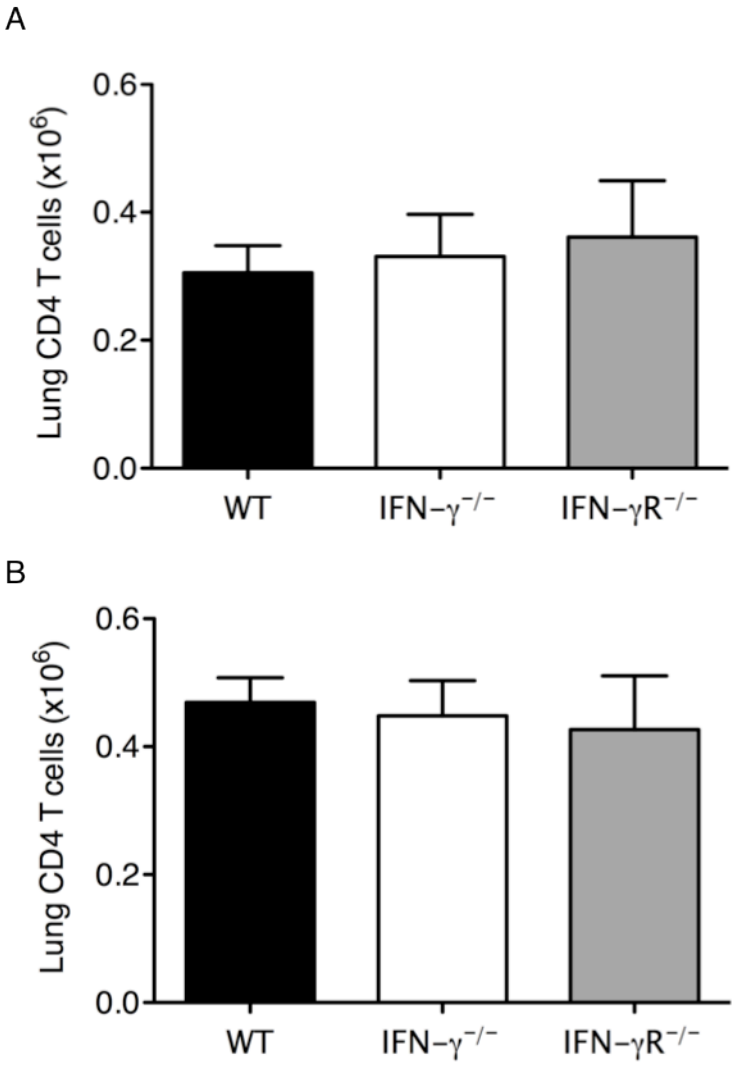

Figure 6.10 Total CD4$^+$ T cell response after 500 PFU PR8 re-infection

C57BL/6 WT, IFN-γ$^{-/-}$ and IFN-γR$^{-/-}$ mice were infected with a sub-lethal dose of influenza HK/X31 (H3N2) and after 35 days, mice were infected with a second virus A/ PR/8/34 (H1N1) and monitored for 8 days after infection. Total lung cells were harvested and cells were stained for CD3 and CD4. Total CD4$^+$ T cells were calculated by the total number of cells and frequency of cells staining positive on day 4 (A) and day 8 p.i. (B**)**. Data are pooled for two-three independent experiments with 4-5 mice/group.

6.10 Viral clearance after re-infection with 500 PFU of PR8

Finally, we examined the kinetics of lung viral RNA by qRT-PCR (Figure 6.11). We observed high viral titers in the lungs of mice with a primary infection of 500PFU PR/8 whereas all the re-infected mice showed much lower titers. The high titer of virus was maintained until day 8 after the primary infection. However, as with the primary infection with a low dose of 5 PFU PR/8, there was no difference in viral loads in the WT, IFN-$\gamma^{-/-}$ and IFN-$\gamma R^{-/-}$ mice after a primary infection with a high dose of 500 PFU.

In the re-infected mice however, we saw that the levels of viral RNA peaked at day 2 but from then on decreased steadily and were much lower by day 8 p.i. We also observed that levels of viral RNA in the lungs of the IFN-$\gamma^{-/-}$ and IFN-$\gamma R^{-/-}$ were significantly reduced compared to WT mice on day 8 after re-infection. This demonstrates that persisting antigen-specific $CD8^+$ T cells in IFN-$\gamma^{-/-}$ and IFN-$\gamma R^{-/-}$ mice after resolution of the primary infection indeed lead to higher frequencies of memory precursors and hence produced better recall responses and better viral resolution in the absence of IFN-γ signaling.

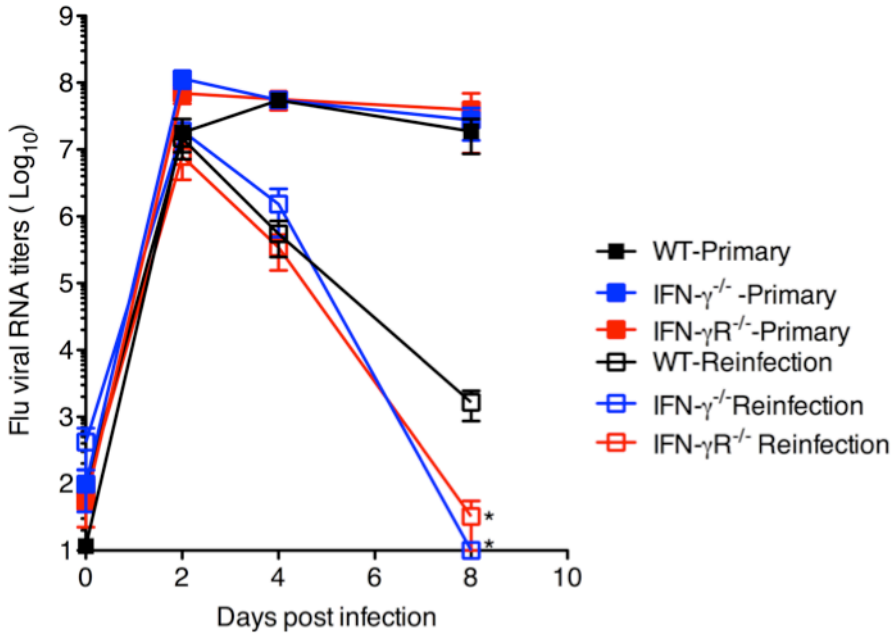

Figure 6.11 Viral clearance after primary infection or re-infection with 500 PFU PR8

Graph showing relative RNA levels of viral M-protein in the lungs of infected mice after primary infection and re-infection with 500 PFU PR/8. (*p<0.05 and **p<0.01 were determined using Mann-Whitney test). n=5/group

6.11 Discussion

Heterosubtypic immunity is defined as cross-protection against a virus of a different subtype to a virus previously encountered. This is mediated by antigen-specific $CD8^+$ T cells which are generally targeted against the internal proteins of the influenza virus, such as the nucleoprotein (NP). We were interested to determine if the increased memory precursor cells generated in the absence of IFN-γ signaling could provide heterosubtypic immunity and if the higher numbers of memory $CD8^+$ T cells would translate to better protection from a re-challenge.

We have shown in the earlier chapters that IFN-γ directly regulates effector $CD8^+$ T-cell survival by controlling the proportion of antigen specific $CD8^+$ T cells that expressed IL-7Rα, which was functionally important for survival of effector cells during the contraction phase of the response. In the current chapter, we show that in a recall response to a secondary challenge with a heterologous strain of influenza, higher numbers of influenza specific $CD8^+$ T cells were found in the IFN-$\gamma^{-/-}$ and IFN-$\gamma R^{-/-}$ compared with WT mice, confirming that higher frequencies of memory precursors are indeed formed in the absence of IFN-γ signaling which subsequently conferred the ability to clear virus faster than WT mice.

Our findings with IFN-$\gamma^{-/-}$ mice infected with a primary infection of both PR/8 or HK-x31 strains of influenza differ from the previously published data using IFN-$\gamma^{-/-}$ mice (Turner et al. 2007), wherein a defect in migration of the antigen specific $CD8^+$ T cells to the lung and concomitant accumulation in the spleen was reported. However, our results are consistent with their observations in

terms of lung viral load and resolution of infection (no difference seen in the absence of IFN-γ signaling), an aspect controlled by the CD8$^+$ T cell response in the lung. Furthermore, it is important to note that evaluation of the BAL does not provide a comprehensive evaluation of the CD8$^+$ T cell response in the lung and could explain differences observed between the studies. Furthermore the emergence of Norovirus as a pathogen in mice around the world may have changed the background status of the animals.

Our studies using the re-infection model are in agreement with previous studies (Bot et al. 1998), which show that IFN-γ is not required for the induction of secondary influenza-specific CD8$^+$ T cell responses and the absence of IFN-γ signaling does not affect the cross-reactive virus-specific immune responses. Although our study is in accordance with most of the findings of the second study (Bot et al. 1998) that IFN-γ does not influence the cytotoxicity of CD8$^+$ T cells, numbers of CD4$^+$ T cells and viral titers, this study showed that the IFN-γ$^{-/-}$ mice displayed reduced survival rates subsequent to a re-challenge. This may have to do with the fact that in that study the primary virus was delivered intraperitoneally, which may not have had the same effect on the memory CD8$^+$ T cell generation in the absence of IFN-γ. Our findings further add to the previous studies by utilizing varying doses of the re-challenge virus, that IFN-γ limits the numbers of memory CD8$^+$ T cells formed against the influenza virus. The higher numbers of antigen-specific memory CD8$^+$ T cells formed in the absence of IFN-γ signaling could lead to slightly faster clearance of the second virus.

Our results suggest that modulation of IFN-γ levels to increase IL-7Rα expression on effector CD8$^+$ T cells represents a potential strategy to increase

the numbers of $CD8^+$ T cell memory precursors, thus permitting the development of an effective memory response to influenza. Our studies provide strong evidence supporting a T cell intrinsic role for IFN-γ in limiting the magnitude of the memory $CD8^+$ T cell pool against influenza. These findings advance our understanding of $CD8^+$ T cell homeostasis and have implications for the development of more effective vaccines against influenza.

Chapter 7: Final discussion and future direction

7.1 Brief Summary of Main Findings

In this thesis, we show that IFN-γ-IFN-γR signaling plays a key role in the modulation of antigen-specific $CD8^+$ T cell contraction and memory development in response to influenza infection. We have shown that in the absence of IFN-γ signaling, the contraction phase of the $CD8^+$ T cell response is aberrant, resulting in the accumulation of antigen-specific $CD8^+$ T cells that is evident as long as 120 days p.i. when the response in WT mice has declined significantly. We could confirm that this was not due to persisting viral loads or extended antigen presentation in the absence of IFN-γ signaling. IFN-γ directly regulates effector $CD8^+$ T-cell survival as we could induce cell death in IFN-$\gamma^{-/-}$ effector cells by culturing them in the presence of IFN-γ. We also identified some of the molecules that are likely to be responsible for IFN-γ induced $CD8^+$ T cell death with a PCR-array. In addition, a larger proportion of antigen specific $CD8^+$ T cells in IFN-$\gamma^{-/-}$ and IFN-$\gamma R^{-/-}$ mice expressed IL-7Rα, which was functionally important for survival of effector cells during the contraction phase of the response. We showed that blocking IL-7 signals in the lungs of the IFN-$\gamma^{-/-}$ mice lead to a reduction in the numbers of antigen specific $CD8^+$ T cells surviving the contraction phase. This was true even in the WT mice, which indicates that IL-7 signals in the lung are indeed important for the survival of influenza-specific $CD8^+$ T cells after the contraction phase. Our studies also show that IFN-γ controls the survival signals received through IL-7 by regulating the expression of IL-7Rα on the

$CD8^+$ T cells. Furthermore, in a recall response to a secondary challenge with a heterologous strain of influenza, higher numbers of influenza specific $CD8^+$ T cells were found in the IFN-$\gamma^{-/-}$ and IFN-$\gamma R^{-/-}$ compared with WT mice, confirming that higher frequencies of memory precursors are indeed formed in the absence of IFN-γ signaling, which can respond to a re-challenge with influenza. Finally, we show that the increased numbers of influenza-specific $CD8^+$ T cells in the IFN-$\gamma^{-/-}$ and IFN-$\gamma R^{-/-}$ mice confer a greater ability to clear virus than WT mice. Collectively, our findings indicate that IFN-γ plays a critical role in regulating antiviral $CD8^+$ T cell responses and memory and hence represents a potential target for improving vaccines aiming to engender protective $CD8^+$ T cell responses.

7.2 Limitations of the study

Exact mechanism of IFN-γ induced cell death

Although in this study we show that IFN-γ induces cell death in influenza specific $CD8^+$ T cells during the contraction phase of the response to infection, we have not identified the exact mechanisms by which this occurs. We used the cell death identifier PCR array to narrow down the molecules whose expression may be controlled by IFN-γ. The IFN-$\gamma^{-/-}$ $NP_{366}{}^+$ $CD8^+$ T cells had up-regulated expression of anti-apoptotic molecules Birc3 and Bcl-2 but had down regulated several genes involved in apoptosis (Akt1 and Casp3), necrosis (Mcl-1, Pvr and Tnfrsf1a) and autophagy (Atg16l1, App, Esr1, Gaa and Irgm1). It is possible that IFN-γ acts on several molecules to activate pathways leading to cell death. Due to redundancy of the molecules involved it is difficult to identify the exact pathway involved using such an array.

Further studies will be required to confirm and assess the exact roles played by these molecules in the cell death induced by IFN-γ.

Physiological significance of the findings

One of the main limitations of this study is the physiological relevance of this finding with respect to human influenza infections. As our model is in mice, it remains to be seen if this is true of humans and if IFN-γ plays a similar role in the contraction of $CD8^+$ T cell responses in individuals after influenza infection. Although there are some IFN-γ deficient humans and indeed there are many who have lesser IFN-γ signaling (Jouanguy et al. 2000; Bogunovic et al. 2012), either due to a pre-existing Th2 phenotype or polymorphisms in the ifn-γ gene (Chong et al. 2006).

Another limitation is the fact that we look at naïve mice and since there are no "naïve" human beings per sse, it is difficult to evaluate the responses in the absence of other micro flora. Also, the presence of other infections, whether bacterial or viral will definitely affect the responses of $CD8^+$ T cells. Further, the presence of a pre-existing Th2 phenotype due to asthma or the aforementioned conditions could have an effect on the immune response influenza infections. In our studies, we noticed an increased eosinophilia in the IFN-γ-signaling deficient mice (chapter 4). Although this did not translate to increased lung damage in the mice in our system, the presence of eosinophilia in humans could lead to increased exacerbation of the infection due to increased allergic airway inflammation after an influenza infection.

7.3 Future direction

7.3.1 Understanding the mechanism behind IFN-γ-induced cell death

Although our study has identified that IFN-γ induces cell death in the activated effector $CD8^+$ T cells after an influenza infection, we are yet to find the exact pathway/mechanism by which this is brought about. Some of the molecules likely to be responsible were identified using a PCR array but further studies will be needed to confirm their roles in the IFN-γ-induced cell death. It will be interesting to study the downstream effectors of IFN-γ, which participate in inducing $CD8^+$ T cell death during the contraction of the immune response after an influenza infection.

7.3.2 Finding how IFN-γ affects the expression of IL-7R

In our study we observed that in the absence of IFN-γ signaling, higher frequencies of influenza-specific $CD8^+$ T cells express IL-7Ra, as a result of which these cells receive signals that lead to increased survival to form memory T cells. But we haven't identified how IFN-γ down-regulates IL-7Ra expression. It also remains to be determined if early IFN-γ signals in T cells directly regulate which effector cells will or will not up regulate IL-7Ra. Thus, determining how antigen-specific $CD8^+$ T cells directly respond to IFN-γ signals during infection may provide important clues as to how the immune system regulates the survival of only a small proportion of effector $CD8^+$ T cells for memory cell generation. T-bet is a transcription factor that was found to regulate the levels of IL-7Ra and T-bet deficiency leads to increased levels of IL-7Ra expressing $CD8^+$ T cells at the peak of the response (Intlekofer et al.

2007). Inhibition of T-bet expression due to IFN-γ deficiency could lead to increased levels of IL-7Ra on the virus-specific $CD8^+$ T cells. But we did not see any differences in the levels of T-bet in the absence of IFN-γ. However, we did observe differences in the levels of its paralog eomesodermin. It remains to be determined if eomes or some other transcription factor affects the expression of IL-7Ra.

7.3.3 Identifying the cells that make IL-7 in the lung tissue

IL-7 is known to be a hematopoietic growth factor that is important for the growth and survival of B and T cells. Stromal cells in the bone marrow and thymus secrete IL-7. It is also produced by keratinocytes (Heufler et al. 1993), dendritic cells (Kroncke et al. 1996), hepatocytes (Sawa et al. 2009) and epithelial cells (Watanabe, M. et al. 1995) but not by T lymphocytes. In our study, we showed that IL-7 provided crucial survival signals that permit antigen specific $CD8^+$ T cells to survive to form memory cells in the lung after influenza infection. Blocking IL-7 in the lung lead to decreased survival of influenza-specific memory $CD8^+$ T cells. However, the cells that make the cytokine in the lung tissue still need to be identified. It remains to be determined whether non-lymphoid cells or the lymphoid cells make IL-7 in the lung tissue and the conditions under which they do so.

7.3.4 Looking at effect of other infections after a primary infection of influenza

In our study we examined the role of IFN-γ in a primary and then a re-infection model, both with influenza infection. Although this helped to delineate and simplify the study, the roles of other infections still need to be studied. It will be interesting to see how the absence of IFN-γ affects a secondary infection with another virus or bacteria, after a primary infection with influenza. It has been shown in one study (Sun, K. and Metzger 2008) that IFN-γ produced during influenza infection in mice inhibits initial bacterial clearance from the lung by alveolar macrophages during a secondary bacterial infection. The effect of having increased influenza-specific memory $CD8^+$ T cell responses on other subsequent infections will need to be studied.

7.3.5 Understanding whether IFN-γ signaling can be blocked to increase memory cell populations

Current vaccination strategies have failed to elicit a strong and lasting $CD8^+$ T cell response against influenza that provides heterosubtypic immunity. One study has shown that limiting the inflammation phase during the infection can reduce the contraction phase thereby increasing the number of memory precursors, also keeping the tissue damage in check (Badovinac et al. 2004). Another study has shown that neutralization of IFN-γ in the lungs of mice during an influenza infection leads to decreased susceptibility to a secondary pneumococcal infection (Sun, K. and Metzger 2008). Our studies provide strong evidence supporting a T cell intrinsic role for IFN-γ in limiting the

magnitude of the memory $CD8^+$ T cell pool against influenza. If the levels of IFN-γ can be controlled during a primary influenza infection by IFN-γ neutralization, this would lead to increased memory influenza-specific $CD8^+$ T cells, which may initiate better protection against subsequent infections with both similar and dissimilar stains of influenza. However, these studies have to be carried out and interpreted with caution as the negative effects of blocking such an important molecule during viral infection may have other negative implications, which have to be weighed against the benefits. It will also be interesting to observe the effect of IFN-γ neutralization during vaccinations for influenza and the effects it has on the memory $CD8^+$ T cell response generated. These findings will advance our understanding of $CD8^+$ T cell homeostasis and will have implications on the development of more effective vaccines against influenza.

References

(2000). "Update: influenza activity--United States and worldwide, 1999-2000 season, and composition of the 2000-01 influenza vaccine." MMWR Morb Mortal Wkly Rep 49(17): 375-381.

Acosta-Rodriguez, E. V., et al. (2007). "Interleukins 1beta and 6 but not transforming growth factor-beta are essential for the differentiation of interleukin 17-producing human T helper cells." Nat Immunol 8(9): 942-949.

Ada, G. L. and P. D. Jones (1986). "The immune response to influenza infection." Curr Top Microbiol Immunol 128: 1-54.

Adachi, M., et al. (1997). "Expression of cytokines on human bronchial epithelial cells induced by influenza virus A." Int Arch Allergy Immunol 113(1-3): 307-311.

Ahmed, R. and D. Gray (1996). "Immunological memory and protective immunity: understanding their relation." Science 272(5258): 54-60.

Akashi, K., et al. (1997). "Bcl-2 rescues T lymphopoiesis in interleukin-7 receptor-deficient mice." Cell 89(7): 1033-1041.

Andrews, D. M., et al. (2008). "The early kinetics of cytomegalovirus-specific CD8+ T-cell responses are not affected by antigen load or the absence of perforin or gamma interferon." J Virol 82(10): 4931-4937.

Arnon, T. I., et al. (2001). "Recognition of viral hemagglutinins by NKp44 but not by NKp30." Eur J Immunol 31(9): 2680-2689.

Bachmann, M. F., et al. (2005). "Functional properties and lineage relationship of CD8+ T cell subsets identified by expression of IL-7 receptor alpha and CD62L." J Immunol 175(7): 4686-4696.

Badovinac, V. P., et al. (2002). "Programmed contraction of CD8(+) T cells after infection." Nat Immunol 3(7): 619-626.

Badovinac, V. P., et al. (2004). "CD8+ T cell contraction is controlled by early inflammation." Nat Immunol 5(8): 809-817.

Badovinac, V. P., et al. (2000). "Regulation of antigen-specific CD8+ T cell homeostasis by perforin and interferon-gamma." Science 290(5495): 1354-1358.

Bannard, O., et al. (2009). "Secondary replicative function of CD8+ T cells that had developed an effector phenotype." Science 323(5913): 505-509.

Bateman, E. D., et al. (2008). "Global strategy for asthma management and prevention: GINA executive summary." Eur Respir J 31(1): 143-178.

Baumgarth, N. and A. Kelso (1996). "In vivo blockade of gamma interferon affects the influenza virus-induced humoral and the local cellular immune response in lung tissue." J Virol 70(7): 4411-4418.

Becker, T. C., et al. (2002). "Interleukin 15 is required for proliferative renewal of virus-specific memory CD8 T cells." J Exp Med 195(12): 1541-1548.

Belz, G. T., et al. (1998). "Characteristics of virus-specific CD8(+) T cells in the liver during the control and resolution phases of influenza pneumonia." Proc Natl Acad Sci U S A 95(23): 13812-13817.

Belz, G. T., et al. (2004). "Distinct migrating and nonmigrating dendritic cell populations are involved in MHC class I-restricted antigen presentation after lung infection with virus." Proc Natl Acad Sci U S A 101(23): 8670-8675.

Belz, G. T., et al. (2002). "Compromised influenza virus-specific CD8(+)-T-cell memory in CD4(+)-T-cell-deficient mice." J Virol 76(23): 12388-12393.

Ben-Sasson, S. Z., et al. (2009). "IL-1 acts directly on CD4 T cells to enhance their antigen-driven expansion and differentiation." Proc Natl Acad Sci U S A 106(17): 7119-7124.

Bender, B. S., et al. (1992). "Transgenic mice lacking class I major histocompatibility complex-restricted T cells have delayed viral clearance and increased mortality after influenza virus challenge." J Exp Med 175(4): 1143-1145.

Bender, B. S. and P. A. Small, Jr. (1992). "Influenza: pathogenesis and host defense." Semin Respir Infect 7(1): 38-45.

Bennink, J., et al. (1978). "Influenzal pneumonia: early appearance of cross-reactive T cells in lungs of mice primed with heterologous type A viruses." Immunology 35(3): 503-509.

Beyer, M., et al. (2004). "Sustained increases in numbers of pulmonary dendritic cells after respiratory syncytial virus infection." J Allergy Clin Immunol 113(1): 127-133.

Bogunovic, D., et al. (2012). "Mycobacterial disease and impaired IFN-gamma immunity in humans with inherited ISG15 deficiency." Science 337(6102): 1684-1688.

Bos, R., et al. (2012). "Functional differences between low- and high-affinity CD8(+) T cells in the tumor environment." Oncoimmunology 1(8): 1239-1247.

Bot, A., et al. (1998). "Protective role of gamma interferon during the recall response to influenza virus." J Virol 72(8): 6637-6645.

Brincks, E. L., et al. (2008). "CD8 T cells utilize TRAIL to control influenza virus infection." J Immunol 181(7): 4918-4925.

Bruder, D., et al. (2006). "Cellular immunity and lung injury in respiratory virus infection." Viral Immunol 19(2): 147-155.

Bullough, P. A., et al. (1994). "Structure of influenza haemagglutinin at the pH of membrane fusion." Nature 371(6492): 37-43.

Cerwenka, A., et al. (1999). "Naive, effector, and memory CD8 T cells in protection against pulmonary influenza virus infection: homing properties rather than initial frequencies are crucial." J Immunol 163(10): 5535-5543.

Chan, M. C., et al. (2005). "Proinflammatory cytokine responses induced by influenza A (H5N1) viruses in primary human alveolar and bronchial epithelial cells." Respir Res 6: 135.

Chong, W. P., et al. (2006). "The interferon gamma gene polymorphism +874 A/T is associated with severe acute respiratory syndrome." BMC Infect Dis 6: 82.

Chowell, G., et al. (2009). "Severe respiratory disease concurrent with the circulation of H1N1 influenza." N Engl J Med 361(7): 674-679.

Christensen, J. E., et al. (2004). "Perforin and IFN-gamma do not significantly regulate the virus-specific CD8+ T cell response in the absence of antiviral effector activity." Eur J Immunol 34(5): 1389-1394.

Chu, C. Q., et al. (2000). "Failure to suppress the expansion of the activated CD4 T cell population in interferon gamma-deficient mice leads to exacerbation of experimental autoimmune encephalomyelitis." J Exp Med 192(1): 123-128.

Cooper, A. M., et al. (1993). "Disseminated tuberculosis in interferon gamma gene-disrupted mice." J Exp Med 178(6): 2243-2247.

Crowe, S. R., et al. (2006). "Uneven distribution of MHC class II epitopes within the influenza virus." Vaccine 24(4): 457-467.

Cruz, A., et al. (2006). "Cutting edge: IFN-gamma regulates the induction and expansion of IL-17-producing CD4 T cells during mycobacterial infection." J Immunol 177(3): 1416-1420.

Dalton, D. K., et al. (2000). "Interferon gamma eliminates responding CD4 T cells during mycobacterial infection by inducing apoptosis of activated CD4 T cells." J Exp Med 192(1): 117-122.

Dalton, D. K., et al. (1993). "Multiple defects of immune cell function in mice with disrupted interferon-gamma genes." Science 259(5102): 1739-1742.

Davies, E. G., et al. (1982). "Defective immune interferon production and natural killer activity associated with poor neutrophil mobility and delayed umbilical cord separation." Clin Exp Immunol 50(2): 454-460.

Decker, T. and P. Kovarik (2000). "Serine phosphorylation of STATs." Oncogene 19(21): 2628-2637.

Derynck, R., et al. (1982). "Human interferon gamma is encoded by a single class of mRNA." Nucleic Acids Res 10(12): 3605-3615.

Diebold, S. S., et al. (2004). "Innate antiviral responses by means of TLR7-mediated recognition of single-stranded RNA." Science 303(5663): 1529-1531.

Doffinger, R., et al. (2004). "Autoantibodies to interferon-gamma in a patient with selective susceptibility to mycobacterial infection and organ-specific autoimmunity." Clin Infect Dis 38(1): e10-14.

Doherty, P. C., et al. (2006). "Influenza and the challenge for immunology." Nat Immunol 7(5): 449-455.

Dolfi, D. V., et al. (2008). "Late signals from CD27 prevent Fas-dependent apoptosis of primary CD8+ T cells." J Immunol 180(5): 2912-2921.

Dupuis, S., et al. (2001). "Impairment of mycobacterial but not viral immunity by a germline human STAT1 mutation." Science 293(5528): 300-303.

Durbin, J. E., et al. (1996). "Targeted disruption of the mouse Stat1 gene results in compromised innate immunity to viral disease." Cell 84(3): 443-450.

Ealick, S. E., et al. (1991). "Three-dimensional structure of recombinant human interferon-gamma." Science 252(5006): 698-702.

Ege, M. J., et al. (2011). "Exposure to environmental microorganisms and childhood asthma." N Engl J Med 364(8): 701-709.

Ekiert, D. C., et al. (2009). "Antibody recognition of a highly conserved influenza virus epitope." Science 324(5924): 246-251.

Ely, K. H., et al. (2003). "Cutting edge: effector memory CD8+ T cells in the lung airways retain the potential to mediate recall responses." J Immunol 171(7): 3338-3342.

Farrar, M. A. and R. D. Schreiber (1993). "The molecular cell biology of interferon-gamma and its receptor." Annu Rev Immunol 11: 571-611.

Feng, C. G., et al. (2008). "The immunity-related GTPase Irgm1 promotes the expansion of activated CD4+ T cell populations by preventing interferon-gamma-induced cell death." Nat Immunol 9(11): 1279-1287.

Fesq, H., et al. (1994). "Programmed cell death (apoptosis) in human monocytes infected by influenza A virus." Immunobiology 190(1-2): 175-182.

Flynn, K. J., et al. (1998). "Virus-specific CD8+ T cells in primary and secondary influenza pneumonia." Immunity 8(6): 683-691.

Flynn, K. J., et al. (1999). "In vivo proliferation of naive and memory influenza-specific CD8(+) T cells." Proc Natl Acad Sci U S A 96(15): 8597-8602.

Fountoulakis, M., et al. (1992). "Stoichiometry of interaction between interferon gamma and its receptor." Eur J Biochem 208(3): 781-787.

Freeman, G. J., et al. (2000). "Engagement of the PD-1 immunoinhibitory receptor by a novel B7 family member leads to negative regulation of lymphocyte activation." J Exp Med 192(7): 1027-1034.

Gajewski, T. F. and F. W. Fitch (1988). "Anti-proliferative effect of IFN-gamma in immune regulation. I. IFN-gamma inhibits the proliferation of Th2 but not Th1 murine helper T lymphocyte clones." J Immunol 140(12): 4245-4252.

Garcia-Zepeda, E. A., et al. (1996). "Human eotaxin is a specific chemoattractant for eosinophil cells and provides a new mechanism to explain tissue eosinophilia." Nat Med 2(4): 449-456.

Garten, R. J., et al. (2009). "Antigenic and genetic characteristics of swine-origin 2009 A(H1N1) influenza viruses circulating in humans." Science 325(5937): 197-201.

Gerhard, W. (2001). "The role of the antibody response in influenza virus infection." Curr Top Microbiol Immunol 260: 171-190.

Gern, J. E. and W. W. Busse (2002). "Relationship of viral infections to wheezing illnesses and asthma." Nat Rev Immunol 2(2): 132-138.

GeurtsvanKessel, C. H., et al. (2008). "Clearance of influenza virus from the lung depends on migratory langerin+CD11b- but not plasmacytoid dendritic cells." J Exp Med 205(7): 1621-1634.

Goldrath, A. W., et al. (2002). "Cytokine requirements for acute and Basal homeostatic proliferation of naive and memory CD8+ T cells." J Exp Med 195(12): 1515-1522.

Gomez-Puertas, P., et al. (2000). "Influenza virus matrix protein is the major driving force in virus budding." J Virol 74(24): 11538-11547.

Gorak-Stolinska, P., et al. (2002). "Activation-induced cell death in human T cells is a suicidal process regulated by cell density but superantigen induces T cell fratricide." Cell Immunol 219(2): 98-107.

Gorak-Stolinska, P., et al. (2001). "Activation-induced cell death of human T-cell subsets is mediated by Fas and granzyme B but is independent of TNF-alpha." J Leukoc Biol 70(5): 756-766.

Gourley, T. S., et al. (2004). "Generation and maintenance of immunological memory." Semin Immunol 16(5): 323-333.

Graham, M. B. and T. J. Braciale (1997). "Resistance to and recovery from lethal influenza virus infection in B lymphocyte-deficient mice." J Exp Med 186(12): 2063-2068.

Graham, M. B., et al. (1994). "Influenza virus-specific CD4+ T helper type 2 T lymphocytes do not promote recovery from experimental virus infection." J Exp Med 180(4): 1273-1282.

Graham, M. B., et al. (1993). "Response to influenza infection in mice with a targeted disruption in the interferon gamma gene." J Exp Med 178(5): 1725-1732.

Hamada, H., et al. (2009). "Tc17, a unique subset of CD8 T cells that can protect against lethal influenza challenge." J Immunol 182(6): 3469-3481.

Hand, T. W. and S. M. Kaech (2009). "Intrinsic and extrinsic control of effector T cell survival and memory T cell development." Immunol Res 45(1): 46-61.

Haring, J. S., et al. (2005). "Dynamic regulation of IFN-gamma signaling in antigen-specific CD8+ T cells responding to infection." J Immunol 174(11): 6791-6802.

Haring, J. S. and J. T. Harty (2006). "Aberrant contraction of antigen-specific CD4 T cells after infection in the absence of gamma interferon or its receptor." Infect Immun 74(11): 6252-6263.

Harty, J. T. and V. P. Badovinac (2008). "Shaping and reshaping CD8+ T-cell memory." Nat Rev Immunol 8(2): 107-119.

Hassantoufighi, A., et al. (2007). "Respiratory syncytial virus replication is prolonged by a concomitant allergic response." Clin Exp Immunol 148(2): 218-229.

Hayden, F. G. (1997). "Antivirals for pandemic influenza." J Infect Dis 176 Suppl 1: S56-61.

Hayden, F. G., et al. (1999). "Use of the selective oral neuraminidase inhibitor oseltamivir to prevent influenza." N Engl J Med 341(18): 1336-1343.

Herold, S., et al. (2006). "Alveolar epithelial cells direct monocyte transepithelial migration upon influenza virus infection: impact of chemokines and adhesion molecules." J Immunol 177(3): 1817-1824.

Heufler, C., et al. (1993). "Interleukin 7 is produced by murine and human keratinocytes." J Exp Med 178(3): 1109-1114.

Ho, A. W., et al. (2011). "Lung CD103+ dendritic cells efficiently transport influenza virus to the lymph node and load viral antigen onto MHC class I for presentation to CD8 T cells." J Immunol 187(11): 6011-6021.

Hofmann, P., et al. (1997). "Susceptibility of mononuclear phagocytes to influenza A virus infection and possible role in the antiviral response." J Leukoc Biol 61(4): 408-414.

Holzinger, D., et al. (2007). "Induction of MxA gene expression by influenza A virus requires type I or type III interferon signaling." J Virol 81(14): 7776-7785.

Horimoto, T. and Y. Kawaoka (2005). "Influenza: lessons from past pandemics, warnings from current incidents." Nat Rev Microbiol 3(8): 591-600.

Hou, S., et al. (1994). "Virus-specific CD8+ T-cell memory determined by clonal burst size." Nature 369(6482): 652-654.

Huang, S., et al. (1993). "Immune response in mice that lack the interferon-gamma receptor." Science 259(5102): 1742-1745.

Hufford, M. M., et al. (2011). "Antiviral CD8+ T cell effector activities in situ are regulated by target cell type." J Exp Med 208(1): 167-180.

Hussell, T., et al. (2001). "Inhibition of tumor necrosis factor reduces the severity of virus-specific lung immunopathology." Eur J Immunol 31(9): 2566-2573.

Igarashi, K., et al. (1994). "Interferon-gamma induces tyrosine phosphorylation of interferon-gamma receptor and regulated association of protein tyrosine kinases, Jak1 and Jak2, with its receptor." J Biol Chem 269(20): 14333-14336.

Intlekofer, A. M., et al. (2007). "Requirement for T-bet in the aberrant differentiation of unhelped memory CD8+ T cells." J Exp Med 204(9): 2015-2021.

Jayasekera, J. P., et al. (2007). "Natural antibody and complement mediate neutralization of influenza virus in the absence of prior immunity." J Virol 81(7): 3487-3494.

Jayasekera, J. P., et al. (2006). "Enhanced antiviral antibody secretion and attenuated immunopathology during influenza virus infection in nitric oxide synthase-2-deficient mice." J Gen Virol 87(Pt 11): 3361-3371.

Joshi, N. S., et al. (2007). "Inflammation directs memory precursor and short-lived effector CD8(+) T cell fates via the graded expression of T-bet transcription factor." Immunity 27(2): 281-295.

Jouanguy, E., et al. (1996). "Interferon-gamma-receptor deficiency in an infant with fatal bacille Calmette-Guerin infection." N Engl J Med 335(26): 1956-1961.

Jouanguy, E., et al. (2000). "In a novel form of IFN-gamma receptor 1 deficiency, cell surface receptors fail to bind IFN-gamma." J Clin Invest 105(10): 1429-1436.

Jouanguy, E., et al. (1997). "Partial interferon-gamma receptor 1 deficiency in a child with tuberculoid bacillus Calmette-Guerin infection and a sibling with clinical tuberculosis." J Clin Invest 100(11): 2658-2664.

Julkunen, I., et al. (2000). "Inflammatory responses in influenza A virus infection." Vaccine 19 Suppl 1: S32-37.

Julkunen, I., et al. (2001). "Molecular pathogenesis of influenza A virus infection and virus-induced regulation of cytokine gene expression." Cytokine Growth Factor Rev 12(2-3): 171-180.

Kaech, S. M., et al. (2003). "Selective expression of the interleukin 7 receptor identifies effector CD8 T cells that give rise to long-lived memory cells." Nat Immunol 4(12): 1191-1198.

Kaech, S. M. and E. J. Wherry (2007). "Heterogeneity and cell-fate decisions in effector and memory CD8+ T cell differentiation during viral infection." Immunity 27(3): 393-405.

Kaech, S. M., et al. (2002). "Effector and memory T-cell differentiation: implications for vaccine development." Nat Rev Immunol 2(4): 251-262.

Kalia, V., et al. (2010). "Prolonged interleukin-2Ralpha expression on virus-specific CD8+ T cells favors terminal-effector differentiation in vivo." Immunity 32(1): 91-103.

Kelchtermans, H., et al. (2005). "Defective CD4+CD25+ regulatory T cell functioning in collagen-induced arthritis: an important factor in pathogenesis, counter-regulated by endogenous IFN-gamma." Arthritis Res Ther 7(2): R402-415.

Kemler, I., et al. (1994). "Nuclear import of microinjected influenza virus ribonucleoproteins." Virology 202(2): 1028-1033.

Kennedy, M. K., et al. (2000). "Reversible defects in natural killer and memory CD8 T cell lineages in interleukin 15-deficient mice." J Exp Med 191(5): 771-780.

Kilbourne, E. D. (1969). "Future influenza vaccines and the use of genetic recombinants." Bull World Health Organ 41(3): 643-645.

Kim, E. Y., et al. (2008a). "Persistent activation of an innate immune response translates respiratory viral infection into chronic lung disease." Nat Med 14(6): 633-640.

Kim, H. M., et al. (2008b). "Alveolar macrophages are indispensable for controlling influenza viruses in lungs of pigs." J Virol 82(9): 4265-4274.

Kim, T. S. and T. J. Braciale (2009). "Respiratory dendritic cell subsets differ in their capacity to support the induction of virus-specific cytotoxic CD8+ T cell responses." PLoS One 4(1): e4204.

Klenk, H. D., et al. (1975). "Activation of influenza A viruses by trypsin treatment." Virology 68(2): 426-439.

Kobasa, D., et al. (2004). "Enhanced virulence of influenza A viruses with the haemagglutinin of the 1918 pandemic virus." Nature 431(7009): 703-707.

Kris, R. M., et al. (1985). "Protection and recovery in influenza virus-infected mice immunosuppressed with anti-IgM." J Immunol 134(2): 1230-1235.

Kroncke, R., et al. (1996). "Human follicular dendritic cells and vascular cells produce interleukin-7: a potential role for interleukin-7 in the germinal center reaction." Eur J Immunol 26(10): 2541-2544.

Ku, C. C., et al. (2000). "Control of homeostasis of CD8+ memory T cells by opposing cytokines." Science 288(5466): 675-678.

Kumagai, Y., et al. (2008). "Pathogen recognition by innate receptors." J Infect Chemother 14(2): 86-92.

Kuo, C., et al. (2011). "Rhinovirus infection induces expression of airway remodelling factors in vitro and in vivo." Respirology 16(2): 367-377.

La Gruta, N. L., et al. (2007). "A question of self-preservation: immunopathology in influenza virus infection." Immunol Cell Biol 85(2): 85-92.

Lamb, R. A., et al. (1985). "Influenza virus M2 protein is an integral membrane protein expressed on the infected-cell surface." Cell 40(3): 627-633.

Langrish, C. L., et al. (2005). "IL-23 drives a pathogenic T cell population that induces autoimmune inflammation." J Exp Med 201(2): 233-240.

Lawrence, C. W., et al. (2005). "Frequency, specificity, and sites of expansion of CD8+ T cells during primary pulmonary influenza virus infection." J Immunol 174(9): 5332-5340.

Li, C., et al. (2006). "Autophagy is induced in CD4+ T cells and important for the growth factor-withdrawal cell death." J Immunol 177(8): 5163-5168.

Li, X., et al. (2007). "IFN-gamma acts directly on activated CD4+ T cells during mycobacterial infection to promote apoptosis by inducing components of the intracellular apoptosis machinery and by inducing extracellular proapoptotic signals." J Immunol 179(2): 939-949.

Liu, Y. and C. A. Janeway, Jr. (1990). "Interferon gamma plays a critical role in induced cell death of effector T cell: a possible third mechanism of self-tolerance." J Exp Med 172(6): 1735-1739.

Lodolce, J. P., et al. (1998). "IL-15 receptor maintains lymphoid homeostasis by supporting lymphocyte homing and proliferation." Immunity 9(5): 669-676.

Maggi, E., et al. (1992). "Reciprocal regulatory effects of IFN-gamma and IL-4 on the in vitro development of human Th1 and Th2 clones." J Immunol 148(7): 2142-2147.

Mandelboim, O., et al. (2001). "Recognition of haemagglutinins on virus-infected cells by NKp46 activates lysis by human NK cells." Nature 409(6823): 1055-1060.

Maraskovsky, E., et al. (1997). "Bcl-2 can rescue T lymphocyte development in interleukin-7 receptor-deficient mice but not in mutant rag-1-/- mice." Cell 89(7): 1011-1019.

Maraskovsky, E., et al. (1996). "Impaired survival and proliferation in IL-7 receptor-deficient peripheral T cells." J Immunol 157(12): 5315-5323.

Masopust, D., et al. (2001). "Preferential localization of effector memory cells in nonlymphoid tissue." Science 291(5512): 2413-2417.

Matrosovich, M. N., et al. (2004). "Human and avian influenza viruses target different cell types in cultures of human airway epithelium." Proc Natl Acad Sci U S A 101(13): 4620-4624.

Mazanec, M. B., et al. (1995). "Intracellular neutralization of influenza virus by immunoglobulin A anti-hemagglutinin monoclonal antibodies." J Virol 69(2): 1339-1343.

McGeoch, D., et al. (1976). "Influenza virus genome consists of eight distinct RNA species." Proc Natl Acad Sci U S A 73(9): 3045-3049.

McGill, J. and K. L. Legge (2009). "Cutting edge: contribution of lung-resident T cell proliferation to the overall magnitude of the antigen-specific CD8 T cell response in the lungs following murine influenza virus infection." J Immunol 183(7): 4177-4181.

McGill, J., et al. (2008). "Protective influenza-specific CD8 T cell responses require interactions with dendritic cells in the lungs." J Exp Med 205(7): 1635-1646.

McMichael, A. J., et al. (1983). "Cytotoxic T-cell immunity to influenza." N Engl J Med 309(1): 13-17.

Meraz, M. A., et al. (1996). "Targeted disruption of the Stat1 gene in mice reveals unexpected physiologic specificity in the JAK-STAT signaling pathway." Cell 84(3): 431-442.

Message, S. D., et al. (2008). "Rhinovirus-induced lower respiratory illness is increased in asthma and related to virus load and Th1/2 cytokine and IL-10 production." Proc Natl Acad Sci U S A 105(36): 13562-13567.

Miller, E. K., et al. (2008). "Influenza burden for children with asthma." Pediatrics 121(1): 1-8.

Morens, D. M., et al. (2008). "Predominant role of bacterial pneumonia as a cause of death in pandemic influenza: implications for pandemic influenza preparedness." J Infect Dis 198(7): 962-970.

Moskophidis, D. and D. Kioussis (1998). "Contribution of virus-specific CD8+ cytotoxic T cells to virus clearance or pathologic manifestations of influenza virus infection in a T cell receptor transgenic mouse model." J Exp Med 188(2): 223-232.

Mosmann, T. R. and R. L. Coffman (1989). "TH1 and TH2 cells: different patterns of lymphokine secretion lead to different functional properties." Annu Rev Immunol 7: 145-173.

Mozdzanowska, K., et al. (1999). "Treatment of influenza virus-infected SCID mice with nonneutralizing antibodies specific for the transmembrane proteins matrix 2 and neuraminidase reduces the pulmonary virus titer but fails to clear the infection." Virology 254(1): 138-146.

Muller, I., et al. (1994). "Expansion of gamma interferon-producing CD8+ T cells following secondary infection of mice immune to Leishmania major." Infect Immun 62(6): 2575-2581.

Mullooly, J. P., et al. (2007). "Influenza- and RSV-associated hospitalizations among adults." Vaccine 25(5): 846-855.

Murphy, B. R., et al. (1982). "Secretory and systemic immunological response in children infected with live attenuated influenza A virus vaccines." Infect Immun 36(3): 1102-1108.

Murphy, C. A., et al. (2003). "Divergent pro- and antiinflammatory roles for IL-23 and IL-12 in joint autoimmune inflammation." J Exp Med 198(12): 1951-1957.

Nguyen, H. H., et al. (2000). "Gamma interferon is not required for mucosal cytotoxic T-lymphocyte responses or heterosubtypic immunity to influenza A virus infection in mice." J Virol 74(12): 5495-5501.

Novelli, F., et al. (1996). "Switching on of the proliferation or apoptosis of activated human T lymphocytes by IFN-gamma is correlated with the differential expression of the alpha- and beta-chains of its receptor." J Immunol 157(5): 1935-1943.

O'Neill, R. E., et al. (1995). "Nuclear import of influenza virus RNA can be mediated by viral nucleoprotein and transport factors required for protein import." J Biol Chem 270(39): 22701-22704.

Paget, C., et al. (2011). "Potential role of invariant NKT cells in the control of pulmonary inflammation and CD8+ T cell response during acute influenza A virus H3N2 pneumonia." J Immunol 186(10): 5590-5602.

Pang, I. K. and A. Iwasaki (2011). "Inflammasomes as mediators of immunity against influenza virus." Trends Immunol 32(1): 34-41.

Peper, R. L. and H. Van Campen (1995). "Tumor necrosis factor as a mediator of inflammation in influenza A viral pneumonia." Microb Pathog 19(3): 175-183.

Peperzak, V., et al. (2010). "CD27 sustains survival of CTLs in virus-infected nonlymphoid tissue in mice by inducing autocrine IL-2 production." J Clin Invest 120(1): 168-178.

Perrone, L. A., et al. (2008). "H5N1 and 1918 pandemic influenza virus infection results in early and excessive infiltration of macrophages and neutrophils in the lungs of mice." PLoS Pathog 4(8): e1000115.

Perussia, B. (1991). "Lymphokine-activated killer cells, natural killer cells and cytokines." Curr Opin Immunol 3(1): 49-55.

Picard, C. and J. L. Casanova (2004). "Inherited disorders of cytokines." Curr Opin Pediatr 16(6): 648-658.

Pichlmair, A., et al. (2006). "RIG-I-mediated antiviral responses to single-stranded RNA bearing 5'-phosphates." Science 314(5801): 997-1001.

Pipkin, M. E., et al. (2010). "Interleukin-2 and inflammation induce distinct transcriptional programs that promote the differentiation of effector cytolytic T cells." Immunity 32(1): 79-90.

Potter, C. W. and J. S. Oxford (1979). "Determinants of immunity to influenza infection in man." Br Med Bull 35(1): 69-75.

Prabhu, N., et al. (2009). "Monoclonal antibodies against the fusion peptide of hemagglutinin protect mice from lethal influenza A virus H5N1 infection." J Virol 83(6): 2553-2562.

Pulendran, B. and R. Ahmed (2006). "Translating innate immunity into immunological memory: implications for vaccine development." Cell 124(4): 849-863.

Pulendran, B. and R. Ahmed (2011). "Immunological mechanisms of vaccination." Nat Immunol 12(6): 509-517.

Quan, F. S., et al. (2008). "A bivalent influenza VLP vaccine confers complete inhibition of virus replication in lungs." Vaccine 26(26): 3352-3361.

Reading, P. C., et al. (1997). "Collectin-mediated antiviral host defense of the lung: evidence from influenza virus infection of mice." J Virol 71(11): 8204-8212.

Refaeli, Y., et al. (2002). "Interferon gamma is required for activation-induced death of T lymphocytes." J Exp Med 196(7): 999-1005.

Reid, A. H., et al. (2001). "The 1918 Spanish influenza: integrating history and biology." Microbes Infect 3(1): 81-87.

Rinderknecht, E., et al. (1984). "Natural human interferon-gamma. Complete amino acid sequence and determination of sites of glycosylation." J Biol Chem 259(11): 6790-6797.

Robertson, J. S., et al. (1992). "High growth reassortant influenza vaccine viruses: new approaches to their control." Biologicals 20(3): 213-220.

Rothbarth, P. H., et al. (1999). "Influenza virus serology--a comparative study." J Virol Methods 78(1-2): 163-169.

Sad, S., et al. (1995). "Cytokine-induced differentiation of precursor mouse CD8+ T cells into cytotoxic CD8+ T cells secreting Th1 or Th2 cytokines." Immunity 2(3): 271-279.

Sallusto, F., et al. (2010). "From vaccines to memory and back." Immunity 33(4): 451-463.

Sallusto, F., et al. (1999). "Two subsets of memory T lymphocytes with distinct homing potentials and effector functions." Nature 401(6754): 708-712.

Sarawar, S. R., et al. (1994). "Administration of anti-IFN-gamma antibody to beta 2-microglobulin-deficient mice delays influenza virus clearance but does not switch the response to a T helper cell 2 phenotype." J Immunol 153(3): 1246-1253.

Sarkar, S., et al. (2008). "Functional and genomic profiling of effector CD8 T cell subsets with distinct memory fates." J Exp Med 205(3): 625-640.

Sawa, Y., et al. (2009). "Hepatic interleukin-7 expression regulates T cell responses." Immunity 30(3): 447-457.

Schlub, T. E., et al. (2010). "Predicting CD62L expression during the CD8+ T-cell response in vivo." Immunol Cell Biol 88(2): 157-164.

Schluns, K. S., et al. (2000). "Interleukin-7 mediates the homeostasis of naive and memory CD8 T cells in vivo." Nat Immunol 1(5): 426-432.

Schluns, K. S., et al. (2002). "Cutting edge: requirement for IL-15 in the generation of primary and memory antigen-specific CD8 T cells." J Immunol 168(10): 4827-4831.

Schnell, J. R. and J. J. Chou (2008). "Structure and mechanism of the M2 proton channel of influenza A virus." Nature 451(7178): 591-595.

Scholzen, T. and J. Gerdes (2000). "The Ki-67 protein: from the known and the unknown." J Cell Physiol 182(3): 311-322.

Schroder, K., et al. (2004). "Interferon-gamma: an overview of signals, mechanisms and functions." J Leukoc Biol 75(2): 163-189.

Shope, R. E. (1931). "Swine Influenza : I. Experimental Transmission and Pathology." J Exp Med 54(3): 349-359.

Shope, R. E. (1934). "The Infection of Ferrets with Swine Influenza Virus." J Exp Med 60(1): 49-61.

Shope, R. E. (1935). "The Infection of Mice with Swine Influenza Virus." J Exp Med 62(4): 561-572.

Sprenger, H., et al. (1996). "Selective induction of monocyte and not neutrophil-attracting chemokines after influenza A virus infection." J Exp Med 184(3): 1191-1196.

Stegmann, T., et al. (1991). "The HA2 subunit of influenza hemagglutinin inserts into the target membrane prior to fusion." J Biol Chem 266(27): 18404-18410.

Subrata, L. S., et al. (2009). "Interactions between innate antiviral and atopic immunoinflammatory pathways precipitate and sustain asthma exacerbations in children." J Immunol 183(4): 2793-2800.

Sun, J., et al. (2009). "Effector T cells control lung inflammation during acute influenza virus infection by producing IL-10." Nat Med 15(3): 277-284.

Sun, K. and D. W. Metzger (2008). "Inhibition of pulmonary antibacterial defense by interferon-gamma during recovery from influenza infection." Nat Med 14(5): 558-564.

Suptawiwat, O., et al. (2010). "Enhanced susceptibility of nasal polyp tissues to avian and human influenza viruses." PLoS One 5(9): e12973.

Swain, S. L., et al. (2004). "T cell responses to influenza virus infection: effector and memory cells." Viral Immunol 17(2): 197-209.

Tacon, C. E., et al. (2010). "Human rhinovirus infection up-regulates MMP-9 production in airway epithelial cells via NF-{kappa}B." Am J Respir Cell Mol Biol 43(2): 201-209.

Tanchot, C., et al. (1997). "Differential requirements for survival and proliferation of CD8 naive or memory T cells." Science 276(5321): 2057-2062.

Taubenberger, J. K. and S. P. Layne (2001). "Diagnosis of influenza virus: coming to grips with the molecular era." Mol Diagn 6(4): 291-305.

Taubenberger, J. K. and D. M. Morens (2008). "The pathology of influenza virus infections." Annu Rev Pathol 3: 499-522.

Taubenberger, J. K., et al. (1997). "Initial genetic characterization of the 1918 "Spanish" influenza virus." Science 275(5307): 1793-1796.

Tewari, K., et al. (2007). "Role of direct effects of IFN-gamma on T cells in the regulation of CD8 T cell homeostasis." J Immunol 179(4): 2115-2125.

Topham, D. J., et al. (1997). "CD8+ T cells clear influenza virus by perforin or Fas-dependent processes." J Immunol 159(11): 5197-5200.

Tumpey, T. M., et al. (2005). "Pathogenicity of influenza viruses with genes from the 1918 pandemic virus: functional roles of alveolar macrophages and neutrophils in limiting virus replication and mortality in mice." J Virol 79(23): 14933-14944.

Turner, S. J., et al. (2007). "Disregulated influenza A virus-specific CD8+ T cell homeostasis in the absence of IFN-gamma signaling." J Immunol 178(12): 7616-7622.

Valente, G., et al. (1992). "Distribution of interferon-gamma receptor in human tissues." Eur J Immunol 22(9): 2403-2412.

Veiga-Fernandes, H., et al. (2000). "Response of naive and memory CD8+ T cells to antigen stimulation in vivo." Nat Immunol 1(1): 47-53.

Vella, A. T., et al. (1998). "Cytokine-induced survival of activated T cells in vitro and in vivo." Proc Natl Acad Sci U S A 95(7): 3810-3815.

Verbist, K. C., et al. (2011). "Cutting edge: IL-15-independent maintenance of mucosally generated memory CD8 T cells." J Immunol 186(12): 6667-6671.

Vukmanovic-Stejic, M., et al. (2000). "Human Tc1 and Tc2/Tc0 CD8 T-cell clones display distinct cell surface and functional phenotypes." Blood 95(1): 231-240.

Walsh, J. J., et al. (1961). "Bronchotracheal response in human influenza. Type A, Asian strain, as studied by light and electron microscopic examination of bronchoscopic biopsies." Arch Intern Med 108: 376-388.

Wang, Z., et al. (2006). "Role of IFN-gamma in induction of Foxp3 and conversion of CD4+ CD25- T cells to CD4+ Tregs." J Clin Invest 116(9): 2434-2441.

Wang, Z. E., et al. (1994). "CD4+ effector cells default to the Th2 pathway in interferon gamma-deficient mice infected with Leishmania major." J Exp Med 179(4): 1367-1371.

Watanabe, M., et al. (1995). "Interleukin 7 is produced by human intestinal epithelial cells and regulates the proliferation of intestinal mucosal lymphocytes." J Clin Invest 95(6): 2945-2953.

Watanabe, T., et al. (2013). "Characterization of H7N9 influenza A viruses isolated from humans." Nature.

Watanabe, Y., et al. (2005). "Augmentation of fatality of influenza in mice by inhibition of phagocytosis." Biochem Biophys Res Commun 337(3): 881-886.

Wheelock, E. F. (1965). "Interferon-like virus-inhibitor induced in human leukocytes by phytohemagglutinin." Science 149(3681): 310-311.

Whitmire, J. K., et al. (2008). "Tentative T cells: memory cells are quick to respond, but slow to divide." PLoS Pathog 4(4): e1000041.

Wiley, J. A., et al. (2001). "Production of interferon-gamma by influenza hemagglutinin-specific CD8 effector T cells influences the

development of pulmonary immunopathology." Am J Pathol 158(1): 119-130.

Williams, M. A. and M. J. Bevan (2007). "Effector and memory CTL differentiation." Annu Rev Immunol 25: 171-192.

Wirth, T. C., et al. (2009). "Differentiation of central memory CD8 T cells is independent of CD62L-mediated trafficking to lymph nodes." J Immunol 182(10): 6195-6206.

Yap, K. L., et al. (1978). "Transfer of specific cytotoxic T lymphocytes protects mice inoculated with influenza virus." Nature 273(5659): 238-239.

Yasuda, J., et al. (1993). "Molecular assembly of influenza virus: association of the NS2 protein with virion matrix." Virology 196(1): 249-255.

Young, H. A. and K. J. Hardy (1995). "Role of interferon-gamma in immune cell regulation." J Leukoc Biol 58(4): 373-381.

Zhang, W. J., et al. (1996). "Lethal synergism between influenza infection and staphylococcal enterotoxin B in mice." J Immunol 157(11): 5049-5060.